ELECTROPHYSIOLOGY OF INTERSTITIAL CELLS OF CAJAL

ELECTROPHYSIOLOGY OF INTERSTITIAL CELLS OF CAJAL

By

GEORGE W.J. WRIGHT, B.SC. (HONS.)

A Thesis

Submitted to the School of Graduate Studies

In Partial Fulfillment of the Requirements

For the Degree Doctor of Philosophy

McMaster University

DOCTOR OF PHILOSOPHY (2016) McMaster University

(Medical Sciences) Hamilton, Ontario

TTLE: Electrophysiology of interstitial cells of Cajal

AUTHOR: George W.J. Wright, B.Sc. (Hons.) (McMaster University)

SUPERVISOR: Professor Jan D. Huizinga (Ph.D.)

NUMBER OF PAGES: xiv, 201

LAY ABSTRACT

The gut is essential for digestion and absorption of food. The gut has special cells called interstitial cells of Cajal (ICC), which control the contractions of the gut muscle. ICC are pacemaker cells, like those that pace heart beats. To pace gut muscle contractions, ICC generate electrical signals which cause the muscle to contract in an organized rhythmic manner, which promotes mixing or propulsion of gut contents, called motility. I used tiny electrodes to record electrical activity from ICC or gut muscle, to improve our understanding of how ICC pacemaker activity controls motility. My research characterised ion channels, which are microscopic protein pores that allow cells to make electrical currents, that enable generation of pacemaker signals by ICC. I also investigated activation of ICC electrical activity that causes propulsive colonic motility. This will hopefully lead to treatment improvements for patients with motility disorders in the future.

ABSTRACT

This thesis focuses on elucidating the electrical mechanisms underlying excitation of small intestinal and colonic smooth muscle initiated by interstitial cells of Cajal (ICC). All the ICC subtypes are involved in the orchestration, generation, and/or transmission of electrical signals to smooth muscle to pace gut motor patterns. Some ICC types have intrinsic activity leading to omnipresent rhythmic changes in smooth muscle excitability; others respond to stimuli, inducing pacemaker activity as required. Together they orchestrate motor patterns such as propulsion and segmentation, essential functions of the gut. To study ICC electrophysiology, I utilized patch clamping to record ion channel currents from single intestinal ICC and sharp microelectrodes to record colonic smooth muscle membrane potentials. I have made several discoveries contributing to our understanding of ICC electrophysiology. Firstly, my research increased our understanding of the properties of intrinsic pacemaker activity. I showed that maxi Cl^- channels from small intestinal ICC make a significant contribution to slow wave depolarization triggered by intracellular calcium. Secondly, I showed that colonic intramuscular ICC (ICC-IM) selectively express $K_V7.5$ channels, which are suppressed by cholinergic agonists, meaning that excitatory stimuli triggering acetylcholine release deactivate $K_V7.5$ channels, leading to increased excitability. Thirdly, I have shown that the bile acid chenodeoxycholic acid and the nitric oxide donor sodium nitroprusside both induce pacemaker activity, rhythmic transient depolarisations in mouse colonic muscle, which led to the hypothesis that nitrergic nerves are involved in generating inducible myenteric plexus ICC (ICC-MP) pacemaker activity. It is only when ICC are suitably stimulated by intracellular processes such as rhythmic Ca^{2+} transients or extracellular signalling from neurotransmitters or small molecules, that ICC produce membrane potential rhythmicity,

required for generation of intrinsic slow waves, low-frequency rhythmic transient depolarisations and transmission of excitation into the muscle.

ACKNOWLEDGEMENTS

I would like to gratefully acknowledge my graduate supervisor Dr. Jan Huizinga for his support, insight and advice. His supervision and guidance have brought me a long way from my days working with him as an undergraduate coop student. I appreciate all the time, money and input that he has given me over the years which have enabled me to complete this degree, travel to conferences and publish numerous papers. I have always been encouraged by Jan's excitement and enthusiasm for science and his appreciation of the beauty of a good recording. I would like to thank Dr. Sean Parsons for his technical expertise and hands on training regarding patch clamping, dissections, preparing electrodes, and many other skills. I have also appreciated his excellent programming and analysis contributions for many of my projects. I would like to thank Dr. Xuan Yu Wang for her help with immunohistochemistry, staining and other important contributions to my projects. I would also like to thank Dr. Yong Fang Zhu for her help and advice with intracellular recording techniques and providing the FFT and continuous wavelet transform analysis programs.

I would also like to thank the members of my supervisory committee Drs. Michael O'Donnell and Luke Janssen, who have provided excellent critical feedback on my work throughout the years. I appreciate their advice and suggestions on both my written and presented work as they have helped refine and improve them considerably.

I would also like to thank and acknowledge the many colleagues with whom I had the pleasure of working over the years including Marc Pistilli, Amir Khoshdel, Raul Loera-Valencia, Andrew Pawelka, Sarah Martz, David Chen, Bobbi-Jo Lowie, Victor Gil, Hong Fei Li, Zain-

ab Al Harraq, Yasmeen Maurice, Xiao Jing Quan, Alex Vincent and many others. I value the friendships I have made working in the lab with these people and they have made it thoroughly enjoyable.

I am very grateful to the granting agencies that have provided scholarships to me during my Ph.D. studies. I would like to thank the Government of Ontario for the George and Alice Rivett Ontario Graduate Scholarship that I received. I would also like to thank the Natural Science and Engineering Research Council (NSERC) for both the NSERC Postgraduate Scholarship – Doctoral and the NSERC Alexander Graham Bell Canada Graduate Scholarship – Doctoral that I received. Each of these scholarships provided essential financial support that enabled me to complete my degree.

I would not have completed this degree without the love and support of my wife Emily. She has encouraged me after tough days of experiments and celebrated all the successes with me along the way. I would like to dedicate this thesis to my son Daniel, who at the time of writing this is a few months old.

TABLE OF CONTENTS

LIST OF FIGURES

LIST OF TABLES

LIST OF ABBREVIATIONS AND SYMBOLS

AM	Acetoxymethyl ester
Ano1	Anoctamin 1 Ca^{2+}-activated Cl^- channel
ATP	Adenosine triphosphate
BK_{Ca}	Large conductance Ca^{2+}-activated K^+ channels
Ca^{2+}_i	Intracellular calcium ions
CFTR	Cystic fibrosis transmembrane conductance regulator
CPA	Cyclopiazonic acid
CWT	Continuous wavelet transform
DIDS	4,4'-Diisothiocyanato-2,2'-stilbenedisulfonic acid
DMSO	Dimethyl sulphoxide
E_{rev}	Reversal potential
ERG K^+	Ether-a-go-go related gene K^+ channels
GFP	Green fluorescent protein
GI	Gastrointestinal
HEPES	4-(2-Hydroxyethyl)piperazine-1-ethanesulfonic acid
HS	HEPES-buffered saline
ICC	Interstitial cells of Cajal
ICC-DMP	ICC associated with the deep muscular plexus
ICC-IM	Intramuscular ICC
ICC-MP	ICC associated with the myenteric plexus
ICC-SMP	ICC associated with the submuscular plexus
IPAN	Intrinsic primary afferent neuron
I/V	Current versus voltage
$K_V7.5$	Voltage-gated K^+ channel 7.5
Li-NCX	Li^+ and La^{3+} containing NCX blocking solution
M_3	Muscarinic acetylcholine receptor 3
mAChRs	Muscarinic acetylcholine receptors
MCl_{ir}	Inwardly rectifying maxi Cl^- currents
MCl_{or}	Outwardly rectifying maxi Cl^- currents
NC	No cell control
NCX	Na^+/Ca^{2+} exchanger
NO	Nitric oxide
NPPB	5-Nitro-2-(3-phenylpropylamino)benzoic acid
NSCC	Non-selective cation channel
PBS	Phosphate buffered saline
PKA	Protein kinase A
PMCA	Plasma membrane Ca^{2+} ATPase
P_o	Open probability
Rrmp	Relative to resting membrane potential
SANC	Sinoatrial node cells
SEM	Standard error of the mean

SERCA	Sarco/endoplasmic reticulum Ca^{2+} ATPase
SNP	Sodium nitroprusside
SR	Sarcoplasmic reticulum
TTX	Tetrodotoxin
VAChT	Vesicular acetylcholine transporter

DECLARATION OF ACADEMIC ACHIEVEMENT

During my time as a PhD student in the Physiology and Pharmacology stream of the Medical Sciences graduate program in the faculty of Health Sciences at McMaster University I have made the following research contributions contained within this thesis. My three major projects on the activation of low-frequency rhythmic transient depolarisations by chenodeoxycholic acid in mouse colon, Ca^{2+} activation of the maxi chloride channel from small intestinal interstitial cells of Cajal (ICC) and the $K_V7.5$ channels expressed in colonic intramuscular ICC have been included here as full manuscripts. I contributed to these manuscripts by planning the studies, performing the experiments, analyzing the data, writing and editing the drafts, and creating the figures. I was also able to contribute to several other projects as a co-author where I performed experiments, calculated statistics and wrote and edited manuscripts.

I would like to gratefully acknowledge the input of my supervisor Dr. Jan Huizinga without whom the writing of this thesis would not have been possible. He contributed to it via planning, providing references from the literature, and by making editorial comments. I would also like to acknowledge my coauthors on all the papers contained herein, whose specific contributions are described in the prefaces of each of the chapters.

CHAPTER 1: GENERAL INTRODUCTION

1.1 Gastrointestinal Motility and Interstitial Cells of Cajal

Normal motility is required for proper digestion, absorption and excretion. Motility is often affected in diseases that involve the gastrointestinal (GI) tract. Interstitial cells of Cajal (ICC) were first proposed as gastrointestinal pacemaker cells in the late 1970s and early 1980s (Rumessen, et al., 1982; Huizinga, et al., 2011; Thuneberg, 1982; Faussone Pellegrini, et al., 1977). There are several different populations of ICC in both the small intestine and the colon. They differ in location, morphology, role and protein expression (Huizinga, et al., 2011; Komuro, 2006). Small intestinal ICC associated with the myenteric plexus (ICC-MP) are the best studied ICC subtype; they generate rhythmic depolarising electrical activity called slow waves which pace rhythmic muscle contractions required for motility (Thomsen, et al., 1998; Barajas-Lopez, et al., 1989; Kito and Suzuki, 2003; Huizinga, et al., 1998; van Helden, et al., 2010). ICC associated with the colonic submuscular plexus generate rhythmic slow waves analogous to those generated by small intestinal ICC-MP (Pluja, et al., 2001; Huizinga, et al., 2011; Yoneda, et al., 2002). ICC-MP from the colon, on the other hand, may pace the propulsive motor pattern of the colon associated with content movement (Huizinga, et al., 2011).

Evidence for the role of interstitial cells of Cajal (ICC) in motor patterns in the stomach and small intestine is strong. Individual small intestinal ICC with functional c-kit, a tyrosine kinase receptor that is a selective marker of ICC required for their development and differenti-

ation (Huizinga, et al., 1995; Ward, et al., 1994), generate slow waves (Thomsen, et al., 1998), which occur at the same frequency as associated peristaltic contractions (Der-Silaphet, et al., 1998). Animals with heterozygous mutations leading to loss of functional c-kit receptors (W/W^V mice) do not exhibit slow waves (Thomsen, et al., 1998; Ward, et al., 1994) or slow wave driven peristaltic contractions (Der-Silaphet, et al., 1998). Neutralizing antibodies against c-kit administered to neonatal mice disrupt development of their ICC-MP networks and their small intestines lose electrical rhythmicity (Torihashi, et al., 1995). In the stomach ICC-MP are not lost in W/W^V mice, but intramuscular ICC (ICC-IM) are absent (Hirst and Edwards, 2004). Consequently, slow waves are observed in the antra of W/W^V mice, but the secondary component generated by ICC-IM was not recorded from mouse gastric muscles (Dickens, et al., 2001; Hirst, et al., 2002).

Nerves and interstitial cells of Cajal are closely connected in the myenteric plexus and within the muscle (Hirst and Edwards, 2004). Many research papers have been written with the assumption that nerves alone can generate the rhythmicity required for gut motor patterns; however, it is well established that pacemaker orchestrated rhythmicity continues in the presence of neuronal Na^+ channel blockers like lidocaine and TTX (Pawelka and Huizinga, 2015; Keef, et al., 1997). Considering several studies on neuronal activation or modulation of ICC activity (Zhu, et al., 2011; Bayguinov, et al., 2010; So, et al., 2009), the interplay between nerves and ICC is very important. Attempting to explain the complex motor patterns of the gut solely invoking neuronal activity is, thus, misguided. Therefore, investigating how nerves and ICC interact to generate different motility patterns, especially focusing on the electro-

physiological mechanism underlying changes in pacemaker activity, is essential for understanding how gut motility is orchestrated.

1.2 Intrinsic ICC Pacemaker Activity

Determining the contributions of ion channels to ICC-MP pacemaker potentials is essential for understanding how intrinsic pacemaker activity is generated. Prior to my thesis, studies had focused on the roles of non-selective cation channels (Thomsen, et al., 1998; Koh, et al., 2002), Ano1 (Zhu, et al., 2009), ether-a-go-go related gene (ERG) K^+ channels (McKay and Huizinga, 2006), large conductance Ca^{2+}-activated K^+ channels (BK_{Ca}) (Corrias and Buist, 2008), SCN5A Na^+ channels (Strege, et al., 2003), $K_V1.1$ K^+ channels (Hatton, et al., 2001), dihydropyridine insensitive voltage-gated Ca^{2+} channels (Kim, et al., 2002), and transient outward K^+ channels (Parsons and Huizinga, 2010) in the ICC-MP pacemaker potential (Fig. 1.1). I wanted to determine the role of maxi chloride channels in the generation of the pacemaker potential upstroke and prove or disprove that it is the fundamental pacemaker channel (Fig. 1.1). ICC-MP pacemaker potentials occur at the same frequency as rhythmic intracellular Ca^{2+} transients (Lowie, et al., 2011; Torihashi, et al., 2002; Lee, et al., 2007), thus, it is likely that ICC-MP possess a Ca^{2+} clock like sinoatrial node cells (SANCs) which are the pacemaker cells from the heart (Lakatta, et al., 2010). To link the Ca^{2+} clock to the membrane potential depolarisations required for the ICC-MP pacemaker potential, the pacemaker channel crucial for the pacemaker potential upstroke should be sensitive to the intracellular Ca^{2+} signalling pathway. If the maxi Cl^- channel is Ca^{2+}-activated, then its role as the ICC-MP pacemaker channel would be solidified.

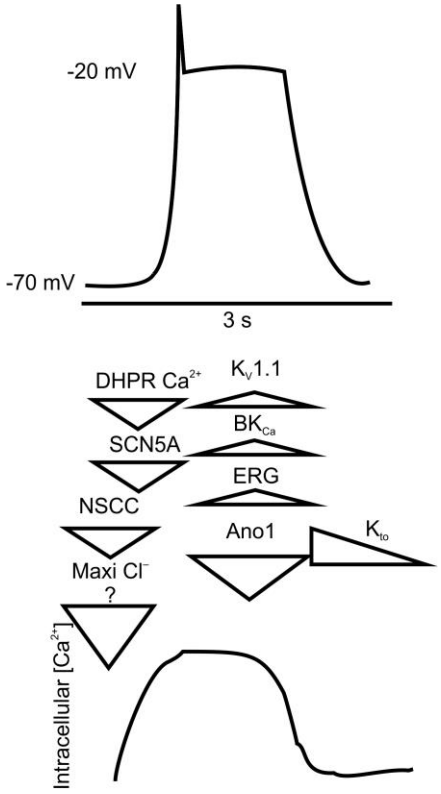

Figure 1.1: Schematic diagram of ion channel involvement in the interstitial cells of Cajal associated with the myenteric plexus (ICC-MP) pacemaker potential. Top trace represents a slow wave pacemaker potential generated by ICC-MP. Below, triangles represent current contributions from: dihydropyridine-resistant (DHPR) Ca^{2+} channels, SCN5A Na^{+} channels, non-selective cation channels (NSCC), voltage gated K^{+} channel 1.1 ($K_V1.1$), large conductance Ca^{2+}-activated K^{+} channels (BK_{Ca}), ether-a-go-go related gene (ERG) K^{+} channels, anoctamin 1 (Ano1) Ca^{2+}-activated Cl^{-} channels, and transient outward K^{+} channels (K_{to}). The maxi Cl^{-} channel is possibly involved in the upstroke of pacemaker potential, which occurs in concert with rhythmic intracellular Ca^{2+} transients in ICC-MP (bottom trace). Downward triangles indicate inward currents and upward triangles indicate outward currents.

ICC pacemaker mechanisms may have some commonalities with the primary cardiac pacemaker system provided by sinoatrial node cells (SANC) (Lakatta, et al., 2010). Mechanisms of cardiac pacemaking are better understood than those of ICC. It is important to make comparisons between the pacemaker systems of SANCs and ICC to develop testable hypotheses about ICC pacemaker mechanisms. Lakatta and colleagues have suggested that a Ca^{2+} clock is inextricably linked to a membrane delimited clock (see Figure 1A of Lakatta (2010)); both are vital for pacemaker function. Central to the coupled membrane and Ca^{2+} clock schema is the Na^{+}/Ca^{2+} exchanger (NCX) (Bogdanov, et al., 2001; Lakatta, et al., 2010). Li^{+}, an NCX blocker, was shown to inhibit action potential firing in SANCs; Li^{+} also affected Ca^{2+} handling, reducing Ca^{2+} transient magnitude (Bogdanov, et al., 2001). It seems that electrogenic NCX activity is required for adequate depolarization for voltage-gated Ca^{2+} channel activation and in turn NCX reduces cytosolic Ca^{2+} from rhythmic Ca^{2+} transients (Lakatta, et al., 2010).

NCX also has an important role in small intestinal ICC-MP pacemaking; reverse mode NCX is required for sarcoplasmic reticulum Ca^{2+} store refilling after Ca^{2+} transients since the NCX inhibitor KB-R7943 reduced Ca^{2+} oscillation frequency (Lowie, et al., 2011). Rhythmic Ca^{2+} transients are not blocked by nicardipine or mibefradil, L-type and T-type Ca^{2+} channel blockers, suggesting that voltage-gated Ca^{2+} channels do not play a major role in these transients (Lowie, et al., 2011). Although NCX is involved in the Ca^{2+} clock, it is unclear how the electrogenic properties of NCX are involved in ICC-MP pacemaker potentials. There may be

more parallels and contrasts between SANCs and ICC that provide promising avenues for pacemaker research.

1.3 Interactions of Multiple Pacemakers Generate Gut Motor Patterns

Unlike small intestinal ICC-MP, not all ICC subtypes possess intrinsic pacemaker activity. Small intestinal ICC associated with the deep muscular plexus (ICC-DMP) generate low-frequency electrical activity when stimulated by decanoic acid or butyric acid (Pawelka and Huizinga, 2015). The low-frequency electrical activity evoked by decanoic acid caused the amplitude of the ICC-MP slow wave (Fig. 1.2A) to wax and wane (Fig. 1.2B). Continuous wavlet transform (CWT) analysis (see section 1.7.3) was used to determine that there were two frequency components in the waxing and waning electrical recordings at ~2 cpm and ~32 cpm (Pawelka and Huizinga, 2015; Huizinga, et al., 2015). Our laboratory went on to show that these two frequency components interacted with each other by phase amplitude coupling.

Whole small intestine contractility experiments in the organ bath showed rhythmic propulsive contractions paced by ICC-MP slow waves (Fig. 1.2C). After addition of decanoic acid, the activity changed to a non-propulsive segmentation pattern charaterised by "checkered" spatiotemporal maps where the slow wave-paced contrations waxed and waned in amplitude (Fig. 1.2D) (Huizinga, et al., 2015). The reason that the segmentation pattern became non-propulsive was because the phase of the low-frequency activity modulated the amplitude of the high frequency. With these small intestinal pacemaker properties in mind, I

wanted to determine how the inducible pacemaker in the colon is activated and whether or not phase amplitude coupling is a method of motor pattern generation employed by the colon . To fully understand the different types of ICC, their functions and how they interact to generate distinct motor patterns, we need to understand the characteristics of the pacemaker activities (intrinsic or inducible) of the different subtyptes in the different organs of the gut, and how these activities interact.

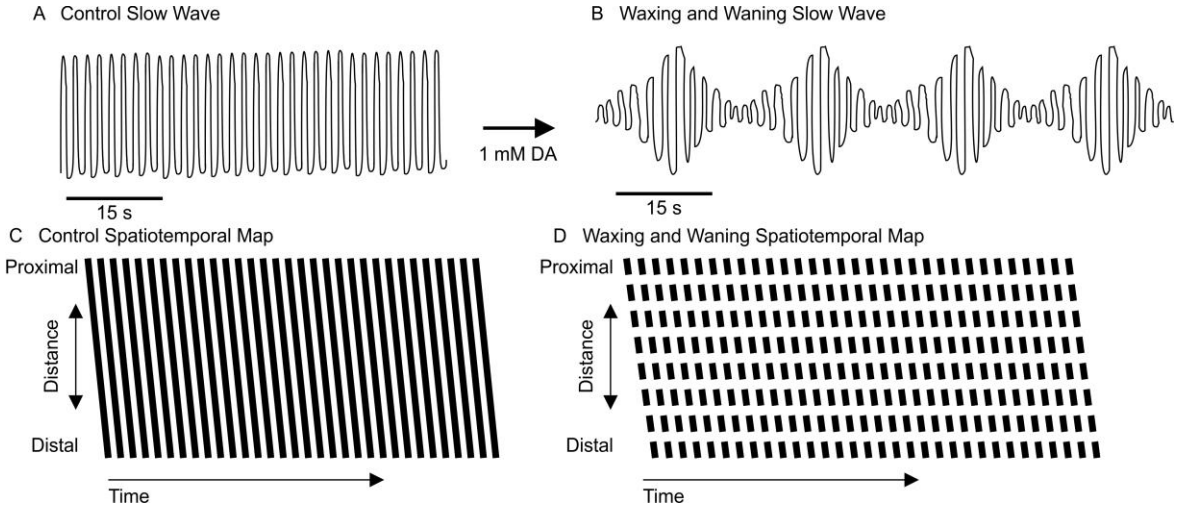

Figure 1.2: Pacemaker interactions in the small intestine. A) Cartoon trace depicting slow waves recorded in control conditions from small intestinal circular muscle using intracellular microelectrodes. B) Cartoon trace depicting waxing and waning slow waves evoked by 1 mM decanoic acid (DA) recorded from circular muscle. C) Simulated spatiotemporal map typical of those generated from video recordings of whole small intestine contractility, depicting rhythmic propulsive contractions paced by slow waves like those in (A). D) Simulated spatio-temporal map typical of contractility recordings after addition of decanoic acid. "Checkered" contractions exhibiting amplitude modulation leading to a non-propulsive, mixing pattern

called segmentation. Dark lines on spatiotemporal map represent more contracted intestine (smaller diameter) and white areas represent more relaxed intestine (larger diameter).

1.4 Three Research Questions and Hypotheses

The following sections contain the three main questions I tried to answer in my thesis. I will give some specific background to the questions and give the hypothesis that determined our methods of study.

1.5 How is the Maxi Cl^- Channel from ICC-MP Activated?

Previous studies identified a high conductance chloride channel in ICC-MP which has several conductance states, and may be able to generate the initial depolarisation required for the upstroke (Fig. 1.1) of the pacemaker potential (Huizinga, et al., 2002; Parsons and Sanders, 2008; Wang, et al., 2008). ICC-MP exhibit spontaneous rhythmic Ca^{2+} transients (Lowie, et al., 2011; Torihashi, et al., 2002; Lee, et al., 2007), which occur at the same frequency as the ICC-MP slow wave. As introduced above, the maxi Cl^- channel is a candidate for the pacemaker channel for intrinsic ICC-MP pacemaker activity, but to drive periodic membrane potential depolarisations with the rhythmic Ca^{2+} transients, the pacemaker channel requires sensitivity to intracellular Ca^{2+} or its effectors (Zhu, et al., 2009). This led to the ***research question:*** how is the maxi Cl^- channel from ICC-MP is activated? ***Our hypothesis*** was that the maxi Cl^- channel is activated by increased intracellular Ca^{2+}. If proved true, then the maxi Cl^- channel would respond to the rhythmic Ca^{2+} transients in ICC-MP and drive rhythmic membrane potential depolarisations required for the upstroke of the pacemaker potential underly-

ing the small intestinal slow wave. To answer this question, we utilized patch clamp electrophysiology, Ca^{2+} imaging and immunohistochemistry, discussed in the next section.

1.5.1 Patch Clamp Electrophysiology Methods

Since my aim was to test the hypothesis that the maxi Cl^- channel from ICC-MP was activated by intracellular Ca^{2+}, I needed to choose a technique to accurately detect and measure currents flowing through specific types of ion channels. Therefore, I used patch clamp electrophysiology to record the ion channel activity from individual ICC, because it is a uniquely powerful technique that uses fine glass microelectrodes to record tiny electrical currents from single cells (Hamill, et al., 1981). This is possible due to the formation of a high resistance gigaohm seal between the glass electrode and the cell membrane, which insulates the ion channels such that picoamp currents can be recorded with high signal to noise ratios, with the help of a specialized amplifier and software (Molleman, 2003).

I used cell-attached patches and inside-out patches, which enabled measurement of currents from a few ion channels at a time (1-~6). Cell-attached patch clamping is unique in that the intracellular machinery remains intact such that pharmacological activation of receptors or modulation intracellular pathways (such as increasing intracellular Ca^{2+}) can be tested to determine effects on ion channel activity. Since the cell membrane is intact in the cell-attached configuration, the cell maintains its resting membrane potential. Therefore, the potentials that the ion channels in the cell-attached patch experience are the sum of the command potential applied by the voltage protocol and the membrane potential. I chose to use repeating ramp protocols to provide a snapshot of channel voltage dependence and to make creating

current/voltage plots and calculating reversal potentials easier than using voltage steps. I used ion substitution to eliminate the contribution of ionic currents other than those which we wished to record. I used NMDGCl pipette solution to remove any contribution of inward monovalent cation currents (i.e from Na^+ channels), since $NMDG^+$ is an impermeant ion. The specific protocols I used to increase intracellular Ca^{2+} in ICC-MP to test the effects on maxi Cl^- channel activation were the following: adding the Ca^{2+} selective ionophore, ionomycin (1 in Fig. 1.3), which is a small molecule that facilitates transport of Ca^{2+} across cell membranes, and cyclopiazonic acid (2 in Fig. 1.3), which is a sarco/endoplasmic reticulum Ca^{2+} ATPase inhibitor. I also used a solution with Na^+ substituted with Li^+, and containing La^{3+}, which prevents Ca^{2+} efflux by the Na^+/Ca^{2+} exchanger (4 in Fig. 1.3) and blocks P-type ATPases including PMCA (5 in Fig. 1.3), respectively. Another goal of my study was to settle a controversy about the rectification properties of the maxi Cl^- channel; if maxi channels were outwardly rectifying, the magnitude of inward Cl^- currents required for depolarisation would not be very large, which would affect its ability to generate the pacemaker potential upstroke. Outward rectification means that channels allow outward current more readily than inward current. Outward current through Cl^- channels means that Cl^- ions enter the cell, since current direction is defined as the direction of positive charge flow, due to convention. When Cl^- enters the cell, it makes the interior of the membrane more negative, hyperpolarising the cell, which is the opposite of the depolarisation required for pacemaker potential upstroke initiation. Therefore, if the maxi Cl^- channel was inwardly rectifying, meaning that it allows inward current more readily than outward, then it would be more likely to generate the inward depolarising currents required to be the pacemaker channel. One way I used to

test the maxi Cl^- channel rectification was recording them in the inside-out patch clamp configuration. The inside-out patch clamp configuration involves pulling a cell-attached patch away from a cell (3 in Fig. 1.3), allowing access to the intracellular face of the channel.

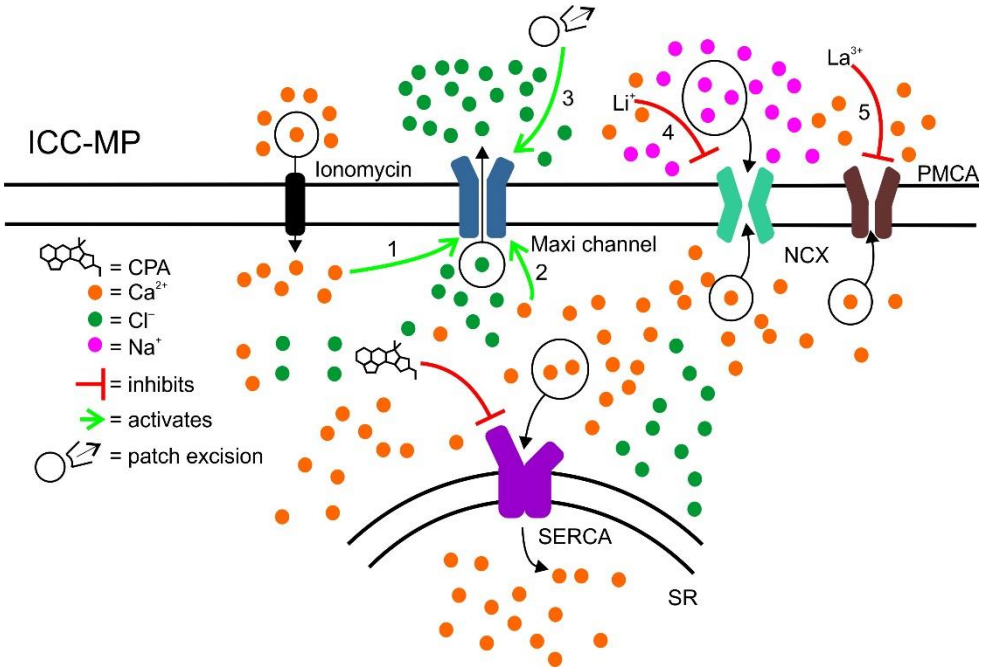

Figure 1.3: Schematic diagram depicting strategies by which maxi chloride channels could be activated by intracellular Ca^{2+}. We investigated whether ionomycin – a Ca^{2+} ionophore (1) – or cyclopiazonic acid (CPA) – a Sarco/endoplasmic reticulum Ca^{2+} ATPase (SERCA) inhibitor (2) – could activate maxi chloride channels by increasing intracellular Ca^{2+}. We also wanted to elucidate the effect of patch excision into the inside-out configuration on channel activation and rectification properties (3). Another method we used to increase intracellular Ca^{2+} was a solution with Na^+ substituted with Li^+ to prevent Ca^{2+} efflux via the Na^+/Ca^{2+} exchanger (NCX; 4) and La^{3+} to block P-type ATPases, including the plasma membrane Ca^{2+} ATPase (PMCA; 5).

1.5.2 Ca^{2+} Imaging Methods

Dr. Sean Parsons and I used Fluo-4 AM Ca^{2+} dye to measure relative Ca^{2+} fluorescence in ICC. The Fluo-4 with acetoxymethyl ester (AM) groups is not fluorescent and they enable loading of the dye into the cells. Once loaded, the AM groups are cleaved, the Fluo-4 chelates Ca^{2+}, and then fluoresces when excited by light with a wavelength of 488 nm, enabling measurement of changes in relative Ca^{2+} fluorescence in the cells. I used this technique to confirm whether ionomycin and CPA could increase ICC-MP intracellular Ca^{2+}.

1.5.3 Immunohistochemistry Methods

Dr. Xuan Yu Wang performed the immunohistochemistry in our studies to selectively stain various cell surface proteins to differentiate nerve cells from ICC and show which proteins are colocalized with selective markers of ICC. We also used it to determine the structure of ICC networks and how they connect to each other. In our study of maxi Cl^- channel activation, we used an antibody against Ano1, which is a Ca^{2+}-activated Cl^- channel and a selective marker of ICC (Gomez-Pinilla, et al., 2009), to stain cultured cells and confirm their identity.

1.6 How is the Cholinergic Agonist Carbachol Able to Excite Intramuscular ICC?

An important factor linking inducible and intrinsic pacemaker activities in ICC is the possibility of neuronal stimulation or modulation of those activities. ICC networks are highly innervated (Zhang, et al., 2011; Ward and Sanders, 2006; Ward, et al., 2000), and can be modulated by excitatory neurotransmitters, like acetylcholine (ACh) from cholinergic nerves, which causes changes in intrinsic pacemaker activity (So, et al., 2009), and possibly ICC ex-

citability and inducible pacemaker activity. However, the ion channels potentially modulated by cholinergic activity to alter ICC excitability and activate inducible pacemakers require more study. Due to the primary culture technique I used to isolate cells for patch clamping, both ICC-MP and ICC-IM were present in cultures. We wanted to test whether carbachol, a non-hydrolysable ACh analogue, could activate colonic ICC maxi chloride channels. A previous study showed that carbachol could modulate the activity of small intestinal ICC-MP via M_3 acetylcholine receptors (So, et al., 2009). Colonic ICC-MP do not generate intrinsic pacemaker activity, but we hypothesized that cholinergic nerves are able stimulate them to generate inducible pacemaker activity.

Colonic intramuscular ICC (ICC-IM) are found between the smooth muscle cells, as opposed to associated with a nerve plexus like other ICC networks (Komuro, 2006). They are involved in the transmission of neuronal stimulation to the smooth muscle (Wang, et al., 2003), but the electrical mechanism underlying ICC-IM increased excitability in response to cholinergic stimulation was unknown. Our second aim was to determine how ICC-IM responded to carbachol. This led to the ***research question:*** how is the cholinergic agonist carbachol able to excite colonic ICC-IM? Therefore, it was important to determine from which ICC subtype I was recording. ***I hypothesized*** that carbachol activates maxi Cl^- channels and inhibits K_V7 K^+ channels from ICC-IM. To test this hypothesis, I utilized cell-attached patch clamp electrophysiology, single cell PCR and immunohistochemistry.

1.6.1 Patch Clamp Electrophysiology Methods

The patch clamping methods I used for this study were largely the same as those discussed above in section 1.5.1 for the study of small intestinal ICC-MP maxi Cl^- channels, but with a few key differences. The pipette solution I used was 150 mM KCl, chosen because it enhances the amplitude of K^+ currents (Shibasaki, 1987; Block and Jones, 1997; Parsons and Huizinga, 2010). Using a K^+ concentration in the pipette that is higher than that inside the cells will reverse the normal concentration gradient from outward to inward. This is helpful because inward currents observed could only be carried by K^+ or Cl^- and pharmacology could then be used to determine the identity of the currents. If physiological extracellular solution with K^+ (~5 mM) and Na^+ (~140 mM) was used, one would not be able to eliminate the possible contribution of outward Na^+ currents to the outward K^+ currents without the use of additional pharmacological agents.

To test the hypothesis that carbachol inhibits K^+ channels (1 in Fig. 1.4) and activates maxi Cl^- channels (5 in Fig. 1.4), I recorded currents from cell attached patches and applied carbachol. I used XE991, a selective K_V7 channel blocker, to test whether the K^+ currents I recorded were from those channels. I tested whether K^+ channel blockers (XE991) in the pipette (2 in Fig. 1.4) or added to the bath (3 in Fig. 1.4) could block the K^+ currents. I was also interested in the effects of patch excision into the inside-out configuration on K^+ currents (4 in Fig. 1.4) and I hypothesized that it would turn off K^+ currents, based on previous studies of small intestinal ICC-MP (Parsons and Huizinga, 2010).

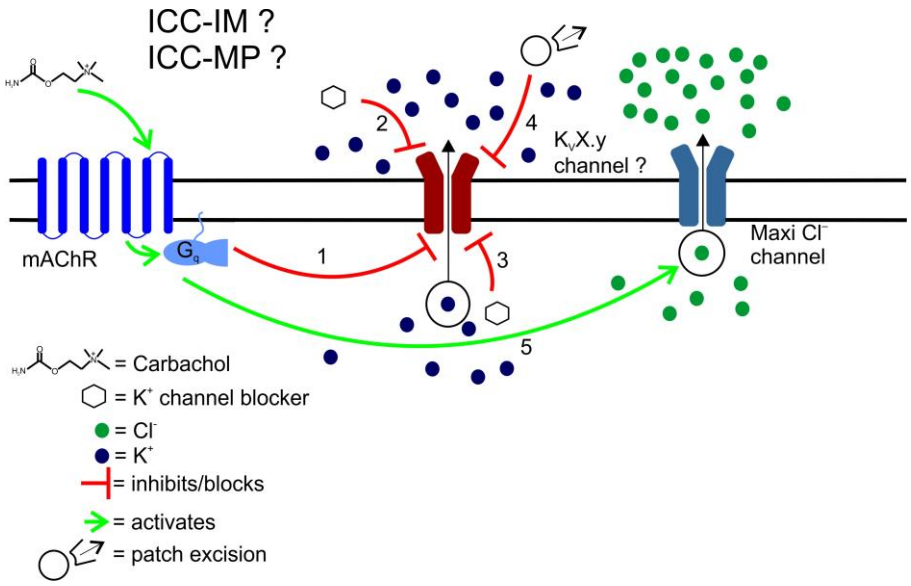

Figure 1.4: Schematic diagram depicting strategies to investigate the effects of carbachol on K^+ and Cl^- currents from ICC. I tested whether carbachol – a non-hydrolysable cholinergic agonist – could inhibit K^+ currents from ICC (1). Next, I used selective blockers to determine the identity of the channels responsible for carrying the K^+ current by adding them to the pipette (2) or the bath (3). I also wanted to determine whether patch excision would turn off K^+ currents (4). In addition, I wanted to assess whether muscarinic acetylcholine receptor (mAChR) activation by carbachol could activate maxi chloride currents (5).

1.6.2 Single Cell PCR Methods

To confirm the cultured cells from which I was recording were ICC, Raúl Loera-Valencia performed single cell PCR on them. I collected single ICC – selected using the same criteria as those that were chosen for patch clamping – by aspiration with low-resistance patch pipettes. Then Raúl extracted the genetic material by lysing the cells and created cDNA from the cell mRNA with reverse transcriptase. With the cDNA synthesised, Raúl amplified both

c-Kit – a selective marker of ICC – and K_V channel genes, in this case K_V7.5, with PCR. Showing that c-Kit is transcribed in cells chosen for patching would support the cell selection criteria; showing that both are transcribed would be valuable supporting evidence that K_V7.5 channels are expressed in ICC-IM.

1.6.3 Immunohistochemistry Methods

Dr. Xuan Yu Wang performed immunohistochemistry to show co-localisation of selective markers for ICC and nerves as well as K_V7 channels. To confirm that at least one member of K_V7 channel family was expressed in ICC, I prepared cultures that Xuan Yu double labelled with c-kit and a selective antibody for one of K_V7.2-5. She also checked intact tissue for colocalization of K_V7 channels and c-kit or a selective cholinergic neuronal marker vesicular acetylcholine transporter, with ICC and nerves arranged with their physiological connections. This staining was essential to determine which types of ICC expressed K_V7 channel subtypes (Fig. 1.4), since the cultured cells had both dispersed ICC-MP and ICC-IM present.

1.7 How is the Inducible Colonic Pacemaker Activated?

The mouse colon has three networks of ICC, one associated with the myenteric plexus (ICC-MP) and one with the submuscular plexus (ICC-SMP). The third one is located between the circular muscle (ICC-IM). ICC-SMP are the source of the intrinsic slow wave in the colon (Pluja, et al., 2001; Yoneda, et al., 2002). The ICC-MP of the colon, in contrast to the small intestine, do not generate intrinsic pacemaker activity, but we hypothesized that they require stimulation in order to generate rhythmic activity (Bayguinov, et al., 2010). The colon is the

waste storage and water reabsorption site of the gastrointestinal (GI) tract and in concert with these roles it does not exhibit propulsive motility all the time. I was interested in how inducible pacemaker activity is evoked in response to certain stimuli, which likely underlies propulsive colonic motility. This led to the ***research question***: how is the colonic inducible pacemaker activated?

In our preliminary studies of rabbit colon contractility using spatiotemporal mapping, we showed that the bile acid chenodeoxycholic acid could evoke low-frequency rhythmic contractions in the 3-taeniated segment of the colon. A possible mechanism, underlying the evoked contractility is the activation of TGR5 7-TM/G-protein coupled receptors, expressed on both intrinsic primary afferent neurons (IPANs) and enterochromaffin cells, which are activated by bile acids (Alemi, et al., 2013). Over 80% of NO synthase-expressing inhibitory nerves have TGR5 receptors (Poole, et al., 2010). Thus, ***I hypothesized*** that the activation of inducible ICC pacemaker activity in the mouse colon, by non-cholinergic (possibly nitrergic) myenteric neurons stimulated by chenodeoxycholic acid, leads to generation of low-frequency rhythmic transient depolarisations. To do this I investigated the actions of chenodeoxycholic acid and the NO donor sodium nitroprusside (SNP) on ICC electrical activity *in situ* by using intracellular recording with sharp microelectrodes on mouse colonic smooth muscle.

1.7.1 Multiple Pacemakers and Their Interactions

Our laboratory has pioneered the concept that many motor patterns are orchestrated via interaction of two different ICC pacemaker activities. For example, ICC associated with the myenteric plexus (ICC-MP) interacting with ICC associated with the deep muscular plexus (ICC-DMP) in the small intestine produces segmentation (Huizinga, et al., 2014a; Huizinga, et al., 2014b). The second pacemaker can be activated by decanoic acid (DA) and butyric acid via different mechanisms (Pawelka and Huizinga, 2015). It is possible that pacemakers in the colon interact to produce complex motor patterns, such as segmentation, through phase-amplitude coupling, like the small intestine. The pacemaker networks in the canine colon produce 6 cpm slow waves, recorded from the circular muscle, as well as 20 cpm oscillations when closer to the myenteric border (Smith, et al., 1987). The authors suggested that the two frequencies, produced by ICC-SMP and ICC-MP, interact by addition in the circular muscle. The 20 cpm frequency appears to increase in amplitude with the depolarisation phase of the ICC-MP slow wave in their figure 2 (Smith, et al., 1987), which suggests phase amplitude coupling. Rat colon also exhibits two pacemakers; ICC-MP produce a low-frequency (1-2 cpm) high amplitude activity and ICC-SMP produce higher frequency (10-12 cpm) low-amplitude slow waves (Pluja, et al., 2001; Alberti and Jimenez, 2005; Kato, et al., 2009; Quan, et al., 2015). Thus, I formulated the hypothesis that inducible pacemaker activity interacted by phase amplitude coupling with intrinsic slow waves or rhythmic pacemaker activity from ICC-SMP.

1.7.2 Intracellular Recording Methods

To test whether the drugs I selected could activate the inducible pacemaker in the colon, I used sharp microelectrodes to perform intracellular recording of colonic smooth muscle membrane potentials. Intracellular recording works by impaling a cell with a sharp microelectrode such that the tip of the electrode is inside the cell membrane. To impale a cell, the electrode was brought into contact with the tissue and a large amplitude current was injected into the cell for 10-20 ms. Once impaled, setting the holding current at 0 nA enabled measurement of the potential across the cell membrane as it changed spontaneously or when stimulated pharmacologically. After achieving impalements from circular muscle preparations with (Fig. 1.5) or without (Fig. 1.6) submucosa attached, I recorded smooth muscle membrane potentials which are affected by ICC pacemaker activity. To test whether I could evoke activity from the inducible pacemaker, I added the bile acid chenodeoxycholic acid or sodium nitroprusside (an NO donor) during recordings (2a & b in both Figs. 1.5 & 1.6). I chose to use chenodeoxycholic based on preliminary studies from our laboratory and because it is one of the most abundant endogenously synthesized primary bile acids (Bajor, et al., 2010) Chenodeoxycholic acid also causes diarrhea when it reaches the colon (Lee, 2015), which led me to hypothesize that it could activate the inducible colonic pacemaker activity. I chose to use SNP based on preliminary experiments where it evoked low-frequency pacemaker activity in mouse small intestine (unpublished data). Another reason for using SNP is because NO is the main neurotransmitter of nitrergic nerves which have TGR5 receptors, which respond to bile acids (Alemi, et al., 2013; Poole, et al., 2010). Also, in previous studies of dog colon, 0.3-1 μM SNP evoked low-frequency electrical activity (Keef, et al., 2002).

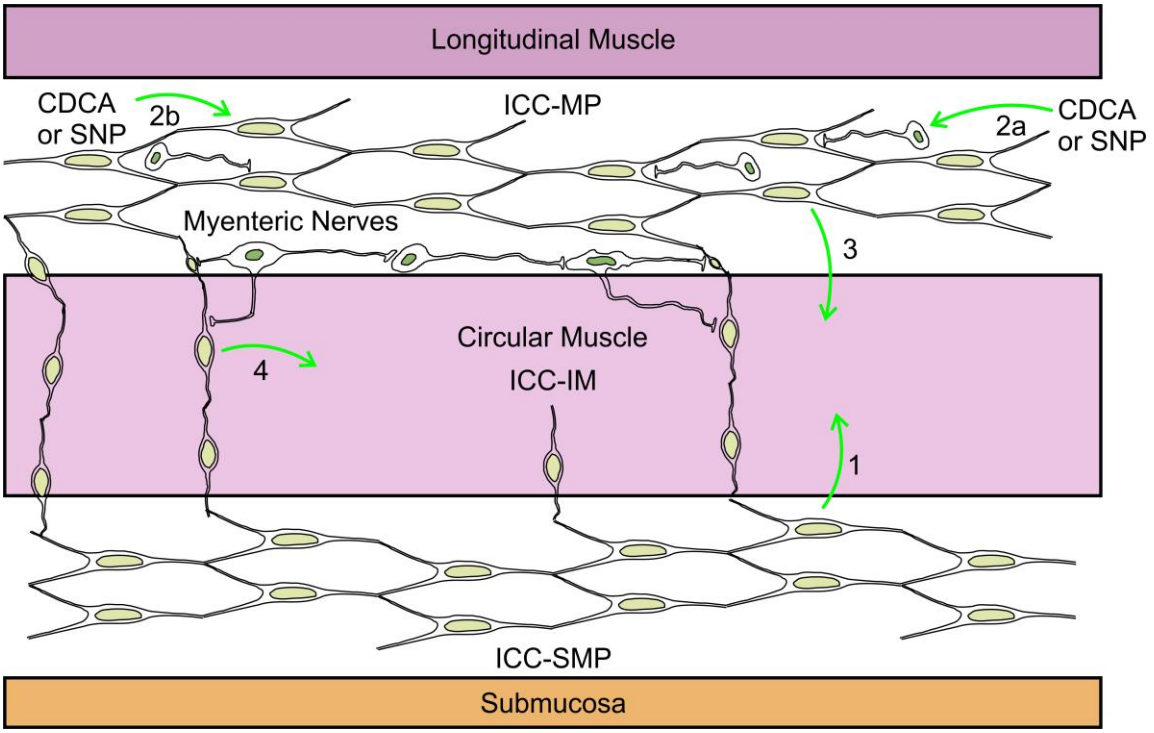

Figure 1.5: Schematic diagram depicting strategies to activate the mouse colon inducible pacemaker (part 1). Gut wall in cross-section showing pacemaker activity sources and possible mechanisms to activate inducible pacemaker activity. The interstitial cells of Cajal associated with the submuscular plexus (ICC-SMP) are the intrinsic pacemakers of the colon and in control conditions slow waves from them should be detectable in smooth muscle intracellular recordings (1). The myenteric plexus contains a highly connected network of nerves arranged in ganglia, with which a network of interstital cells of Cajal is associated (ICC-MP). One possible mechanism underlying activation of the inducible pacemaker may involve activation of myenteric nitrergic nerves (2a) via TGR5 receptors by chenodeoxycholic acid (CDCA) or guanylate cyclase by the NO donor sodium nitroprusside (SNP). Alternatively, CDCA and SNP may act directly on ICC-MP to activate inducible pacemaker activity (2b). It is also possible that intramuscular ICC (ICC-IM) may generate

electrical activity detectable in circular muscle (4). If pacemaker activities from (1) and (3) are present at the same time, it is possible that they could interact by phase amplitude coupling.

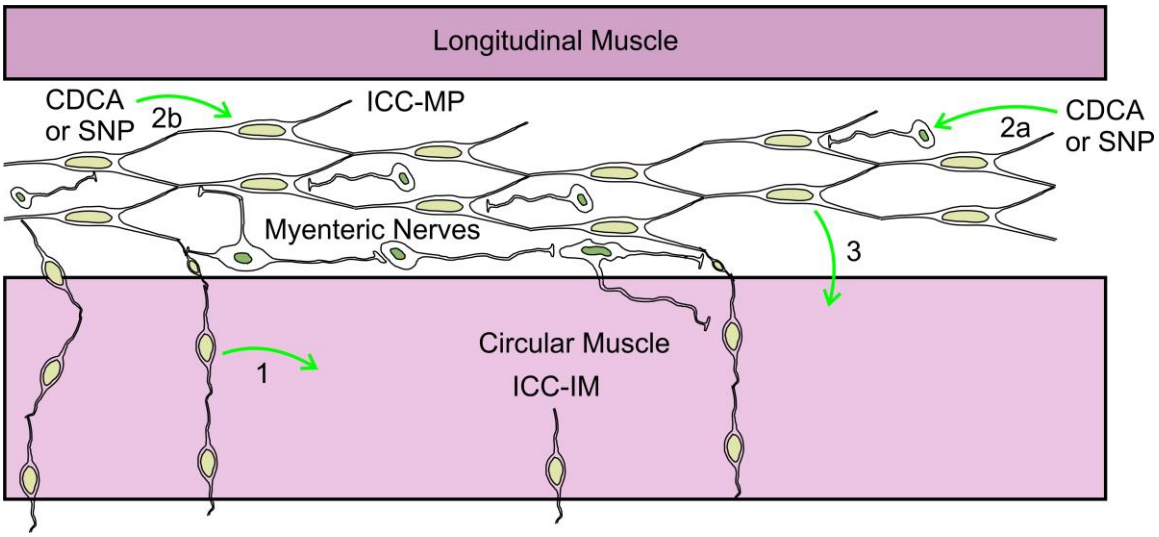

Figure 1.6: Schematic diagram of dissected colonic muscle depicting strategies to activate the mouse colon inducible pacemaker (part 2). Gut wall in cross-section with submucosa and interstitial cells of Cajal associated with the submuscular plexus (ICC-SMP) removed. Thus, we do not expect to see ICC-MP intrinsic slow waves in recordings from these preparations. It is possible that intramuscular ICC (ICC-IM) may generate electrical activity detectable in circular muscle (1). One possible mechanism underlying activation of the inducible pacemaker may involve activation of myenteric nitrergic nerves (2a) via TGR5 receptors by chenodeoxycholic acid (CDCA) or guanylate cyclase by the NO donor sodium nitroprusside (SNP). Alternatively, CDCA and SNP may act directly on ICC-MP to activate inducible pacemaker activity (2b). If pacemaker activities from (1) and (3) are present at the same time, it is possible that they could interact by phase amplitude coupling.

1.7.3 Frequency Component and Phase Amplitude Coupling Analysis

I used continuous wavelet transform (CWT) analysis to dissect the frequency components from membrane potential recordings containing signals suspected to originate from multiple pacemakers. The reason that I chose to use CWT analysis in addition to fast Fourier transform (FFT) analysis is because CWT enables one to determine which frequency components are present over time. In contrast, FFT decomposes the time function of a signal, only showing which frequencies were present and not when they occurred (Fig. 1.7B), or how strong they were at a given timepoint. The analysis program I used was programmed in MATLAB with tab delimited excel files as inputs, containing a column with time in ms and a corresponding column with membrane potentials in mV. The program used the predefined Morlet wavelet function and it divided the continuous time function of the membrane potential recordings into wavelets, decomposing the recording into its component frequencies. These frequencies were then plotted versus time on contour plots (Fig. 1.7C).

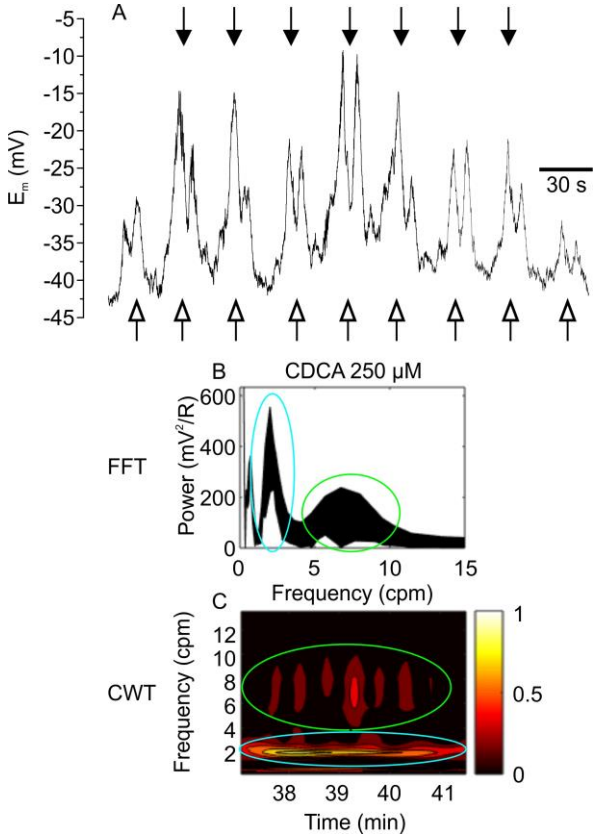

Figure 1.7: Explanation of fast Fourier transform (FFT) and continuous wavelet transform (CWT) analyses. A) Membrane potential recording from mouse colon without submucosa exhibiting rhythmic transient depolarizations evoked by chenodeoxycholic acid (CDCA). A*rrows* indicate occurrence of 8 cpm depolarizing activity, *open arrows* indicate occurrence of rhythmic transient depolarizations. B) FFT analysis revealed the strength of the frequency components present from the membrane potential recording in (A), one at ~2 cpm (*blue circled peak; open arrows in A*) and another at ~8 cpm (*green circled peak; arrows in A*). C) CWT analysis revealed the time course of the frequency components present in (A) and their relative strength as indicated by colour intensity on the contour plot. The recording exhibited a con-

sistent low-frequency (2 cpm; *blue circled band*) and an intermittent 8 cpm activity (*green circled peaks; arrows in A*).

Phase amplitude coupling analysis was used to determine whether two different frequencies from membrane potential recordings were interacting such that the phase of the low-frequency modulated the amplitude of the high frequency, other than by addition. The analysis software I used was an ImageJ plugin with tab delimited text files as inputs, containing membrane potentials in mV. The parameters required for the analysis were stipulating the frequency ranges in which one expected to find the high- and low-frequency components in the membrane potential recordings. Once those ranges were defined, the software filtered out frequencies outside of those ranges and then calculated the phase of the frequency component in the low-frequency range. The amplitude of the high-frequency component was calculated from the membrane potential recording. The phase of the low-frequency and the amplitude of the high-frequency were then plugged into the phase amplitude coupling function to determine if there was an interaction between the two signals.

1.8 Summary of Research Questions and Hypotheses

The research questions for my studies on ICC electrophysiology were the following: how is the maxi Cl^- channel from ICC-MP is activated, how is the cholinergic agonist carbachol able to excite colonic ICC-IM, and how is the colonic inducible pacemaker activated? My hypotheses regarding these questions were the following: the maxi Cl^- channel is activated by increased intracellular Ca^{2+}, carbachol activates maxi Cl^- channels and inhibits K_V7 K^+ channels

from ICC-IM, and the activation of inducible ICC pacemaker activity in the mouse colon, by non-cholinergic (possibly nitrergic) myenteric neurons stimulated by chenodeoxycholic acid, leads to generation of low-frequency rhythmic transient depolarisations. These questions and corresponding hypotheses are addressed in chapters 2, 3 and 4, respectively.

CHAPTER 2: CA^{2+} SENSITIVITY OF THE MAXI CHLORIDE CHANNEL IN INTERSTITIAL CELLS OF CAJAL

2.1 Preface

The body of this chapter was reproduced from a journal article, published in Neurogastroenterology and Motility, of which I am the first author, with permission from the publisher John Wiley and Sons © 2012:

Wright GW, Parsons SP and Huizinga JD (2012) Ca^{2+} sensitivity of the maxi chloride channel from interstitial cells of Cajal. *Neurogastroenterol Motil* **24:** e221-e234. DOI # 10.1111/j.1365-2982.2012.01881.x

As the first author of this paper I planned the study, performed 80% of the patch clamping experiments (119/148) and 75% of the Ca^{2+} imaging experiments (114/153), analyzed all the data, prepared all the figures, wrote the manuscript and edited it during review. Sean Parsons initiated and planned the study, performed 20% of the patch clamping experiments (29/148) and 25% of the Ca^{2+} imaging experiments (39/153), taught me the techniques, and assisted with the analysis. Jan D Huizinga supervised and planned the study, provided the funding, and edited the manuscript during review.

2.2 Paper Full Text

Neurogastroenterology & Motility

Neurogastroenterol Motil (2012) 24, e221-e234 doi: 10.1111/j.1365-2982.2012.01881.x

Ca^{2+} sensitivity of the maxi chloride channel in interstitial cells of Cajal

G. W. J. WRIGHT, S. P. PARSONS & J. D. HUIZINGA
Department of Medicine, Farncombe Family Digestive Health Research Institute, McMaster University, Hamilton, ON, Canada

Abstract

Background *Interstitial cells of Cajal (ICC) associated with the myenteric plexus of the small intestine express maxi chloride channels. Our aim was to investigate whether or not these channels would be activated by increases in intracellular Ca^{2+}, as that would strengthen evidence for their potential role in ICC pacemaking. A further aim was to examine whether inwardly and outwardly rectifying maxi chloride currents signify different channels.* ***Methods*** *We used Fluo-4 AM Ca^{2+} imaging and patch clamp electrophysiology (cell-attached and inside-out) on isolated ICC in short term culture.* ***Key Results*** *Increasing intracellular Ca^{2+} by three functionally distinct mechanisms (blocking sarcoplasmic reticulum Ca^{2+} refilling, creating membrane Ca^{2+} pores and a solution designed to block plasmalemmal Ca^{2+} extrusion) was followed by inwardly rectifying maxi chloride channel activation assessed in the cell-attached configuration. Furthermore, in the inside-out configuration, increased outwardly rectifying maxi-chloride channel activity followed an increase in Ca^{2+} to 2 $mmol^{-1}$ at the cytoplasmic face of the channel.* ***Conclusions & Inferences*** *Increase in intracellular Ca^{2+} will activate the maxi chloride channels. Maxi chloride currents are inwardly rectifying in the cell-attached*

patch clamp configuration under physiological conditions and are outwardly rectifying in the inside-out configuration. The same channel is responsible for both currents. Ca^{2+} does not appear to regulate the rectification.

Address for Correspondence

Jan D. Huizinga, Farncombe Family Digestive Health

Research Institute, McMaster University, HSC 3N46-9, 1280 Main Street West, Hamilton, ON L8S 4K1, Canada. Tel: +1 905-525-9140 x22590; fax: +1 905-522-3454; e-mail: huizinga@mcmaster.ca

Received: 24 October 2011

Accepted for publication: 6 January 2012

Keywords *Ca^{2+} imaging, chloride channel, cyclopiazonic acid, gastrointestinal motility, patch clamp electrophysiology.*

Abbreviations: CPA, cyclopiazonic acid; E_{rev}, reversal potential; HS, HEPES-buffered saline; ICC, interstitial cells of Cajal; Li-NCX, Li^+ and La^{3+} containing NCX blocking solution; NCX, Na^+/Ca^{2+} exchanger; PBS, phosphate-buffered saline; P_o, open probability; PMCA, plasma membrane Ca^{2+} ATPase; SR, sarcoplasmic reticulum; SERCA, sarco/endoplasmic reticulum Ca^{2+} ATPase

INTRODUCTION

Slow waves are rhythmic depolarizations recordable from smooth muscle cells throughout most of the gastrointestinal (GI) tract. They are the basis of certain rhythmic motor activities

of the GI tract. Interstitial cells of Cajal (ICC) are the pacemaker cells from which slow waves originate[1–3] and they pace the musculature into its rhythm. The complete mechanism behind ICC pacemaker activity is still unresolved, but we know that rhythmic intracellular Ca^{2+} transients in ICC occur at the same frequency as the slow wave activity.[4–6] These Ca^{2+} transients likely take part in activating the channels involved in slow wave generation. The objective of this study was to investigate potential Ca^{2+} activation of ICC chloride currents; firstly in the cell-attached patch clamp configuration, with the intracellular machinery intact, and secondly

in the inside-out configuration, with direct access to the cytoplasmic face of the channel. One of the channels likely involved in slow wave generation is the high conductance chloride channel.[7] This chloride channel had oscillatory activity in cell-attached patches similar in frequency to slow wave activity suggesting an association with the slow wave.[7] The Ca^{2+} sensitivity of this channel has been insufficiently explored.

Several papers have appeared on high conductance chloride channels in different patch clamp configurations.[7–11] The type of rectification these channels possess needs clarification. Because both strong outward and strong inward rectification is observed, the question arises whether more than one type of channel is described in these studies. In the first paper,[7] the rectification properties were not emphasized but the figures show an example in the inside-out configuration of outward rectification and another example of a linear current voltage relationship between -60 and +80 mV. In another study on inside-out patches, outward recti-

fication was clearly dominant.[11] In the whole-cell configuration, inwardly rectifying chloride currents were observed that were associated with a high conductance chloride channel, partly because inward rectification was observed in the cell-attached configuration.[10] Our most recent study again showed dominant inward rectification in the cell-attached configuration.[12] A second objective of the present study was to clarify whether differences in rectification properties relate to different channels or to the patch clamp configuration used. We will refer to these channels as maxi chloride channels/currents distinguishing between inward (MCl_{ir}) and outward (MCl_{or}) rectification.

MATERIALS AND METHODS

Cell preparation and culture

Primary cultures of ICC were prepared as described previously.[12] All procedures were carried out in accordance with regulations from the Animal Research Ethics Board (AREB) of McMaster University. Briefly, pieces of small intestine muscle from 5 to 15 day old CD-1 mice (Charles River Laboratories, St-Constant, QC, Canada) were incubated for 15 min at 36°C in HEPES buffered saline (HS) with the addition of 1 mg mL^{-1} type F collagenase, 1 mg mL^{-1} bovine serum albumin, 0.5 mg mL^{-1} papain, 0.5 mg mL^{-1} soybean trypsin inhibitor and 0.2 mg mL^{-1} ())-1,4-Dithio-L-threitol (all from Sigma Aldrich, Oakville, ON, Canada). The muscle was then triturated to give a cell suspension. Cells were settled on collagen-coated cover slips and cultured for 3–4 days before use, using the Clonetics SmGM-2 system (Lomax; supplied by Cedarlane, Burlington, ON, Canada). Cells were identified by their roughly triangular shape with a process at each apex, found in small networks or singly. This

study focuses on maxi chloride channels that have been identified by us in in situ preparations,[9] hence cannot be construed as being present as a consequence of culturing.

Electrophysiology

Two patch-clamp rigs were employed. The first consisted of an Eclipse FN1 microscope (Nikon, Mississauga, ON, Canada), Axon MultiClamp 700B amplifier (Molecular Devices, Sunnyvale, CA, USA), Axon Digidata 1440A, Axon CV-7B headstage and PCS-6000 micromanipulator (Burleigh, Thorlabs Inc., Newton, NJ, USA). The second consisted of a Nikon Diaphot inverted microscope, Axon 200B amplifier, Axon Digidata 1322A, Axon CV-203BU headstage and an MHW-3 micromanipulator (Narishige International Inc., East Meadow, NY, USA). Acquisition software was Clampex (Molecular Devices). Currents were filtered by the amplifier with a 2 kHz cut-off, low-pass, 8-pole Bessel filter and digitized at 5 kHz. Pipettes had resistances of 5–10 MW.

The bath solution was HS, containing (mmol L^{-1}): 135 NaCl, 5 KCl, 10 glucose, 10 HEPES, 2 $CaCl_2$, 1.2 $MgCl_2$. The pipette solution (referred to as NMDG pipette solution from hereon) contained (mmol L^{-1}): 140 N-methyl-D-glucamine chloride, 10 glucose, 10 HEPES.[11] In some experiments the bath solution was changed to 'Li-NCX', a solution containing (mmol L^{-1}): 110 LiCl, 25 $CaCl_2$, 5 KCl, 10 glucose, 10 HEPES, 1 $LaCl_3$. All solutions were adjusted to pH 7.35 with Tris base. NaCl, glucose, HEPES and Tris base were from BioShop Canada Inc., All other chemicals were purchased from Sigma Aldrich (Oakville, ON, Canada). The drugs ionomycin (a Ca^{2+} ionophore that forms channels in the plasma membrane that allow

for the entry of extracellular Ca^{2+} into the cell) and cyclopiazonic acid [a mycotoxin derived from members of the Aspergillus and Penicillium fungal genera and a potent and selective inhibitor of the sarcoplasmic reticulum (SR) Ca^{2+} ATPase (SERCA)] were used to increase intracellular Ca^{2+}. Drugs were prepared by dilution in bath solution to concentrations specified in the results from stock solutions in DMSO.

Voltage protocols were adjusted according to the junction potential between the pipette and bath solutions.[11,12] For experiments in the cell-attached configuration, potentials are expressed as relative to resting membrane potential throughout the study.

Ca^{2+} imaging

Interstitial cells of Cajal was loaded with 5 μmol L^{-1} Fluo-4 AM (Invitrogen Canada Inc.), a fluorescent Ca^{2+} indicator, for 15 min before experiments. Ca^{2+} imaging experiments were performed using the FN1 microscope rig as above, with a QuantEM 512SC camera (Photometrics, Tucson, AZ, USA) and a Lambda DG-4 xenon arc lamp (Sutter Instruments, Novato, CA, USA). Images were acquired with NIS Elements AR 3.0 imaging software (Nikon). All procedures were performed at 22°C in a dark room.

ANO1 staining

Staining protocols were adapted from those described previously.[13] The cells were rinsed three times with phosphate buffered saline (PBS, pH 7.4) to wash away the culture medium, fixed in 4% paraformaldehyde in 0.1 mol L^{-1} phosphate buffer (PB, pH 7.4) at room temperature for 10 min and rinsed three times with PBS again. Non-specific staining was blocked by

incubating the cells with 5% normal goat serum for 1 h at room temperature. The cells were then incubated overnight at 4°C with anti-ANO1 antibody (1: 100; AbCam Inc., Cambridge, MA, USA). On the second day, the cells were washed three times in PBS, and immunoreactivity was detected by incubation for 1 h at room temperature in Cy3-conjugated anti-rabbit IgG (1: 500; Jackson Immuno Research Laboratories Inc., West Grove, PA, USA). For negative controls, cells were treated only with the secondary antibody. All PBS for rinsing and antibody dilution was 0.05 mol L^{-1} PBS with 0.3% Triton-X 100. The cells were washed three times with PBS and cover slips were mounted using anti-fading GEL/MOUNT (Biomeda, Foster City, CA, USA). Reactions were examined with a confocal microscope (Zeiss LSM 510, Germany) with an excitation wavelength appropriate for the Cy3 (595 nm).

Analysis

Currents were evoked using voltage ramp protocols from -80 to +80 mV for 1200 ms every 6 s (Fig. 1B). Current and voltage traces were inverted to account for current direction according to convention. The reversal potential (E_{rev}), absolute conductance and open probability (P_o) of the currents were calculated with the aid of programs written in C++. Current traces were smoothed with a boxcar function seven samples in width. The measured E_{rev} is the potential where the current is 0 pA. The absolute conductance at given voltage (g_E) was $I_E/(E-E_{rev})$. P_o was g_E/g_{max}, where g_{max} was the maximum conductance. Values of g_E 10 mV either side of the E_{rev} were excluded because they are prone to artifacts. Theoretical E_{rev} values were calculated using the Nernst equation based on assumed ICC intracellular [Cl^-] of 10 or 30 mmol L^{-1} and the [Cl^-] in the pipette solution. In current over time plots, the mean cur-

rents during the 200 ms -80 and +80 mV sections of the ramp protocol were calculated for each sweep (every 6 s). The traces in Figs 2, 4, 7 and 8 and Supplementary Fig. S2 represent currents for each experiment and/or the mean values of each corresponding sweep from all experiments. Both the positive and negative traces display one point per sweep.

Initial analysis of Ca^{2+} imaging data was performed as described previously.[6] Further analysis was performed using a program to calculate the normalized fluorescence. Data were smoothed with a boxcar function eleven samples in width. For CPA alone and CPA and Li-NCX experiments data were normalized to the first minute of recording (0–60 s); for ionomycin experiments data were normalized to the 20 samples before ionomycin application. These regions were defined as F0. Each fluorescence measurement was transformed into a percentage of F0 fluorescence. Then the maximum, onset and area above half-maximum (and below the curve) were calculated for the Ca^{2+} transients. The derivatives of fluorescence were calculated from the normalized fluorescence.

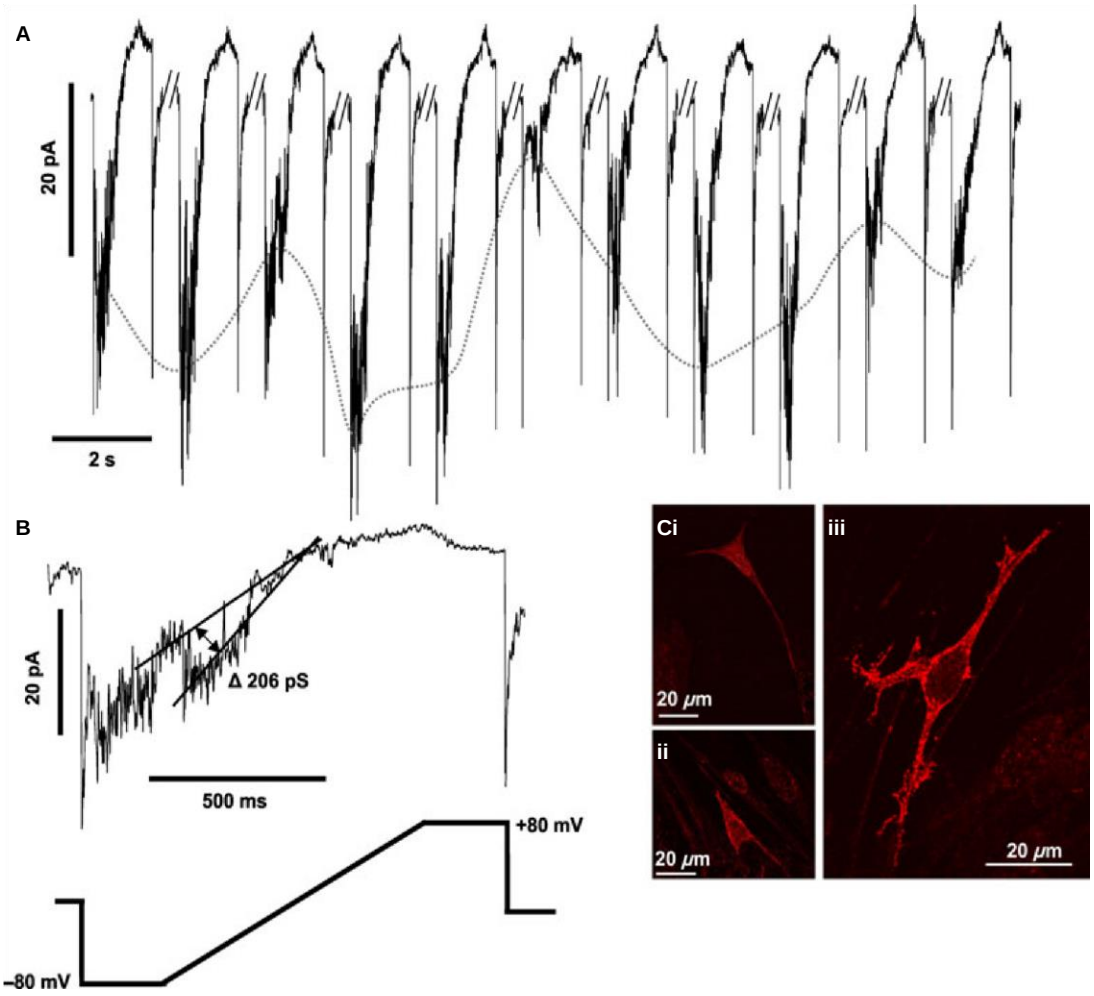

Figure 1 Activity in the absence of protocols that increase intracellular Ca^{2+}. (A) Inwardly rectifying maxi chloride (MCl_{ir}) currents recorded in the cell-attached configuration. No pharmacological agents or strong depolarizing protocols were used to evoke this activity. Break markers exclude 4.5 s segments where voltage was 0 mV; all ramps are sequential. Dotted line indicates rhythmic variation in current magnitude. (B) Enlarged MCl_{ir} currents from A and ramp protocol used to evoke currents. Sloped lines drawn by eye indicate 206 pS conductance, typical of the maxi chloride channel. (Ci–iii) Immunohistochemical staining of

interstitial cells of Cajal using an antibody against ANO1 (red). Interstitial cells of Cajal are typical of those patched in this study.

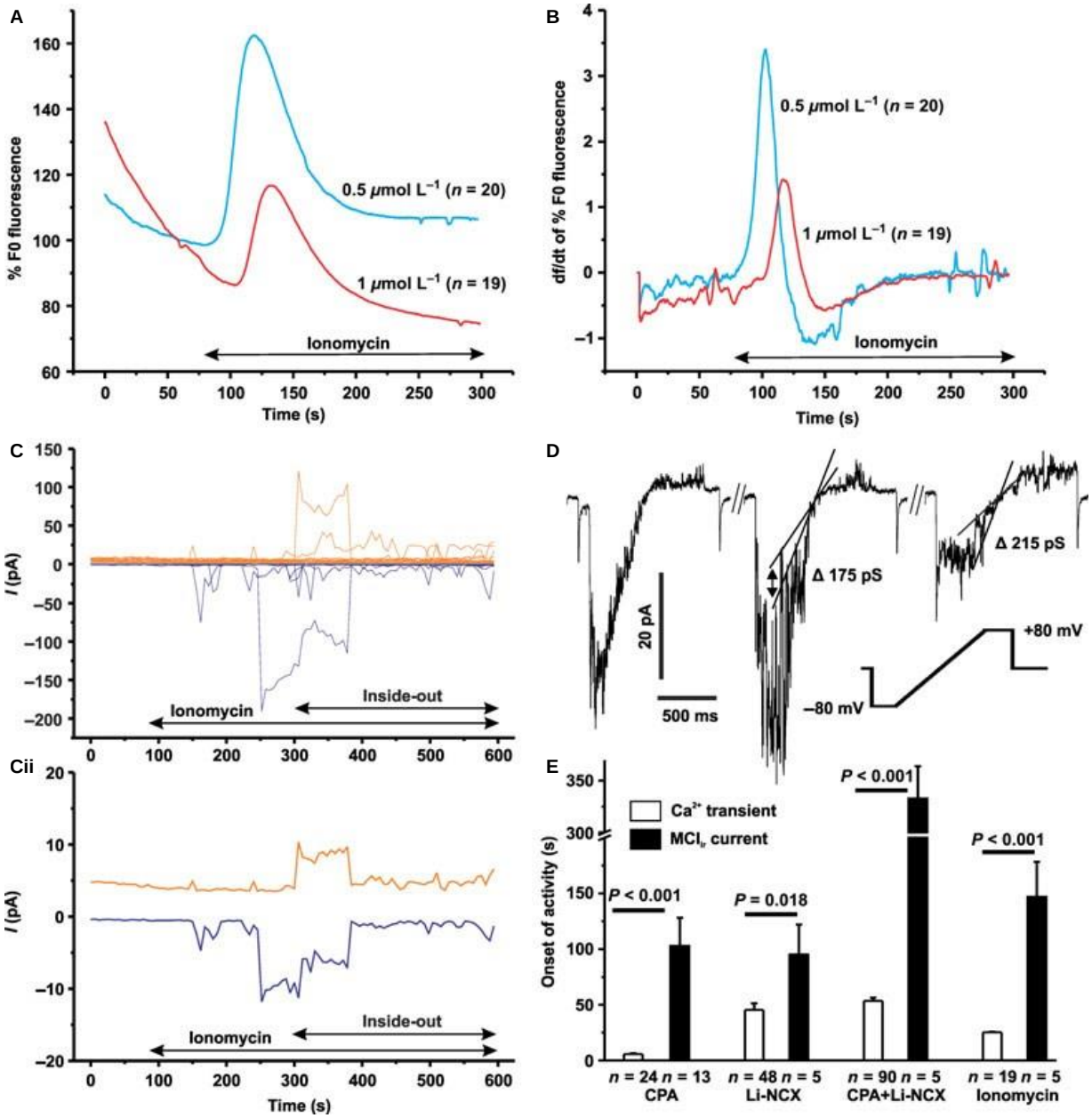

Figure 2 Effects of ionomycin. (A) Effects of ionomycin on Fluo-4 fluorescence over time. (B) Derivatives of Fluo-4 fluorescence in A. (Ci, ii) Ionomycin activated maxi chloride (MCl_{ir}) currents at -80 (dark blue) and +80 mV (orange) portions of the ramp over

time (see Materials and methods). Panels show currents from individual cells (i) and the mean of all cells (ii; $n = 18$). (D) Ionomycin-activated (1 μmol L^{-1}) MCl_{ir} currents. Sloped lines drawn by eye indicate conductance states. Break markers exclude 4.5 s segments where voltage was 0 mV. Inset: ramp protocol used to evoke currents. (E) Comparison of Ca^{2+} transient and MCl_{ir} current onsets.

Half the maximum fluorescence and the full-width at half maximum of the Ca^{2+} transient were calculated to find the area above half maximum (Fig. S2 insets for graphical representation of analysis). Onsets of Ca^{2+} transients and currents were calculated from the beginning of solution/drug perfusion; 20 s was subtracted from each value to account for perfusion system latency.

Statistics and data presentation

Excel was used to calculate two-tailed Student's t-tests. Origin 7.0 graphing software (OriginLab Corporation, Northampton, MA, USA) was used to perform one-way ANOVA when comparing three groups for the same variable. Post hoc Bonferroni corrections were used to determine true differences between means. For both tests $P < 0.05$ was considered significant. Data are expressed as mean ± SEM; n refers to number of cells. Current traces for figures were inverted and filtered in Clampfit with a 200 Hz-cutoff, low-pass, 8-pole Bessel software filter. Figures were created using Origin 7.0 (OriginLab Corporation, Northampton, MA, USA) and Corel Draw X5 (Corel, Ottawa, ON, Canada). Images of ICC from Ca^{2+}

imaging were from slices of the NIS Elements recordings and pseudo-colored with ImageJ software (National Institutes of Health).

RESULTS

Activity in the absence of protocols that increase intracellular Ca^{2+}

Voltage ramps from -80 to +80 mV were applied to cell-attached patches of cultured ICC. $NMDG^+$ was the only cation in the pipette solution, thus any inward currents were carried by Cl^-.[11] 61% of patches (90/148) exhibited transient outward K^+ currents (I_{to}, a voltage-dependent potassium channel).[12] In 6% of patches (9/148), inwardly rectifying maxi chloride (MCl_{ir}) currents, previously termed $I_{flicker}$,[12] were observed within the first 2 min of recording (Fig. 1). However, chloride currents were not present in most ramps. Thus, when the currents were present the ramp voltage change itself was not the only contributor to activation of channel activity. Ramps with activity showed a high degree of variation in current amplitude; the turning off and on of the currents suggested changes in intracellular activity, possibly Ca^{2+}, affecting the chloride currents (Fig. 1A). Inwardly rectifying maxi chloride currents transitioned between conductance states; 211 and 180 pS were dominant (Fig. 1B).[7,11] In these cell-attached experiments the reversal potential (E_{rev}) was 8.2 ± 3.8 mV (n = 5). The calculated E_{rev} is -2.1 mV with assumed $[Cl^-]_i$ = 10 mmol L^{-1} and 25.8 mV with assumed $[Cl^-]_i$ = 30 mmol L^{-1} (T = 22°C and pipette $[Cl^-]_o$ = 140 mmol L^{-1}). Cells identified morphologically as ICC stained positive for ANO1, a selective marker of ICC[13] (Fig. 1C).

Effects of ionomycin

Ionomycin [0.5 (n = 20) and 1 μmol L^{-1} (n = 19)] caused Ca^{2+} transients in all ICC tested (Fig. 2A and B, Fig. S1). Inwardly rectifying maxi chloride currents were activated by 1 μmol L^{-1} ionomycin in 5/18 patches while cell-attached (Fig. 2C and D). Channel activity after patch excision was observed in 7/18 of the patches, including three experiments where maxi chloride currents were not activated by ionomycin in the cell-attached configuration. Inwardly rectifying maxi chloride currents, activated cell-attached, transitioned to MCl_{or} once inside-out. The onset of Ca^{2+} transients caused by 1 μmol L^{-1} ionomycin was significantly sooner than the onset of currents activated by ionomycin (Fig. 2E).

Effects of CPA

Cyclopiazonic acid (CPA; 10 μmol L^{-1}) caused Ca^{2+} transients in an ICC network (Fig. 3A). Note that once Ca^{2+} transients reached their maximum they decreased before washout of CPA. Cyclopiazonic acid caused Ca^{2+} transients in all ICC tested (n = 24 cells; Fig. 3B). The derivative of Fluo-4 fluorescence shows that the rate of change increased dramatically after CPA was applied and decreased before CPA was washed out (Fig. 3C). The maximum, full-width at half-maximum, area above half maximum of Ca^{2+} transients caused by CPA were significantly larger than those of Ca^{2+} transients caused by 1 mol L^{-1} ionomycin (Supplementary Fig. S1A and B).

Inwardly rectifying maxi chloride currents were activated by CPA (10 μmol L^{-1}) in 13/36 patches with control conditions exhibiting only I_{to} (Fig. 4A and B). The MCl_{ir} currents had

large conductance states (Fig. 4B–D) characteristic of maxi chloride currents.[7,11] Dominant conductances were 211 and 180 pS. Current activation occurred after 15 s in some experiments but in others a substantial amount of time elapsed before channel activity was seen (Figs 4Ei and 2E). Inward currents remained active when a 1.5 s hyperpolarizing voltage step followed different depolarizing steps (Fig. 4F, $n = 10$) indicating no time-dependent inactivation. The relationship between current and voltage as well as open probability (P_o) and voltage for CPA activated MCl_{ir} currents ($n = 13$) are shown in Fig. 5. The P_o was highest at -80 mV and decreased to its minimum at +80 mV (Fig. 5A) and the I/V plot displays inward rectification (Fig. 5B). The E_{rev} for CPA activated MCl_{ir} currents was 12.7 ± 2.5 mV ($n = 8$). The onset of Ca^{2+} transients caused by CPA was significantly sooner than the onset of MCl_{ir} currents activated by CPA (Fig. 2E).

Effects of Li-NCX and CPA

To investigate if sustained intracellular Ca^{2+} transients would cause sustained activity of chloride channels, Li-NCX solution (see Materials and methods) was introduced. Li-NCX has low Na^+ and high Ca^{2+} and is predicted to prevent Ca^{2+} extrusion by the plasmalemmal Na^+/Ca^{2+} exchanger (NCX).[14] It also has La^{3+} that blocks Ca^{2+} extrusion by the P-type ATPases (which include SERCA and the plasma membrane Ca^{2+} ATPase or PMCA).[15] Using Fluo-4 Ca^{2+} imaging with Li-NCX applied at 0 s, 10 μmol L^{-1} CPA applied at 240 s caused Ca^{2+} transients in ICC networks (Fig. 6). Ca^{2+} remained elevated in 39/90 cells after the peak of the CPA induced transients (Fig. 6B), in contrast to CPA alone (Fig. 3B). The derivative of Fluo-4 fluorescence shows that the rate of change increased dramatically after

CPA was applied and decreased when CPA and Li-NCX were washed out (Fig. 6C). Before the application of CPA, Li-NCX caused Ca^{2+} transients in half of the ICC (48/90, Fig. 6B and D). Ca^{2+} transients caused by CPA in Li-NCX were significantly larger than those caused by CPA alone (Fig. S1B and C).

Li-NCX activated MCl_{ir} currents in 5/26 patches, with control conditions only showing I_{to} (Fig. 7A and B).

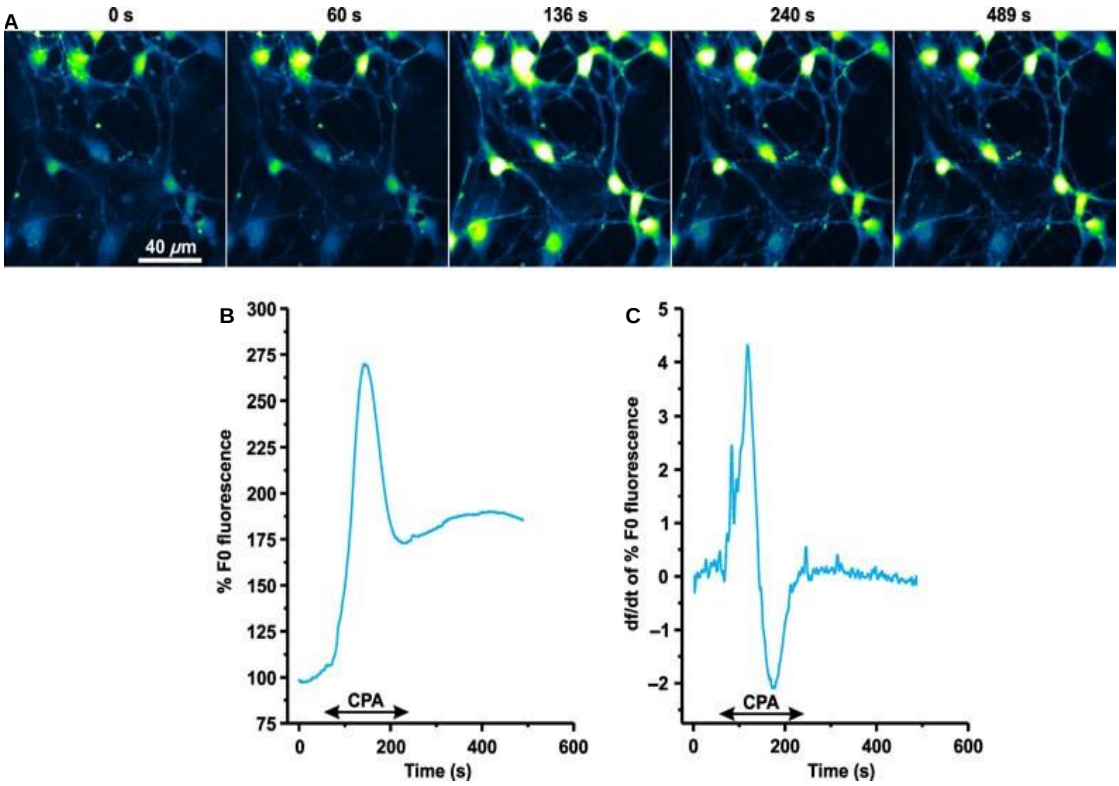

Figure 3 Effect of cyclopiazonic acid (CPA): Ca^{2+} transients. (A) Fluo-4 fluorescence intensity images of a network of ICC illustrating Ca^{2+} transients caused by CPA (10 μmol L^{-1}, applied at 60 s) at time points indicated. Blue/dark coloration represents areas of low fluores-

cence while white/light coloration represents high fluorescence. (B) Average effect of CPA on Fluo-4 fluorescence over time (n = 24). Note the rapid onset of Ca^{2+} transients caused by CPA. (C) Derivative of Fluo-4 fluorescence from B.

Cyclopiazonic acid enhanced MCl_{ir} currents in the presence of Li-NCX and evoked MCl_{ir} currents in an additional 5/26 patches where there was no activation by Li-NCX alone (Fig. 7C). Ramps again show several channels with conductance states typical of MCl_{or} channels (Fig. 7D). Inwardly rectifying maxi chloride currents activated by CPA in Li-NCX were larger in magnitude than those activated by Li-NCX alone (Fig. 7E). When CPA and Li-NCX were washed out, channel activity continued at the increased level or continued to increase (Fig. 7E). The E_{rev} of currents after CPA was applied was 4.2 ± 2.5 mV (n = 10). The onsets of Ca^{2+} transients caused by either Li-NCX or CPA were significantly sooner than the onsets of MCl_{ir} currents activated by Li-NCX or CPA (Fig. 2E).

Effect of La^{3+}

We investigated if La^{3+}, a component of Li-NCX, could activate MCl_{ir} currents. La^{3+} (1 mmol L^{-1}) activated MCl_{ir} currents (Fig. S2A) in 4/15 ICC. P_o decreased as potentials increased similar to the other treatments (Fig. S2B). The I/V relationship shows inward rectification similar to those recorded in the cell-attached configuration with other treatments (Fig. S2C). The magnitude of inward and outward currents activated by La^{3+} is shown in Fig. S2Di,ii (compared with Fig. 7D). The E_{rev} of La^{3+} activated MCl_{ir} currents was -1.0 ± 5.6 mV (n = 4).

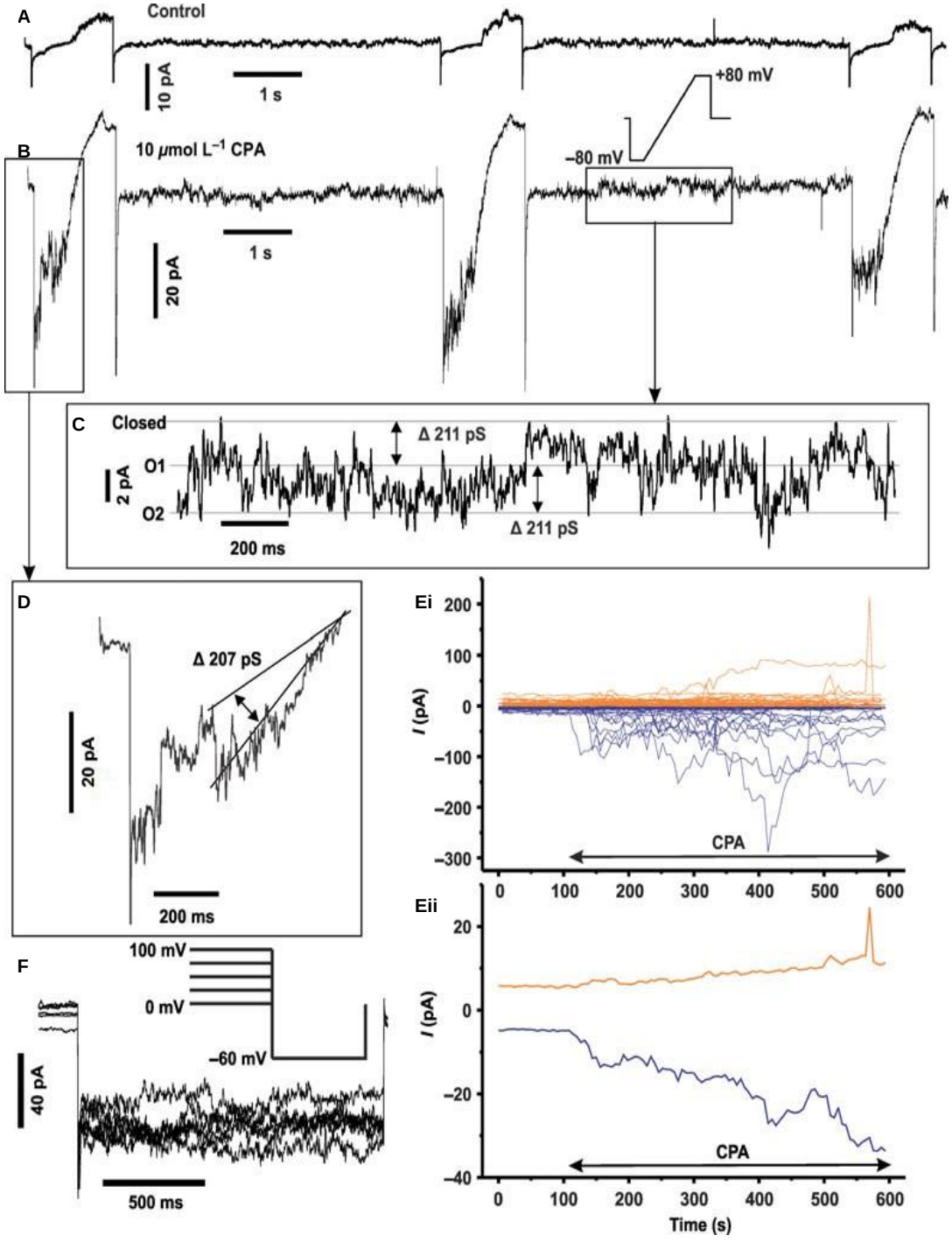

Figure 4 Effect of cyclopiazonic acid (CPA): maxi chloride currents. Currents in A and B were recorded from the same cell. (A) Control conditions show transient outward K^+ cur-

rents (I_{to}). Inset: ramp protocol used to evoke the currents. (B) CPA activated inwardly rectifying maxi chloride (MCl_{ir}) currents. (C) Enlarged MCl_{ir} currents from B recorded at 0 mV. Note conductance states at O1 and O2 as well as sub-conductance states between them. (D) Enlarged MCl_{ir} currents from B. Sloped lines drawn by eye indicate conductance state. (Ei and ii) CPA activated MCl_{ir} currents at both -80 (blue) and +80 mV (orange) portions of the ramp over time (see Materials and methods). Panels show currents from individual cells (i) and the mean of all cells (ii; n = 36). Note the inward rectification. (F) CPA activated MCl_{ir} currents, which did not turn off during the hyperpolarizing voltage steps. Inset: voltage steps used to evoke currents.

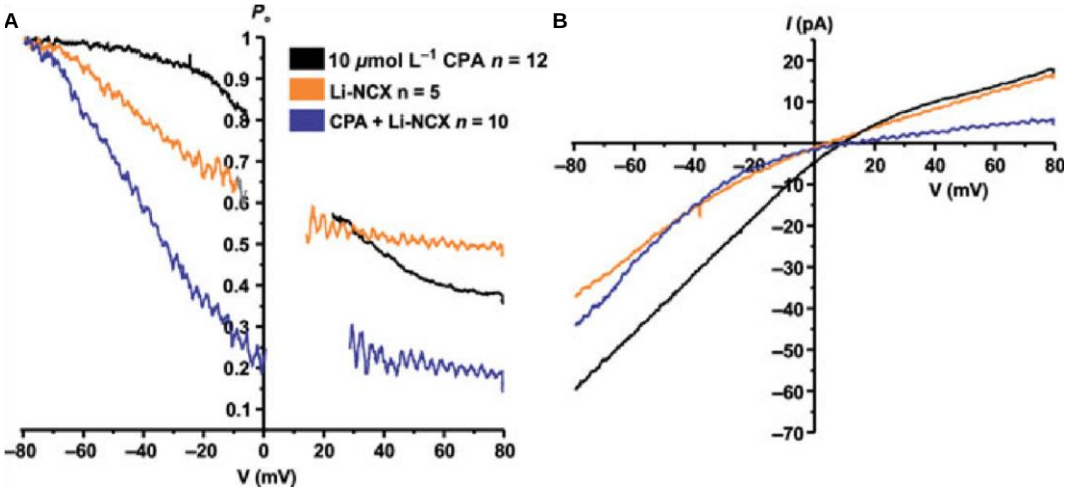

Figure 5 Maxi chloride current open probability and current/voltage relationship. (A) Open probability (P_o) vs voltage from a -80 to +80 mV voltage ramp. Values within 10 mV of the E_{rev} of each treatment were removed (see Materials and methods). (B) Current–voltage relationship for MCl_{ir} currents from -80 to +80 mV voltage ramp. Note that currents from all treatments were inwardly rectifying. Key in A also applies to B.

Rectification of maxi chloride currents in the cell-attached vs inside out configuration

As shown above, all of the CPA induced maxi chloride currents in the cell-attached configuration were inwardly rectifying. In another set of experiments cell-attached patches exposed to CPA, in which MCl_{ir} currents were activated (14/26), were subsequently excised into the inside-out configuration. Currents became either outward rectifying (n = 4, Fig. 8A), linear (6/26) or turned off (4/26). The currents had sharp transitions as different channels or sub-conductance states opened and closed (Fig. 8A). There is a marked difference in rectification between currents recorded in the cell-attached and inside-out configurations (Fig. 8B and C), indicating that a single channel type shows different rectification properties, dependent on the patch configuration (see Discussion).

Effect of Ca^{2+} on maxi chloride currents in the inside out configuration

Outwardly rectifying maxi chloride currents were present in 6/18 in inside-out patches. These include experiments where MCl_{or} was activated by excision or when there was activity prior to excision that continued afterwards. Low Ca^{2+} HS is HS without added Ca^{2+} or Mg^{2+}, but Ca^{2+} content of water and Ca^{2+} contamination in other salts used may add up to 10 μmol L^{-1} Ca^{2+}.[16] When the inside of the patch was subsequently exposed to 2 mmol L^{-1} Ca^{2+}, the MCl_{or} current magnitude at +80 mV increased 2.9 ± 0.6 times and at -80 mV increased 1.7 ± 0.5 times (n = 6, Fig. 8D). Outwardly rectifying maxi chloride currents increased in magnitude and were active in more sweeps when 2 mmol L^{-1} Ca^{2+} containing HS was applied (Fig. 8E). In 2/18 patches where no channel activity was present, exposure to 2 mmol L^{-1} Ca^{2+} evoked MCl_{or} activity.

DISCUSSION

The present data show that activation of the maxi chloride channel follows a Ca^{2+} transient in ICC associated with the myenteric plexus of the small intestine (ICC-MP). We have shown that, in the cell attached configuration with the inside of the channel in a physiological intracellular environment, a Ca^{2+} ionophore (ionomycin), inhibition of the sarco/endoplasmic reticulum Ca^{2+} ATPase (SERCA) by CPA, blockade of the Na^{+}/Ca^{2+} exchanger (NCX) and the plasma membrane Ca^{2+} ATPase (PMCA), and CPA in the presence of NCX and PMCA blockade, all cause Ca^{2+} transients followed by chloride channel activation.

Our data are consistent with (but do not prove) the hypothesis that the fluctuating current amplitude seen when MCl_{ir} currents are recorded in the cell-attached configuration without manipulation to increase intracellular calcium, is due to fluctuations in intracellular Ca^{2+}. The fact that the fluctuating activity is lost when Ca^{2+} levels are sustained in the presence of CPA is in line with the hypothesis.

The activation of the maxi chloride channels may be due to direct interaction between Ca^{2+} ions and the channel because Ca^{2+} activated MCl_{or} currents without delay in the inside-out patch configuration. In the cell-attached configuration, in some experiments, channel activation was rapid, with CPA alone as well as with Li-NCX. The delay between Ca^{2+} transients and channel activation seen in other experiments (although not measured in the same cells) may be due to delay in Ca^{2+} reaching the channels in the patch.

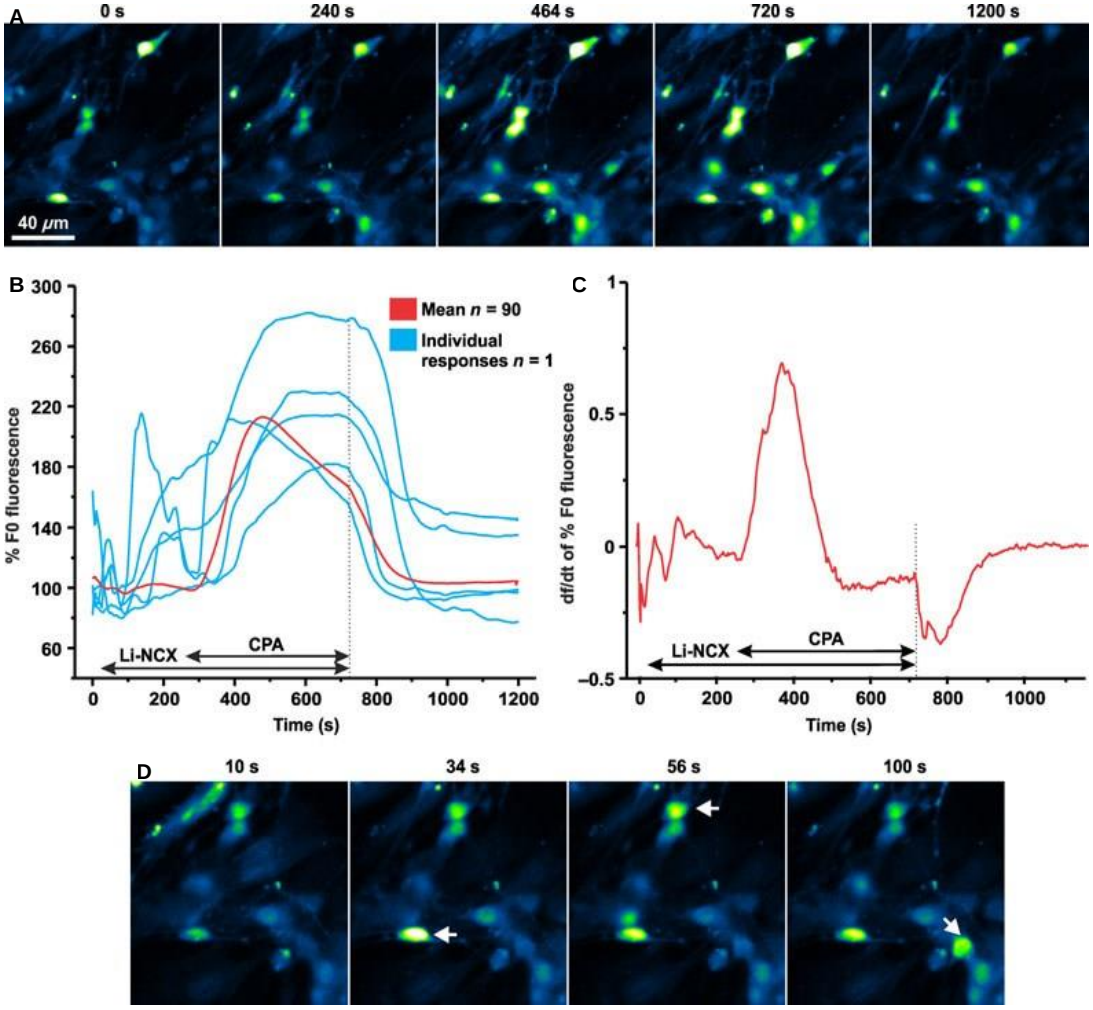

Figure 6 Effect of Li-NCX and cyclopiazonic acid (CPA): Ca^{2+} transients. (A) Fluo-4 fluorescence intensity images of a cluster of ICC illustrating Ca^{2+} transients caused by CPA (10 μmol L^{-1}, applied at 240 s) in the presence of Li-NCX at time points indicated. Blue/dark coloration represents areas of low fluorescence while white/light coloration represents high fluorescence. (B) Effect of CPA and Li-NCX on Fluo-4 fluorescence over time. Blue traces represent individual cells in which Li-NCX caused Ca^{2+} transients prior to those caused by CPA. Acquisition frequency was 0.5 Hz. (C) Derivative of Fluo-4 fluorescence from average value in B. (D) Fluo-4 fluorescence intensity images of ICC illustrating Ca^{2+} transients caused

by Li-NCX (applied at 20 s) at time points indicated. Colouration and scale are the same as A; white arrows indicate cells at highest fluorescence in sequence of four images.

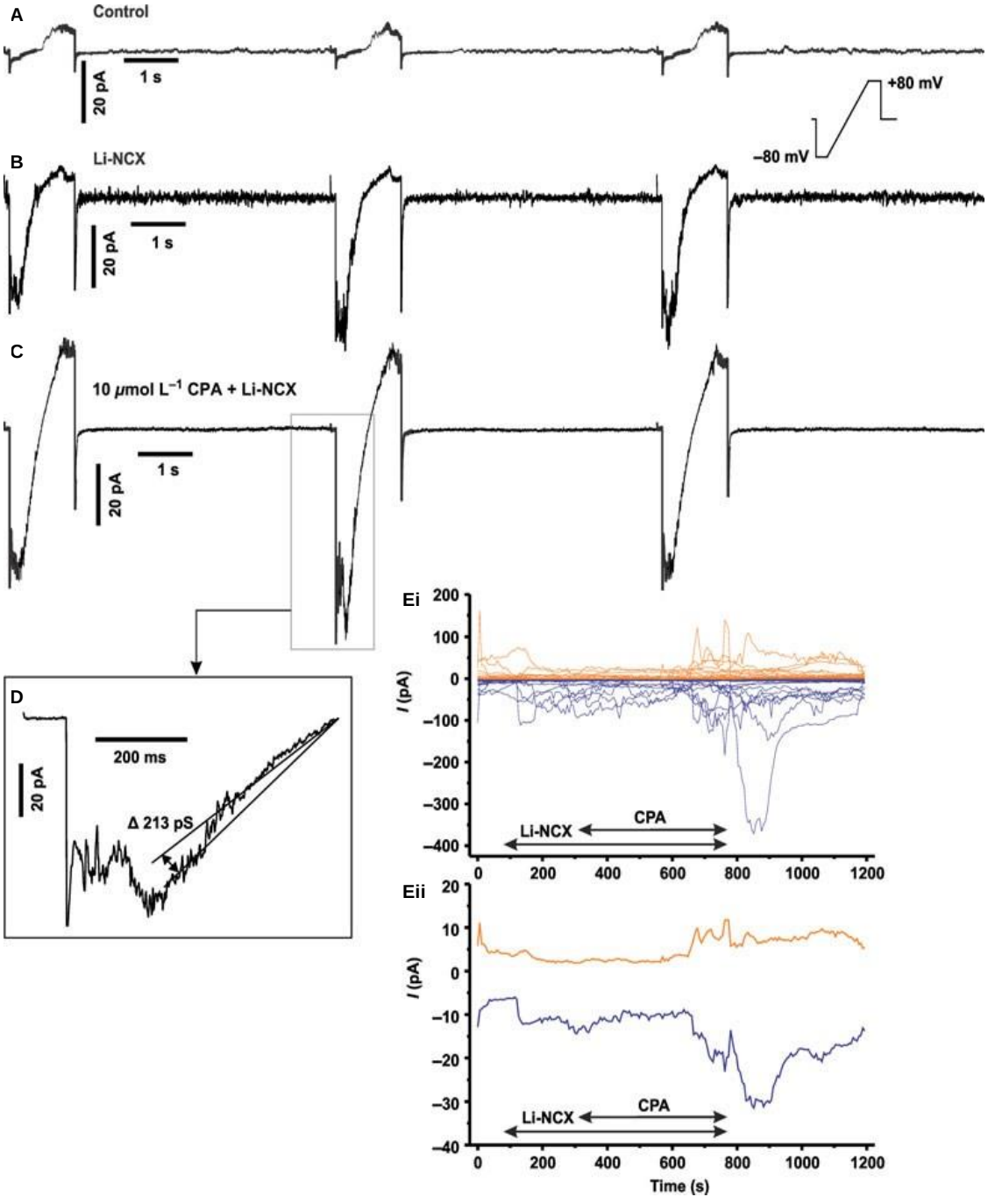

Figure 7 Effect of Li-NCX and cyclopiazonic acid (CPA): maxi chloride currents. (A) Control conditions show transient outward K^+ currents (I_{to}) (compare with Fig. 4A). Inset: ramp protocol used to evoke currents. (B) Li-NCX activated inwardly rectifying maxi chloride

(MCl_{ir}) currents. (C) CPA and Li-NCX activated MCl_{ir} currents (compare with Fig. 4B). Traces A and C were obtained from the same cell. (D) Enlarged MCl_{ir} currents from C. Sloped lines drawn by eye indicate conductance state. (Ei and ii) Li-NCX and CPA both activated MCl_{ir} currents at both -80 (blue) and +80 mV (orange) portions of the ramp over time. Panels show currents from individual cells (i) and the mean of all cells (ii; n = 26). These traces represent experiments where currents were activated either by Li-NCX or by both CPA and Li-NCX.

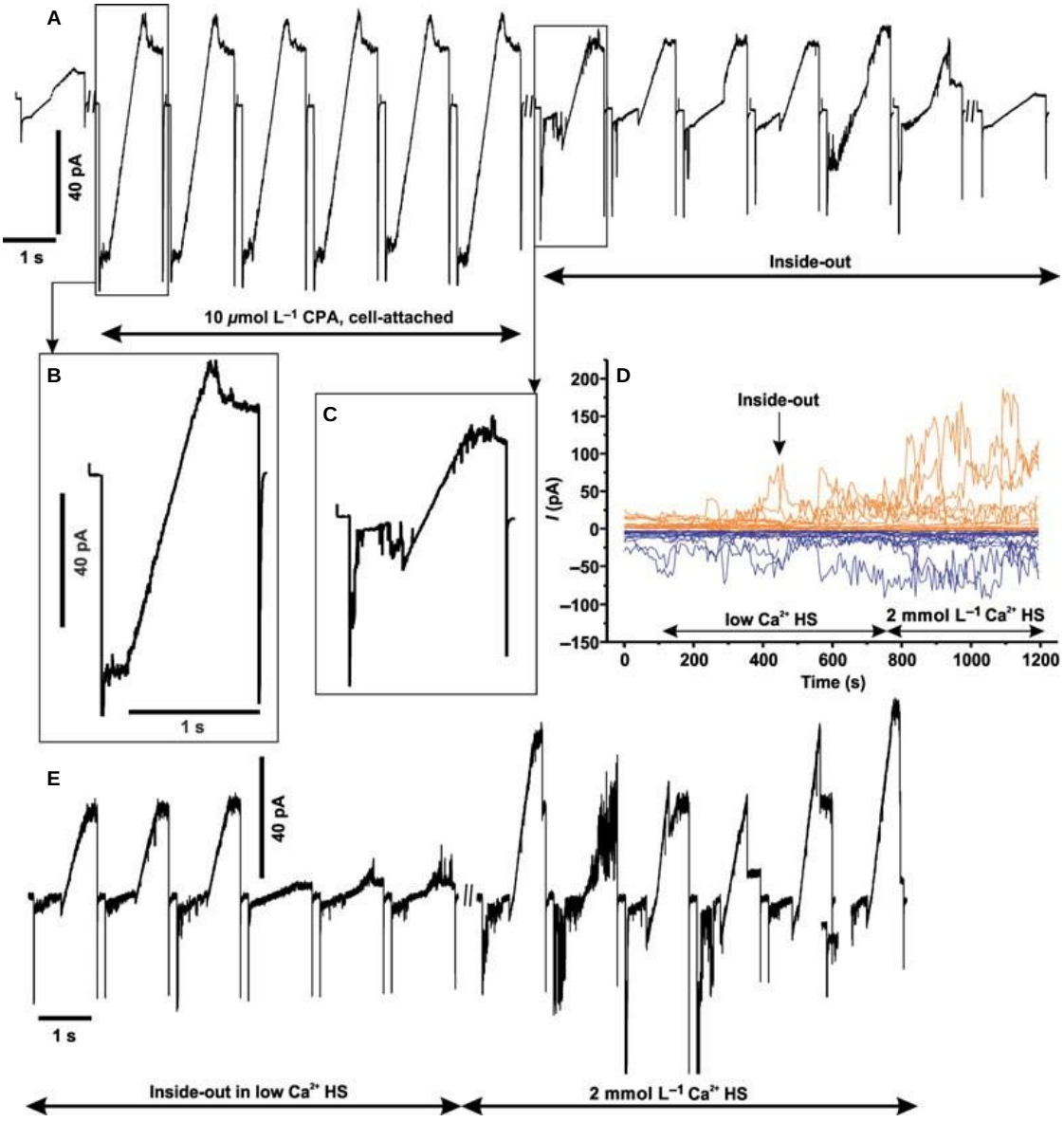

Figure 8 Maxi chloride current rectification and effect of Ca^{2+} while inside-out. (A) Cyclopiazonic acid activated inwardly rectifying maxi chloride (MCl_{ir}) currents while cell-attached with an onset of 16 s. Currents became outwardly rectifying with distinct sharp We hypothesize that maxi chloride channels are situated between the sarcoplasmic reticulum (SR) and the plasma membrane as they are activated by SR Ca^{2+} release. Hence, the chloride channels will

be associated channel transitions after patches were excised into the inside-out configuration. The first and last ramps show background currents while cell-attached and inside-out, respectively. The 4.8 s segments where voltage was 0 mV were removed. (B) Enlarged MCl_{ir} current from A. (C) Enlarged outwardly rectifying maxi chloride (MCl_{or}) current from A. Scale bars in B also apply to C. (D) Maxi chloride current magnitude increased on application of 2 mmol L^{-1} Ca^{2+}. Traces show both currents at -80 (blue) and +80 mV (orange) portions of the ramp over time (see Materials and methods). (E) MCl_{or} current magnitude increased after 2 mmol L^{-1} Ca^{2+} was applied to inside-out patches. The 4.8 s segments where voltage was 0 mV were removed.

We hypothesize that maxi chloride channels are situated between the sarcoplasmic reticulum (SR) and the plasma membrane as they are activated by SR Ca^{2+} release. Hence, the chloride channels will be associated with the superficial buffer barrier,[17] and access from the general cytoplasmic compartment may be restricted, which explains differences in channel activation times observed in this study.

The brevity of MCl_{ir} activity in ionomycin experiments may relate to the brevity of the Ca^{2+} transients in corresponding experiments. Compared with CPA and CPA + Li-NCX, Ca^{2+} transients caused by ionomycin were smaller in magnitude, duration and area above half maximum. Another explanation of the weak channel activation by ionomycin is that the pipette access to Ca^{2+} from ionomycin may be different to pipette access of Ca^{2+} from another source such as blocked intracellular stores. Ca^{2+} entering through an ionomycin pore may

have restricted access to the inside of the patch as well as the cytosolic face of the channel (possibly because of the buffer barrier). It is possible that maxi chloride channels are store-operated similar to TRP Ca^{2+} channels.[18] This hypothesis is consistent with the fact that Li-NCX and CPA both interfere with store fill status but ionomycin does not. In this study we identified all patches where a good seal was maintained and the baseline noise level was less than 0.8 rms. In 76/139 patches, no maxi chloride channel activity was observed under conditions of increased intracellular calcium. We assume that no channels were present in these patches indicating that one has a 50% chance of getting maxi chloride channels in a patch. When no channel activity was observed we cannot exclude that channels refractory to Ca^{2+} were present.

In the present study we show that exposing ICC to Li-NCX solution, that blocks the Na^+/Ca^{2+} exchanger, causes a Ca^{2+} transient and activation of chloride currents. This suggests that the NCX is important in ICC Ca^{2+} homeostasis. Indeed, we observed that the ICC plasma membrane is rich in the NCX protein and that inhibition of the exchanger in reverse mode abolished rhythmic Ca^{2+} transients in situ.[6] The Li-NCX solution also blocks the PMCA, which will contribute to the observed increase in intracellular Ca^{2+}.[15]

Although examining inactivation or deactivation properties of the channel was not an objective of the present study, a number of observations are worth noting. MCl_{ir} currents do not often turn off in the presence of CPA, even though high Ca^{2+} is not sustained under these conditions. Also, washing out CPA and Li-NCX does not turn off MCl_{ir} currents. Hence,

there does not appear to be a simple linear relationship between level of Ca^{2+} and activation/deactivation of the channel. This study shows that maxi chloride currents were predominantly inwardly rectifying in the cell-attached configuration whereas this became predominantly outwardly rectifying in the inside-out configuration. Published studies on the maxi chloride channel have shown either inward rectification or outward rectification, usually associated with a specific patch clamp configuration (see Introduction). A possible explanation is that when the inside-out configuration is formed, a cytoplasmic component is lost that caused inward rectification in the cell-attached configuration.

It is also possible that changing the ionic gradients affects the rectification. The present study gives no reason to assume that outward and inward rectification suggests different channels. It may be similar in principle to the cardiac myocyte inwardly rectifying K^+ channels; its rectification is influenced by changes in internal or external K^+, by removal of intracellular Mg^{2+} and can be switched on and off by physiological changes in intracellular Ca^{2+}.[19] The precise regulatory mechanisms of the maxi chloride channel rectification are yet to be investigated, but the present study suggests that it is not Ca^{2+} as rectification properties in both configurations did not change when marked changes in Ca^{2+} at the inside of the channel were introduced.

Changing the exposure of inside-out patches from 10 μmol L^{-1} to 2 mmol L^{-1} Ca^{2+} activated the MCl_{or} channels markedly. Interestingly, in a previous study, changing the exposure from <10 to 100 nmol L^{-1} or 2 μmol L^{-1} did not increase MCl_{or} current magnitude.[11] Hence it ap-

pears that the concentration needed to activate the current is in the millimolar range. This may in part explain the delay in channel activation in the cell-attached configuration because of the time to reach critical [Ca^{2+}] at the mouth of the channel. A high concentration is quickly achieved in the space between SR and plasma membrane under physiological conditions of SR Ca^{2+} extrusion.[17]

The precise role of chloride channels in slow wave generation is not resolved (see Introduction). One view holds that an initial depolarization (primary component) is generated by voltage-dependent ion channels acting either as pacemakers or in response to depolarization by a propagating slow wave. Some of these voltage-dependent channels pass Ca^{2+}, which then causes further Ca^{2+} release from the ICC's SR which in turn would trigger Ca^{2+}-activated chloride channels. This results in a secondary, plateau depolarization.[20] Another view is that the initial slow wave depolarization is caused by Ca^{2+}-activated channels (including chloride channels) activated by rhythmic Ca^{2+} release from the SR without the need for voltage dependent Ca^{2+} entry.[6] This Ca^{2+} could activate channels that take part in the initial phase of depolarization as well as the plateau potential. One pacemaker channel candidate in ICC is the protein ANO1[13,21] which gives a Ca^{2+} activated chloride current when expressed in several cells.[22] Possibly associated with ANO1 was a voltage dependent chloride current recorded from freshly isolated ICC by whole cell patch clamping, which was dependent on extracellular Ca^{2+}.[23] Another pacemaker channel candidate, the focus of this study, is the high conductance (or maxi-) chloride channel.[7] This chloride channel has oscillatory activity in cell-attached patches similar in frequency to slow wave activity suggesting an association with the

slow wave.[7] The present study strengthens the evidence that the maxi chloride channel is activated in ICC by Ca^{2+} transients.

The following schema is consistent with the current data and data observed in previous experiments. Inwardly rectifying maxi chloride channels are activated by Ca^{2+} release from the SR in the narrow space between SR and plasma membrane. The channel has little activity in very low Ca^{2+} [11] and is activated by exposure to Ca^{2+} in the millimolar range. It does not necessarily inactivate when Ca^{2+} is washed out. All this obviously does not exclude other factors that might influence chloride channel opening and closing. Our data are consistent with calcium activating the channel directly, however it cannot be excluded that an intermediary step is involved.

ACKNOWLEDGMENTS

We would like to thank Dr. Xuan-Yu Wang for performing the ANO1 staining.

FUNDING

This study was supported by the Canadian Institutes of Health Research (MOP-12874 to JH) and NSERC (#386877 to JH). Most of this work was conducted during co-op work terms and as a senior thesis project by GW as part of his studies in the Honours Biology Pharmacology program for which he received the Jensen Medal. GW was supported in part by a scholarship from the Farncombe Family Digestive Health Research Institute.

DISCLOSURE

The authors have no competing interests.

AUTHOR CONTRIBUTION

SP initiated the study by performing the ionomycin experiments and starting the CPA experiments; SP and GW performed CPA Ca^{2+} imaging studies; GW continued with the CPA experiments, executed all other experiments and analyzed the data; GW, SP and JH collaborated on study design, protocol design, and manuscript preparation.

REFERENCES

1 Huizinga JD, Thuneberg L, Kluppel M, Malysz J, Mikkelsen HB, Bernstein A. W/kit gene required for interstitial cells of Cajal and for intestinal pacemaker activity. Nature 1995; 373: 347–9.
2 Thomsen L, Robinson TL, Lee JC et al. Interstitial cells of Cajal generate a rhythmic pacemaker current. Nat Med 1998; 4: 848–51.
3 Koh SD, Sanders KM, Ward SM. Spontaneous electrical rhythmicity in cultured interstitial cells of cajal from the murine small intestine. J Physiol 1998; 513: 203–13.
4 Torihashi S, Fujimoto T, Trost C, Nakayama S. Calcium oscillation linked to pacemaking of interstitial cells of Cajal: requirement of calcium influx and localization of TRP4 in caveolae. J Biol Chem 2002; 277: 19191–7.
5 Lee HT, Hennig GW, Fleming NW et al. The mechanism and spread of pacemaker activity through myenteric interstitial cells of Cajal in human small intestine. Gastroenterology 2007; 132: 1852–65.
6 Lowie BJ, Wang XY, White EJ, Huizinga JD. On the origin of rhythmic calcium transients in the ICC-MP of the mouse small intestine. Am J Physiol Gastrointest Liver Physiol 2011; 301: G835–45.
7 Huizinga JD, Zhu Y, Ye J, Molleman A. High-conductance chloride channels generate pacemaker currents in interstitial cells of Cajal. Gastroenterology 2002; 123: 1627–36.
8 Park SJ, McKay CM, Zhu Y, Huizinga JD. Volume-activated chloride currents in interstitial cells of Cajal. Am J Physiol Gastrointest Liver Physiol 2005; 289: G791–7.
9 Wang B, Kunze WA, Zhu Y, Huizinga JD. In situ recording from gut pacemaker cells. Pflugers Arch 2008; 457: 243–51.
10 Zhu Y, Mucci A, Huizinga JD. Inwardly rectifying chloride channel activity in intestinal pacemaker cells. Am J Physiol Gastrointest Liver Physiol 2005; 288: G809–21.

11 Parsons SP, Sanders KM. An outwardly rectifying and deactivating chloride channel expressed by interstitial cells of cajal from the murine small intestine. J Membr Biol 2008; 221: 123–32.
12 Parsons SP, Huizinga JD. Transient outward potassium current in ICC. Am J Physiol Gastrointest Liver Physiol 2010; 298: G456–66.
13 Gomez-Pinilla PJ, Gibbons SJ, Bardsley MR et al. Ano1 is a selective marker of interstitial cells of Cajal in the human and mouse gastrointestinal tract. Am J Physiol Gastrointest Liver Physiol 2009; 296: G1370–81.
14 Shimizu H, Borin ML, Blaustein MP. Use of La3+ to distinguish activity of the plasmalemmal Ca2+ pump from Na+/Ca2+ exchange in arterial myocytes. Cell Calcium 1997; 21: 31– 41.
15 Brini M, Carafoli E. Calcium pumps in health and disease. Physiol Rev 2009; 89: 1341–78.
16 Bers DM, Patton CW, Nuccitelli R. A practical guide to the preparation of Ca(2+) buffers. Methods Cell Biol 2010; 99: 1–26.
17 van Breemen C, Chen Q, Laher I.
Superficial buffer barrier function of smooth muscle sarcoplasmic reticulum. Trends Pharmacol Sci 1995; 16: 98–105.
18 Guibert C, Ducret T, Savineau JP. Expression and physiological roles of
TRP channels in smooth muscle cells. Transient Receptor Potential Channels 2011; 704: 687–706.
19 Mazzanti M, DiFrancesco D. Intracellular Ca modulates K-inward rectification in cardiac myocytes. Pflugers Arch 1989; 413: 322–4.
20 Kito Y, Suzuki H. Properties of pacemaker potentials recorded from myenteric interstitial cells of Cajal distributed in the mouse small intestine. J Physiol 2003; 553: 803–18.
21 Huang F, Rock JR, Harfe BD et al. Studies on expression and function of the TMEM16A calcium-activated chloride channel. Proc Natl Acad Sci USA 2009; 106: 21413–8.
22 Kunzelmann K, Kongsuphol P, Alde- 23 hni F et al. Bestrophin and TMEM16Ca(2+) activated Cl(-) channels with different functions. Cell Calcium 2009; 46: 233–41.
23 Zhu MH, Kim TW, Ro S et al. A Ca(2+)-activated Cl(-) conductance in interstitial cells of Cajal linked to slow wave currents and pacemaker activity. J Physiol 2009; 587: 4905–18.

SUPPORTING INFORMATION

Additional Supporting Information may be found in the online version of this article:

Figure S1. Properties of Ca^{2+} transients. (A) The maximums of Ca^{2+} transients caused by ionomycin, cyclopiazonic acid (CPA) and CPA + Li-NCX in % F0 fluorescence. (B) The full-width at half-maximum (FWHM) of Ca^{2+} transients caused by ionomycin, CPA and CPA + Li-NCX in s. (C) The area above the half maximum line of Ca^{2+} transients caused by ionomycin, CPA and CPA + Li-NCX in % F0 fluorescences · 10^2. Key applies to panels (A–C). Insets beneath each panel represent different Ca^{2+} transient parameters.

Figure S2. Effect of La^{3+}: maxi chloride currents. (A) La^{3+} (1 mmol L^{-1}) activated inwardly rectifying maxi chloride (MCl_{ir}) currents. (B) MCl_{ir} current open probability (P_o) vs voltage; average n = 3. (C) La^{3+} activated MCl_{ir} channel current–voltage relationship; average n = 3. Note that currents exhibit slight inward rectification. (Di and ii) La^{3+} activated MCl_{ir} currents at -80 (blue) and +80 mV (orange) portions of the ramp over time (n = 3). Panels show currents from individual cells (i) and the mean of all cells (ii; n = 15).

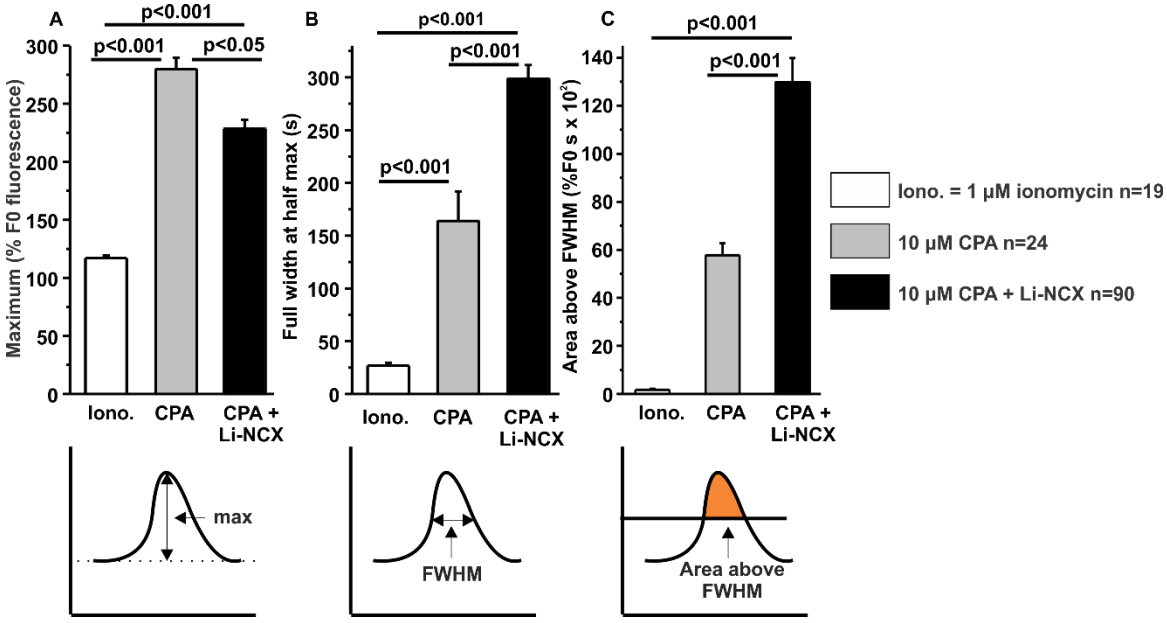

Supplementary Fig. S1.

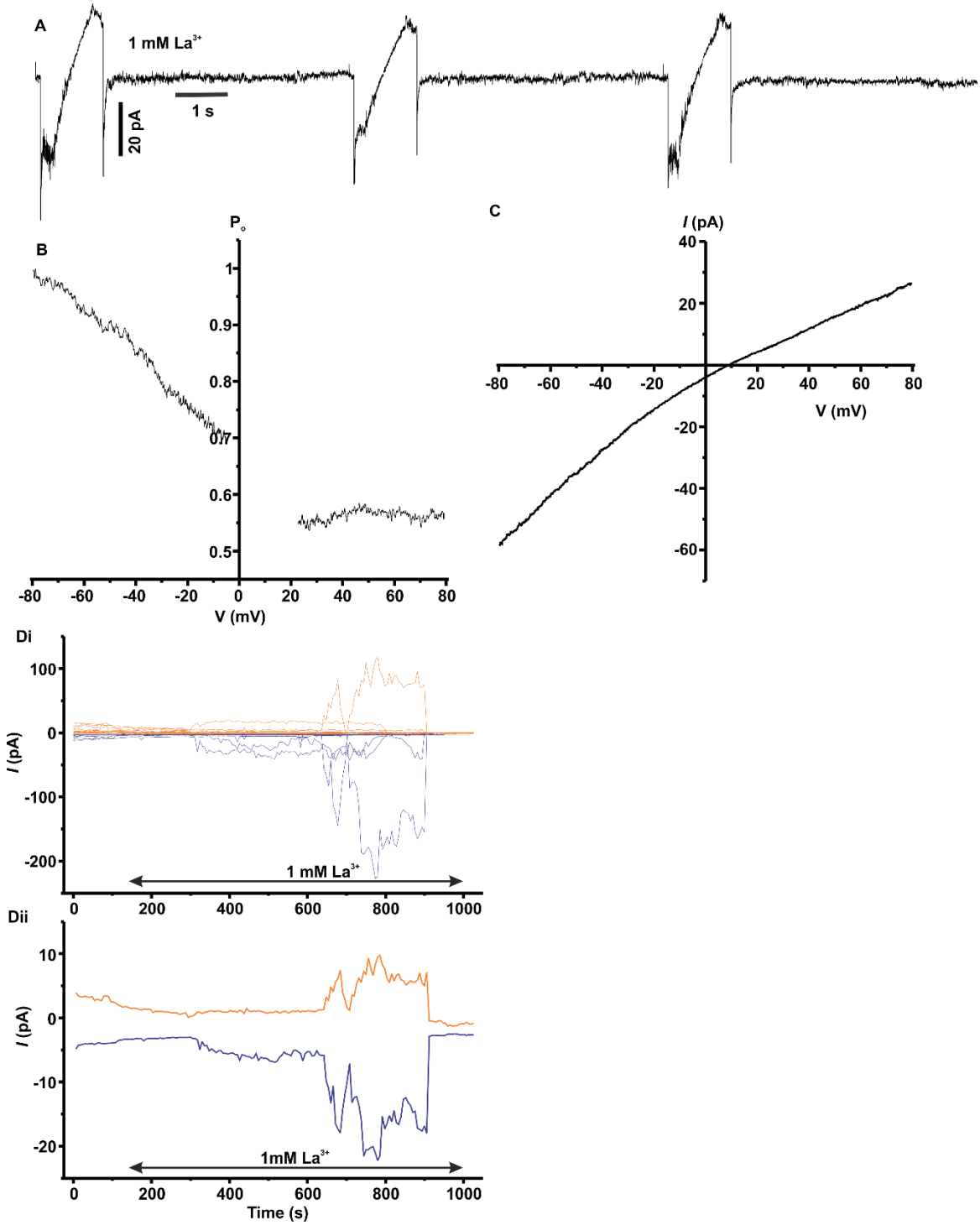

Supplementary Fig. S2.

CHAPTER 3: CHOLINERGIC SIGNALLING-REGULATED $K_V7.5$ CURRENTS ARE EXPRESSED IN COLONIC ICC-IM BUT NOT ICC-MP

3.1 Preface

The body of this chapter was reproduced from a journal article, published in Pflügers Archiv European Journal of Physiology, of which I am the first author, with permission from the publisher Springer-Verlag Berlin Heidelberg © 2013:

Wright GWJ, Parsons SP, Loera-Valencia R, Wang XY, Barajas-López C, and Huizinga JD (2013) Cholinergic signalling-regulated $K_V7.5$ currents are expressed in colonic ICC-IM but not ICC-MP. *Pflugers Arch* **466:** 1805-1818. DOI # 10.1007/s00424-013-1425-7

As the first author of this paper I planned the study, performed all the electrophysiology experiments, cell culture and cell isolation for single-cell PCR, analyzed all the data, prepared all the figures, wrote the manuscript and edited it during review. Sean P Parsons contributed to the electrophysiology analysis and interpretation. Raul Loera-Valencia performed the single-cell PCR and provided the gel images for figures. Xuan Yu Wang performed the immunohistochemistry and provided the images of stained cells for figures. Carlos Barajas-López supervised Raul Loera-Valencia. Jan D Huizinga supervised and planned the study, provided the funding, and edited the manuscript during review.

3.2 Paper Full Text

DOI 10.1007/s00424-013-1425-7

ION CHANNELS, RECEPTORS AND TRANSPORTERS

Cholinergic signalling-regulated $K_V7.5$ currents are expressed in colonic ICC-IM but not ICC-MP

George W. J. Wright · Sean P. Parsons · Raúl Loera-Valencia Xuan-Yu Wang · Carlos Barajas-López · Jan D. Huizinga

Received: 8 November 2013 /Revised: 2 December 2013 /Accepted: 10 December 2013
/Published online: 28 December 2013

Abstract Interstitial cells of Cajal (ICC) and the enteric nervous system orchestrate the various rhythmic motor patterns of the colon. Excitation of ICC may evoke stimulus-dependent pacemaker activity and will therefore have a profound effect on colonic motility. The objective of the present study was to evaluate the potential role of K^+ channels in the regulation of ICC excitability. We employed the cell-attached patch clamp technique to assess single channel activity from mouse colon ICC, immunohistochemistry to determine ICC K^+ channel expression and single cell RT-PCR to identify K^+ channel RNA. Single channel activity revealed voltage-sensitive K^+ channels, which were blocked by the K_V7 blocker XE991 (n=8), which also evoked inward maxi channel activity. Muscarinic acetylcholine receptor stimulation with carbachol inhibited K^+ channel activity (n=8). The single channel conductance was

3.4±0.1 pS (*n*=8), but with high extracellular K^+, it was 18.1±0.6 pS (*n*=22). Single cell RTPCR revealed Ano1-positive ICC that were positive for $K_V7.5$. Double immunohistochemical staining of colons for c-Kit and $K_V7.5$ in situ revealed that intramuscular ICC (ICC-IM), but not ICC associated with the myenteric plexus (ICC-MP), were positive for $K_V7.5$. It also revealed dense cholinergic innervation of ICC-IM. ICC-IM and ICC-MP networks were found to be connected. We propose that the pacemaker network in the colon consists of both ICC-MP and ICC-IM and that one way of exciting this network is via cholinergic $K_V7.5$ channel inhibition in ICC-IM.

Keywords Interstitial cells of Cajal · Pacemaking · Colonic motility · K_V7 channels · Intramuscular ICC · XE991

Abbreviations

GI	Gastrointestinal
ICC	Interstitial cells of Cajal
ICC-MP	Interstitial cells of Cajal associated with the myenteric plexus
ICC-IM	Intramuscular interstitial cells of Cajal
ICC-SMP	Interstitial cells of Cajal associated with the submuscular plexus
$K_V7.5$	Voltage-gated K^+ channel 7.5
mAChRs	Muscarinic acetylcholine receptors
rrmp	Relative to resting membrane potential
VAChT	Vesicular acetylcholine transporter

Electronic supplementary material The online version of this article (doi:10.1007/s00424-013-1425-7) contains supplementary material, which is available to authorized users.

G. W. J. Wright (✉) · S. P. Parsons · R. Loera-Valencia · X.-Y. Wang · J. D. Huizinga (✉)

Farncombe Family Digestive Health Research Institute, Department of Medicine, McMaster University, HSC-3N8, 1200 Main Street West, Hamilton, ON L8N 3Z5, Canada e-mail: wrightgw@mcmaster.ca e-mail: huizinga@mcmaster.ca

R. Loera-Valencia · C. Barajas-López

IPICYT (Instituto Potosino de Investigación Científica y Technológica), San Luis Potosí, SLP, Mexico

Introduction

Interstitial cells of Cajal (ICC) were proposed as gastrointestinal (GI) pacemaker cells in the late 1970s and early 1980s based on correlations between electrophysiological studies and ultrastructural observations by electron microscopy [12, 18, 35, 41]. There are several populations of ICC in every organ of the GI tract that differ in location, morphology, role and protein expression [18, 23]. With respect to the colon, although initial physiological studies were carried out on dog colonic circular muscle, most subsequent studies on ICC pacemaker mechanisms and ion channels have focused on small intestine and stomach [17, 36, 42]. Hence, our knowledge of the colonic pacemaker mechanisms and ion channels involved is still limited. ICC associated with the myenteric plexus (ICC-MP) of the small intestine generate the omnipresent slow waves [40] that orchestrate rhythmic propulsive muscle contractions in the proximal intestine. In the colon, the omnipresent slow waves are generated by ICC associated with the submuscular plexus (ICC-SMP) in the canine [27, 39], rat [32], mouse [47] and human [33]. ICC-MP from the rat [32] and mouse [47] colon do not generate omnipresent slow waves, but generate rhythmic transient depolarisations of low and variable

frequency, that might depend on activation of L-type calcium channels. Based on these findings, it was proposed that ICC-MP can be induced to generate the pacemaker activity governing a propulsive motor pattern of the colon at that frequency [8, 9, 18]. Carbachol strongly promotes this rhythmic activity, even in the presence of TTX [8, 9]. The objective of the present study was to find mechanisms of excitation of the ICC-MP. Our specific hypothesis was that cholinergic inhibition of K^+ channels is involved.

Materials and methods

Cultured cells

The preparation and electrophysiology for the cultured cells were the same as those described previously [29, 46], except that colons from 8- to 15-day-old CD-1 mice were used instead of small intestine. All procedures were approved by the Animal Research Ethics Board (AREB) of McMaster University.

Solutions, drugs and electrophysiology

Carbachol and XE991 were purchased from Sigma Aldrich, Oakville, ON, Canada. Drugs were prepared by dilution in bath solution to concentrations specified in the results from stock solutions in DMSO. Voltage protocols were adjusted according to the junction potential between the pipette and bath solutions [29, 31]. The potential that the patch "sees" (E_{patch}) is the summation of the cell membrane potential (E_{cell}) and the potential applied to the patch relative to resting membrane potential (E_{rrmp}).

$$E_{patch} = E_{rrmp} + E_{cell}$$

In the results, potentials are expressed as E_{rrmp} followed in parentheses by E_{patch}, assuming an E_{cell} of −60 mV [28]. See Table 1 for the contents of bath and pipette solutions.

Data analysis and statistics

Current traces for figures were filtered with a 140-dB eight-pole Bessel filter on Clampfit (Molecular Devices, Sunnyvale, CA, USA) and a notch electrical interference filter where necessary. The difference in current (ΔI) for the channel transition between one current level and another at a certain potential was measured, and this was repeated for channel transitions at different potentials. The ΔI values plotted versus potential were fitted with linear regression, the slope of which was used to determine the conductance; the x-intercept was used to determine the reversal potential of the currents. Mean reversal potentials and conductances were calculated from the linear fits of ΔI values from individual experiments; pooled data are shown in the figures fitted with linear regression.

Current voltage plots were created by averaging the currents evoked by the voltage ramps from control sweeps or from sweeps after inhibition by drugs. For control sweeps, the linear slope of the current from −80 (−140) to −20 (−80) mV, where no K^+ channels were active, was subtracted from the current evoked by the −80 (−140) to +80 (20) mV voltage ramp. For sweeps after inhibition by drugs, the linear slope of the current from −80 (−140) to + 80 (20) mV was subtracted. A Z-test for proportions was used to determine differences between proportions with a significance level of α=0.05.

ICC RNA extraction and reverse transcription

RNA was obtained from CD-1 mouse brain tissue or single cultured ICC to perform RT-PCR. For tissue, the RNA extraction was done using the RNAeasy RNA isolation kit (Qiagen, Toronto, ON, Canada), according to the manufacturer's instructions. Brain RNA (1 μg) was used for reverse transcription. As a measure to control for gDNA PCR products, an RT minus control was used. To collect single cells, the patch clamp rig was used with unpolished, low resistance glass pipettes containing 6 μL of the RT-PCR mix (20 U of RNase inhibitor, 2.3 μM oligo (dT), 150 μM dNTPs, 1.2 mM dTT, 3.6 mM $MgCl_2$ and 10× RT Buffer (Life Technologies Inc., Burlington, ON, Canada)). The same parameters used to identify ICC for electrophysiology were used to select single cells from primary cultures. After collection, we used NP-40 detergent (1:100) to lyse the cells and release the genetic material. Tissue samples and single ICC were brought to a final volume of 20 μL with RT-PCR mix and 200 U of Superscript III RT. Then the samples were incubated at 50°C for 50 min. After the cDNA synthesis, the RT enzyme was deactivated by freezing overnight and subsequent thawing.

Solution	Na^+	Cl^-	K^+	$NMDG^+$	Mg^{2+}	Ca^{2+}	HEPES	pH	Glucose
Bath	135	146.4	5	–	1.2	2	10	7.35[a]	10
KCl pipette	–	150	150	–	–	–	10	7.0[a]	10
NMDG pipette	–	140	–	140	–	–	10	7.35[a]	10

Table 1 Contents of solutions

$NMDG^+$ N-methyl-D-glucamine, *HEPES* 4-(2-hydroxyethyl)piperazine-1-ethanesulfonic acid

[a]pH adjusted with Tris base

Nested PCR protocol

PCR was performed using Platinum Taq DNA Polymerase (Life Technologies Inc.). To detect transcripts coding for K_V7.5 channels, we used the primers K_V7.5 ExtR 5'-TGTG TCGGCGTCTATCACTG. A nested PCR was carried afterwards with internal primers K_V7.5 intF 5'-GCCAGAGCAT TAAGAGCAGAC and K_V7.5 intR 5'-ACTCTTGAGCCGTATGAGG. To amplify Ano1, we first used the primers Ano1 ExtF 5'-TGTACTTTGCCTGGCTTGGAGC and Ano1 ExtR 5'-CACCTGGCAATGCAGCCGTA, in the same way as with potassium channels, a nested PCR was performed next using the primers Ano1 intF 5'-CAACTACCGATGGGACCT CAC and Ano1 intR 5'-AATAGGCTGGGAATCGGTCC. To control for gDNA PCR products from the single cells, the external primers were designed to span at least one intron of the analysed genes. No additional bands of higher size were detected. We omitted the template for negative controls. The PCR protocol was performed as follows on a CFX96

thermal cycler (Bio-Rad Laboratories Canada Ltd., Mississauga, ON, Canada): initial denaturation for 3 min at 94 °C, then 30 amplification rounds with denaturation for 15 s at 94 °C, alignment for 15 s at 50 °C and extension for 1 min 45 s at 72 °C per round. The final extension was 5 min at 72 °C. For the nested PCR, the same protocol was used with 36 cycles and annealing temperature of 58–60 °C per cycle. The resulting products were analysed by electrophoresis in agarose gels (1.5 %, Invitrogen, Burlington, ON, Canada) stained with 1 μg/mL ethidium bromide (Sigma-Aldrich). Images were obtained with Gel-Doc 2000 documentation system (Bio-Rad Laboratories Canada Ltd.). The resulting bands were cut then sequenced by MOBIX Laboratories (McMaster University, Hamilton, ON, Canada).

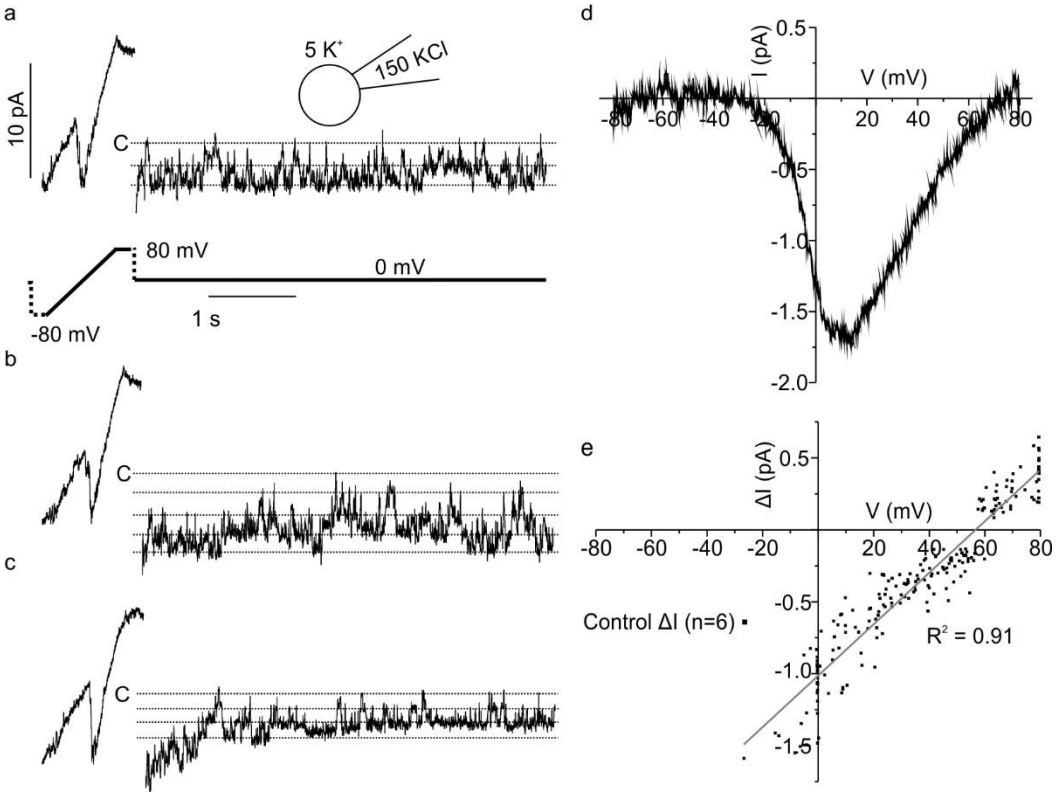

Fig. 1 K^+ currents recorded from cell-attached patches of ICC. Up to four channels were active around 0 (−60) mV. a–c Control inward K^+ currents evoked by ramps and at 0 (−60)

mV. Simultaneous multiple openings were present at 0 (−60) mV. For this and all subsequent figures, grey lines show current levels and C represents the level where all channels are closed. V is the potential applied to the patch relative to resting membrane potential (Errmp) and values in parentheses are patch potentials (Epatch) assuming a cell membrane potential of −60 mV (see "Materials and methods" and "Results"). D Current–voltage plot of average K^+ currents evoked by ramp protocol (n=6). e Single channel current amplitudes from pooled experiments (n=6); grey line is a linear fit of data with slope=17.9 pS and x-interept= 56.7 (−3.3) mV

Immunohistochemical staining

Cell culture preparations were the same as for the electrophysiological study. In addition, the whole (proximal, mid and distal) colon was removed for frozen sections and musculature whole-mount preparations. Whole-mount specimens were prepared by peeling away the mucosa and submucosa. Frozen sections were made by embedding the tissues in Tissue-Tek (Miles Lab., Naperville, IL, USA) and freezing in liquid nitrogen. Ten micrometer sections were cut with the cryostat and mounted on the coated slides. Staining for c-Kit was performed since it is a selective marker of ICC [19]. For whole-mount tissue and culture staining, specimens were fixed in ice-cold acetone for 10 min and then processed for c-Kit staining. After c-Kit staining, specimens were fixed again with 4 % paraformaldehyde for 10 min and then processed for $K_V7.5$ staining or vesicular acetylcholine transporter (VAChT) staining. For frozen section staining, sections were only fixed with 4 % paraformaldehyde for 10 min and processed for $K_V7.5$ and then c-Kit staining. The non-specific binding was blocked with 5 % normal goat serum in all immunohistochemical staining, except for c-Kit/VAChT

staining, in which 2 % bovine serum albumin was applied. Tissues were then incubated overnight at room temperature in the following two groups of primary antibodies: rat anti-c-Kit (1:200, Cedarlane, Oakville, ON, Canada) and rabbit antiK_V7.5 (1:100, Santa Cruz Biotech., Santa Cruz, CA, USA); rat anti c-Kit and goat anti VAChT (1:100, Santa Cruz Biotech.). For c-Kit/K_V7.5 double labelling, secondary antibodies were Cy3-conjugated goat anti-rat IgG (1:400, Jackson Immuno Research, West Grove, PA, USA) and Alexa488-conjugated goat anti-rabbit IgG (1:200, Jackson Immuno Research). For c-Kit/VAChT double labelling, secondary antibodies were Alexa488-conjugated donkey anti-rat IgG (1:200, Jackson Immuno Research) and Cy3conjugated donkey anti-goat IgG (1:400, Jackson Immuno Research). All antibodies were diluted in 0.05 M PBS (pH 7.4) with 0.03 % Triton-X 100. Negative controls included the omission of primary antibodies from the incubation solution. All of the immunostaining was examined using a confocal microscope (Zeiss LSM 510, Göttingen, Germany) with excitation wavelengths (595 nm and 488 nm) appropriate for Cy3 and Alexa488. Confocal micrographs shown were digital composites of Z-series of 1–4 optical sections through a depth of 0–2 μm.

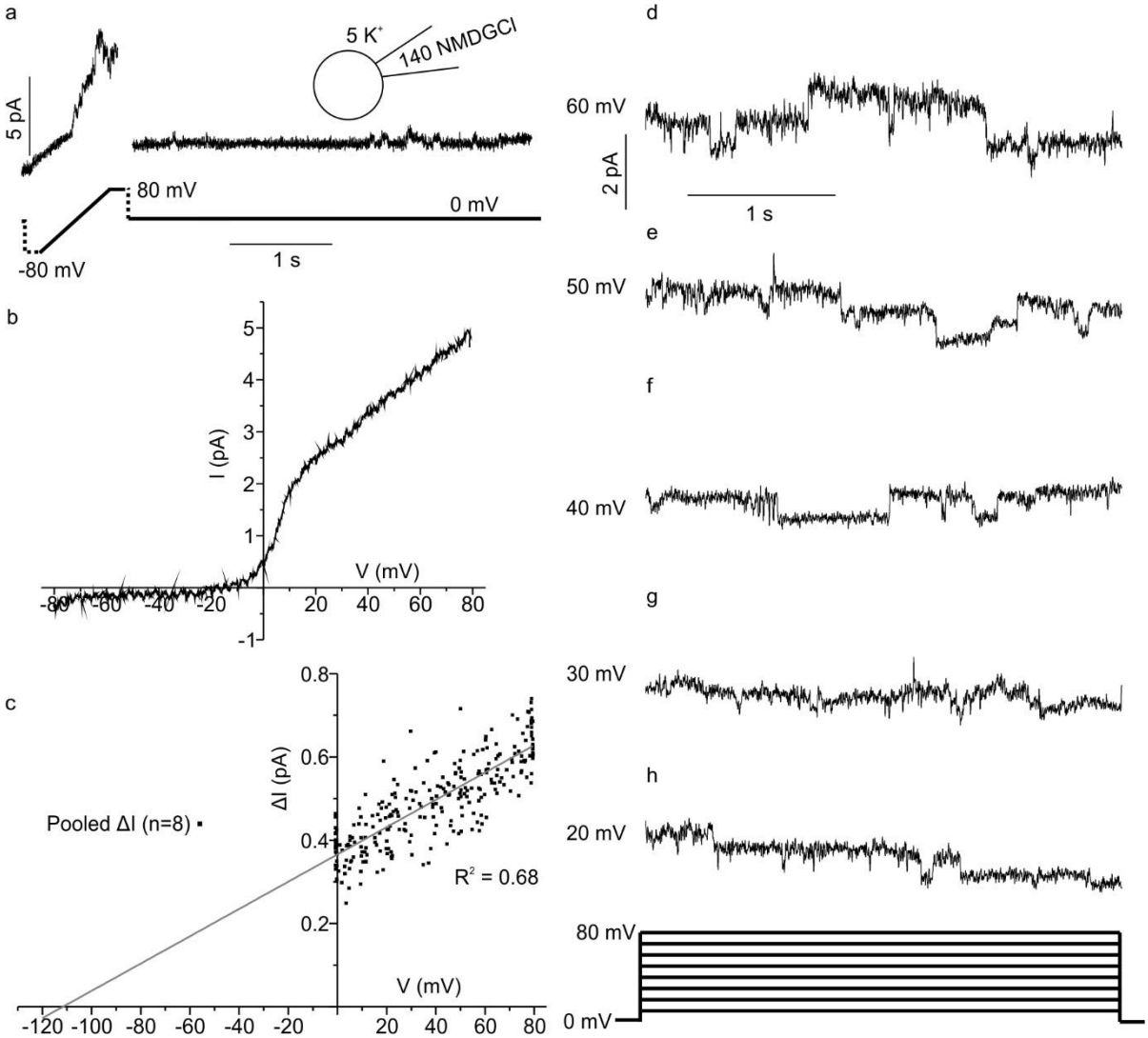

Fig. 2 Outward K^+ currents while cell-attached in 140 mM NMDGCl pipette solution. **a** Outward K^+ currents evoked during depolarising portion of the ramp. **b** Current–voltage plot of average outward K^+ currents recorded from ramp protocols (*n*=8). **c** Single channel current amplitudes from pooled experiments (*n*=8); grey line is a linear fit of data with slope=3.3 pS and x-intercept=−111.6 (−171.6) mV. **d–h** Currents recorded from decreasing depolarising voltage steps (inset) and were inactive below 0 (−60) mV (not shown)

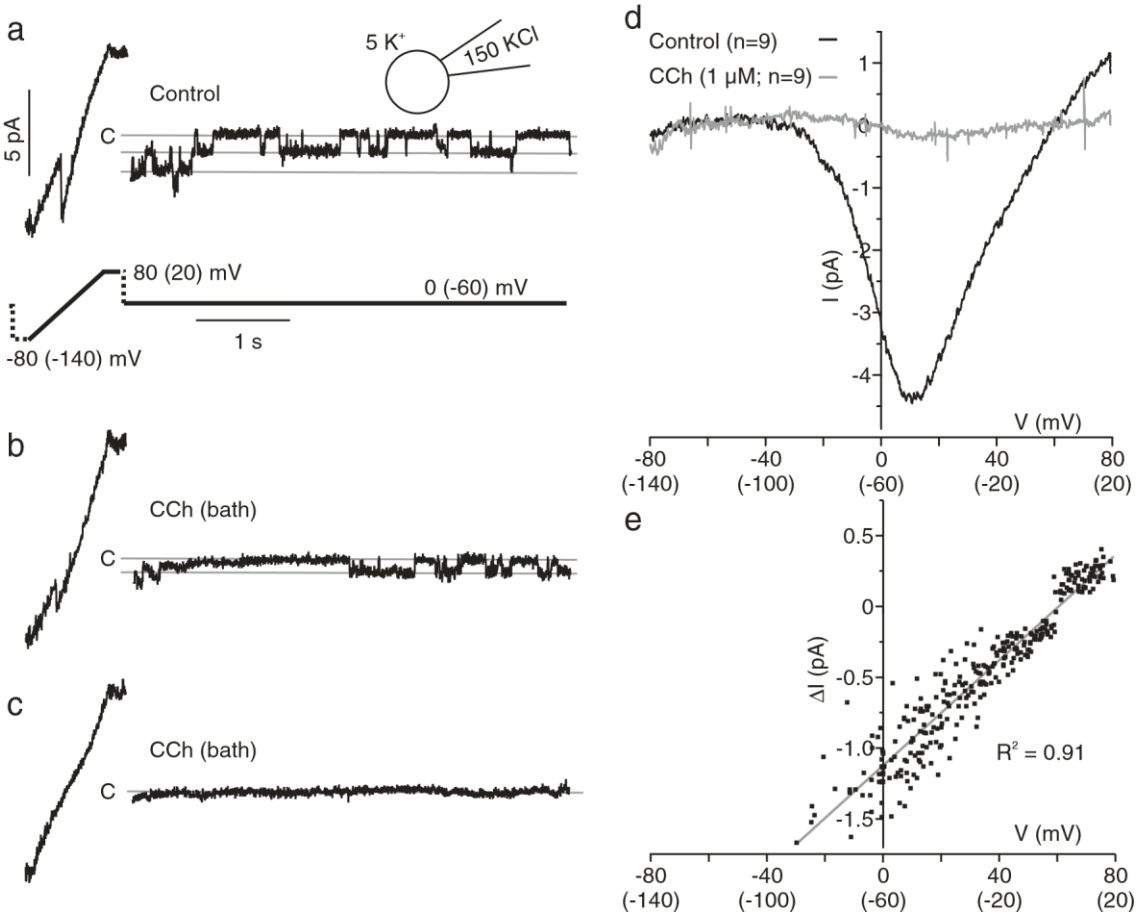

Fig. 3 Effect of carbachol on K^+ current while cell-attached. a Control K^+ currents evoked by the ramp and at 0 (−60) mV. Note inward current in the middle of the ramp. **b, c** Carbachol (CCh; 1 µM) inhibited K^+ currents. **b** Recorded 18 s after CCh addition, **c** was 114 s after **b**. **d** Current–voltage plots of average currents show inhibition of K^+ current by CCh. **e** Single channel current amplitudes from pooled CCh controls (*n*=8); grey line is a linear fit of data with slope=18.6 pS and x-intercept= 60.4 (0.4) mV

Results

Colonic ICC display K^+ channel activity

The potential that the patch "sees" (E_{patch}) is the summation of the cell membrane potential (E_{cell}) and the potential applied to the patch relative to resting membrane potential (E_{rrmp}), $E_{patch}=E_{rrmp}+E_{cell}$. Potentials are expressed as E_{rrmp} followed in parentheses by E_{patch}, assuming an E_{cell} of −60 mV. For example, 20 (−40) mV. One to four channels opened (Fig. 1a–c) at ∼−20 (−80) mV when a ramp protocol from −80 (−140) to +80 (20) mV was applied to cell-attached patches of cultured colonic ICC, using a 150 mM KCl pipette solution. The inward currents were most active at 10 (−50) mV, as shown by the current–voltage (*I–V*) plot (Fig. 1d). The inward currents turned off upon patch excision to the inside-out configuration (without changing the bath solution; data not shown). Based on single channel activity—single channel current amplitude (ΔI) versus voltage (Fig. 1e)—the reversal potential was 56.7 (−3.3)±1.0 mV and the single channel conductance was 17.9±0.9 pS (n=6). Assuming symmetrical K^+ between the cell and pipette, K^+ currents would reverse at a patch potential of 0 mV. Therefore, the reversal potential of 56.7 mV rrmp suggests a cell membrane potential of −56.7 mV ($E_{cell}=E_{patch}-E_{rrmp}$= 0−56.7 mV=−56.7 mV), confirming it to be close to −60 mV.

The current was outward when a 140 mM NMDGCl pipette solution was used and activated at approximately the same voltage in ramps and steps, consistent with the current being carried by a K^+ channel (Fig. 2a, d−h). The I–V plot shows outward K^+ current at positive potentials (Fig. 2b). Based on ΔI versus voltage, the reversal potential (determined as above)

was −112.3 (−172.3)±4.7 mV and the single channel conductance was 3.3±0.1 pS (*n*=8; Fig. 2c). The current turned off when patches were excised into the inside-out configuration (data not shown).

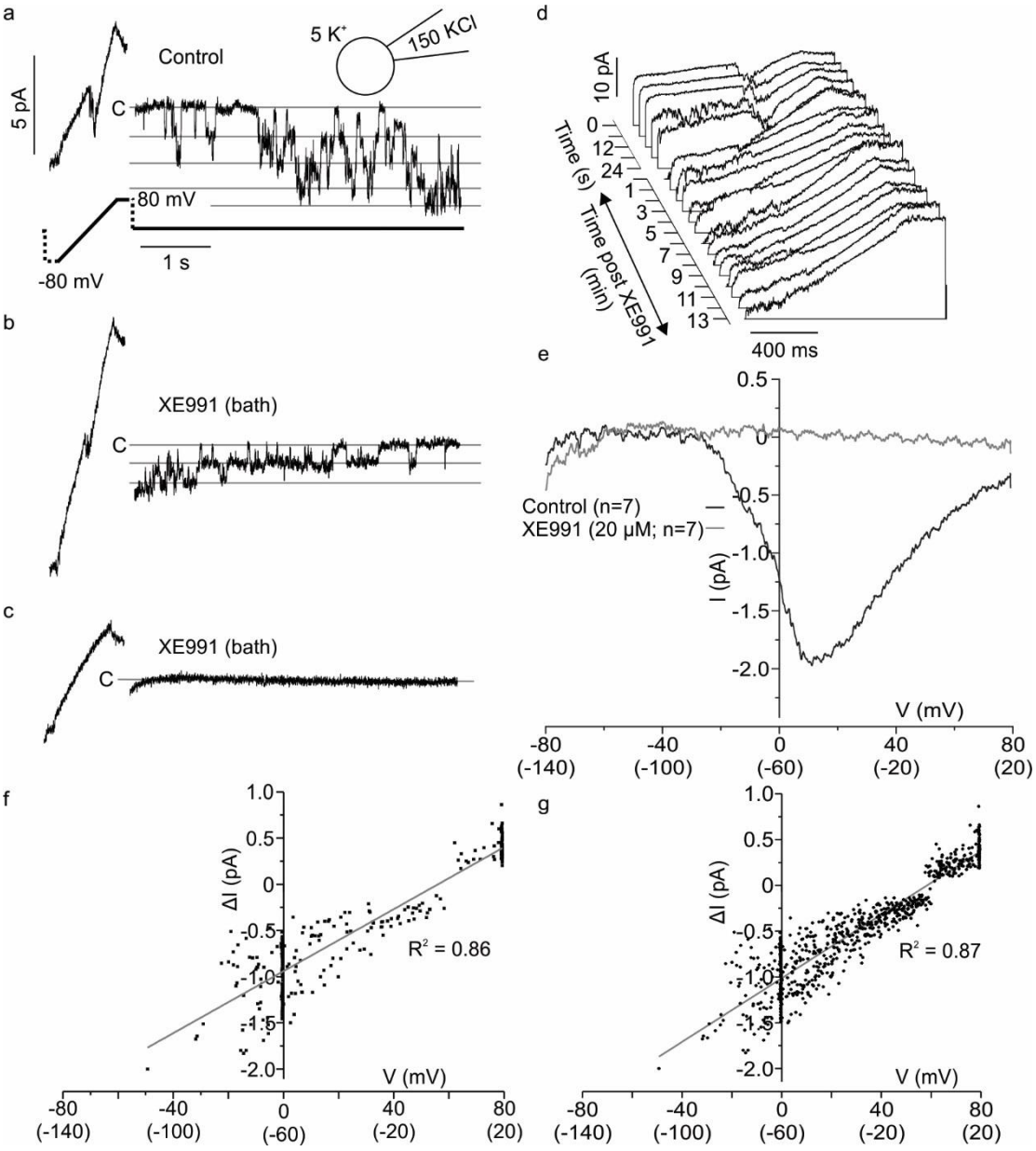

Fig.4 Effect of bath applied XE991 on K^+ currents while cell-attached. **a** Control K^+ currents evoked by the ramp and at 0 (−60) mV. Note inward current in the middle of the

ramp. b, c XE991 (20 μM) blocked K^+ currents; **b** was recorded 138 s after XE991 addition, **c** was 96 s after **b**. **d** Ramp traces where XE991 blocked K^+ currents. The first five traces are sequential from the control with K^+ currents active. The next 15 traces were recorded after XE991 addition at 1 min intervals; note the absence of K^+ currents. **e** Current–voltage plots of average currents show inhibition of K^+ currents by XE991. **f** Single channel current amplitudes from pooled XE991 controls (*n*=8); grey line is a linear fit of data with slope=16.8 pS and x-intercept=56.1 (−3.9) mV. **g** Single channel amplitudes from pooled control K^+ currents (including ΔI values from Figs. 1e, 3e and 4f; *n*=22). *Grey line* is a linear fit of data with slope=17.4 pS and x-intercept=58.4 (−1.6) mV

Effects of carbachol on K^+ currents

Carbachol (CCh; 1 μM) inhibited the K^+ currents completely when added to the bath (*n*=9; Fig. 3a−c). The current amplitude decreased (Fig. 3b) compared to control (Fig. 3a), before the onset of full inhibition (Fig. 3c), which implies that current inhibition began to affect the resting membrane potential, reducing the amplitude of the currents. The I−V plot shows that inward currents were most active at 10 (−50) mV, prior to inhibition by CCh (Fig. 3d). Based on ΔI versus voltage, the reversal potential was 59.9 (−0.1)±0.6 mV and the single channel conductance was 19.1±0.8 pS (*n*=8; Fig. 3e). These data imply that the K^+ current is carried by a cholinergic signalling regulated channel; hence, we tested whether or not the current was carried by Kcnq (K_V7) channels, which are the channels responsible for M-current [5].

Effects of XE991 on K^+ current

XE991 (20 μM), a K_V7 channel blocker [1, 21], completely blocked the currents (*n*=10; Fig. 4a–c). As with CCh, current amplitude was reduced after the addition of XE991 before the onset of complete blockade (Fig. 4a, b). Current blockade by XE991 was sustained as is shown by the absence of the K^+ current from ramps recorded at 1 min intervals after XE991 addition (Fig. 4d). The I–V plot shows that inward currents were most active at 10 (−50) mV and were blocked by XE991 (*n*=8). Based on ΔI versus voltage, K_V7 currents had a reversal potential of 55.1 (−4.9)±2.3 mV and the conductance was 17.1±1.3 pS (*n*=8; Fig. 4f). The ΔI versus voltage when all controls were pooled yielded a reversal potential of 57.3 (−2.7)±1.0 mV and a conductance of 18.1±0.6 pS (*n*=22; Fig. 4g). XE991 blocks K_V7 currents from the ICC causing them to depolarise, leading to activation of a large, inwardly rectifying current (*n*=15; Fig. 5a−c).

In order to confirm that XE991 was blocking the K^+ channels directly, 20 μM XE991 was added to the KCl pipette solution. Time-dependent block was shown in Fig. 6a–c. If there were no K^+ currents at the beginning of an experiment, we could not determine whether the channels were blocked rapidly, or whether there were no channels present in the patches. Therefore, many experiments were performed to gain a sample population large enough to accurately determine the effects of XE991 on cultured ICC K^+ currents. Only 30.0 % of patches exposed to XE991 exhibited K^+ currents (*n*=30), in contrast to 57.1 % of patches with control 150 mM KCl pipette solution (*n*=35). There was a significant reduction in the proportion of patches exhibiting K^+ current when exposed to XE991 (9/30) compared to control (20/35), as determined by a Z-test for proportions ($z=2.19$, $\alpha=0.05$, c.v.=1.96).

Thus, XE991 blocks the K^+ channels directly when applied to the extracellular side of the patch.

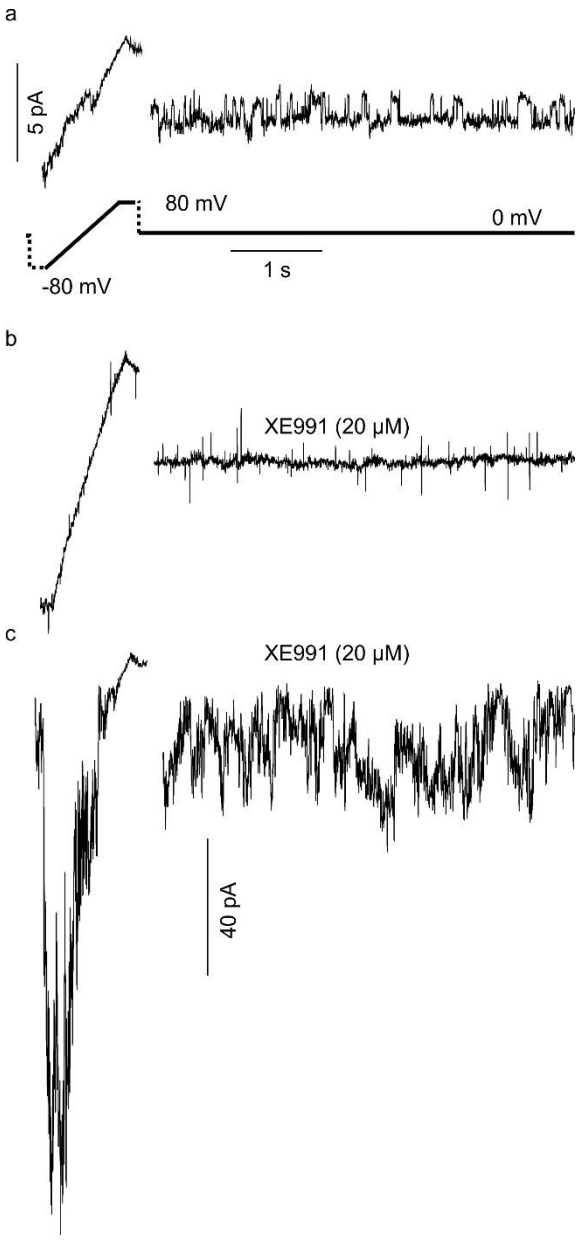

Fig. 5 Activation of an inwardly rectifying current by XE991. **a** Inward K^+ currents were active prior to addition of XE991. b XE991 (20 µM) blocked K^+ currents; **b** was recorded im-

mediately after switch to XE991 bath solution, which takes 120 s. **c** XE991 activated inwardly rectifying currents after 24 s and **c** was recorded 360 s after addition of XE991

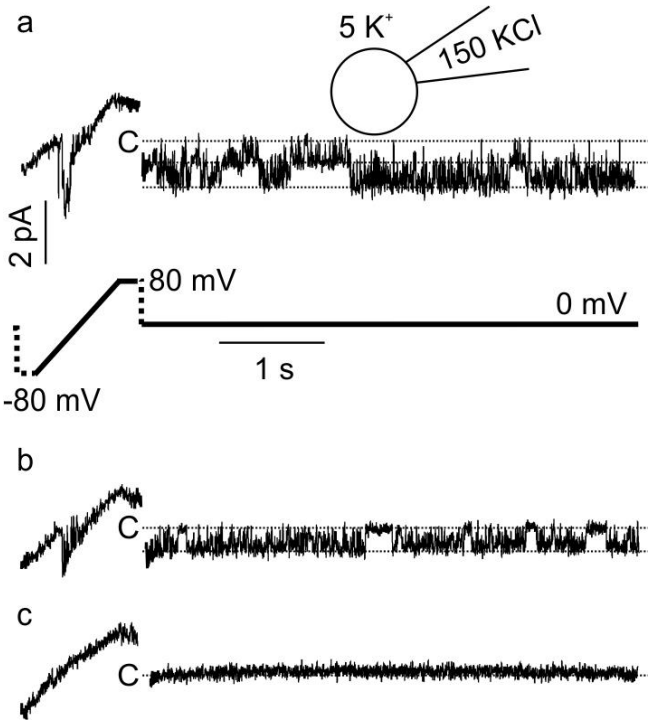

Fig. 6 Effect of XE991 in pipette solution on K^+ currents. **a** K^+ currents active prior to onset of XE991 (20 μM) blockade, recorded 144 s from start. **b** Time-dependent block of current by XE991, 102 s after **a**. **c** Complete current inhibition 18 s after **b**

K_V7 single cell PCR

Since XE991 blocked the K^+ currents in colonic ICC-IM, we looked for $K_V7.5$ using RT-PCR. We isolated single colonic ICC-IM and found that two out of six Ano1-positive cells were also $K_V7.5$ positive (Fig. 7). The identities of the Ano1 and $K_V7.5$ PCR products were confirmed by sequencing.

c-Kit and $K_V7.5$ double immunohistochemical staining

At the level of the myenteric plexus (Fig. 8a), $K_V7.5$ reactivity was found in the enteric neurons of the myenteric ganglia (Fig. 8a2), which were frequently surrounded by c-Kit-positive ICC-MP that were negative for $K_V7.5$ (Fig. 8a3). In the circular muscle layer (Fig. 8b–d), $K_V7.5$ was co-expressed with c-Kit in ICC-IM (Fig. 8b3–d3), both in multipolar and bipolar ICC-IM (arrows in c3). Weak $K_V7.5$ reactivity was also found in the smooth muscle cells (Fig. 8b, c2). Transverse sections confirmed that the colonic ICC network expresses $K_V7.5$, not at the level of the myenteric plexus, but in the ICCIM in the circular muscle (Fig. 8d). $K_V7.5$-positive ICC-IM formed contacts with $K_V7.5$-negative ICC-MP (Fig. 8d3). We also stained for $K_V7.2$–4, all of which were negative in the two ICC networks. However, enteric nerves were positive for $K_V7.2$–4 and the smooth muscle was weakly positive (Supplementary Fig. 1).

Immediately after cell isolation, most cells were rounded and they gained specific shapes after a few days in culture. Three- to 4-day-old c-Kit-positive cultured cells were either multipolar (Fig. 8e, f) or bipolar (Fig. 8g, h). Both bipolar and multipolar ICC were found amongst the cells that were positive for $K_V7.5$ (Fig. 8e3, f–h; solid arrow in h), which is consistent with the observation of $K_V7.5$-positive ICC-IM of both morphologies in situ. c-Kit-positive but $K_V7.5$-negative cells may be ICC-MP (Fig. 8h, open-headed arrow).

Vesicular acetylcholine transporter and c-Kit double immunohistochemical staining

In the mouse colon, anti-vesicular acetylcholine transporter (VAChT) antibodies labelled all the cholinergic nerve varicosities within the myenteric ganglia (Fig. 9a1, b1) and the nerve

fibers in the muscle layer (Fig. 9c1, d1). c-Kit-positive ICCMP were densely distributed around the myenteric plexus ganglia forming a network (Fig. 9a2, b2, a3 and b3). ICCIM were observed in both longitudinal and circular muscle layers, parallel to neighbouring smooth muscle cells, connecting each other to form networks (Fig. 9c2, d2). Intimate apposition between cholinergic varicosities and ICC-IM processes occurred over lengths as long as 250 μm (Fig. 9c3, d3). Unlike the ICC-MP, which only showed point contact with enteric nerves, ICC-IM (both their cell bodies and processes) contacted nerves with varicosities over long distances.

ICC-IM and ICC-MP networks are connected

In order to search for structural evidence for communication between ICC-MP and ICC-IM, we conducted whole-mount c-Kit immunohistochemistry. ICC-IM, running at a 90° angle from the ICC-MP network parallel to the circular muscle cells, were either bi-polar or multipolar in shape, with branches occurring from their cell bodies or major processes (Fig. 10). ICC-IM were not independently scattered in the musculature, but were connected to each other to form a network, although the density of their network was not as high as that of ICC-MP. ICC-IM and ICC-MP were connected (arrows in Fig. 10), providing structural evidence for communication between the two networks.

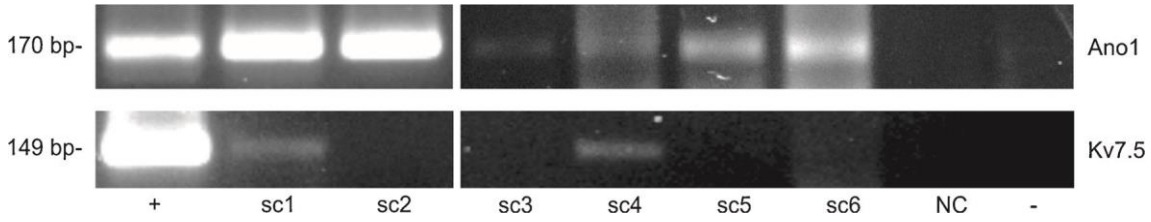

Fig.7 Expression of K_V7 channels in single ICC-IM. Two of six Ano1-positive cells were positive for $K_V7.5$: single cell 1 (sc1) and single cell (sc4). No cell, positive and negative controls are indicated by NC, + and −

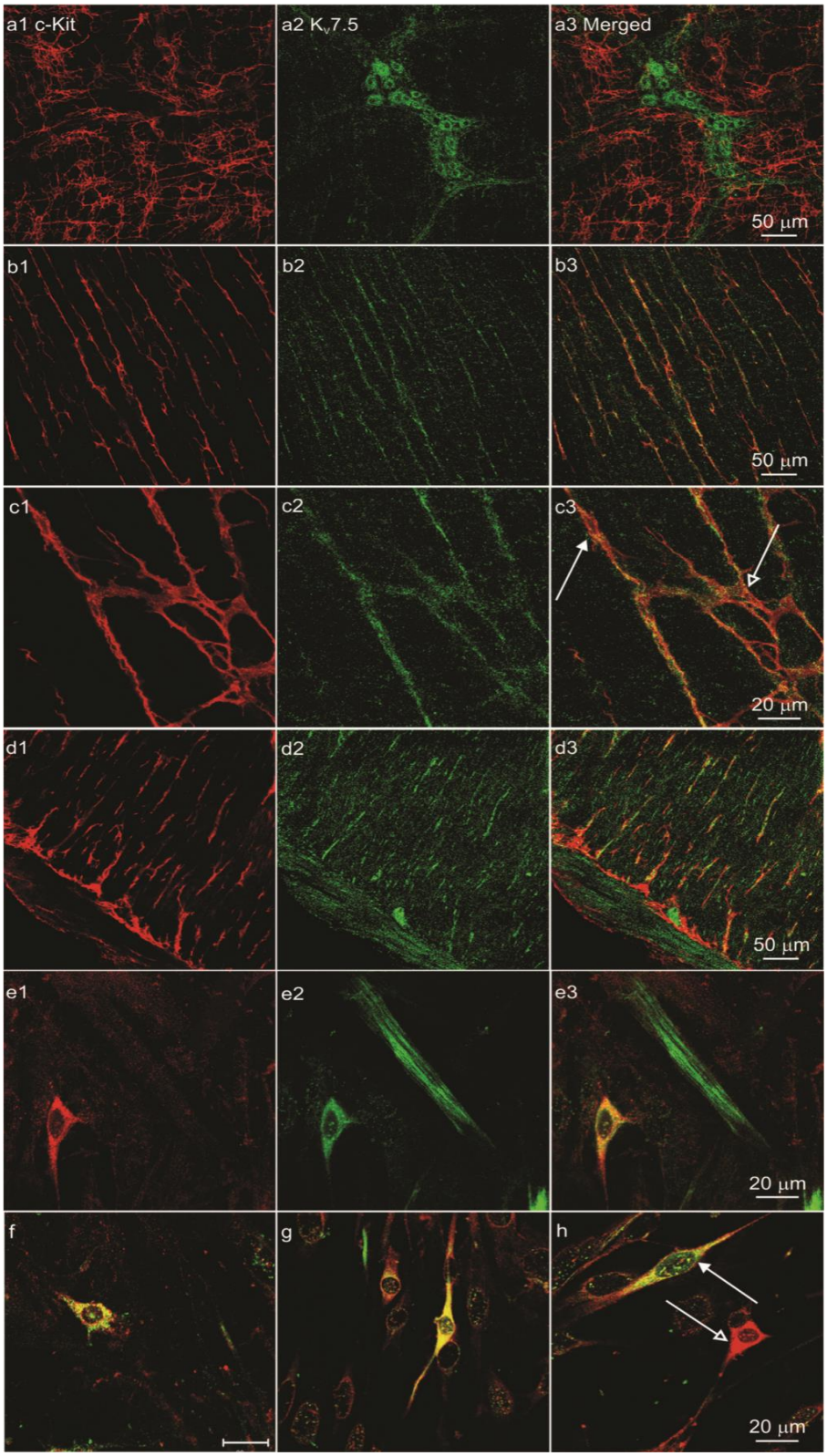
a1 c-Kit
a2 K_v7.5
a3 Merged
50 μm
b1
b2
b3
50 μm
c1
c2
c3
20 μm
d1
d2
d3
50 μm
e1
e2
e3
20 μm
f
g
h
20 μm

Fig. 8 Double labelling of c-Kit (*red*) and K_V7.5 (*green*) in mouse colon whole-mount (**a–c**), frozen sections (**d**) and cultured cells (**e– h**). **a***1–3*) c-Kit-positive ICC-MP network and K_V7.5 positive myenteric neurons. No co-localization was found at the level of myenteric plexus. **b***1-3*) c-Kit-positive ICC-IM and K_V7.5-positive enteric nerves at the level of circular muscle layer. Merged figure shows the co-existence of K_V7.5 and c-Kit within ICC-IM. **c***1–3*) Enlarged images to show co-localization of K_V7.5 and c-Kit in ICC-IM that were either bi-polar (*arrow*) or multi-polar (*open arrow*) in shape. **d***1–3*) Transversal sections show the circular muscle, myenteric plexus and longitudinal muscle layers. c-Kit-positive ICC-MP surrounded K_V7.5-positive myenteric neurons; both c-Kit and K_V7.5 immunoreactivities were seen in ICC-IM. Smooth muscle cells also expressed weak immunoreactivity for K_V7.5. **e–h** Cultured cell staining. **e*1–3***) A triangle-shaped ICC with three processes was positive for K_V7.5. **f–h** Merged images show a multipolar-shaped ICC that was K_V7.5 positive (**f**), a spindle-shaped bipolar ICC that was K_V7.5 positive (**g**) and a multi-polar-shaped ICC that was K_V7.5 negative (*open arrow*), and a spindle-shaped ICC (*arrow*) that was K_V7.5 positive (**h**)

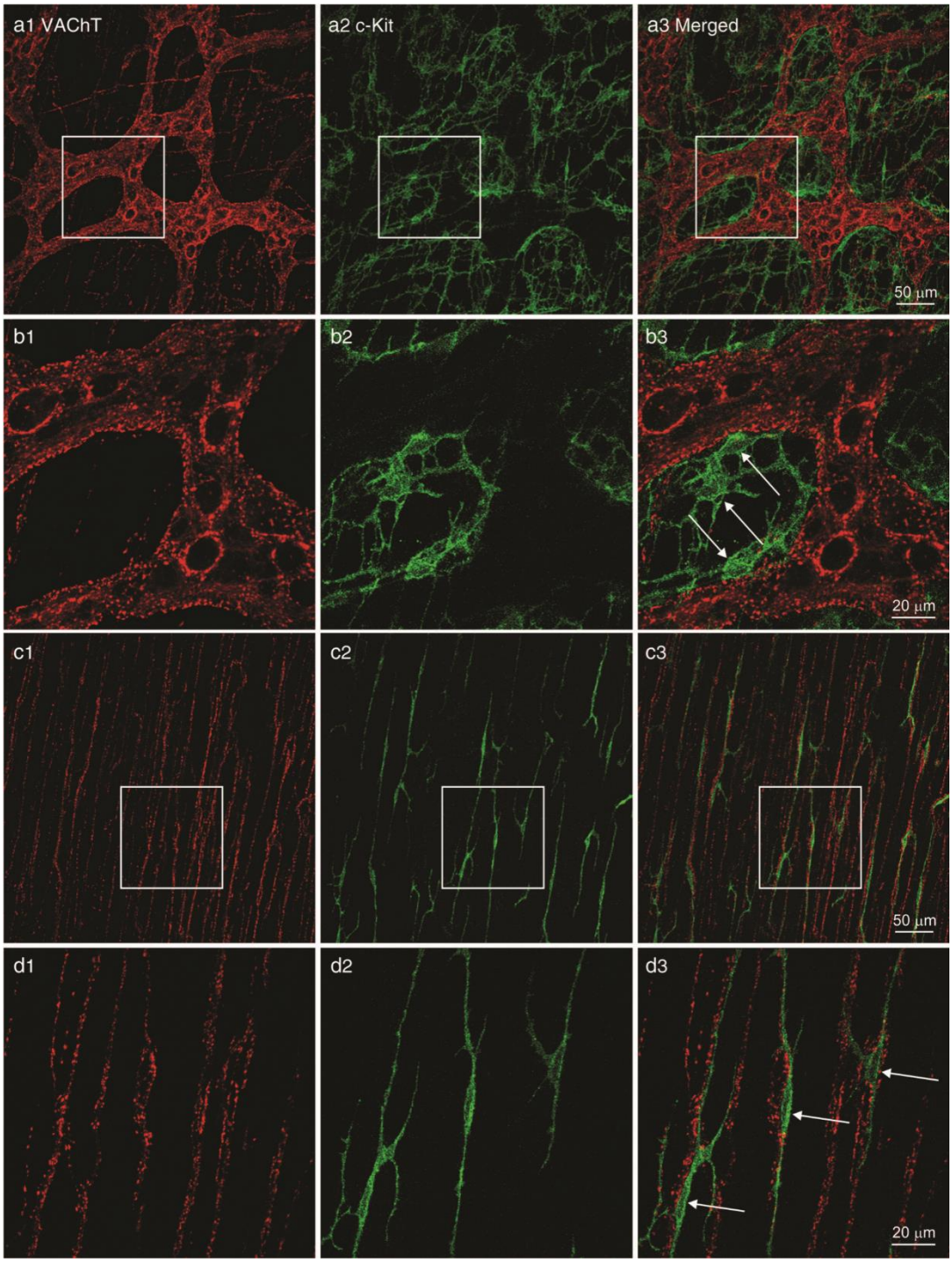

Fig. 9 Double labelling of c-Kit (*green*) and VAChT (*red*) in mouse colon whole-mount preparation. **a***1–3*) VAChT-positive nerve varicosities within the myenteric ganglia and c-Kit-

positive ICC-MP encompassing the ganglia. **b***1–3* Enlarged images (single scan confocal micrographs) from the boxes in figures **a***1–3*. Three ICC-MP (*arrows*) connecting to each other to form network closely aligned the boundaries of the ganglia but never penetrated inside the ganglia. The processes of ICC-MP were not seen lining along the VAChT-positive varicosities. **c***1–3*) VAChT-positive nerves and c-Kit-positive ICC-IM within the circular muscle layer. **d***1–3*) Enlarged images (single scan confocal micrographs) from the boxes in figures **c***1–3*). Three ICC-IM (*arrows*) with different shapes were all running along cholinergic nerves within the circular muscle layer. Both their cell bodies and processes were surrounded by dotted cholinergic varicosities

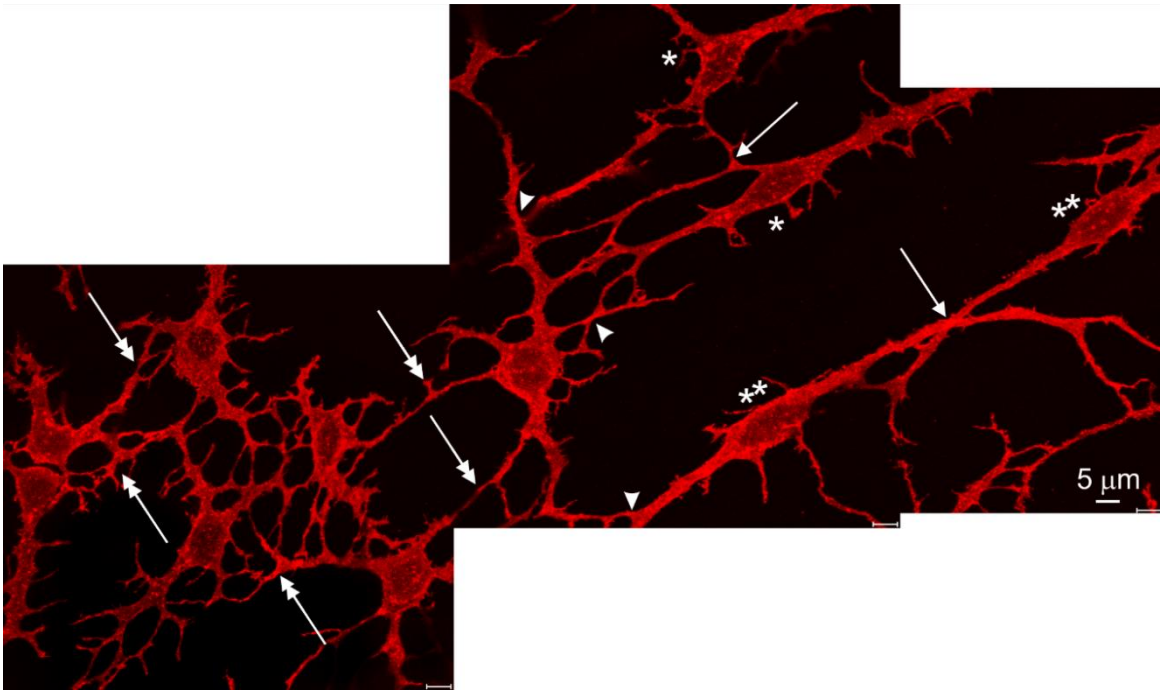

Fig. 10 Combined confocal images with scanning thickness of 1−2 µm (focused on all connections) showing direct connections between ICC-IM, between ICC-MP and between ICC-IM and ICC-MP in mouse colon. *On the right side*, four ICC-IM in the circular muscle layer

close to the level the myenteric plexus were bipolar (*double asterisks*) or multipolar (single asterisk) in shape. They were directly connected to each other (*arrows*) and to nearby ICC-MP (*arrowheads*). On the left side, several ICC-MP with multipolar shape were closely associated to each other (*double arrows*) to form a dense network at the myenteric plexus level

Discussion

Our hypothesis that ICC-MP excitation was regulated by cholinergic inhibition of K^+ channels was not substantiated. Instead, evidence is provided for the regulation of ICC-IM excitability by cholinergic inhibition of $K_V7.5$ channels. Therefore, our hypothesis is that ICC-IM have a special role in neurally mediated regulation of pacemaker activity, since we provide evidence that ICC-IM communicate directly with ICC-MP. The notion that ICC-MP and ICC-IM collaborate is well established in the stomach where they cooperate in the generation of pacemaker activity [11, 14–16]. In the stomach, the ICC-MP appear to generate the primary pacemaker, and when triggered by the primary pacemaker, the ICCIM appear to generate a secondary component of the slow wave; this was substantiated by the observation that calcium transients occurred in the ICC-IM following this activity in ICC-MP [13].

Identity of the $K_V7.5$-positive cells

Immunohistochemistry showed that in tissue ICC-IM, but not ICC-MP, were positive for $K_V7.5$. ICC-MP are primarily branching cells, whereas ICC-IM are a mix of branching and bipolar cells. This was corroborated in the cultured cells where we found branching and bipolar cells, positive both for c-Kit and $K_V7.5$. Although cells in the short-term culture may differentiate in unpredictable ways, the composition and structural features of c-Kit-positive

cells in culture were similar to that in tissue: a mix of branching and bipolar cells with some, but not all, branching cells positive for $K_V7.5$. We confirmed using single cell RT-PCR that in our culture, all of the $K_V7.5$positive ICC were positive for Ano1. Therefore, $K_V7.5$ appears to identify mouse colonic ICC-IM when used in conjunction with Ano1.

Cholinergic stimulation of ICC: relationship between ICC-MP and ICC-IM

ICC-IM were shown to be heavily innervated by cholinergic neurons (much more so that ICC-MP) and have the $K_V7.5$ channel; inhibition of K_V7 channels by cholinergic neurotransmitters will enhance cell excitability. When an ICC becomes excited, it is possible that pacemaker mechanisms are activated. Cholinergic stimulation causes ICC-IM depolarisation since current amplitude decreased before the onset of full current inhibition by CCh or blockade by XE991. Cholinergic stimulation leads to depolarisation and increased intracellular Ca^{2+}, which activates maxi chloride channels in small intestinal ICC [46], which may be involved in generating the ICC pacemaker potential [20, 30, 44, 49]. In the present study, we show that high conductance inwardly rectifying currents were activated in colonic ICC-IM by XE991. This strongly supports the hypothesis that cholinergic signalling activates ICC-IM by inhibition of K_V7 channels, resulting in increased cell excitability. We hypothesize that depolarisation caused by blockade of K_V7 channels by XE991 led to activation of the inward currents. The currents resembled inwardly rectifying maxi chloride currents that we have previously recorded from small intestinal ICC-MP [20, 30, 31, 44, 46, 49]. In neurons, XE991 enhances cell excitability as evidenced by more frequent action potentials observed during intracellular microelectrode recordings [6]. ICC-MP and ICC-IM may cooperate in the generation of pacemaker activity; their excitability may be regulated by cholinergic inhibition of

K_V7.5 in ICC-IM and cholinergic modulation of ICC-MP pacemaker activity may occur through ICC-IM.

Comparison to other systems

M-current was first isolated and described in frog sympathetic neurons [4], and subsequently expression in skeletal muscle [34], blood vessels [48] and other smooth muscle cells has been reported. Previous studies have shown expression of K_V7.5 in the microarray analysis of small intestinal ICC [7]. K_V7.5 is also expressed in mouse colonic smooth muscle [22]. K_V7 currents have also been found in ICC from the guinea pig bladder [1]. The features of the K_V7.5 channel activity described in the present study are similar to those of K_V7 channels in Chinese hamster ovary cells transfected with human KCNQ5, where the single channel conductance was 2.2±0.1 pS [25], which is close to our observation of 3.3±0.1 pS (in NMDGCl pipette solution). The K_V7 single channel amplitude versus voltage relationship we reported was similar to that reported for transfected K_V7.5 channels [25]. The activation at ~−20 (−80) mV of K_V7.5 currents recorded from ICC-IM was the same as observed in neurons [6]. The conductance of the K_V7.5 channel currents increased dramatically when high extracellular K^+ pipette solution is used. This is because extracellular monovalent cations (such as $NMDG^+$ or Na^+ etc.) can block K_V channels [3, 29, 38], reducing their conductance, which is why studies on K_V currents are often performed with high K^+ pipette solutions.

K_V7 channel regulation

There are five members of the K_V7 family; channels composed of K_V7.2–5 are responsible for M-current [5, 22, 24]. M-current is often carried by heteromeric K_V7 channels composed

of $K_V7.2$ and $K_V7.3$ [37], $K_V7.3$ and $K_V7.5$ [24] or $K_V7.4$ and $K_V7.5$ [2]. However, currents we recorded were likely carried exclusively by $K_V7.5$ homomers since we provided negative evidence for the expression of $K_V7.2$–4 proteins in ICC-IM and ICC-MP. It is not known which subtype(s) of muscarinic acetylcholine receptors (mAChRs) are involved in the inhibition of $K_V7.5$ currents in colonic ICCIM. K_V7 channel inhibition can occur via PiP_2 degradation [5, 6] or Ca^{2+}-calmodulin [10, 26]; the relative contribution of the two K_V7 inhibition mechanisms requires investigation. Close proximity of mAChRs to the sarcoplasmic reticulum, as proposed for small intestinal ICC-MP, may favour Ca^{2+}-dependent inhibition in ICC-IM because of the superficial buffer barrier [43, 46].

In summary, colonic ICC-IM have a voltage-sensitive K^+ current, activated around the resting membrane potential of the cell, inhibited by cholinergic stimulation and blocked by a K_V7 channel blocker. These data imply inhibition of K_V7 channels as a possible mechanism for excitation of colonic ICC-IM by enteric cholinergic nerves. The close association of ICC-IM with ICC-MP and the presence of the maxi chloride channel in ICC-IM suggest the possibility that ICC-IM and ICC-MP cooperate in generating and regulating colonic pacemaker activity associated with propulsive motility [8, 18].

Acknowledgments This study was supported by the Natural Sciences and Engineering Research Council (NSERC) operating grant #386877 to JH. GW was supported by both a doctoral NSERC Postgraduate Scholarship and an Ontario Graduate Scholarship. Additional support was obtained from the Canadian Institutes of Health Research #MOP-12874 to JH. RLV was supported by CONACYT (Consejo Nacional de Ciencia y Tecnología, México,

scholarship 290618). Some of the data in this manuscript were previously published in abstract form [45]. We thankfully acknowledge Dr. Waliul Khan for the use of his thermal cycler and documentation system. We also acknowledge Drs. Luke Janssen and Wolfgang Kunze for their helpful discussions on analysis.

Ethical standards The experiments described herein were performed in accordance with the guidelines of the Canadian Council on Animal Care (CCAC) and received approval from the McMaster University Animal Research Ethics Board (AREB).

Conflicts of interest The authors declare that they have no conflicts of interest.

References

1. Anderson UA, Carson C, McCloskey KD (2009) KCNQ currents and their contribution to resting membrane potential and the excitability of interstitial cells of Cajal from the guinea pig bladder. J Urol 182:330–336
2. Bal M, Zhang J, Zaika O, Hernandez CC, Shapiro MS (2008) Homomeric and heteromeric assembly of KCNQ (Kv7) K+ channels assayed by total internal reflection fluorescence/fluorescence resonance energy transfer and patch clamp analysis. J Biol Chem 283:30668–30676
3. Block BM, Jones SW (1997) Delayed rectifier current of bullfrog sympathetic neurons: ion-ion competition, asymmetrical block and effects of ions on gating. J Physiol 499(Pt 2): 403–416
4. Brown DA, Adams PR (1980) Muscarinic suppression of a novel voltage-sensitive K+ current in a vertebrate neurone. Nature 283: 673–676
5. Brown DA, Hughes SA, Marsh SJ, Tinker A (2007) Regulation ofM(Kv7.2/7.3) channels in neurons by PIP(2) and products of PIP(2) hydrolysis: significance for receptor-mediated inhibition. J Physiol 582:917–925
6. Brown DA, Passmore GM (2009) Neural KCNQ (Kv7) channels. BrJ Pharmacol 156:1185–1195
7. Chen H, Ordog T, Chen J, Young DL, Bardsley MR, Redelman D, Ward SM, Sanders KM (2007) Differential gene expression in functional classes of interstitial cells of Cajal in murine small intestine. Physiol Genomics 31:492–509

8. Chen JH, Zhang Q, Yu Y, Li K, Liao H, Jiang L, Hong L, Du X, Hu X, Chen S, Yin S, Gao Q, Yin X, Luo H, Huizinga JD (2013) Neurogenic and myogenic properties of pan-colonic motor patterns and their spatiotemporal organization in rats. PLoS One 8:e60474
9. Costa M, Dodds KN, Wiklendt L, Spencer NJ, Brookes SJ, Dinning PG (2013) Neurogenic and myogenic motor activity in the colon of the guinea-pig, mouse, rabbit and rat. Am J Physiol Gastrointest Liver Physiol 305:G749–G759
10. Delmas P, Brown DA (2005) Pathways modulating neural KCNQ/M(Kv7) potassium channels. Nat Rev Neurosci 6:850–862
11. Edwards FR, Hirst GD (2006) An electrical analysis of slow wave propagation in the guinea-pig gastric antrum. J Physiol 571:179–189
12. Faussone Pellegrini MS, Cortesini C, Romagnoli P (1977) Ultrastructure of the tunica muscularis of the cardial portion of the human esophagus and stomach, with special reference to the so-called Cajal's interstitial cells. Arch Ital Anat Embriol 82:157–177
13. Hennig GW, Hirst GD, Park KJ, Smith CB, Sanders KM, Ward SM, Smith TK (2004) Propagation of pacemaker activity in the guinea-pig antrum. J Physiol 556:585–599
14. Hirst GD, Beckett EA, Sanders KM, Ward SM (2002) Regional variation in contribution of myenteric and intramuscular interstitial cells of Cajal to generation of slow waves in mouse gastric antrum. J Physiol 540:1003–1012
15. Hirst GD, Dickens EJ, Edwards FR (2002) Pacemaker shift in the gastric antrum of guinea-pigs produced by excitatory vagal stimulation involves intramuscular interstitial cells. J Physiol 541:917–928
16. Hirst GD, Garcia-Londono AP, Edwards FR (2006) Propagation of slow waves in the guinea-pig gastric antrum. J Physiol 571:165–177
17. Huizinga JD and Chen JH (2014) Interstitial cells of Cajal: update on clinical and basic science. Curr Gastroenterol Rep 16:363–374
18. Huizinga JD, Martz S, Gil V, Wang XY, Jimenez M, Parsons S (2011) Two independent networks of interstitial cells of Cajal work cooperatively with the enteric nervous system to create colonic motor patterns. Front Neurosci 5:93
19. Huizinga JD, Thuneberg L, Kluppel M, Malysz J, Mikkelsen HB, Bernstein A (1995) W/kit gene required for interstitial cells of Cajal and for intestinal pacemaker activity. Nature 373:347–349
20. Huizinga JD, Zhu Y, Ye J, Molleman A (2002) High-conductance chloride channels generate pacemaker currents in interstitial cells of Cajal. Gastroenterology 123:1627–1636
21. Ipavec V, Martire M, Barrese V, Taglialatela M, Curro D (2011) KV7 channels regulate muscle tone and non-adrenergic noncholinergic relaxation of the rat gastric fundus. Pharmacol Res 64:397–409
22. Jepps TA, Greenwood IA, Moffatt JD, Sanders KM, Ohya S (2009) Molecular and functional characterization of Kv7 K+ channel in murine gastrointestinal smooth muscles. Am J Physiol Gastrointest Liver Physiol 297:G107–G115
23. Komuro T (2006) Structure and organization of interstitial cells of Cajal in the gastrointestinal tract. J Physiol 576:653– 658
24. Lerche C, Scherer CR, Seebohm G, Derst C, Wei AD, Busch AE, Steinmeyer K (2000) Molecular cloning and functional expression of KCNQ5, a potassium channel subunit that may contribute to neuronal M-current diversity. J Biol Chem 275:22395–22400

25. Li Y, Gamper N, Shapiro MS (2004) Single-channel analysis of KCNQ K+ channels reveals the mechanism of augmentation by a cysteine-modifying reagent. J Neurosci 24:5079–5090
26. Linley JE, Pettinger L, Huang D, Gamper N (2012) M channel enhancers and physiological M channel block. J Physiol 590:793– 807
27. Liu LW, Huizinga JD (1993) Electrical coupling of circular muscle to longitudinal muscle and interstitial cells of Cajal in canine colon. J Physiol 470:445–461
28. Molleman A (2003) Patch clamping an introductory guide to patch clamp electrophysiology. Wiley, New York
29. Parsons SP, Huizinga JD (2010) Transient outward potassium current in ICC. Am J Physiol Gastrointest Liver Physiol 298: G456–G466
30. Parsons SP, Kunze WA, Huizinga JD (2012) Maxi-channels recorded in situ from ICC and pericytes associated with the mouse myenteric plexus. Am J Physiol Cell Physiol 302:C1055–C1069
31. Parsons SP, Sanders KM (2008) An outwardly rectifying and deactivating chloride channel expressed by interstitial cells of Cajal from the murine small intestine. J Membr Biol 221:123–132
32. Pluja L, Alberti E, Fernandez E, Mikkelsen HB, Thuneberg L, Jimenez M (2001) Evidence supporting presence of two pacemakers in rat colon. Am J Physiol Gastrointest Liver Physiol 281:G255– G266
33. Rae MG, Fleming N, McGregor DB, Sanders KM, Keef KD (1998) Control of motility patterns in the human colonic circular muscle layer by pacemaker activity. J Physiol 510(Pt 1):309–320
34. Roura-Ferrer M, Etxebarria A, Sole L, Oliveras A, Comes N, Villarroel A, Felipe A (2009) Functional implications of KCNE subunit expression for the Kv7.5 (KCNQ5) channel. Cell Physiol Biochem 24:325–334
35. Rumessen JJ, Thuneberg L, Mikkelsen HB (1982) Plexus muscularis profundus and associated interstitial cells. II. Ultrastructural studies of mouse small intestine. Anat Rec 203:129–146
36. Sanders KM, Koh SD, Ward SM (2006) Interstitial cells of Cajal as pacemakers in the gastrointestinal tract. Annu Rev Physiol 68:307– 343
37. Schroeder BC, Hechenberger M, Weinreich F, Kubisch C, Jentsch TJ (2000) KCNQ5, a novel potassium channel broadly expressed in brain, mediates M-type currents. J Biol Chem 275:24089– 24095Shibasaki T (1987) Conductance and kinetics of delayed rectifier potassium channels in nodal cells of the rabbit heart. J Physiol 387: 227–250
38. Smith TK, Reed JB, Sanders KM (1987) Interaction of two electrical pacemakers in muscularis of canine proximal colon. Am J Physiol 252:C290–C299
39. Thomsen L, Robinson TL, Lee JC, Farraway LA, Hughes MJ, Andrews DW, Huizinga JD (1998) Interstitial cells of Cajal generate a rhythmic pacemaker current. Nat Med 4:848–851
40. Thuneberg L (1982) Interstitial cells of Cajal: intestinal pacemaker cells? Adv Anat Embryol Cell Biol 71:1–130
41. Thuneberg L (1999) One hundred years of interstitial cells of Cajal. Microsc Res Tech 47:223–238

42. van Breemen C, Chen Q, Laher I (1995) Superficial buffer barrier function of smooth muscle sarcoplasmic reticulum. Trends Pharmacol Sci 16:98–105
43. Wang B, Kunze WA, Zhu Y, Huizinga JD (2008) In situ recording from gut pacemaker cells. Pflugers Arch 457:243–251
44. Wright G, Parsons SP, Huizinga JD (2012) Colonic interstitial cells of Cajal associated with the myenteric plexus harbour ion channels regulated by excitatory neurotransmitters. Neurogastroenterol Motil 24(S2):156
45. Wright GW, Parsons SP, Huizinga JD (2012) Ca(2+) sensitivity of the maxi chloride channel in interstitial cells of Cajal. Neurogastroenterol Motil 24:e221–e234
46. Yoneda S, Fukui H, Takaki M (2004) Pacemaker activity from submucosal interstitial cells of Cajal drives high-frequency and low-amplitude circular muscle contractions in the mouse proximal colon. Neurogastroenterol Motil 16:621–627
47. Zhong XZ, Harhun MI, Olesen SP, Ohya S, Moffatt JD, Cole WC, Greenwood IA (2010) Participation of KCNQ (Kv7) potassium channels in myogenic control of cerebral arterial diameter. J Physiol 588:3277–3293
48. Zhu MH, Kim TW, Ro S, Yan W, Ward SM, Koh SD, Sanders KM (2009) A Ca(2+)-activated Cl(−) conductance in interstitial cells of Cajal linked to slow wave currents and pacemaker activity. J Physiol 587:4905–4918

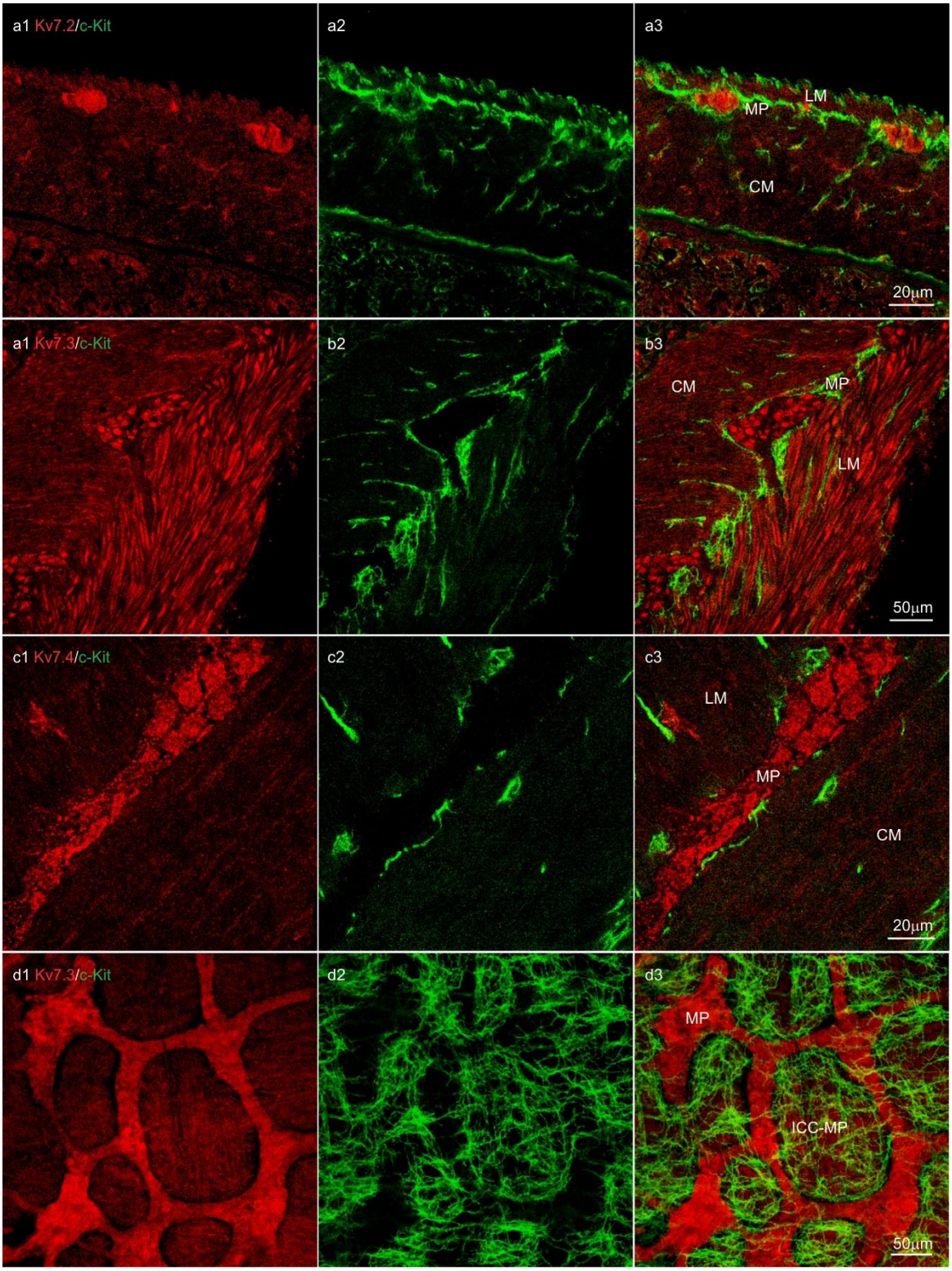
a1 Kv7.2/c-Kit
a2
a3
LM
MP
CM
20μm
a1 Kv7.3/c-Kit
b2
b3
CM
MP
LM
50μm
c1 Kv7.4/c-Kit
c2
c3
LM
MP
CM
20μm
d1 Kv7.3/c-Kit
d2
d3
MP
ICC-MP
50μm

Supplementary Fig. 1: Double labeling of c-Kit (green) and K_V7.2/7.3/7.4 (red) in mouse colon. Top three groups of figures were from cross sections, bottom group from musculature wholemount preparation. Enteric nerves at the level of myenteric plexus (MP) were positive for K_V7.2 and K_V7.4. Enteric nerves and smooth muscles in the longitudinal muscle (LM) layer were positive for K_V7.3. No co-localization was found between K_V7.2/7.3/7.4 and c-Kit. CM: circular muscle.

CHAPTER 4: CHENODEOXYCHOLIC ACID ACTIVATES THE MOUSE COLONIC INDUCIBLE PACEMAKER VIA STIMULATION OF NITRERGIC NERVES

4.1 Preface

The body of this chapter was reproduced from a journal article, submitted to The Journal of Neurogastroenterology and Motility, of which I am the first author. Permission to use this material is mine as I hold the copyright until it is transferred to the publisher, The Korean Society of Neurogastroenterology and Motility, once the article is published.

Wright GWJ, Parsons SP, Zhu YF and Huizinga JD (2016) Chenodeoxycholic acid activates the mouse colonic inducible pacemaker via stimulation of nitrergic nerves. *J Neurogastroenterol Motil* (Submitted)

As the first author of this paper I planned the study, performed all the electrophysiology experiments, analyzed all the data, wrote the manuscript, prepared the figures and edited the manuscript during review. Sean P Parsons provided the phase-amplitude analysis ImageJ plugin and helped with interpretation. Yong Fang Zhu taught me intracellular recording and provided the MATLAB continuous wavelet transform analysis and fast Fourier transform analysis program and helped with interpretation. Jan D Huizinga supervised and planned the study, provided the funding, and edited the manuscript during review.

4.2 Paper Full Text

Chenodeoxycholic acid activates the mouse colonic inducible pacemaker via stimulation of nitrergic nerves

George WJ Wright, Sean P Parsons, Yong Fang Zhu and Jan D Huizinga

McMaster University, Department of Medicine, Farncombe Family Digestive Health Research Institute, Hamilton, ON, Canada

Running Title:

CDCA activates colonic inducible ICC-MP

Address for Correspondence:

Dr. Jan D. Huizinga,

McMaster University,

HSC 3N8,

1280 Main St. W.,

Hamilton,

ON,

L8S 4K1,

Canada

Phone: 1-905-525-9140 x22584 Fax: 1-905-522-3454

Abstract

Background/Aims The mouse colon has networks of interstitial cells of Cajal (ICC) associated with the myenteric plexus (ICC-MP) and with the submuscular plexus (ICC-SMP). Our

aim was to determine stimuli that could evoke low-frequency rhythmic depolarising activity from the mouse colon inducible pacemaker, putatively found in ICC-MP. **Methods** We recorded mouse colonic smooth muscle membrane potentials with sharp microelectrodes from preparations with or without submucosa. **Results** In control conditions, preparations with submucosa exhibited slow waves at 19.9 ± 3.0 cpm (n=17). In preparations without submucosa and associated ICC-SMP a rhythmic depolarising activity at 8.0 ± 0.6 cpm (n=29) was present in the absence of ~20 cpm slow waves. The bile acid chenodeoxycholic acid (250 μM) evoked low-frequency rhythmic transient depolarisations (n=9); in submucosa intact preparations at 3.6 ± 0.9 cpm (n=5), and at 2.5 ± 0.8 cpm (n=4) in preparations without submucosa. With submucosa intact, rhythmic transient depolarisations interacted with the ICC-SMP slow waves by phase amplitude coupling, with submucosa removed the rhythmic transient depolarisations interacted with the 8 cpm slow wave by phase amplitude coupling. Chenodeoxycholic acid evoked rhythmic IJPs at 22.5 ± 11.8 cpm (n=7), implying the activation of nitrergic nerves. The NO donor sodium nitroprusside (1 μM) evoked rhythmic transient depolarisations at 1.7 ± 1.3 cpm (n=7) in preparations without submucosa. **Conclusions** This study highlights a mechanism by which ICC generate rhythmic transient depolarisations, which contribute the creation of motility patterns in the colon. It provides the hypothesis that chenodeoxycholic acid evokes low-frequency pacemaker activity in ICC-MP via TGR5 receptor activation on nitrergic nerves.

Key Words

Colon; Interstitial cells of Cajal; Chenodeoxycholic acid; Nitric oxide, Nitrergic nerves

Introduction

Ever since interstitial cells of Cajal (ICC) were proven to be pacemaker cells for gastrointestinal motility (Huizinga, et al., 1995; Thomsen, et al., 1998), understanding the relative roles of ICC and enteric nerves in generating motor patterns has been a major focus of research. With respect to the colon, this has been reinforced by studies that identify ICC dysfunction as a potential cause of colonic dysmotility; Farrugia wrote that "the marked reduction of ICC is the only consistent pathology finding in patients with chronic constipation" (Knowles and Farrugia, 2011). It is not assumed that ICC lesions are the only cause, but their importance was also highlighted by a high-resolution colonic motility study that showed a correlation between the absence of ICC and the inability to generate propulsive contractile activity in children with chronic constipation (Giorgio, et al., 2013). In many cases, the role of ICC in motor pattern generation is uncontested, such as the regular 3 cpm propulsive contractions in the stomach (Edwards and Hirst, 2006; Koch, et al., 1987), and the role of ICC in generating the 40 cpm propulsive contractions in the mouse proximal intestine are also without dispute (Der-Silaphet, et al., 1998).

Dissecting tissues to isolate a specific ICC network, together with associated muscle layers, has given us much insight into the role of those ICC networks. For the colon, this started with studies in the canine that showed the ICC-SMP to be the source of the dominant slow wave activity (Sabourin, et al., 1990), many confirmatory studies followed (Liu and Huizinga, 1993; Liu, et al., 1998; Smith, et al., 1987). Recent studies in the mouse and rat colon have confirmed this role of ICC-SMP, and they gave further insight into the potential role of ICC-MP in generating a second low-frequency stimulus-dependent electrical activity (Yoneda, et

al., 2002; Yoneda, et al., 2004; Pluja, et al., 2001; Huizinga, et al., 2011). The second pacemaker activity of the colon, generated by ICC-MP has several characteristics that are different from the primary pacemaker. The activity is not omnipresent, is abolished by calcium channel blockers, and hence, it appears to be dependent on driving the membrane potential above threshold for calcium channel activation, thus, its occurrence will then be dependent on a stimulus. Stimulus-dependent pacemaking also occurs in mouse small intestine and it was shown to interact with the primary pacemaker system to generate the typical segmentation motor pattern of the small intestine (Huizinga, et al., 2014; Pawelka and Huizinga, 2015). This opened the research field of interactions between different ICC networks as a basis for the generation of certain motor patterns (Huizinga, et al., 2015).

The elucidation of the precise role of ICC has been hampered by the fact that ICC and the enteric nervous system (ENS) are so closely intertwined. Not only are ICC essential for the transmission of certain neural excitatory or inhibitory pathways to smooth muscle (Ward, et al., 2000; Wang, et al., 2003; Ward and Sanders, 2006; Zhu, et al., 2014; Lies, et al., 2014), neurotransmitters might also be the prime stimulators for the induced pacemaker activity of certain ICC networks. An excellent example of this was shown by Bayguinov and colleagues (2010), who utilized Ca^{2+} imaging to record from colonic ICC-MP, which are under tonic inhibition by nitrergic nerves, but respond to mechanical stimulus-induced release of acetylcholine and substance P with rhythmic Ca^{2+} transients.

Bile acids are endogenously synthesized detergent molecules released into the duodenum, via the gall bladder and bile ducts, to emulsify fats facilitating digestion and absorption (Camilleri

and Gores, 2015; Bajor, et al., 2010). The two main primary bile acids are cholic acid and chenodeoxycholic acid, which are synthesized from cholesterol in the liver and recirculated from the distal ileum via Na^+-dependent bile salt transporters in the epithelial cells, back into the enterohepatic circulation (Camilleri and Gores, 2015; Frommherz, et al., 2016). In certain diseases, high concentrations of bile acids enter the colon and can cause diarrhea (Lee, 2015). Both intrinsic primary afferent neurons (IPANs) and enterochromaffin cells have TGR5 G-protein coupled receptors that are activated by bile acids (Alemi, et al., 2013). Interestingly, the bile acid receptor is also found in the myenteric plexus where over 80% of NO synthase-expressing inhibitory nerves are positive for the TGR5 receptor (Poole, et al., 2010). Bile acids may not only influence the colon through the lumen, but they also circulate in the blood (Frommherz, et al., 2016), so that they can affect myenteric plexus function, possibly activating nitrergic nerves. Activation of nitrergic nerves can result in inhibitory junction potentials and subsequent inhibition of motor activities, but it can also play a role in the orchestration of rhythmic propulsive motor activities (Diamant, 1989; Bogeski, et al., 2005; Ferens, et al., 2007; Matchkov, 2010). The objective of the present study was to investigate potential action of the bile acid chenodeoxycholic acid on the electrical activity of the circular muscle of the mouse colon, as well as the action of a NO donor, so that a potential mechanism of action of the bile acid on inhibitory nerves could be postulated.

Materials and Methods

Animals

All procedures were approved by the Animal Research Ethics Board (AREB) of McMaster University as per guidelines from the Canadian Council on Animal Care. Female CD-1 mice

(Charles River Laboratories, St Constant, QC) were housed in the McMaster University central animal facility with *ad libitum* access to food and water. Mice >6 weeks old were killed via cervical dislocation.

Dissection

Mouse intestines were removed and placed into Krebs bubbled with 95% O_2 5% CO_2, with 5 μM atropine. Then the whole colon was cut open along the mesenteric border. Two different preparations were used in this study; in the first, the submucosa and mucosa were removed and in the second, only the mucosa was removed, leaving the submucosal plexus intact, with associated ICC. Proximal and mid colon muscle tissues were prepared and pinned out circular muscle face up or Sylgard® coated dishes.

Electrophysiology

Intracellular recording was performed on colonic smooth muscle preparations using Zeiss Axiovert S100 TV inverted microscope (Carl Zeiss Canada Ltd., Toronto, ON, CA). Cells were impaled with microelectrodes made from borosilicate glass capillaries (BF150-86-10, OD: 1.5 mm, ID: 0.86 mm, Sutter Instruments, Novato, CA, USA) pulled to a resistance of 25-45 MΩ with a Flaming/Brown model P-97 pipette puller (Sutter Instruments), filled with 3 M KCl. Microelectrodes were attached to a CV-7B headstage, connected to a Multiclamp 700B amplifier, then to a Digidata 1322A digitizer (all from Molecular Devices, Sunnyvale, CA, USA). The digitizer was connected to a PC running Clampex 9.2 and Multiclamp commander software (both from Molecular Devices). The headstage was mounted on a MC-35A micromanipulator (Narishige International Inc., East Meadow, NY) connected to a Newport

stand (model 150 magnetic base, model 45 post and model 340-RC clamp; Newport Corporation, Irvine, CA, USA) mounted on a Micro-g vibration isolation table (Technical Manufacturing Corporation, San Francisco, CA, USA), all enclosed in a custom-built, grounded, Faraday cage. Preparations were perfused constantly with 30-35°C Krebs by a Peri-Star Pro peristaltic pump (World Precision Instruments, Sarasota, FL, USA). Membrane potentials were sampled at 20 kHz and filtered with a 10 kHz Bessel filter.

We recorded membrane potentials of mouse proximal colon smooth muscle cells using sharp microelectrodes. Very little spontaneous electrical activity was observed in the presence of 2 μM nicardipine (data not shown). In the presence of 5 μM atropine and absence of nicardipine, some spontaneous contractility was observed, yet we could record electrical activity. Nicardipine was thus avoided to allow observation of calcium channel-dependent activities.

Solutions and Drugs

Tissues were kept in Krebs solution containing (in mM): 118.1 NaCl, 4.8 KCl, 1.0 NaH_2PO_4, 1.2 $MgCl_2$, 2.5 $CaCl_2$, 11.1 dextrose and 25 $NaHCO_3$, with pH 7.35. All drugs were purchased from Sigma-Aldrich, Burlington, ON unless otherwise indicated. Atropine was dissolved in DMSO, nicardipine in 50% ethanol, chenodeoxycholic acid (Cayman Chemicals, Ann Arbor, MI) in ethanol and both tetrodotoxin and sodium nitroprusside in distilled water. DMSO never exceeded 0.1% of the final solution. All drugs were kept at -20°C once aliquoted apart from sodium nitroprusside, which was prepared before experiments as required.

Data Analysis and Statistics

Differences between control and drug treated states were assessed using two-tailed homoscedastic Student's t-tests with $\alpha=0.05$. Means are reported as the average of n experiments ± standard deviation. Membrane potential traces in figures were filtered in Clampfit with an 8-pole Bessel low pass filter, followed by a notch electrical interference filter to eliminate 60 Hz noise. Then the data were decimated to either 4 kHz or 0.2 kHz for plotting. Figures were created using Corel Draw X5 (Corel Corporation, Ottawa, ON) and Origin 8.0 graphing software (OriginLab Corporation, Northampton, MA).

Fast Fourier Transform (FFT) analysis was performed on membrane potential recordings to decompose the time series of membrane potentials and separate them into their component frequencies (Huizinga, et al., 2014). This was performed using a program written in MATLAB (MathWorks, Natick, MA), calling the predefined FFT function. The output of the program produced one-sided power/frequency plots. Continuous wavelet transform (CWT) analysis was performed on membrane potential recordings, using the same MATLAB program for FFT, to determine the frequency components present in each recording over time. Phase amplitude coupling analysis was performed on membrane potential recordings using a plugin programmed for ImageJ (NIH, Bethesda, MD). Potentials were analyzed to determine whether the phase of one frequency component present in the recording interacted with the amplitude of another frequency component. Frequency ranges were chosen to capture the relative low-frequency and high-frequency components from the recordings. For a more detailed description of these methods see Huizinga et al. (2015).

Results

Preparation with Submucosa and ICC-SMP Intact

Spontaneous Slow Wave Activity

In preparations with submucosa and associated ICC-SMP intact, slow wave activity occurred at 19.9 ± 3.0 cpm (n=17; Fig. 1A-C).

Chenodeoxycholic Acid Induced Activity

Chenodeoxycholic acid (250 μM) evoked rhythmic transient depolarizations at 3.6 ± 0.9 cpm (n=5) with an amplitude of 2.2 ± 0.7 mV (n=5; Fig. 1D & E) in preparations with submucosa intact. In some experiments, smooth muscle action potentials were triggered by the upstroke of the rhythmic transient depolarisations (Fig. 1 D & E). Continuous wavelet transform (CWT) analysis of the example trace in Figure 1D revealed frequencies at ~3 cpm and ~20 cpm (Fig. 1F); the power spectrum of those frequencies determined by fast Fourier transform analysis (FFT) is shown in Figure 1G. After the addition of chenodeoxycholic acid, the frequency of the slow wave was 18.5 ± 1.9 cpm (n=11; Fig. 1E), which was not significantly different from the control frequency (19.9 ± 3.0 cpm, n=17; p=0.188). The rhythmic transient depolarisations interacted by phase amplitude coupling with the slow waves (Fig. 1H); the amplitudes of the slow waves were enhanced by the phase of the rhythmic transient depolarizations.

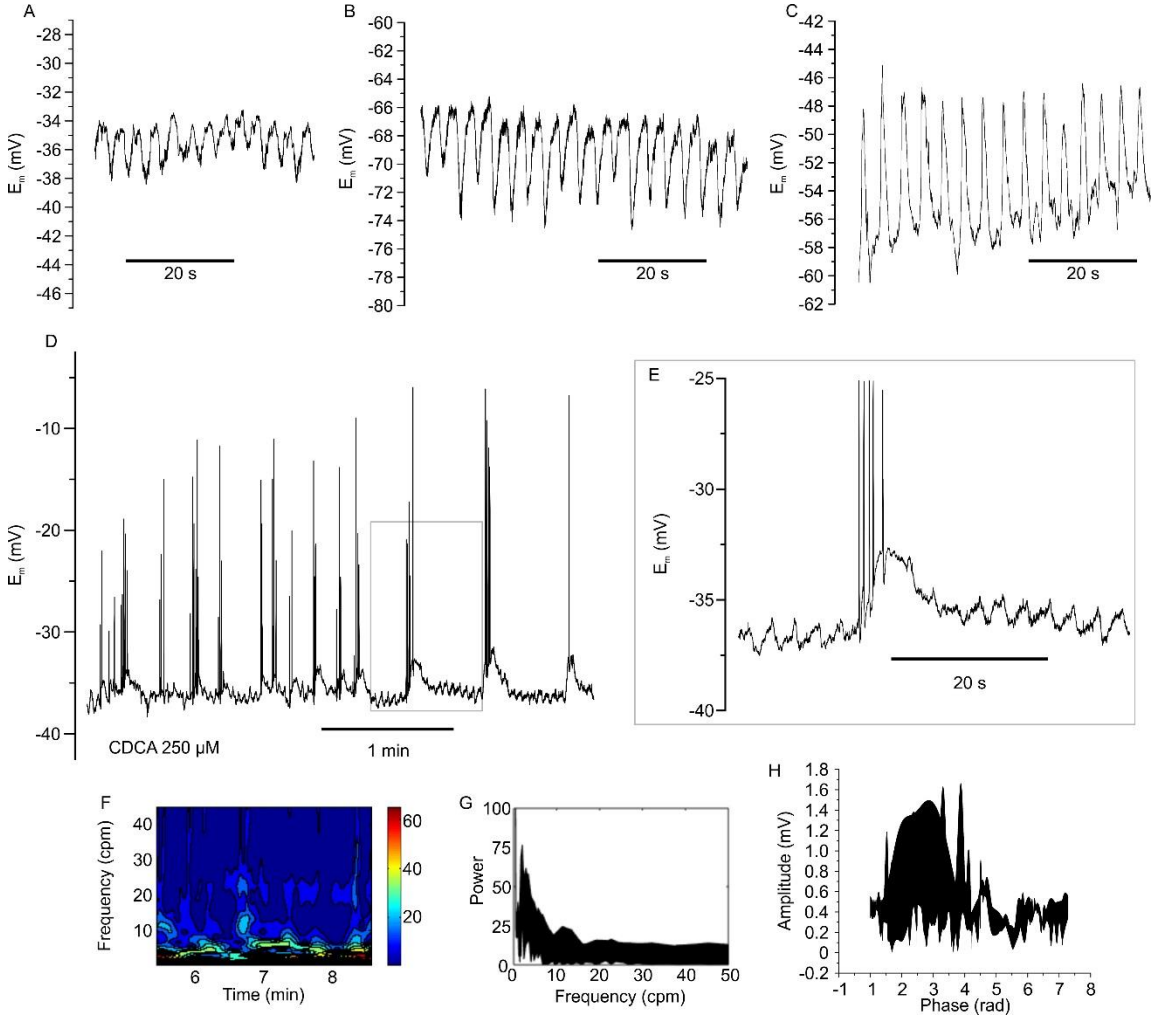

Fig. 1: Chenodeoxycholic acid (CDCA; 250 µM) evoked rhythmic transient depolarisations in preparations with intact submucosa. A) Rhythmic ICC-SMP slow wave activity example trace exhibiting 19 cpm slow waves from proximal colon. B) Example trace exhibiting 20 cpm slow waves from mid colon. C) Second example trace of proximal colon slow waves at 17 cpm. D) Rhythmic transient depolarisations evoked by chenodeoxycholic acid. Rhythmic transient depolarisations evoked smooth muscle action potentials (APs); 19 cpm slow wave depolarizations are also visible. E) Magnified potential trace from box in D. Frequency analysis of control and chenodeoxycholic acid evoked electrical activity from trace in (D). F)

Phase amplitude plot depicting interaction between 0.2-5 cpm and 15-30 cpm frequency components in (D). G) Time-frequency contour plots showing the frequency components from (D) calculated using CWT. H) Power spectrum-frequency distribution of recordings depicting the strength of frequency components evoked by chenodeoxycholic acid calculated using FFT. Potentials recorded in the presence of 5 μM atropine.

Chenodeoxycholic acid also evoked rhythmic inhibitory junction potentials (IJPs) in previously quiescent preparations with ICC-SMP intact, which occurred at 22.5 ± 11.8 cpm, with an amplitude of -8.6 ± 5.2 mV (n=7; Fig. 2A & B). In another set of experiments without chenodeoxycholic acid, rhythmic IJPs also occurred spontaneously at 21.7 ± 5.0 cpm with an amplitude of IJPs, -9.4 ± 4.2 mV (n=3), these values were not significantly different from the frequency (p=0.915) and amplitude (p=0.810) of IJPs evoked by chenodeoxycholic acid.

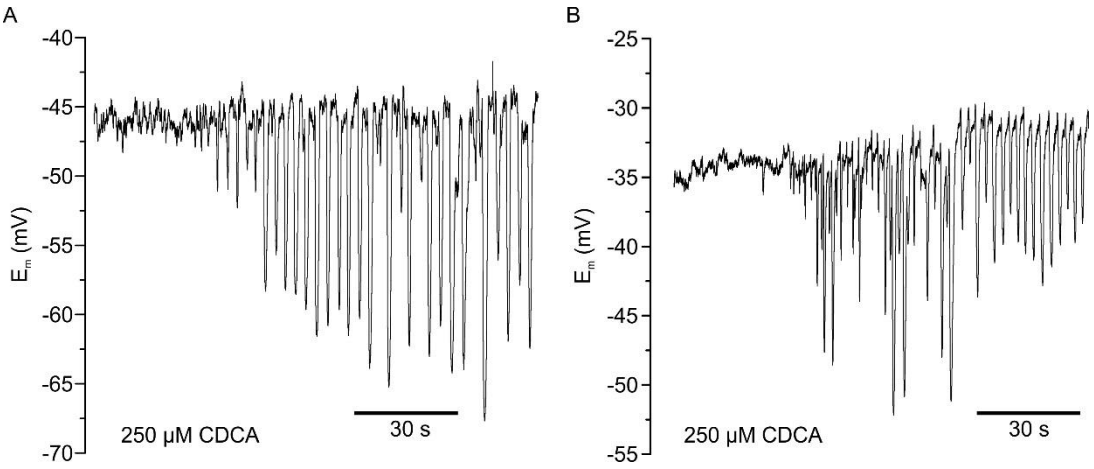

Fig. 2: Chenodeoxycholic acid (CDCA; 250 μM) evoked inhibitory junction potentials (IJPs) shown from two different preparations with submucosa intact; recorded in the presence of 5 μM atropine.

Preparation with Submucosa and ICC-SMP Removed

Spontaneous Electrical Activity

The most common electrical activity in the muscle preparations without submucosa (and associated ICC-SMP) had a frequency of 8.0 ± 0.6 cpm (n=29; Fig. 3B) and an amplitude of 1.3 ± 0.7 mV (n=29). Action potential activity was frequently observed at 221.7 ± 60.8 cpm (n=24) before and at 240.5 ± 63.0 cpm (n=22) after chenodeoxycholic acid (p=0.31). Rhythmic transient depolarisations were observed spontaneously at a frequency of 2.3 ± 0.7 cpm (n=13), excluding the possibility that they originated from the ICC-SMP.

Chenodeoxycholic Acid Induced Activity

In spontaneously quiescent preparations, chenodeoxycholic acid induced rhythmic transient depolarisations with a frequency of 2.1 ± 0.1 cpm and an amplitude of 6.5 ± 8.1 mV (n=4; Fig. 3C). The power and time distribution of frequencies from example traces in Fig. 3, calculated with FFT and CWT analyses, show both the ~2 cpm and ~8 cpm frequencies (Fig. 3D-I). Rhythmic transient depolarisations in the range of 0.1-3 cpm enhanced the amplitude 8 cpm slow wave (range 6-12 cpm) by phase-amplitude coupling (Fig. 3J).

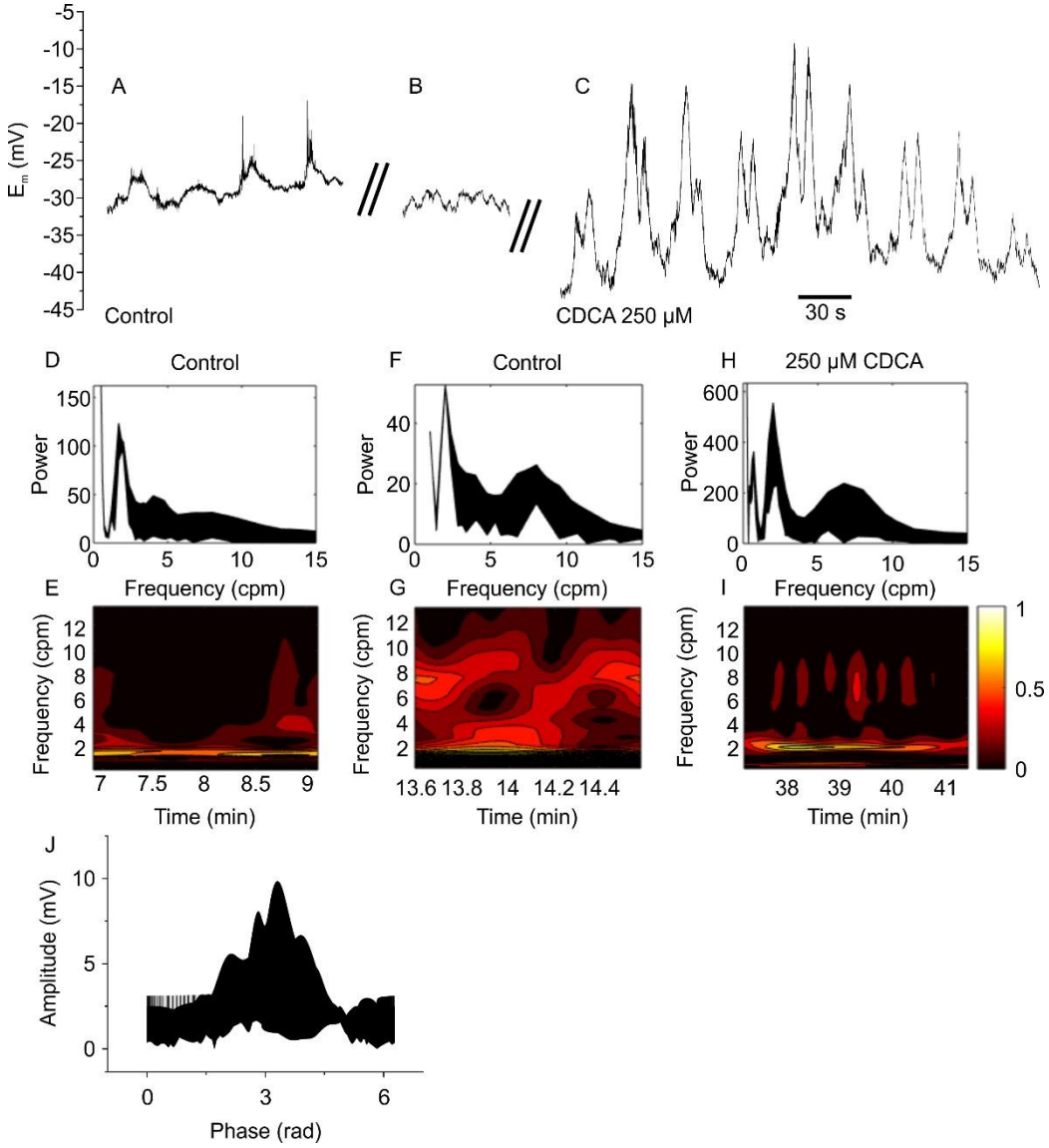

Fig. 3: Chenodeoxycholic acid (250 µM; CDCA) activated low-frequency high-amplitude rhythmic transient depolarizations in preparations without submucosa. A) Control recordings exhibiting low-amplitude rhythmic transient depolarisations and 8 cpm slow wave (B) prior to addition of chenodeoxycholic acid. C) Rhythmic transient depolarisations evoked by chenodeoxycholic acid, which occurred concurrently with the 8 cpm slow wave. Trace in B was recorded 4.5 min after trace in A; trace in C recorded 22.5 min after trace in B. D-I) Fre-

quency analysis of control and chenodeoxycholic acid evoked electrical activity from traces A, B and C. D, F and H) Power spectrum-frequency distribution of recordings depicting the strength of frequency components from control (A and B) and chenodeoxycholic acid (C) calculated using FFT. E, G, and I) Time-frequency contour plots showing the frequency components of control (A and B) and chenodeoxycholic acid (C) recordings over time calculated using CWT. J) Phase amplitude plot depicting interaction between 0.1-3 cpm and 6-12 cpm frequency components in (C). Potentials recorded in the presence of 5 μM atropine.

Sodium Nitroprusside Evoked Activity

Sodium nitroprusside evoked rhythmic transient depolarisations at 1.7 ± 1.3 cpm; at an amplitude of 6.3 ± 6.8 mV (Fig 4B; n=7). TTX blocked the rhythmic transient depolarisations (Fig. 4B & C). The power and time distribution of frequencies from example traces in Fig. 4, calculated with FFT and CWT analyses, show the ~2 cpm frequency evoked by sodium nitroprusside and blocked by TTX (Fig. 4D-I). The phase of the rhythmic transient depolarisations (0.2-3 cpm) enhanced the amplitude of the 8 cpm slow wave (5-12 cpm; Figs. 4J-L).

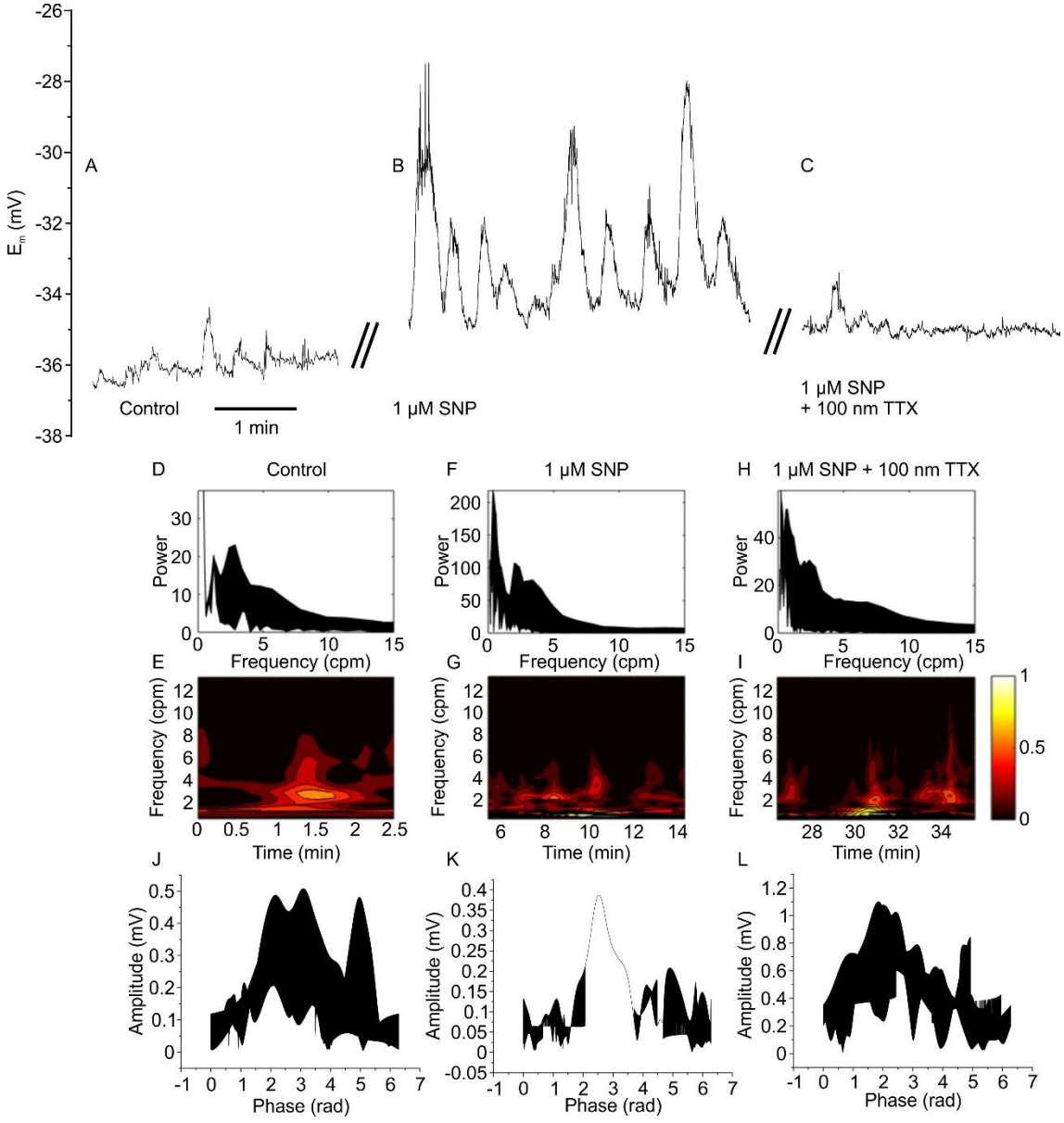

Fig. 4: Sodium nitroprusside (SNP; 1 µM) evoked rhythmic transient depolarizations. A) Control recording with sporadic rhythmic transient depolarisations. B) Sodium nitroprusside activated rhythmic transient depolarisations, enhanced their amplitude and increased the regularity of the frequency. Note that smooth muscle action potentials were triggered by some of the rhythmic transient depolarisations. C) TTX (100 nM) blocked rhythmic transient de-

polarisations evoked by sodium nitroprusside, which was added with TTX. Trace in B was recorded 2 min after A, and trace in C was recorded 17.25 min after B. D-I) Frequency analysis of control, sodium nitroprusside evoked electrical activity from traces A, B and C. D, F, and H) Power spectrum-frequency distributions of recordings depicting the strength of frequency components from control (A), sodium nitroprusside (B) and sodium nitroprusside + TTX (C) calculated using FFT. E, G, and I) Time-frequency contour plots showing the frequency components of control (A), sodium nitroprusside (B) and sodium nitroprusside + TTX (C) recordings over time calculated using CWT. J-L) Phase amplitude plots depicting the interacting between 0.2-3 and 5-12 cpm frequency components in (A, B and C). Potentials recorded in the presence of 5 μM atropine.

Prior to the addition of sodium nitroprusside (1 μM), rhythmic depolarizing activity was present in preparations without submucosa, with a frequency of 8.2 ± 0.9 cpm and an amplitude of 1.41 ± 0.62 mV (n=27). After the addition of sodium nitroprusside, the frequency was 8.0 ± 0.1 cpm (n=17) and the amplitude was 1.23 ± 0.81 mV (n=15; Fig. 5), these values were not significantly different from the frequency (p=0.28) and amplitude (p=0.42) of control values. Action potential activity was observed at 211 ± 91 cpm (n=55) which was not influenced by sodium nitroprusside (p=0.81).

Sodium nitroprusside (1 μM) also evoked rhythmic IJPs in previously quiescent preparations, at 10.0 ± 8.1 cpm, with an amplitude of -4.4 ± 2.8 mV (n=14; Fig. 5B). In another set of experiments without sodium nitroprusside, IJPs occurred spontaneously at 7.4 ± 5.2 cpm, with

an amplitude of -3.3 ± 1.1 mV (n=5), these values were not significantly different from the frequency (p=0.53) and amplitude (p=0.42) of IJPs evoked by sodium nitroprusside.

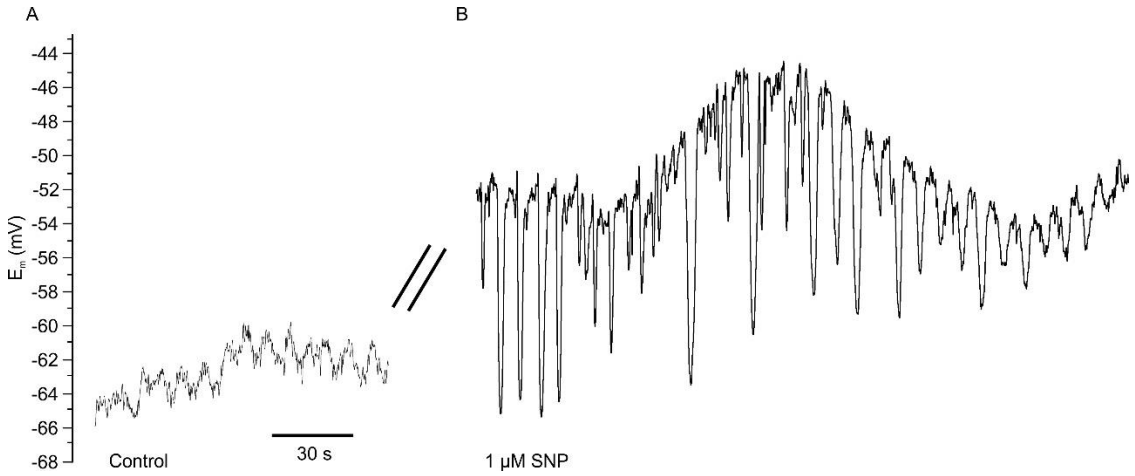

Fig. 5: Sodium nitroprusside (SNP; 1 μM) evoked IJPs. A) Control recording with 7 cpm activity. B) Inhibitory junction potentials evoked by sodium nitroprusside. Trace in B was recorded 35.5 mins after trace in A. Potentials recorded in the presence of 5 μM atropine.

Discussion

In the mouse colon, ICC associated with the submuscular plexus (ICC-SMP) produce stable rhythmic slow waves (Yoneda, et al., 2004; Yoneda, et al., 2002; Hanani, et al., 1998; Lee, et al., 2009; Huizinga, et al., 2011) that are not abolished by nerve conduction block. In the present study, we confirmed that the 20 cpm slow waves originate from the ICC-SMP, since it was present in preparations with submucosa, and absent from preparations without submucosa, similar to the corresponding activity of 13-15 cpm in the rat colon (Pluja, et al., 2001).

In both the mouse and rat colon, a second prominent lower frequency rhythmicity is present that is dependent on calcium channel activation(Yoneda, et al., 2002; Yoneda, et al., 2004; Pluja, et al., 2001). This means that this rhythmicity is stimulus-dependent, it must depolarize the smooth muscle membrane above threshold for calcium channel activation. These are called "rhythmic transient depolarizations" consistent with their counterpart in the small intestine (Huizinga, et al., 2014).

The present study shows that rhythmic transient depolarisations were activated by 250 μM chenodeoxycholic acid or 1 μM sodium nitroprusside. The fact that sodium nitroprusside evoked rhythmicity indicates that a constant level of nitric oxide appears to facilitate rhythmicity; nitric oxide plays a similar role in the generation of rhythmic vasomotion (Matchkov, 2010). We hypothesize that nitrergic nerves can generate a constant level of nitric oxide facilitated by the fact that they are coupled by gap junctions (Nagy, et al., 2014). Since nitrergic nerves exhibit abundant TGR5 receptors (Alemi, et al., 2013; Poole, et al., 2010), we postulate that chenodeoxycholic acid evokes rhythmicity by activating nitrergic nerves that in turn activate ICC to generate the rhythmicity, since ICC are heavily innervated by nitrergic nerves (Ward, et al., 2000; Wang, et al., 2003; Ward and Sanders, 2006; Zhu, et al., 2014; Lies, et al., 2014). Rhythmic transient depolarizations were evoked in preparations with or without the submucosa, thus, the ICC associated with the myenteric plexus (ICC-MP) are a likely candidate, [consistent with the data from Takaki and Jimenez (Yoneda, et al., 2002; Yoneda, et al., 2004; Pluja, et al., 2001)]. Since our experiments were performed in the presence of 5 μM atropine, it is unlikely that cholinergic nerves were responsible for activating the ICC-MP. Since atropine blocks muscarinic acetylcholine receptors, even acetylcholine (ACh) from ni-

trergic nerves would not be able to activate the inducible pacemaker (Harrington, et al., 2010).

Previous studies have shown that low-frequency high-amplitude electrical activity in canine colon, termed slow electrical oscillations, which occurred at 1.3 cpm, were evoked by 0.3 μM sodium nitroprusside and blocked by 1 μM TTX (Keef, et al., 2002; Keef, et al., 1997). We also observed that low-frequency rhythmic transient depolarizations were evoked by 1 μM sodium nitroprusside and blocked by 100 nM TTX. Similar activity called spike complexes, with associated smooth muscle action potentials, were observed spontaneously in proximal colon from Balb/c mice on post-natal day 20 at 3.1 cpm (Ward, et al., 1997). Other studies of Balb/c mice also exhibited these low frequency oscillations, which occurred spontaneously at 3.9 or 4.6 cpm, called spike bursts because of the smooth muscle actions potentials evoked by the depolarisations (Yoneda, et al., 2002; Yoneda, et al., 2004). Rhythmic low-frequency activity at 2 cpm was also observed in cultured colonic ICC (Wu, et al., 2015). The rhythmic transient depolarizations we observed sometimes evoked smooth muscle action potentials as described previously in rat, mouse and dog (Pluja, et al., 2001; Ward, et al., 1997; Keef, et al., 2002). We propose that once stimulated, ICC-MP pace low-frequency smooth muscle contractile activity via the generation of rhythmic transient depolarizations. It is likely that they result in a low-frequency propulsive motor pattern, for instance long distance contractions, described previously by Yu, et al. (2015).

Atropine (5 μM) was used to improve the stability of the muscle and enable continuous recording from smooth muscle cells. A previous study found that 3.5 μM atropine reduced the

amplitude of slow oscillations (~0.5 cpm) in mouse circular muscle (Bywater, et al., 1989), which would explain why the average amplitudes of the rhythmic transient depolarizations we observed were lower than those for other mouse studies (Bywater, et al., 1989; Ward, et al., 1997). We did not use nifedipine or nicardipine on our preparations, even though it enhances the stability of electrical recordings (Lyster, et al., 1995), because 1 μM nifedipine has been shown to inhibit spontaneous rhythmic transient depolarizations (or cyclic depolarisations with associated action potentials) in rat colon (Pluja, et al., 2001); nifedipine (0.1 μM) was shown to block rhythmic transient depolarizations (spike potentials/bursts) in mouse colonic smooth muscle (Yoneda, et al., 2002).

In the submucosa-free preparation, 8 cpm slow wave was observed in 30 out of 45 preparations, but in was only observed in 1 out of 40 preparations with the submucosa intact. Hence, removing the submucosa disinhibited the 8 cpm slow wave. We hypothesize that the presence of the 20 cpm slow waves prevented the occurrence of the 8 cpm slow wave. It is possible that the source of the 8 cpm slow wave is the ICC-IM, which normally conduct ICC-SMP pacemaker activity into the muscle, but in the absence of ICC-SMP and their slow waves, their intrinsic 8 cpm slow wave may be revealed.

IJPs were evoked by chenodeoxycholic acid, the two neurotransmitters responsible for biphasic colonic IJPs are NO and adenosine or ATP (Alberti, et al., 2005; Lies, et al., 2014; Gallego, et al., 2014; Mane, et al., 2014a; Mane, et al., 2014b; Sanders, 2016). A previous study showed that NO-sensitive guanylate cyclase expressed in ICC and smooth muscle are essential for generation of IJPs (Lies, et al., 2014). Since chenodeoxycholic acid evoked IJPs

in addition to rhythmic transient depolarizations, we postulate that it did so by activating the inhibitory neurons of the myenteric plexus. This is similar to small intestinal ICC associated with the deep muscular plexus (ICC-DMP), which also seem to generate on-demand pacemaker activity, while being controlled by inhibitory nitrergic nerves (Huizinga, et al., 2014; Pawelka and Huizinga, 2015; Baker, et al., 2016; Zhu, et al., 2016). This is further supported by our observation that SNP activated rhythmic IJPs as well. Thus, it is likely that chenodeoxycholic acid and SNP act through similar pathways since they both activated IJPs and rhythmic transient depolarisations.

Networks of nerves in the brain communicate through phase amplitude coupling (Zalay and Bardakjian, 2009; Canolty and Knight, 2010) and the same phenomenon appears to orchestrate interaction of networks of pacemaker cells in the gut. In the small intestine, phase amplitude coupling underlies the interaction between pacemaker activity of the ICC-MP and ICC-DMP to generate the classical segmentation motor pattern (Huizinga, et al., 2014), but, dependent on the nature of the pacemaker activities, it is likely that low-frequency propulsive activity can also be a consequence of phase amplitude coupling (Huizinga, et al., 2015). The interaction of the two pacemaker activities in the small intestine generates waxing and waning in amplitude of the dominant pacemaker activity of ICC-MP. We did not see evidence of waxing and waning in the mouse colon, the phase amplitude coupling resulted in enhancement of the slow wave amplitude by rhythmic transient depolarisations. This was obvious in the interaction of rhythmic transient depolarizations evoked by chenodeoxycholic acid and the 8 cpm slow wave purportedly generated by ICC-IM; the interaction with the 20 cpm slow wave was less pronounced. It is possible that the enhanced slow wave amplitude caused by

the phase of the rhythmic transient depolarisations was masked by the decrease in slow wave amplitude which occurs as the membrane depolarizes (Liu, et al., 1994; Kim, et al., 2014). Slow wave amplitude decreases as the membrane potential approaches the reversal potential of the ion channels responsible for its upstroke. Chenodeoxycholic acid evokes low-frequency propulsive contractions in the human colon (Bampton, et al., 2002), and the present study puts forth the hypothesis that this is evoked by induction of low-frequency rhythmic transient depolarizations in ICC-MP, via nitrergic nerves, which then interact with slow wave activity within the musculature and to generate low-frequency propulsive activity. Hence, the electrical activity within the musculature is a combination of low-frequency oscillations with superimposed enhanced amplitude slow wave activity. The consequence of the phase amplitude coupling of rhythmic transient depolarisations and slow waves is likely an enhancement in the amplitude of the ripple contractions, which occur at the ICC-SMP frequency, after long distance contractions (Yu, et al., 2015). More research is needed to confirm this and reveal how the low-frequency rhythmic transient depolarizations propagate within the musculature.

In conclusion, chenodeoxycholic acid evoked rhythmic transient depolarisations in the mouse colon. The data are consistent with chenodeoxycholic acid acting on nitrergic nerves via TGR5 receptors, thereby creating a constant increase in NO around ICC-MP which evokes rhythmic transient depolarizations.

Acknowledgements

This study was supported by CIHR and NSERC grants to JH. GW was supported by NSERC Alexander Graham Bell PGS-D and CGS-D scholarships.

References

Alberti E, Mikkelsen HB, Larsen JO and Jimenez M (2005) Motility patterns and distribution of interstitial cells of Cajal and nitrergic neurons in the proximal, mid- and distal-colon of the rat. *Neurogastroenterol Motil* **17**:133-147.

Alemi F, Poole DP, Chiu J, Schoonjans K, Cattaruzza F, Grider JR, Bunnett NW and Corvera CU (2013) The receptor TGR5 mediates the prokinetic actions of intestinal bile acids and is required for normal defecation in mice. *Gastroenterology* **144**:145-154.

Bajor A, Gillberg PG and Abrahamsson H (2010) Bile acids: short and long term effects in the intestine. *Scand J Gastroenterol* **45**:645-664.

Baker SA, Drumm BT, Saur D, Hennig GW, Ward SM and Sanders KM (2016) Spontaneous Ca(2+) transients in interstitial cells of Cajal located within the deep muscular plexus of the murine small intestine. *J Physiol* **594**:3317-3338.

Bampton PA, Dinning PG, Kennedy ML, Lubowski DZ and Cook IJ (2002) The proximal colonic motor response to rectal mechanical and chemical stimulation. *Am J Physiol Gastrointest Liver Physiol* **282**:G443-G449.

Bayguinov PO, Hennig GW and Smith TK (2010) Ca2+ imaging of activity in ICC-MY during local mucosal reflexes and the colonic migrating motor complex in the murine large intestine. *J Physiol* **588**:4453-4474.

Bogeski G, Shafton AD, Kitchener PD, Ferens DM and Furness JB (2005) A quantitative approach to recording peristaltic activity from segments of rat small intestine in vivo. *Neurogastroenterol Motil* **17**:262-272.

Bywater RA, Small RC and Taylor GS (1989) Neurogenic slow depolarizations and rapid oscillations in the membrane potential of circular muscle of mouse colon. *J Physiol* **413**:505-519.

Camilleri M and Gores GJ (2015) Therapeutic targeting of bile acids. *Am J Physiol Gastrointest Liver Physiol* **309**:G209-G215.

Canolty RT and Knight RT (2010) The functional role of cross-frequency coupling. *Trends Cogn Sci* **14**:506-515.

Der-Silaphet T, Malysz J, Hagel S, Larry AA and Huizinga JD (1998) Interstitial cells of cajal direct normal propulsive contractile activity in the mouse small intestine. *Gastroenterology* **114**:724-736.

Diamant NE (1989) Physiology of esophageal motor function. *Gastroenterol Clin North Am* **18**:179-194.

Edwards FR and Hirst GD (2006) An electrical analysis of slow wave propagation in the guinea-pig gastric antrum. *J Physiol* **571**:179-189.

Ferens D, Baell J, Lessene G, Smith JE and Furness JB (2007) Effects of modulators of Ca(2+)-activated, intermediate-conductance potassium channels on motility of the rat small intestine, in vivo. *Neurogastroenterol Motil* **19**:383-389.

Frommherz L, Bub A, Hummel E, Rist MJ, Roth A, Watzl B and Kulling SE (2016) Age-Related Changes of Plasma Bile Acid Concentrations in Healthy Adults--Results from the Cross-Sectional KarMeN Study. *PLoS One* **11**:e0153959.

Gallego D, Malagelada C, Accarino A, De GR, Malagelada JR, Azpiroz F and Jimenez M (2014) Nitrergic and purinergic mechanisms evoke inhibitory neuromuscular transmission in the human small intestine. *Neurogastroenterol Motil* **26**:419-429.

Giorgio V, Borrelli O, Smith VV, Rampling D, Koglmeier J, Shah N, Thapar N, Curry J and Lindley KJ (2013) High-resolution colonic manometry accurately predicts colonic neuromuscular pathological phenotype in pediatric slow transit constipation. *Neurogastroenterol Motil* **25**:70-78.

Hanani M, Louzon V, Miller SM and Faussone-Pellegrini MS (1998) Visualization of interstitial cells of Cajal in the mouse colon by vital staining. *Cell Tissue Res* **292**:275-282.

Harrington AM, Lee M, Ong SY, Yong E, Farmer P, Peck CJ, Chow CW, Hutson JM and Southwell BR (2010) Immunoreactivity for high-affinity choline transporter colocalises with VAChT in human enteric nervous system. *Cell Tissue Res* **341**:33-48.

Huizinga JD, Chen JH, Zhu YF, Pawelka A, McGinn RJ, Bardakjian BL, Parsons SP, Kunze WA, Wu RY, Bercik P, Khoshdel A, Chen S, Yin S, Zhang Q, Yu Y, Gao Q, Li K, Hu X, Zarate N, Collins P, Pistilli M, Ma J, Zhang R and Chen D (2014) The origin of segmentation motor activity in the intestine. *Nat Commun* **5**:3326.

Huizinga JD, Martz S, Gil V, Wang XY, Jimenez M and Parsons S (2011) Two independent networks of interstitial cells of cajal work cooperatively with the enteric nervous system to create colonic motor patterns. *Front Neurosci* **5**:93.

Huizinga JD, Parsons SP, Chen JH, Pawelka A, Pistilli M, Li C, Yu Y, Ye P, Liu Q, Tong M, Zhu YF and Wei D (2015) Motor patterns of the small intestine explained by phase-amplitude coupling of two pacemaker activities: the critical importance of propagation velocity. *Am J Physiol Cell Physiol* **309**:C403-C414.

Huizinga JD, Thuneberg L, Kluppel M, Malysz J, Mikkelsen HB and Bernstein A (1995) W/kit gene required for interstitial cells of Cajal and for intestinal pacemaker activity. *Nature* **373**:347-349.

Keef KD, Anderson U, O'Driscoll K, Ward SM and Sanders KM (2002) Electrical activity induced by nitric oxide in canine colonic circular muscle. *Am J Physiol Gastrointest Liver Physiol* **282**:G123-G129.

Keef KD, Murray DC, Sanders KM and Smith TK (1997) Basal release of nitric oxide induces an oscillatory motor pattern in canine colon. *J Physiol* **499 (Pt 3)**:773-786.

Kim BJ, Nam JH, Kim KH, Joo M, Ha TS, Weon KY, Choi S, Jun JY, Park EJ, Wie J, So I and Nah SY (2014) Characteristics of gintonin-mediated membrane depolarization of pacemaker activity in cultured interstitial cells of Cajal. *Cell Physiol Biochem* **34**:873-890.

Knowles CH and Farrugia G (2011) Gastrointestinal neuromuscular pathology in chronic constipation. *Best Pract Res Clin Gastroenterol* **25**:43-57.

Koch KL, Stewart WR and Stern RM (1987) Effect of barium meals on gastric electromechanical activity in man. A fluoroscopic-electrogastrographic study. *Dig Dis Sci* **32**:1217-1222.

Lee HT, Hennig GW, Park KJ, Bayguinov PO, Ward SM, Sanders KM and Smith TK (2009) Heterogeneities in ICC Ca2+ activity within canine large intestine. *Gastroenterology* **136**:2226-2236.

Lee KJ (2015) Pharmacologic Agents for Chronic Diarrhea. *Intest Res* **13**:306-312.

Lies B, Gil V, Groneberg D, Seidler B, Saur D, Wischmeyer E, Jimenez M and Friebe A (2014) Interstitial cells of Cajal mediate nitrergic inhibitory neurotransmission in the murine gastrointestinal tract. *Am J Physiol Gastrointest Liver Physiol* **307**:G98-106.

Liu LW, Farraway L, Berezin I and Huizinga JD (1998) Interstitial cells of Cajal: mediators of communication between circular and longitudinal muscle layers of canine colon. *Cell Tissue Res* **294**:69-79.

Liu LW and Huizinga JD (1993) Electrical coupling of circular muscle to longitudinal muscle and interstitial cells of Cajal in canine colon. *J Physiol* **470**:445-461.

Liu LW, Thuneberg L and Huizinga JD (1994) Selective lesioning of interstitial cells of Cajal by methylene blue and light leads to loss of slow waves. *Am J Physiol* **266**:G485-G496.

Lyster DJ, Bywater RA and Taylor GS (1995) Neurogenic control of myoelectric complexes in the mouse isolated colon. *Gastroenterology* **108**:1371-1378.

Mane N, Gil V, Martinez-Cutillas M, Clave P, Gallego D and Jimenez M (2014a) Differential functional role of purinergic and nitrergic inhibitory cotransmitters in human colonic relaxation. *Acta Physiol (Oxf)* **212**:293-305.

Mane N, Gil V, Martinez-Cutillas M, Martin MT, Gallego D and Jimenez M (2014b) Dynamics of inhibitory co-transmission, membrane potential and pacemaker activity determine neuromyogenic function in the rat colon. *Pflugers Arch* **466**:2305-2321.

Matchkov VV (2010) Mechanisms of cellular synchronization in the vascular wall. Mechanisms of vasomotion. *Dan Med Bull* **57**:B4191.

Nagy JI, Urena-Ramirez V and Ghia JE (2014) Functional alterations in gut contractility after connexin36 ablation and evidence for gap junctions forming electrical synapses between nitrergic enteric neurons. *FEBS Lett* **588**:1480-1490.

Pawelka AJ and Huizinga JD (2015) Induction of rhythmic transient depolarizations associated with waxing and waning of slow wave activity in intestinal smooth muscle. *Am J Physiol Gastrointest Liver Physiol* **308**:G427-G433.

Pluja L, Alberti E, Fernandez E, Mikkelsen HB, Thuneberg L and Jimenez M (2001) Evidence supporting presence of two pacemakers in rat colon. *Am J Physiol Gastrointest Liver Physiol* **281**:G255-G266.

Poole DP, Godfrey C, Cattaruzza F, Cottrell GS, Kirkland JG, Pelayo JC, Bunnett NW and Corvera CU (2010) Expression and function of the bile acid receptor GpBAR1 (TGR5) in the murine enteric nervous system. *Neurogastroenterol Motil* **22**:814-818.

Sabourin PJ, Kingma YJ and Bowes KL (1990) Electrical and mechanical interactions between the muscle layers of canine proximal colon. *Am J Physiol* **258**:G484-G491.

Sanders KM (2016) Enteric Inhibitory Neurotransmission, Starting Down Under. *Adv Exp Med Biol* **891**:21-29.

Smith TK, Reed JB and Sanders KM (1987) Origin and propagation of electrical slow waves in circular muscle of canine proximal colon. *Am J Physiol* **252**:C215-C224.

Thomsen L, Robinson TL, Lee JC, Farraway LA, Hughes MJ, Andrews DW and Huizinga JD (1998) Interstitial cells of Cajal generate a rhythmic pacemaker current. *Nat Med* **4**:848-851.

Wang XY, Paterson C and Huizinga JD (2003) Cholinergic and nitrergic innervation of ICC-DMP and ICC-IM in the human small intestine. *Neurogastroenterol Motil* **15**:531-543.

Ward SM, Beckett EA, Wang X, Baker F, Khoyi M and Sanders KM (2000) Interstitial cells of Cajal mediate cholinergic neurotransmission from enteric motor neurons. *J Neurosci* **20**:1393-1403.

Ward SM, Harney SC, Bayguinov JR, McLaren GJ and Sanders KM (1997) Development of electrical rhythmicity in the murine gastrointestinal tract is specifically encoded in the tunica muscularis. *J Physiol* **505 (Pt 1)**:241-258.

Ward SM and Sanders KM (2006) Involvement of intramuscular interstitial cells of Cajal in neuroeffector transmission in the gastrointestinal tract. *J Physiol* **576**:675-682.

Wu MJ, Kee KH, Na J, Kim SW, Bae Y, Shin DH, Choi S, Jun JY, Jeong HS and Park JS (2015) Pituitary Adenylate Cyclase-activating Polypeptide Inhibits Pacemaker Activity of Colonic Interstitial Cells of Cajal. *Korean J Physiol Pharmacol* **19**:435-440.

Yoneda S, Fukui H and Takaki M (2004) Pacemaker activity from submucosal interstitial cells of Cajal drives high-frequency and low-amplitude circular muscle contractions in the mouse proximal colon. *Neurogastroenterol Motil* **16**:621-627.

Yoneda S, Takano H, Takaki M and Suzuki H (2002) Properties of spontaneously active cells distributed in the submucosal layer of mouse proximal colon. *J Physiol* **542**:887-897.

Yu Y, Chen JH, Li H, Yang Z, Du X, Hong L, Liao H, Jiang L, Shi J, Zhao L, Tan S, Luo H and Huizinga JD (2015) Involvement of 5-HT3 and 5-HT4 receptors in colonic motor patterns in rats. *Neurogastroenterol Motil* **27**:914-928.

Zalay OC and Bardakjian BL (2009) Theta phase precession and phase selectivity: a cognitive device description of neural coding. *J Neural Eng* **6**:036002.

Zhu YF, Wang XY, Lowie BJ, Parsons S, White L, Kunze W, Pawelka A and Huizinga JD (2014) Enteric sensory neurons communicate with interstitial cells of Cajal to affect pacemaker activity in the small intestine. *Pflugers Arch* **466**:1467-1475.

Zhu YF, Wang XY, Parsons SP and Huizinga JD (2016) Stimulus-induced pacemaker activity in interstitial cells of Cajal associated with the deep muscular plexus of the small intestine. *Neurogastroenterol Motil* **28**:1064-1074.

CHAPTER 5: DISCUSSION

5.1 Addressing the Three Research Questions

In my published works included here I successfully addressed the three research questions proposed in the introduction. The three research questions were the following: how is the maxi Cl^- channel from ICC-MP is activated, how is the cholinergic agonist carbachol able to excite colonic ICC-IM, and how is the colonic inducible pacemaker activated? I proved that the maxi Cl^- channel from ICC-MP is activated by intracellular Ca2+, that carbachol excites colonic ICC-IM via suppression of currents from $K_V7.5$ channels and that the colonic inducible pacemaker is activated by chenodeoxycholic acid. Here I will discuss the implications of these studies in the context of the literature and synthesize how they advance our understanding of the electrophysiology of interstitial cells of Cajal (ICC) regarding their intrinsic and inducible pacemaker activities.

5.2 How is the Maxi Cl^- Channel from ICC-MP Activated?

Determining the identity of the pacemaker channel in ICC-MP was essential to understand how gut motility is orchestrated. I showed that a Ca^{2+} ionophore (ionomycin; 1 in Fig. 5.1), a sarco/ endoplasmic reticulum Ca^{2+}-ATPase (SERCA) inhibitor in cyclopiazonic acid (2 in Fig. 5.1) and biophysical block of Ca^{2+} extrusion with La^{3+} (4 in Fig. 5.1) and Na^+ substitution (5 in Fig. 5.1) each activated the maxi Cl^- channel from small intestinal ICC-MP. I also showed that these interventions were able increase ICC-MP intracellular Ca^{2+}. From these data, we can conclude that maxi Cl^- channels are activated by intracellular Ca^{2+}. The hypothesis that maxi Cl^- channels are the pacemaker channel from ICC-MP was deficient because

there was no clear evidence it was periodically activated by Ca^{2+} (Zhu, et al., 2009), prior to my study on its Ca^{2+} sensitivity. However, I have shown a mechanism by which maxi Cl^- channels may become periodically activated and drive rhythmic pacemaker potentials which underlie slow waves transmitted to the smooth muscle.

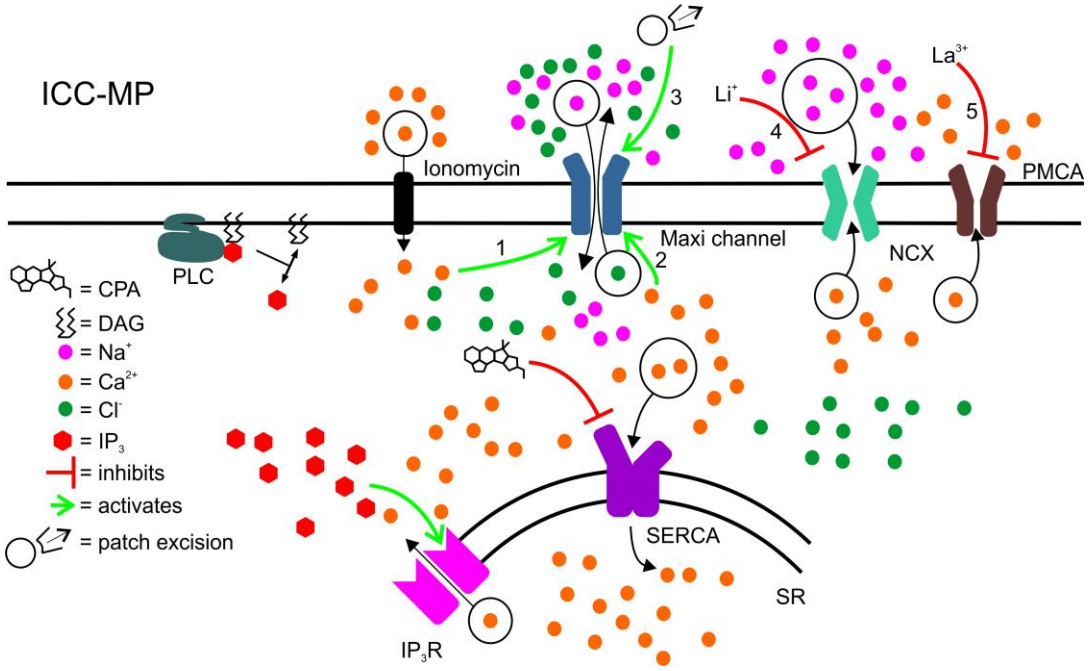

Figure 5.1: Schematic diagram depicting the strategies which increased intracellular Ca^{2+} and activated the maxi Cl^- channel from ICC-MP. We showed that ionomycin – a Ca^{2+} ionophore (1) – and cyclopiazonic acid (CPA) – a sarco/endoplasmic reticulum Ca^{2+} ATPase (SERCA) inhibitor (2) –activated maxi Cl^- channels by increasing intracellular Ca^{2+}. We showed that patch excision into the inside-out configuration changed inwardly rectifying maxi Cl^- currents to outwardly rectifying indicating that the currents come from the same channels (3). Another method we used to increase intracellular Ca^{2+} was solution with Na^+ substituted with Li^+ to prevent Ca^{2+} efflux via the Na^+/Ca^{2+} exchanger (NCX; 4) and La^{3+} to block P-type ATPases, including the plasma membrane Ca^{2+} ATPase (PMCA; 5).

5.2.1 Novel Implications

An important contribution I made with this study was that the rectification properties of the maxi Cl^- channel are dependent on patch configuration. This settled the controversy regarding the rectification of maxi Cl^- channels, showing that maxi Cl^- channels are inwardly rectifying while in patch clamp configurations that mirror physiological conditions: cell-attached (Parsons and Huizinga, 2010) or whole-cell (Zhu, et al., 2005). This proves that the maxi Cl^- channel can generate the inward currents required for pacemaker potential upstroke initiation. I showed that the outward rectification observed in the inside-out configuration (Parsons and Sanders, 2008; Huizinga, et al., 2002) is not due to a different class of maxi Cl^- channels, since inwardly rectifying currents in cell-attached patches switch to outwardly rectifying without turning off. This observation is important because it means that the maxi Cl^- channel can be studied more easily in the inside-out configuration, since we know it is the same channel as those responsible for inwardly rectifying cell-attached maxi Cl^- currents. Maintaining cell-attached patch stability can be challenging, thus, using the inside-out configuration is more attractive and is required for biophysical studies of channel permeability (Parsons, et al., 2012).

5.2.2 Which Ca^{2+}-Sensitive Ion Channel is the Pacemaker Channel?

Since the pacemaker channel from ICC requires sensitivity to the rhythmic Ca^{2+} clock to generate slow waves, researchers have proposed the non-selective cation channel, which is inhibited by intracellular Ca^{2+}, might be the pacemaker channel (Koh, et al., 2002; Corrias and Buist, 2008). It is possible that both maxi Cl^- channels and NSCCs contribute to the pacemaker potential upstroke as co-pacemaker channels, but this seems unlikely since they

have opposite sensitivities to Ca^{2+}. If NSCCs are the pacemaker channels, one has to invoke a complicated mechanism where mitochondria uptake more Ca^{2+} from the subspace between the interior leaflet of the membrane and the sarcoplasmic reticulum (SR) than is exported by inositol trisphosphate (IP_3) receptors on the SR membrane (Corrias and Buist, 2008). If this were the case, the pacemaker potentials and rhythmic Ca^{2+} transients that drive the rhythmicity of the ICC would have to be at least partially out of phase, because NSCC activation requires reduction of intracellular Ca^{2+} (Koh, et al., 2002). It is possible that local Ca^{2+} events may behave independently from whole cell Ca^{2+} transients, but some level of Ca^{2+} event coordination is required to evoke currents strong enough to depolarize ICC and initiate the pacemaker potential upstroke. In ICC associated with the deep muscular plexus (ICC-DMP), local Ca^{2+} events and small Ca^{2+} waves are not synchronised across the whole network in unstimulated conditions (Zhu, et al., 2016; Baker, et al., 2016). When Ca^{2+} transients in ICC-DMP are evoked by sustained application of substance P, they become synchronized across the whole network (Zhu, et al., 2016). ICC-MP networks exhibit synchronised whole cell Ca^{2+} transients spontaneously (Lowie, et al., 2011). Therefore, it seems unlikely that localized depletion of Ca^{2+} could occur simultaneously with these whole cell Ca^{2+} transients, which are required for network synchronisation and propagation of slow waves along the entire intestine. Also, Ano1 and BK_{Ca} which are involved in the pacemaker potential plateau are Ca^{2+}-activated, therefore, it is likely that ICC peak intracellular Ca^{2+} and the pacemaker potential plateau occur synchronously, the opposite of which would be required for NSCC activation.

In our explanation of maxi Cl^- channel Ca^{2+} sensitivity, we invoked the superficial buffer barrier (van Breemen, et al., 1995), which is similar to the idea of a sub-compartment where mi-

tochondria uptake Ca^{2+} released by the SR (Corrias and Buist, 2008). However, in our explanation the compartment between the inner leaflet of the membrane and the closely apposed SR would have increased intracellular Ca^{2+} in concert with whole ICC increased intracellular Ca^{2+}. This is not only simpler than an explanation where local sub-compartments of ICC exhibit Ca^{2+} events that are opposite to those of the whole cell Ca^{2+} events, but also fits better with the hypothesis that ICC Ca^{2+} transients and pacemaker potentials occur synchronously and not completely out of phase. Simultaneous Ca^{2+} imaging and patch clamp or intracellular recording experiments would enable determination of whether pacemaker potentials and Ca^{2+} transients are in phase or out of phase and which channels initiate the upstroke of the pacemaker potential, subsequently activating all the other voltage-dependent channels.

5.2.3 Challenges and Limitations

The Ca^{2+} activation of the maxi Cl^- channel study outlined in Chapter 2 had a few challenges that I overcame to complete the study. The first was identifying ICC by morphology without using fluorescent markers of any kind. To ensure accurate identification of ICC in future experiments, I would use transgenic mice expressing GFP labelled c-kit (Sanders, et al., 2012). Choosing to patch cells that were arranged in networks connected by tripolar processes was the best available method to positively identify the ICC. Another challenge was using cyclopiazonic acid, since it caused Ca^{2+} transients in cells, which sometimes caused ICC to move even in the presence of nicardipine. Using excitatory drugs and neurotransmitters with patch clamping can be difficult since they will often cause the cell under investigation to move, disrupting cell-attached patches.

One of the potential limitations of the Ca^{2+} activation of the maxi Cl^- channel study was the use of cultured cells. We chose to use primary cultured cells as our model for studying the maxi Cl^- channel since they have been used previously (Huizinga, et al., 2002; Parsons and Sanders, 2008; Parsons and Huizinga, 2010), but others have criticized their use because of the potential for ion channel expression and behaviour to change due to culture conditions (Zhu, et al., 2009). We published a study (Appendix 1) showing that ICC mRNA levels for c-kit mRNA changes over the course of 4 days in primary cultured cells, so the criticism that ion channel expression is altered in cultured cells is not unwarranted. However, we do not believe that the primary cultured ICC are completely different from their *in vivo* counterparts, as the properties of the maxi Cl^- channel when recorded from *in situ* patches of small intestinal and colonic ICC were not markedly different from those of primary cultured cells (Parsons, et al., 2012; Wright et al., unpublished observations).

Another potential limitation is the high Ca^{2+} required to activate the maxi Cl^- channel reliably. However, The fact that channels were active spontaneously, without need for Ca^{2+} transient-activating drugs, and that the effective $[Ca^{2+}]$ between the inside of the cell membrane and closely apposed sarcoplasmic reticulum reaches the millimolar range (van Breemen, et al., 1995), refute the notion that maxi Cl^- channel activation by intracellular Ca^{2+} is not a physiological phenomenon.

5.2.4 Future Directions

For future experiments, it would be better to use the *in situ* patch clamping technique in order to ensure the highest similarity to physiological channel activity, while enabling access to

the cell membrane ion channels for recording. The *in situ* dissection and preparation technique is described in Fig. 6.2. Due to patch instability because of contractile activity and because the ICC are not firmly attached to a solid surface, but the malleable tissue around them, *in situ* patch clamping is not ideal for cell-attached patches.

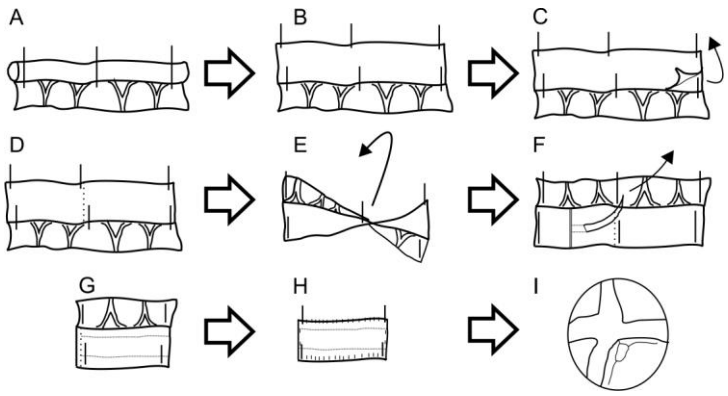

Figure 5.2: Schematic diagram of the *in situ* patch clamping dissection. A) After removing the colon, it was pinned out along the mesenteric border. B) Fine scissors were used to cut along the mesenteric border and pin the tissue flat, mucosa facing up. C) Then the mucosa and submucosa were peeled from two thirds of the tissue, and the loose peeled mucosa was then cut off (D). E) the entire preparation was flipped over so that the serosa was face up. F) A microscalpel was used to cut through the serosa and longitudinal muscle perpendicular to the tissue, on the section of tissue with mucosa still attached, approximately 1 cm proximal to the edge of the section with mucosa removed. Then fine forceps were used to peel strips of longitudinal muscle, starting at the cut, peeling from proximal to distal. G) The middle section of the preparation was peeled such that the myenteric plexus was revealed and the portion of tissue with mucosa still attached was removed. H) Then the mesentery was removed and the preparation pinned out taught on a microscope dish. I) Using

a high-powered phase contrast microscope I was able to visualize the interstitial cells of Cajal found closely apposed to myenteric ganglia, after treating the with a protease solution (Parsons, et al., 2012).

The next avenue of research on the maxi Cl^- channel is identifying the gene which encodes it. One interesting feature of the maxi Cl^- channel that might assist in its identification is that it is irreversibly blocked by the Cl^- channel blocker DIDS. DIDS has been shown to irreversibly block CFTR (Assef, et al., 2003) and anion exchanger 1 (Schopfer and Salhany, 1995). If one were to construct a tagged DIDS molecule with a fluorescent probe attached or a protein linker that could be extracted with covalently bound maxi Cl^- channels using molecular techniques, the protein identity of the channels could be determined. ICC-MP could be extracted by using flow cytometry using selective markers such as c-kit (Huizinga, et al., 1995; Ward, et al., 1994) and Ano1 (Zhu, et al., 2009; Gomez-Pinilla, et al., 2009). The isolated ICC could then be treated with the tagged DIDS to create covalent bonds between the maxi Cl^- channels and the blocker and then isolated using column chromatography. The final step in the process would be sequencing the eluted protein.

Whichever ion channel candidate turns out to encode the maxi Cl^- channel, its role as an initiator of ICC-MP slow wave upstroke is vital for intrinsic pacemaker activity and its activation by Ca^{2+} cements its role as a channel that can respond to the Ca^{2+} clock from ICC. Finding the initiator of the slow wave upstroke is an important part of the slow wave pacemaker potential schema (compare Fig. 5.7 and 1.1) and provides a potential pharmacological target for modulating the intrinsic slow wave of the ICC-MP.

5.3 How is the Cholinergic Agonist Carbachol Able to Excite Colonic ICC-IM?

The goal of our study was to determine the effects of the cholinergic excitatory neurotransmitter analogue carbachol on ICC ion channel activity. Having shown that the maxi chloride channel in small intestinal ICC-MP was Ca^{2+} activated, it was logical to test whether drugs that potentially cause increased intracellular Ca^{2+} through activation of muscarinic acetylcholine receptors (mAChRs) could modulate ICC ion channel activity. My hypothesis was that carbachol activates maxi Cl^- channels and inhibits K_V7 K^+ channels from ICC-IM. I showed that carbachol could inhibit K^+ channels (1 or 2 in Fig. 5.3), by recording currents from cell attached patches to which I applied carbachol. I also showed that the K_V7 channel blocker XE991 in the pipette (3a in Fig. 5.3) or added to the bath (3b in Fig. 5.3) could block the K^+ currents. I then showed that patch excision into the inside-out configuration turned off K^+ currents (4 in Fig. 5.3). XE991 also activated maxi Cl^- currents, likely indirectly through causing ICC-IM to depolarize (5 in Fig. 5.3). In collaboration with Raúl Loera Valencia, who performed single cell PCR, we showed that ICC co-expressed Ano1 mRNA and $K_V7.5$ mRNA. In collaboration with Dr. Xuan Yu Wang, who used immunohistochemistry on c-Kit, vesicular acetylcholine transporter (VAChT), and the K_V7 subfamily members $K_V7.2$-5, we showed that colonic ICC-IM express $K_V7.5$ proteins and ICC-MP do not. Myenteric nerves also express $K_V7.2$ and $K_V7.4$ while the longitudinal muscle expressed $K_V7.3$. Therefore, we proved the hypothesis that carbachol excites ICC-IM by inhibiting $K_V7.5$ channels. I also showed that XE991 could indirectly activate maxi Cl^- channels by inhibiting $K_V7.5$ channels, which may have occurred because blocking $K_V7.5$ channels depolarized the cells and maxi Cl^- channels are voltage sensitive (Parsons and Sanders, 2008; Parsons and Huizinga, 2010; Huizinga, et al., 2002; Wang, et al., 2008; Zhu, et al., 2005).

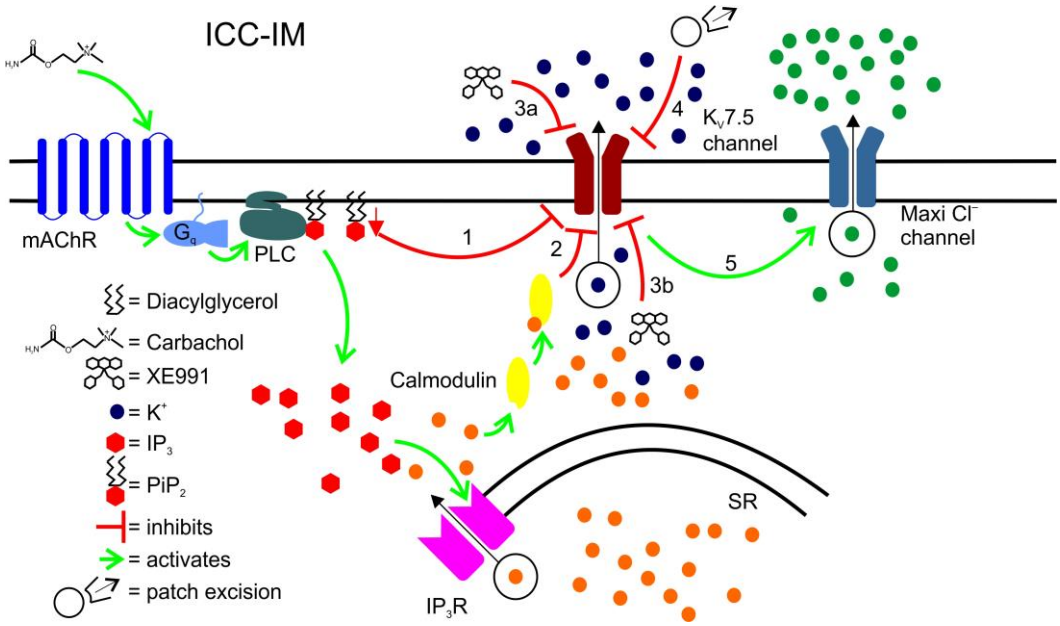

Figure 5.3: Schematic diagram depicting mechanisms which suppress or block colonic ICC-IM K_V7.5 channel currents. I showed that colonic ICC-IM express K_V7.5 channels because their K^+ currents were suppressed by cholinergic signalling pathways activated by carbachol (1 and 2). The selective K_V7 channel blocker XE991 blocked K^+ currents when it was added to the pipette (3a) or bath (3b) solutions. Patch excision caused the K^+ currents to turn off (4). Blockade of K_V7 currents with XE991 indirectly activated maxi Cl^- channels (5).

5.3.1 Mechanisms of K_V7 Current Suppression

K_V7 currents are often called M-current, a term that was originally coined because the currents were suppressed by mAChR signalling (Hernandez, et al., 2008; Brown and Adams, 1980). The pathway activated by mAChRs, which suppresses K_V7 currents, couples with $G_{q/11}$ which activates phospholipase C (PLC) to cleave phosphatidylinositol 4,5-bisphosphate

(PiP_2) into IP_3 and membrane-delimited diacyl glycerol (DAG; Fig. 5.3) (Brown and Passmore, 2009). The main mode by which K_V7 channels become suppressed is the depletion of PiP_2 from the membrane by PLC (1 in Fig. 5.3), since PiP_2 is a lipid required for channel activation (Brown, et al., 2007; Brown and Passmore, 2009). Another mode K_V7 current suppression is release of intracellular Ca^{2+} via the hydrolysis of PiP_2 yielding IP_3, which activates IP_3 receptors on the sarcoplasmic reticulum, releasing intracellular Ca^{2+}; increased intracellular Ca^{2+} leads to calmodulin activation (2 in Fig. 5.3) which can also suppress K_V7 currents (Brown, et al., 2007). The calmodulin mechanism was predominant with bradykinin receptor suppression of K_V7 currents (Brown, et al., 2007).

5.3.2 Challenges and Limitations

The original goal of the colonic ICC study was to assess the effect of the cholinergic agonist carbachol on the activation of the inducible pacemaker in colonic ICC-MP. Through some of the methodological challenges and some fortunate serendipity, we ended up performing a study on the colonic ICC-IM instead. This was because it was very tricky to isolate intact networks of ICC-MP from the colon using the primary cell culture technique (described in methods sections of Chapters 2.2 and 3.2) compared to the small intestinal ICC-MP. Because of this I resorted to patching isolated ICC, often exhibiting triangular or bipolar morphology. One of the results of the study was immunohistochemistry showing that ICC-IM do not always present with bipolar morphology, rather some have multiple processes (Chapter 3.2 Fig. 7). Like the small intestinal ICC-MP maxi Cl^- channel study, positively identifying the ICC before patching them was not exact, and was made even more difficult by the fact that multiple subtypes of ICC were present in primary cultures

and their morphological characteristics constitute a spectrum rather than distinct categories.

The study was strengthened by utilization of both immunohistochemistry to identify the K_V7 subtype present in the ICC and patch clamping to record the carbachol-sensitive currents. However, we were not able to stain the exact cells from which we recorded $K_V7.5$ currents. It is possible that cells that did not exhibit the $K_V7.5$ currents, which were either suppressed by carbachol or blocked by XE991, were ICC-MP, which do not express any of the K_V7 genes tested. Furthermore, we were only able to confirm that ICC-MP did not express K_V7 channels via staining, not with electrophysiology, thus, the use of GFP labelled ICC-MP (Sanders, et al., 2012) or *in situ* patch clamping (Parsons, et al., 2012) would aid analysis of $K_V7.5$ channel properties, the strengths and limitations of which were discussed in section 5.2.3.

5.3.3 Novel Implications

There are several important implications of ICC-IM $K_V7.5$ current study, the first of which is that ICC-IM express K^+ channels suppressed by cholinergic signalling, which provides a mechanism by which they can become electrically excited by neuronal stimuli. Prior to this study there were no other published studies on single channel patch clamping from the colonic ICC-IM subtype. Another implication is that $K_V7.5$ can be used as a selective marker to differentiate colonic ICC-IM from ICC-MP, since the latter do not express any K_V7 channels. I also showed that the selective K_V7 channel blocker XE991 works on both sides of the channel, as it blocked currents when added to the bath while cell-attached (Chapter

3 Fig. 4) and it also blocked them when added to the pipette solution (Chapter 3 Fig. 6), which had not been demonstrated previously. Since I was recording from cell-attached patches, if channel blockers added to the bath could block K^+ currents, those blockers would either cross the membrane and block the intracellular face of the channel, or become incorporated in the membrane and interact with the transmembrane structures of the channels to block them by changing their confirmation. This is not an unprecedented phenomenon as K_V7 channels require the presence of PiP_2 lipids in the membrane for current conduction (Brown, et al., 2007; Brown and Passmore, 2009). I hypothesize that carbachol may also lead to activation of maxi Cl^- channels in ICC-IM, but were not able to definitively distinguish them from ICC-MP, which were also present in the primary cultures. The evidence that XE991 could indirectly activate maxi Cl^- currents by blocking $K_V7.5$ currents certainly confirms that ICC-IM have those channels like small intestinal ICC-MP.

This study bridges the gap between intrinsic ICC pacemaker activity and inducible activity evoked by enteric nerve stimulation. ICC-IM do not normally exhibit their own pacemaker activity, but they facilitate the transmission of neuronal and ICC-MP signals into the muscle. Thus, proof that ICC-IM possess cholinergic signalling-sensitive $K_V7.5$ channels provides an explanation of the response of ICC-IM to acetylcholine (ACh) excitation.

5.3.4 Future Directions

Determining how the $K_V7.5$ channels from ICC-IM are supressed may help to clarify their role in transmitting neuronal signals and ICC pacemaker activity to smooth muscle. It is unclear which mAChR subtypes are present on colonic ICC-IM. It is possible that they express

M_3 receptors like small intestinal ICC-MP (So, et al., 2009). M_3 receptor expression would be consistent with the suppression of $K_V7.5$ currents I observed because carbachol activates both M_1 and M_3 receptors, which couple with $G_{q/11}$ to activate the PLC pathway (Brown and Passmore, 2009). Selective antibodies against the two mAChR subtypes M_1 and M_3 could be used to determine whether they are expressed by ICC-IM or if they have both.

Since both ICC-IM and ICC-MP were present in cultures for the $K_V7.5$ channel study, it is possible that carbachol could have activated maxi Cl^- channels from either cell type. Since morphology was not a reliable characteristic by which to differentiate the two ICC subtypes (see Challenges and Limitations), we could not include data showing carbachol activation of maxi Cl^- channels in ICC-IM. The strategies that I would use to investigate carbachol activation of maxi Cl^- channels in colonic ICC-MP could involve *in situ* patch clamping, however, since carbachol causes the smooth muscle to contract strongly, maintaining a cell-attached patch can be challenging. One way around this could be using wortmannin which is a myosin light chain kinase inhibitor that irreversibly binds to its catalytic domain (Nakanishi, et al., 1992). *In situ* patch clamping is not feasible for recording from ICC-IM since they are too deeply embedded in the muscle layer for exposure by the *in situ* dissection. To assess whether carbachol activates maxi Cl^- channels from ICC-IM, I would use primary cultured cells, but from animals with GFP-tagged $K_V7.5$ to distinguish them from ICC-MP. One problem with using wortmannin on ICC-IM is that inhibits PI4-kinase, which would reduce the concentration of PiP_2 in the membrane. As I showed, inhibiting K_V7 currents with XE991 indirectly activated the maxi Cl^-, therefore, activating K_V7 by reducing PiP_2 and indirectly activating maxi Cl^- channels by depolarizing the cells, would confound the results with carbachol.

Thus, using nicardipine to block L-type Ca^{2+} channels would be another option. It is unclear how the L-type Ca^{2+} channel is involved in colonic ICC pacemaker activity, but it warrants further investigation.

5.4 How is the Inducible Colonic Pacemaker Activated?

After considering neuronal modulation of colonic ICC-IM my next goal was to investigate the inducible pacemaker from the colon, likely found in ICC-MP. My hypothesis was that the activation of inducible ICC pacemaker activity in the mouse colon, by non-cholinergic nitrergic myenteric neurons, stimulated by chenodeoxycholic acid, leads to generation of low-frequency rhythmic transient depolarisations. I recorded ICC-SMP slow waves from colonic circular muscle using sharp microelectrodes (1 in Fig. 5.4). I showed that the bile acid chenodeoxycholic acid (2a & 2b in Fig. 5.4 & 5.5) could induce rhythmic transient depolarisations in preparations with (3 in Fig. 5.4) and without (3 in Fig. 5.5) submucosa and associated ICC-SMP intact. In preparations with submucosa intact, I showed that the phase of rhythmic transient depolarisation generated by ICC-MP (5 in Fig. 5.4) interacted with the amplitude of slow waves from ICC-SMP determined by phase amplitude coupling analysis. I showed that preparations without submucosa exhibited an 8 cpm rhythmic depolarizing electrical activity (1 in Fig. 5.5) likely from ICC-IM and this was absent in preparations with submucosa intact (4 in Fig. 5.4). The phase of the low-frequency rhythmic transient depolarisations interacted with the amplitude of the 8 cpm activity (4 in Fig. 5.5), as determined by phase-amplitude coupling analysis.

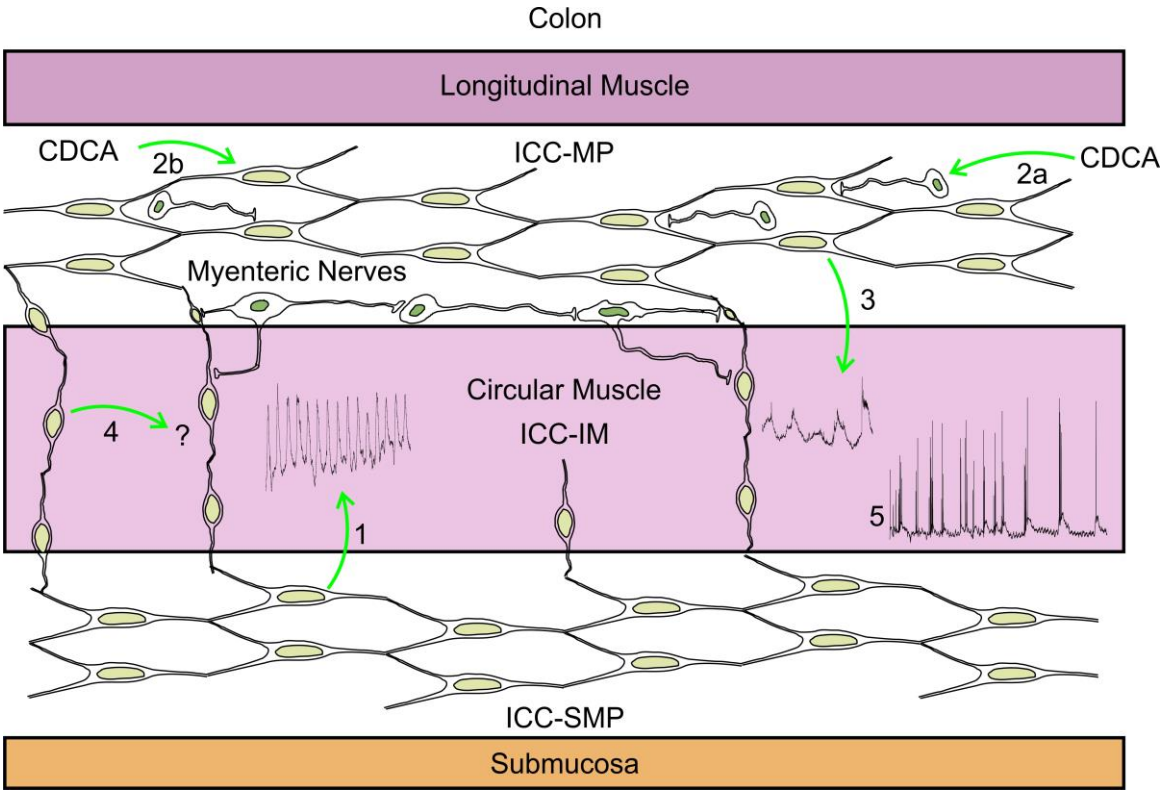

Figure 5.4: Schematic diagram depicting the colonic interstitial cells of Cajal (ICC) pacemaker networks in cross-section and the mechanism of inducible pacemaker activation. ICC associated with the submuscular plexus of the colon (ICC-SMP) generated intrinsic pacemaker activity which paced slow waves recorded from circular muscle (1). Chenodeoxycholic acid (CDCA) activated ICC associated with the myenteric plexus (ICC-MP) via activation of nitrergic nerves likely through TGR5 receptors (2a) or directly (2b). Activation of the inducible pacemaker in ICC-MP led to rhythmic transient depolarizations (3) recorded from the muscle. Intramuscular ICC (ICC-IM) generated intrinsic activity that I observed with submucosa removed was absent with ICC-SMP present (4). Intrinsic ICC-SMP slow waves and inducible ICC-MP rhythmic transient depolarisations activated by CDCA or SNP were both present in the muscle and they interacted by phase amplitude coupling.

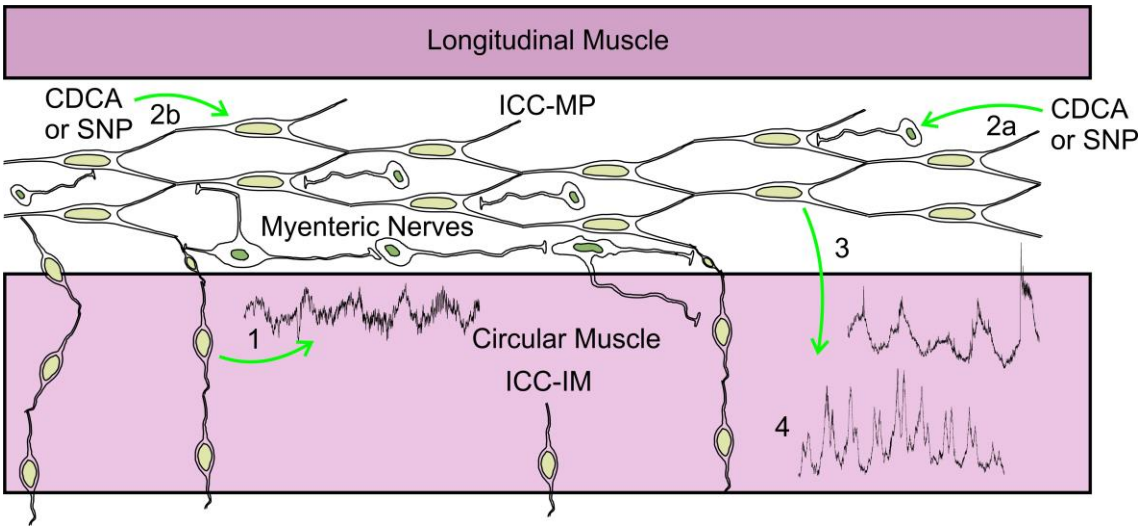

Figure 5.5: Schematic diagram depicting the colonic interstitial cells of Cajal (ICC) pacemaker networks in cross-section and the mechanism of inducible pacemaker activation with submucosa removed. Intramuscular ICC (ICC-IM) generated intrinsic 8 cpm rhythmic depolarisations recorded from circular muscle (1). Chenodeoxycholic acid (CDCA) or sodium nitroprusside (SNP) activated ICC associated with the myenteric plexus (ICC-MP) via activation of nitrergic nerves likely through TGR5 receptors (2a) or directly (2b). Activation of the inducible pacemaker in ICC-MP led to rhythmic transient depolarizations (3) recorded from the muscle. Intrinsic ICC-IM 8 cpm depolarizations and inducible ICC-MP rhythmic transient depolarisations activated by CDCA or SNP were both present in the muscle and they interacted by phase amplitude coupling.

5.4.1 Colonic Electrical Activity

Previous studies of the mouse colon have shown several distinct electrical activities, including slow waves from ICC associated with the myenteric plexus (ICC-SMP) at 14-16 cpm

(Yoneda, et al., 2004; Yoneda, et al., 2002) and low-frequency high amplitude activity with synchronized bursts of action potentials at ~3.5 cpm (Yoneda, et al., 2004). The slow waves that we observed occurred at 20 cpm which is slightly faster than those recorded by Yoneda et al., (2002), but still within the range of frequencies they observed (10-22 cpm). Studies of the canine colon electrical activity revealed three types of electrical activity: ICC-SMP slow waves at 4.5-5 cpm, slow electrical oscillations at 1 cpm and myenteric potential oscillations at 16 cpm (Keef, et al., 1997; Keef, et al., 2002). Slow electrical oscillations (SEOs) are activated by NO in the canine colon and seem to rely on neuronal stimulation, as the spontaneous variety were blocked by 1 μM TTX (Keef, et al., 2002). Slow electrical oscillations may be the canine equivalent of the rhythmic transient depolarisations that I observed, especially since I showed that they could be activated by SNP and blocked by TTX.

5.4.2 Multiple Pacemakers and their Interactions

Since ICC associated with the myenteric plexus (ICC-MP) and ICC associated with the deep muscular plexus (ICC-DMP) in the small intestine produce segmentation by phase amplitude coupling (Huizinga, et al., 2014a; Huizinga, et al., 2014b), I wanted to determine if the colon exhibited similar pacemaker interactions. The small intestinal second pacemaker can be activated by decanoic acid (DA) and butyric acid via different mechanisms (Pawelka and Huizinga, 2015). The pacemaker networks in the canine colon produce 6 cpm slow waves, recorded from the circular muscle, as well as 20 cpm oscillations when closer to the myenteric border (Smith, et al., 1987). The authors suggested that the two frequencies, produced by ICC-SMP and ICC-MP, interact by addition in the circular muscle. The 20 cpm frequency appears to increase in amplitude with the depolarisation phase of the ICC-MP slow wave in

their figure 2 (Smith, et al., 1987), which suggests phase amplitude coupling. Rat colon also exhibits two pacemakers; ICC-MP produce a low-frequency (1-2 cpm) high amplitude activity and ICC-SMP produce higher frequency (10-12 cpm) slow waves (Pluja, et al., 2001; Alberti and Jimenez, 2005; Kato, et al., 2009; Quan, et al., 2015).

In my study of the activation of colonic inducible pacemaker activity I looked for interactions between low-frequency activity and higher frequency slow waves. I did this based on observations of the interactions between low-frequency activity and slow waves from the small intestine, which we called waxing and waning (Huizinga, et al., 2014a; Pawelka and Huizinga, 2015; Huizinga, et al., 2015). Here I explain the rationale behind searching for phase amplitude coupling interactions between low-frequency electrical oscillations and slow waves in the generation multi-frequency electrical activity. An alternate possibility is that two slow waves with similar frequencies could interact to produce the phenomenon.

In the small intestine there is a frequency gradient of pacemaker activity such that the proximal ICC-MP generate higher frequency slow waves than those more distal (Fig. 5.6A) (Code and Szurszewski, 1970; Brown, et al., 1975). ICC-MP distal to the fastest proximal pacemaker become entrained to that higher frequency, up to a certain distance away from that pacemaker site, which is dependent on the strength of electrical coupling in the network (Parsons and Huizinga, 2015). At the limit of the electrical coupling range to the fastest ICC-MP in the proximal small intestine, another pacemaker site emerges at a slightly lower

intrinsic frequency, leading to a "frequency step" in the frequency plot (arrows in Fig. 5.6 A&B).

When the gap junction blocker carbenoxolone was applied to whole small intestine in an organ bath, the interval between frequency steps decreased and more pacemaker sites appeared (Fig. 5.6 B) (Parsons and Huizinga, 2015). Importantly, the waxing and waning pattern from electrical recordings occurred regardless of where the tissue for intracellular recording was collected (Pawelka and Huizinga, 2015), and not just at discrete areas where frequency steps might occur, such that two slightly different frerquencies of slow waves could theoretically be present. Also the preparations were small enough (1 cm^2) such that frequency gradients would not be distinguishable within them (Pawelka and Huizinga, 2015), as frequency steps usually occur every ~10 cm (Parsons and Huizinga, 2015). If the waxing and waning activity was produced by two slow waves occuring at slightly different frequencies interacting by addition in the muscle (ignoring that pacemaker entrainment makes this very unlikely), then one would expect the amplitude of the peak waxed slow waves to be a summation of the two waves, but this was not observed in any of our studies (Huizinga, et al., 2014a; Pawelka and Huizinga, 2015; Huizinga, et al., 2015). Also, unlike airway smooth muscle, gastrointestinal smooth muscle cells are electrically passive and they respond to the excitatory influences of nerves and ICC and are incapable of generating slow waves or rhythmic transient depolarisations in the absence of the ICC networks responsible for pacing them. Therefore, these data taken together support the idea that two pacemaker frequencies in the small intestine, one at ~2 cpm from ICC-DMP induced by decanoic acid and the other at ~32 cpm from the intrinsic ICC-MP, interact by phase amplitude coupling

to produce the waxing and waning electrical activity. These observations led me to test whether low-frequency rhythmic transient depolarisations from the inducible pacemaker, activated by chenodeoxycholic acid, interacted by phase amplitude coupling with slow waves or other rhythmic activities and I showed that this was the case.

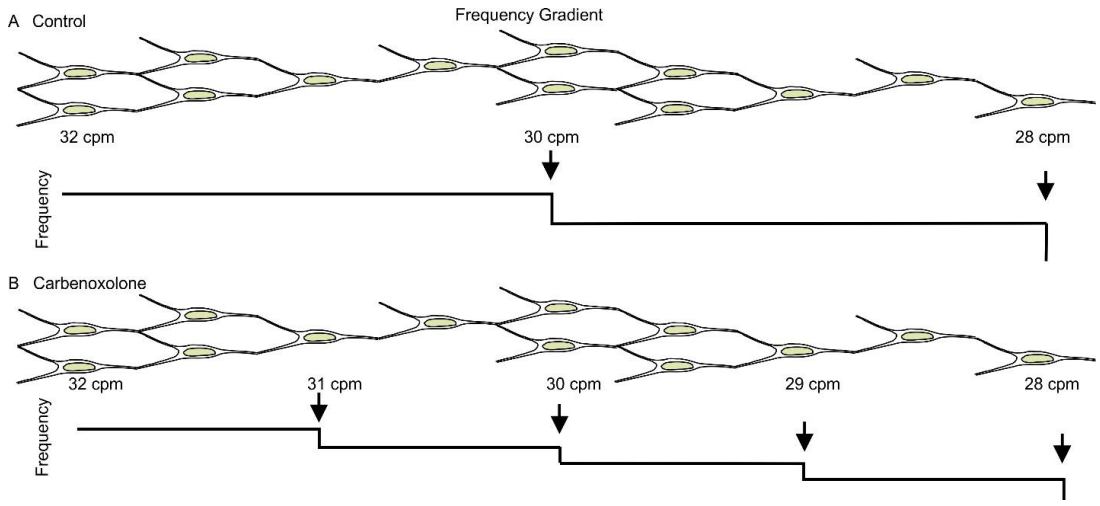

Figure 5.6: Frequency gradient and pacemaker entrainment in the small intestinal network of interstitial cells of Cajal associated with the myenteric plexus (ICC-MP). A) In the absence of drugs the frequency of slow waves generated by the ICC-MP network is determined by the fastest pacemaker in the proximal small intestine (e.g. 32 cpm, *left*). All ICC within the range of electrical coupling of the fastest pacemaker become entrained to its frequency, although their intrinsic frequencies are usually lower than the dominant pacemaker. At the extent of the electrical coupling ranges of ICC pacemaker activity there were "frequency steps" in the space/frequency plots (traces in A & B). Beyond the maximum coupling range, ICC are not longer entrained to the proximal pacemaker, but rather the fastest local pacemaker within coupling range. B) In the presence of the gap junction blocker carbenoxolone the

range of ICC electrical coupling is diminished such that the interval between frequency steps on the space/frequency plot is reduced. Since gap junctions are necessary for electrical coupling over long distances, more local pacemaker sites arose but they were not able to entrain ICC that were further away.

5.4.3 Challenges and Limitations

One of the major challenges with the mouse colonic electrical activity study was the tissue contractility. Unlike the mouse small intestine ICC-MP slow wave (Lowie, et al., 2011), the colonic slow wave is sensitive to L-type Ca^{2+} channel blockers (Pluja, et al., 2001; Yoneda, et al., 2002), hence we could not use nicardipine. Instead we used atropine, which subdued some of the contractility but not all of it, because the intrinsic pacemaker activity is controlled by ICC-SMP without the input of enteric nerves (Huizinga, et al., 2011; Yoneda, et al., 2004).

A possible limitation of the rhythmic transient depolarisation study of mouse colon electrical activity (Chapter 4) is that atropine inhibits the activity induced by bile acids in rabbit (Shiff, et al., 1982). However, a study on the mouse colon showed that atropine did not affect resting membrane potential, frequency of action potential bursts or the number of action potentials within each burst (Yoneda, et al., 2002). We chose to use chenodeoxycholic acid because of its ability to activate low-frequency contractions in rabbit proximal and mid colon, and because it is one of the most prevalent endogenous bile acids at 30-40% of the pool (Bajor, et al., 2010). However, chenodeoxycholic acid has a low potency on TGR5 (Kawamata, et al., 2003), through which we believe it acts to activate nitrergic

nerves (Alemi, et al., 2013; Poole, et al., 2010). This may explain why 250 μM chenodeoxycholic acid was required to evoke inducible ICC-MP pacemaker activity.

5.4.4 Novel Implications

The most important implications from the study in Chapter 4 are the interactivity of the colonic ICC networks, further evidence the ICC-MP harbour an inducible pacemaker and that colonic slow waves and low-frequency rhythmic transient depolarisations interact by phase amplitude coupling, although different from the waxing and waning of the small intestine (Huizinga, et al., 2014a; Pawelka and Huizinga, 2015). The reason that the phase amplitude coupled activity I observed appeared different than the waxing and waning activity from the small intestine (Fig. 1.2B) could be because of the magnitude of the difference between the frequencies that were present. In the small intestine, the coupled frequencies were ~30 cpm slow waves and ~2 cpm rhythmic transient depolarizations (Huizinga, et al., 2014a; Huizinga, et al., 2015; Pawelka and Huizinga, 2015), whereas those I observed were from ~20 cpm slow waves and ~2 cpm rhythmic transient depolarizations. The two frequencies that coupled with submucosa removed were even closer in magnitude, ~8 cpm depolarizing activity and ~2 cpm rhythmic transient depolarizations.

5.4.5 Future Directions

Based on the results and challenges faced during the study there are several potential technical changes to make and questions to address. To combat contractility impeding recording in future experiments, it might be beneficial to use wortmannin, which is a myosin light chain kinase inhibitor (Nakanishi, et al., 1992). Wortmannin has been used previously to paralyze smooth muscle for GI muscle electrophysiology (Bayguinov, et al., 2011). Using

wortmannin would also allow us to investigate the actions of bile acids on cholinergic nerves, since atropine would not be used to block mAChRs. Two reasons that we did not use wortmannin were that it is also a PI3-kinase inhibitor that irreversibly binds to its catalytic domain (Ward, et al., 1999), thus, does not posses a selective pharmacological profile, secondly it is expensive when using it in 1-2.5 L of Krebs in each experiment. I could use A cocktail of neuronal blockers to prevent muscle contractions stimulated by excitatory neurotransmitters, for instance phentolamine to block α-adrenoceptors and propranolol to block β-adrenoceptors. This strategy was used previously, in addition to atropine, to stabilize muscle preparations for intracellular recording (Pluja, et al., 2001). To further investigate the role of NO in inducing ICC-MP generation of rhythmic transient depolarisations, I would use transgenic mice with Cre/loxP elements to excise guanylate cyclase in ICC-MP (Lies, et al., 2014), then determine if bile acids could still evoke rhythmic transient depolarisations. If we were to do more experiments, it might be better to use a secondary bile acid like deoxycholic acid which is more potent than chenodeoxycholic acid (Alemi, et al., 2013). We did not directly prove that nitrergic nerves are involved in the mechanism, but the theory that they are involved is consistent with the data presented in Chapter 4 and the fact that chenodeoxycholic acid is a strong inducer of propulsive contractions in humans (Lee, 2015). Staining for TGR5 receptors would also help clarify the signalling mechanism by which bile acids evoked inducible pacemaker activity in the colon, by determining in which cell types they are expressed.

5.5 Synthesizing the Concepts of Intrinsic and Inducible Pacemaker Activity

Here I discuss some of the broader implications of my research into ICC electrophysiology, some recent developments that affect the interpretation of my work, and clinical implications of the knowledge I have provided.

Since my study on the Ca^{2+} sensitivity of the maxi Cl^- channel there have been some developments in our knowledge of the properties of the channel. Dr. Sean Parsons from our lab showed that maxi channels from small intestinal ICC-MP have a sodium-chloride permeability ratio ($P_{Na/Cl}$) that ranged from 0.76 to 1.64 (Parsons, et al., 2012). The Na^+ permeability of the channel further solidifies its capacity as the pacemaker channel from ICC because inward Na^+ currents would depolarize them to initiate the upstroke of the pacemaker potential. I chose to call the channel the maxi Cl^- channel here, instead of just the "maxi channel" for consistency with the nomenclature used in my studies. Also in the two studies where I recorded the maxi channel, it was inwardly rectifying in the cell-attached configuration and the currents were carried by Cl^- because the pipette solutions did not contain Na^+ or other permeant cations.

Since the maxi Cl^- channel exhibits approximately 1:1 permeability for Na^+ and Cl^-, it prompts the question: how does the channel behave as it approaches the Nernst potential for Cl^- (E_{Cl})? Our best estimate of E_{Cl} can be calculated based on measurements of ICC intracellular [Cl^-] ranging from 10-30 mM (Zhu, et al., 2010), with extracellular [Cl^-] being 140 mM. In my study, I reported the reversal potentials (E_{rev}) relative to resting membrane potential, which was assumed to be -65 mV (Kito and Suzuki, 2003). Thus, Cl^- currents through maxi

Cl^- channels should reverse about 26 mV above resting membrane potential (E_{Cl} = -39 mV), with 30 mM intracellular [Cl^-] (Zhu, et al., 2010).

One reason for reporting potentials relative to resting membrane potential is because in the cell attached configuration, the channels in the patch experience a potential that is the sum of the command potential and the membrane potential (since the cell membrane is intact). Unfortunately, it is not possible to measure the cell membrane potential while cell-attached and to avoid rupturing the cell to measure its membrane potential, we just used previously published values as a guideline for ICC membrane potential (Kito and Suzuki, 2003). The membrane potential of the cell changes over the course of an experiment, especially when I exposed them to excitatory drugs chosen to activate the depolarizing maxi Cl^- channels, but if the reversal potentials were not reported as relative to resting membrane potential, then they would not make sense based on the intra- and extracellular [Cl^-]. My approach in this was informed by the principle of making experiments as physiological as possible to observe ICC ion channel activity in conditions that resemble those present in the living organism. More precision in measuring reversal potentials could have been achieved by bathing the cells in 140 mM KCl, but that could lead to killing the cells and would not allow them to respond physiologically.

Small intestinal pacemaker potentials can be up to 50 mV in amplitude, which lead to 20 mV slow waves in the muscle (Kito and Suzuki, 2003). If the maxi Cl^- channel is responsible for the pacemaker upstroke, then it could not depolarize ICC above -39 mV, but if it is Na^+ permeable it can continue to depolarize ICC as E_m approaches E_{Na}= +66 mV, before plat-

eauing at about -20 mV (Kito and Suzuki, 2003). Without Na^+ permeability, maxi Cl^- channel would not be able to contribute to the entire upstroke of the pacemaker potential and its amplitude would be dependent on just voltage gated Na^+ and Ca^{2+} channels (Fig. 5.7).

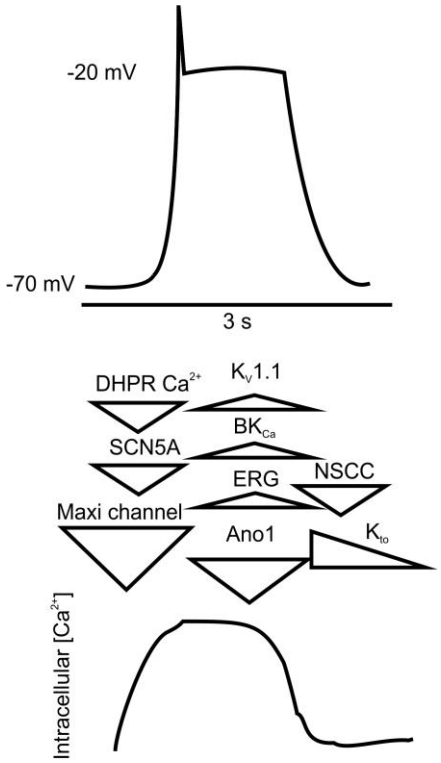

Figure 5.7: Schematic diagram of ion channel involvement in the interstitial cells of Cajal associated with the myenteric plexus (ICC-MP) pacemaker potential after my thesis. Top trace represents a slow wave pacemaker potential generated by ICC-MP. Below, triangles represent current contributions from: dihydropyridine-resistant (DHPR) Ca^{2+} channels, SCN5A Na^+ channels, non-selective cation channels (NSCC), voltage gated K^+ channel 1.1 ($K_V1.1$), large conductance Ca^{2+}-activated K^+ channels (BK_{Ca}), ether-a-go-go related gene (ERG) K^+ channels, anoctamin 1 (Ano1) Ca^{2+}-activated Cl^- channels, and transient outward K^+ channels (K_{to}). The maxi Cl^- channel is involved in the upstroke of pacemaker potential,

which occurs in concert with rhythmic intracellular Ca^{2+} transients in ICC-MP (bottom trace). Downward triangles indicate inward currents and upward triangles indicate outward currents.

5.5.1 Roles of ICC in Gut Motility

The roles of ICC in the gut are varied depending on the location within the gut wall and the specific functions of the organ from which they are derived. Small intestinal ICC-MP (Thomsen, et al., 1998; Barajas-Lopez, et al., 1989; Kito and Suzuki, 2003; Huizinga, et al., 1998; van Helden, et al., 2010) and colonic ICC-SMP (Pluja, et al., 2001; Huizinga, et al., 2011; Yoneda, et al., 2002) both generate intrinsic pacemaker activities that pace the slow waves from their respective organs. For unknown reasons these intrinsic pacemakers are not located in the same layer of the gut wall of their respective organs. Intrinsic pacemaker activity requires a pacemaker channel, which I have shown is the maxi Cl^- channel. Not only was the maxi channel present in small intestinal ICC-MP, but also in the signal transmitting colonic ICC-IM. The maxi Cl^- may also be present in colonic ICC-MP or ICC-SMP, which would make it a hallmark feature of the cell type. Colonic maxi Cl^- channels expression and activity warrants further investigation.

Originally it was thought that ICC networks that did not exhibit intrinsic pacemaker had an unknown function maybe involved in neurotransmission (Huizinga, et al., 1998). Since then we have learned that the ICC networks in the small intestinal deep muscular plexus (ICC-DMP) are involved in pacing inducible low-frequency activity (Huizinga, et al., 2014a; Zhu, et al., 2014; Huizinga, et al., 2015; Zhu, et al., 2016). Colonic ICC-MP appear to play a simi-

lar role to small intestinal ICC-DMP in that they also generate inducible pacemaker activity when activated by certain stimuli (Keef, et al., 1997; Keef, et al., 2002; Pluja, et al., 2001), as I have shown with chenodeoxycholic acid. Another subtype of ICC that does not appear to generate intrinsic pacemaker activity are the highly-innervated networks of ICC-IM. While they may not generate spontaneous electrical activity to pace the muscle, their excitability in response to innervation plays an important role in transmission of signals throughout the muscle layers in which they are embedded (Komuro, 2006; Ward and Sanders, 2006). The function of the 8 cpm activity we observed from ICC-IM in the absence of ICC-SMP remains unknown and may represent a redundant backup pacemaker, inactive in the unperturbed state. Thus, there are three major roles for subtypes of gastrointestinal ICC: generation of intrinsic pacemaker activity leading to slow waves, generation of inducible pacemaker activity when stimulated and transmission of neuronal or other ICC pacemaker signals into the muscle.

5.5.2 Clinical Implications

Recently, our laboratory has turned its attention to determining how the motility patterns in the human colon are orchestrated, so that we may be able to help develop therapeutic strategies to treat patients with refractory dysmotility, like chronic constipation. There are numerous aetiologies of chronic constipation in humans (Giorgio, et al., 2013; Knowles and Farrugia, 2011). If the colon of a chronic constipation patient undergoing high-resolution manometry does not respond to bisacodyl stimulation, there are few options remaining other than surgery. I determined a mechanism by which ICC-paced colonic electrical is activated, which likely underlies increased propulsive motility. This could be translated to provide bet-

ter options to chronic constipation patients, other than colectomy. Since chenodeoxycholic acid is used for treatment of gallstones (Hyun, et al., 2015), and it can cause diarrhea (Alemi, et al., 2013; Lee, 2015; Camilleri and Gores, 2015), a trial using it in chronic constipation patients assessed with high-resolution colonic manometry is warranted. Once activation of inducible pacemaker activity is understood, drugs could be developed to activate propulsive motility in patients with refractory chronic constipation.

Understanding which ion channels are present in ICC and how they are regulated, are not just interesting topics for investigation by basic science, they are essential to enable development better treatments for motility disorders. Since ICC are very important for controlling the rhythm, propagation direction and type of motility present in the gut at a given time, it stands to reason that patients with ICC pathologies would present with dysmotility. This has been observed clinically as patients with loss of ICC present with chronic constipation (Sanders, et al., 2006; Knowles and Farrugia, 2011). Thus, gaining understanding of the ionic mechanisms behind ICC pacemaker activity and excitability may provide potential drug targets treating dysmotility. Knowledge gained from basic scientific discoveries in neuronal patch clamp electrophysiology was later applied in cardiology basic and clinical research, which led to improvements in treating heart arrhythmias (Pugsley, 2002). Mutations in ion channels genes, called channelopathies, can lead to numerous types of motility disorders, which can affect individual patients uniquely (Beyder and Farrugia, 2016). Ion channelopathies in gastrointestinal motility disorders are an emerging area that will lean on our understanding of ICC ion channels and their regulatory mechanisms. Hopefully mapping the ion channel involvement in the pacemaker potential and elucidating the regulatory mechanisms

of ion channels in ICC will lead to advancements in treatments for dysmotility, like those achieved in treating cardiac arrhythmias.

5.6 Summary

My thesis focused on the investigating the electrophysiology of three subtypes of ICC: small intestinal ICC-MP, colonic ICC-IM and colonic ICC-MP. Firstly, I showed that the maxi Cl^- channel is the pacemaker channel from ICC-MP, because it is activated by intracellular Ca^{2+} (Fig. 5.8A-C). Secondly, I showed that colonic ICC-IM are excited by cholinergic agonists because they express $K_V7.5$ channels whose currents are suppressed by activation of mAChRs (Fig. 5.8D-F). Finally, I showed that inducible pacemaker activity from colonic ICC-MP is activated by the endogenous bile acid, chenodeoxycholic acid (Fig. 5.8D, G-J). These three main contributions, along with the details of the papers contained herein, comprise significant contributions to our knowledge of the electrophysiology of ICC. I have advanced our understanding in the three main roles of ICC: generation of intrinsic pacemaker activity, facilitation of signal transmission, and generation of inducible pacemaker activity.

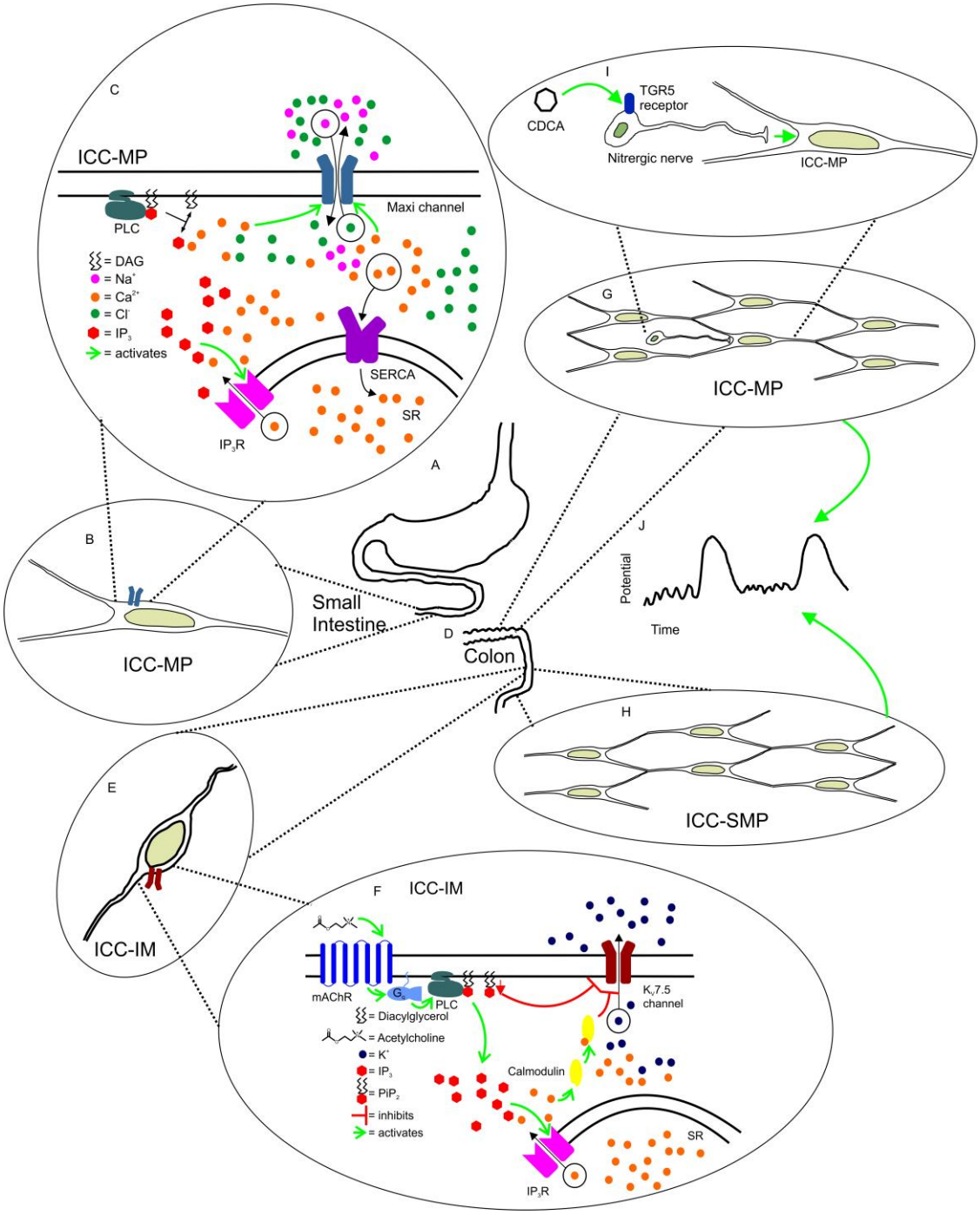

Figure 5.8: Summary of contributions to the understanding interstitial cells of Cajal (ICC) electrophysiology. A) ICC are located throughout the gastrointestinal tract, in one of my studies I focused on the ICC associated with the myentric plexus (ICC-MP) of the small in-

testine which generate intrinsic pacemaker activity responsible for slow waves. B) ICC-MP have maxi Cl^- channels that were pacemaker channel candidates prior to my thesis, but it was not clear if they were sensitive to intracellular Ca^{2+}. C) Maxi Cl^- channels from ICC-MP are activated by intracellular Ca^{2+} released from the sarcoplasmic reticulum (SR) by IP_3 receptors. D) In the colon, intramuscular ICC (ICC-IM) are located between the circular muscle cells. E) ICC-IM do not generate intrinsic pacemaker activity, but I showed that they are highly innervated by cholinergic nerves and express K^+ channels that are sensitive to cholinergic signalling. F) Acetylcholine released from cholinergic nerves activates muscarinic acetylcholine receptors (mAChR) on ICC-IM, leading to activation of G_q which in turn activates phospholipase C (PLC). PLC cleaves PiP_2 into diacylglycerol (DAG) and inositol trisphosphate (IP_3). $K_V7.5$ channels are blocked either by depletion of PiP_2, which is required for channel activity or by blockade by calmodulin which is activated by Ca^{2+} released from the sarcoplasmic reticulum by the IP_3 from PiP_2 hydrolysis. G) Colonic ICC-MP also do not generate intrinsic pacemaker activity, but harbour the inducible pacemaker of the colon. H) ICC-SMP generate intrinsic pacemaker activity which paces the slow waves in colonic circular muscle. I) Chenodeoxycholic acid activates TGR5 receptors on nitrergic nerves which release nitric oxide onto the ICC-MP which they innervate. Once activated the ICC-MP generate inducible pacemaker activity. J) ICC-MP inducible pacemaker activity causes rhythmic transient depolarisations in the muscle which occur in concert with slow waves from ICC-SMP.

APPENDICES

ANO1 IS A BETTER MARKER THAN C-KIT FOR TRANSCRIPT ANALYSIS OF SINGLE INTERSTITIAL CELLS OF CAJAL IN CULTURE

1.1 Preface

The body of this appendix was reproduced from a journal article, published in Cellular & Molecular Biology Letters, of which I am the third author:

Loera-Valencia R, Wang XY, **Wright GWJ**, Barajas-López C, and Huizinga JD (2014) Ano1 is a better marker than c-Kit for transcript analysis of single interstitial cells of Cajal in culture. *Cell Mol Biol Lett* **19:** 601-610. DOI # 10.2478/s11658-014-0214-4

 This article was also published as part of Raul Loera-Valencia's PhD thesis submitted to the Instituto Potosino de Investigación Científica y Tecnológica, Mexico, entitled: Signalling Modulation in Cells that Control Gastrointestinal Motility.

As coauthor of the paper I prepared all the primary cultured ICC, performed the single-cell extractions, and wrote some of the manuscript and edited it during review. Raul Loera-Valencia planned the study, performed 75% of the single-cell PCR, prepared the single-cell PCR figures, wrote most of the manuscript and edited it during review. Xuan Yu Wang performed the 25% of the single-cell PCR and all the immunohistochemistry and staining, prepared the immunohistochemistry figures, and wrote a little of the manuscript. Carlos

Barajas-López supervised Raul Loera-Valencia. Jan D Huizinga supervised and planned the study, provided the funding, and edited the manuscript during review.

1.2 Paper Full Text

VERSITA

CELLULAR & MOLECULAR BIOLOGY LETTERS

http://www.cmbl.org.pl

Received: 23 April 2014 Volume 19 (2014) pp 1-…

Final form accepted: 15 October 2014 DOI: 10.2478/s11658-014-0214-4

Published online:

Short communication

Ano1 IS A BETTER MARKER THAN *c-Kit* FOR TRANSCRIPT ANALYSIS OF SINGLE INTERSTITIAL CELLS OF CAJAL IN CULTURE

RAÚL LOERA-VALENCIA[1, 2, *], XUAN-YU WANG[2], GEORGE W.J. WRIGHT[2], CARLOS BARAJAS-LÓPEZ[1] and JAN D. HUIZINGA[2]

[1] División de Biología Molecular, Instituto Potosino de Investigación Científica y Tecnológica, Camino a la Presa San José 2055, Col. Lomas 4a Sección, C.P.78216 San Luis Potosí, SLP, México, [2]Farncombe Family Digestive Health Research Institute, Department of Medicine, McMaster University, HSC-3N8, 1200 Main Street West, Hamilton, ON, L8N 3Z5, Canada

Abstract: The interstitial cells of Cajal (ICC) drive the slow wave-associated contractions in the small intestine. A commonly used marker for these cells is *c-Kit*, but another marker

named *Ano1* was recently described. This study uses single-cell RT-PCR, qPCR and immunohistochemistry to determine if *Ano1* could be reliably used as a molecular marker for ICC in single-cell mRNA analysis. Here, we report on the relationship between the expression of *c-Kit* and *Ano1* in single ICC in culture. We observed that *Ano1* is expressed in more than 60% of the collected cells, whereas *c-Kit* is found only in 22% of the cells (n = 18). When we stained ICC primary cultures for c-KIT and ANO1 protein, we found complete co-localization in all the preparations. We propose that this difference is due to the regulation of *c-Kit* mRNA in culture. This regulation gives rise to low levels of its transcript, while *Ano1* is expressed more prominently in culture on day 4. We also propose that *Ano1* is more suitable for single-cell expression analysis as a marker for cell identity than *c-Kit* at the mRNA level. We hope this evidence will help to validate and increase the success of future studies characterizing single ICC expression patterns.

Keywords: Interstitial cells of Cajal, *c-Kit*; *Ano1,* Multiplexed RT-PCR, Single-cell PCR, Transcriptional regulation, ICC marker, Small intestine, Primary cultures, Pacemaker cells

---

* Author for correspondence. Email: raul.loera@ipicyt.edu.mx; phone: +52 444 834 2000 x2033; fax: +52 444 834 2010

Abbreviations used: *Ano1* – anoctamin 1, HS – HEPES buffer saline solution, ICC – interstitial cells of Cajal, NC – no cell control

INTRODUCTION

Pacemaker cells called the interstitial cells of Cajal (ICC) drive the slow wave associated contractions in the small intestine [1–3]. Research on the physiology and biochemistry of these cells through patch clamping and other electrophysiological techniques helped to gain insight into their function as the pacemakers of the gut [4–7]. However, other molecular techniques, such as RT-PCR and qPCR have only been used in a limited way because there is no pure culture of ICC or ICC cell line on which to perform gene expression analysis separately from the associated tissues, such as the enteric nerves and smooth muscle [8]. To date, only one transcriptomic analysis of ICC has been achieved after enrichment and purification of cell samples through fluorescence-activated cell sorting [9], but the implementation and validation of such a method requires specialized equipment and considerable economic investment. With the availability of transgenic mice with copGFP-expressing ICC [10], primary cultures have been used to improve identification in electrophysiological or immunohistochemical analyses [11, 12] but not in single cell characterization. One alternative for the molecular analysis of ICC is the single-cell RT-PCR technique, which allows the collection of individual cells from a mixed culture [13]. The use of single-cell RT-PCR has increased in recent years thanks to the introduction of new technologies and the implementation of ready-to-use PCR products. However, the research on single cell expression profiling with ICC has been limited, with only few publications on the subject, mostly dedicated to the identification of the ICC through *c-Kit* expression, which is a broadly accepted ICC marker [1, 3, 14, 15]. Some of the problems encountered performing single-cell RT-

PCR with ICC are the small amount of genetic material obtained and the need to amplify the ICC marker *c-Kit* from every sample, since the most simple form of the protocol allows the amplification of only one target [16].

The large majority of experiments in ICC have been performed in culture, and previous reports have indicated that culture conditions may affect the biochemistry and function of ICC [17, 18]. In particular, *c-Kit* is a gene that can be greatly influenced by the presence of serum factors like TGF-beta, which significantly decreases the half-life of *c-Kit* mRNA [19]. This phenomenon could affect the results of expression studies involving single-cell RT-PCR and using *c-Kit* as a molecular marker. Recent evidence has identified the calcium-activated chloride channel TMEM16A/anoctamin 1 (*Ano1*) in ICC [10]. Immunofluorescence studies reported 100% co-localization of this channel with *c-Kit*, and it is now accepted as an additional marker of ICC identity in both culture and tissue [20, 21].

MATERIALS AND METHODS

ICC primary cell culture

Short-term primary cultures of ICC were generated by enzymatic digestion of dissected small intestinal muscle tissue as previously described [22, 23]. Small intestines were removed from 5- to 15-day old CD-1 mice (Charles River Laboratories) and dissected using blunt dissection. The gut wall was cut open at the mesenteric border, and then the mucosa was removed along with the mesentery. The muscle was cut into pieces and incubated for 15 min at 36ºC in HEPES-buffered saline (HS) with the addition of 1 mg/ml type F colla-

genase, 1 mg/ml bovine serum albumin, 0.5 mg/ml papain, 0.5 mg/ml soybean trypsin inhibitor and 0.2 mg/ml (−)-1,4-dithio-L-threitol (all from Sigma). After trituration of the smooth muscle, the cell suspension was settled on collagen coated cover slips and cultured for 3–4 days before use, using the Clonetics SmGM-2 system (Lomax, supplied by Cedarlane).

All of the procedures were carried out in accordance with regulations from the Animal Research Ethics Board (AREB) of McMaster University in accordance with guidelines from the Canadian Council on Animal Care.

Relative expression RT-PCR

To assess the relative expression of *c-Kit* and *Ano1* compared to GAPDH, primary cultures of ICC were prepared as described above. Day 0 corresponded to a stabilized culture in serum-free solution, while days 2 and 4 correspond to that many days of culture in the normal culture medium. The Ambion Cells to cDNA II Kit for cDNA extraction was used according to the manufacturer's instructions. The internal primers designed for *c-Kit* and *Ano1* are also qPCR compatible. We detected GAPDH expression with the primers GAPDHF 5'-CCATGGAGAAGGCCGGGG and GAPDHR 5'-CAAAGTTGTCATGGATGACC (PCR product: 198 bp). The program included an initial denaturing of 95ºC for 5 min, followed by 35 cycles of 10 s of denaturation at 95ºC and annealing/extension at 60ºC for 5 s. A melting curve was applied to ensure the specificity of the PCR products (65 to 95ºC with 0.5ºC steps every 5 s).

Single cell isolation and RNA extraction

In order to isolate the ICC in primary culture for RT-PCR, we utilized a patch clamp rig as described elsewhere [23]. ICC-MP were identified by their roughly triangular shape with a process at each apex, found singly. Protease (0.1 mg/ml) was used to detach ICC from the collagen-coated coverslips. Unpolished, low-resistance pipettes were used to remove cells from the coverslips. Cells were removed by applying negative pressure to the pipette. A no cell (NC) control was included. For it, we simulated the collection of a cell by lowering the pipette into the bath solution. The pipettes for single cell extraction contained 0.6 μl of RNase-free 10x RT Buffer with RNase inhibitor (20 units per sample) to a final volume of 6 μl. The contents of the pipette were expelled with positive pressure into a PCR tube containing 12.5 μl of RNase-free RT mixture consisting of 2.3 μM oligo (dT), 150 μM dNTPs, 1.2 mM dTT, 3.6 mM $MgCl_2$ and 1.4 μl of 10x RT Buffer (Life Technologies) along with 0.5 μl of 1% NP40 detergent to cause cell membrane disruption.

The reaction was incubated at 65ºC for 2 min. After the addition of 1 μl reverse transcriptase (Superscript III, Invitrogen), the sample was placed at 50ºC for 90 min. For positive controls, tissue extracted from adult CD-1 murine brains was triturated in a mortar with a pestle in liquid nitrogen. Afterwards, we weighed 10–20 mg of tissue and collected it in Eppendorf tubes with 500 μl of lysis solution from an RNeasy RNA isolation kit (Qiagen). The RNA was obtained from the lysis solution using an affinity column and was collected for cDNA synthesis using the instructions of the Superscript III First Strand Synthesis Kit (Invitrogen).

Single-cell RT-PCR

The single cells obtained from primary cultures were tested for *Ano1* and *c-Kit* expression using a nested approach. The external primers for pre-amplification were: Ano1F 5'-TGTACTTTGCCTGGCTTGGAGC and Ano1R 5'-CACCTGGC AATGCAGCCGTA (PCR product: 700 bp); and c-kitF 5'-GCTCAT TGGCTTT-GTGGTTGCAG and c-kitR 5'-ATGCGCCAAGCAGGTTCACAA (PCR product: 404 bp). For nested PCR we used the internal primers: Ano1intF 5'-CAACTACCGATGGGACCTCAC and Ano1intR 5'-AATAGG CTGGGAATCGGTCC (PCR product: 170 bp); and c-kitintF 5'-ATA GACCCGACGCAACTTCCT and c-kitintR 5'-AACTGTCATGGCAGCATCCGAC (PCR product: 150 bp).

Pre-amplification of the targets was carried out on half of the single cell cDNA, or 200 ng of tissue cDNA, by cycling 30 times at 50ºC and extending for 1 min at 72ºC. Then, nested PCR was carried out using internal specific primers. The PCR protocol was performed on a CFX96 thermal cycler (Bio-Rad Laboratories Canada Ltd.): initial denaturation for 3 min at 94ºC, then 35 amplification rounds of denaturation for 15 s at 94ºC, alignment for 15 s at 55–58ºC, and extension for 30 s at 72ºC. The final extension was 5 min at 72ºC.

For both amplifications, recombinant Taq Polymerase was used according to the manufacturer's instructions (Life Technologies). Negative controls were performed without a template; no false amplifications were obtained. The resulting products were analyzed via agarose electrophoresis in 1.5% agarose gels (Invitrogen) stained with 1 μg/ml ethidium bromide (Sigma-Aldrich). Images were obtained with a Gel-Doc 2000 documentation system (Bio-Rad Laboratories Canada Ltd.). The identities of all of the amplicons produced were confirmed by sequencing (MOBIX Laboratories, McMaster University).

ANO1 and c-KIT immunohistochemistry

For immunohistochemistry, both musculature whole-mount tissue and cultured cells were made from the proximal jejunum of CD1 mice processed according to the following protocol. Tissues were fixed in ice-cold acetone for 10 min. After incubation with 5% normal goat serum for 1 h to block non-specific staining, tissues were incubated with monoclonal rat anti-*c-Kit* (ACK4, 1:200, Cedarlane) overnight, followed by Cy3 conjugated goat anti-rat IgG (1:600, Jackson ImmunoResearch) incubation for 1 h at room temperature. After c-Kit staining, the tissues were fixed again with 4% (w/w) paraformaldehyde in phosphate-buffered saline (PBS) for 1 h. The tissues were incubated with rabbit anti-ANO1 (1:100, AbCam Inc.) and then with Alexa 488-conjugated goat anti-rabbit IgG (1:200, Jackson ImmunoResearch). All of the antibodies were diluted in 0.3% Triton X-100 in PBS (pH 7.4). Control tissues were prepared by omitting primary antibodies. Pictures were taken using a confocal microscope (Zeiss LSM 510) with excitation wavelengths (543 nm and 488 nm) appropriate for Cy3 and Alexa 488.

RESULTS AND DISCUSSION

Ano1 and *c-Kit* relative expression

In our relative expression analysis, we observed that *c-Kit* levels remain constant during primary culture, but they were low on day 4 compared to *Ano1*, which increased around fourfold ($p < 0.05$, Fig. 1A). This suggests that Ano1 is a better candidate for ICC identification in single cell expression analyses. The effect of serum on *c-Kit* mRNA regulation has

been shown in other cell types [19], but the precise dynamics of *c-Kit* transcription, translation and *cys*-acting mechanisms in ICC require further investigation.

Standard single-cell *Ano1* and *c-Kit* RT-PCR

Since Ano1 levels were highest on day 4, we looked for Ano1 and c-Kit expression in single ICC at this point during culture. We were able to amplify two genes from single interstitial cells of Cajal: *Ano1* and *c-Kit*. We found that of the eight *Ano1*-positive cells, only one exhibited *c-Kit* expression (Fig. 1B). Of 11 cells tested, 3 cells did not exhibit *Ano1* or *c-Kit* amplification. These cells were not taken into account in the percentage reported because we cannot be sure that any PCR product could be amplified from their cDNA.

Multiplexed RT-PCR and immunohistochemistry

The possibility of a multiplexed approach to increase the number of targets amplified has been reported elsewhere [24]. We applied this methodology to single ICC for this study. We revisited the ratio of *Ano1* and/or *c-Kit* expression in these multiplexed experiments with similar results (n = 18 cells; 12 *Ano1*-positive cells; 4 *c-Kit*-positive cells). Additional genes were amplified from the *Ano1*-positive cells (voltage-gated porins and potassium channels, data not shown), confirming that cDNA had been synthesized correctly and the lack of *c-Kit* expression was not an artifact of the technique used.

At the protein level we found 100% co-localization between *Ano1* and *c-Kit* in both tissue and cultured cells (Fig. 2), which is consistent with previous reports. This suggests that our negative *c-Kit* results could be the product of the low levels of *c-Kit* mRNA present in the

cells at the moment of the extraction, a diminished half-life of its mRNA, or a combination of the two factors, whereas the *Ano1* transcript levels increased.

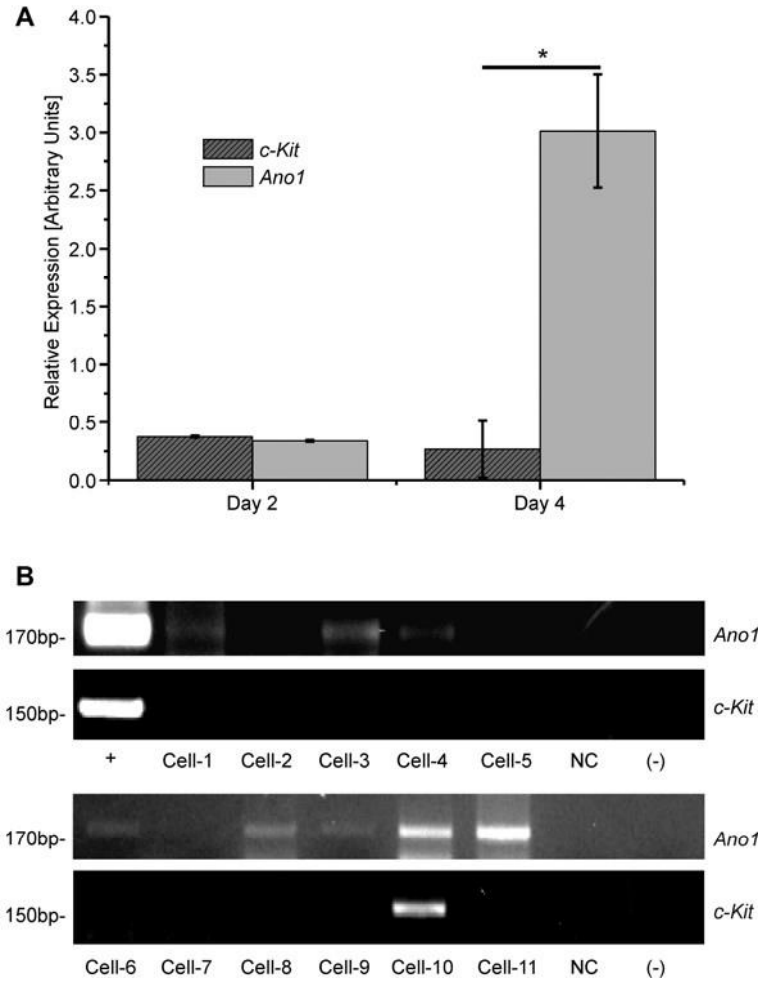

Fig. 1. *Ano1* abundance over *c-Kit* in single isolated interstitial cells of Cajal (ICC). A – Relative expression quantification of *Ano1* and *c-Kit* transcripts from whole small intestinal ICC primary cultures. The data was normalized to the level on day 0 of culture. The asterisk indicates statistical significance (n = 3 per group; $p < 0.05$) between the expression of *Ano1* and *c-Kit* in primary ICC cultures on day 4. B – *Ano1* and *c-Kit* RT-PCR from single ICC in

culture. Whole intestine cDNA (0.2 μg) was used as a positive control. Every column represents the PCR products obtained from a single ICC cDNA.

NC denotes a no cell control, while the negative control was performed without template. The identity of the products was confirmed by sequencing.

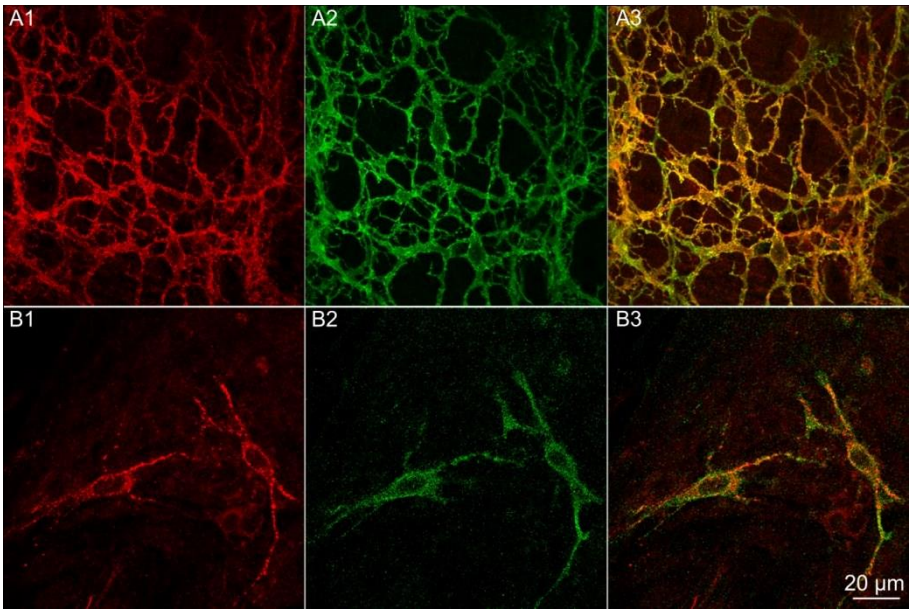

Fig. 2. c-Kit (red) and ANO1 (green) immunoreactivities in mouse jejunum musculature. A1 through A3 – Wholemount preparations show a dense ICC-MP network. B1 through B3 – Cultured preparations show triangle or multipolar-shaped ICC. Co-localization of c-Kit and ANO1 was 100% in ICC-MP of both tissue (A3) and cultured cells (B3).

While *Ano1* transcript levels in cultures seem to increase by day 4, it is likely that they reach a steady-state level. This mainly because Ano1 is required for the generation of slow waves [25] and also because the recorded slow waves maintain their characteristics stably after several days in culture [26].

ANO1 has been previously related to cell division and regulatory volume decrease (RVD) [27–29]. Therefore, the expression of ANO1 in our system could be related to compensation of osmotic homeostasis after stress produced by the tissue disruption process needed to generate ICC primary cultures. In prostate cancer, evidence suggests that ANO1 could regulate swelling-activated Ca^{2+} entry through BCL2 activation and could thus regulate calcium homeostasis in these cells [28]. ANO1 has also been found overexpressed in gastrointestinal stromal tumors [30, 31], which originate from the ICC and present high BCL2 levels. However, the role of ANO1 expression regulation over BCL2 and over calcium oscillations remains to be investigated.

ANO1 Ca^{2+}-activated Cl^- channels play an important role in slow wave generation. A recent study with *Tmem16a*$^{-/-}$ mice showed the complete loss of pacemaker activity in the muscle of the *Tmem16a*$^{-/-}$ mouse antrum and small intestine, whereas the ICC network and *c-Kit* immunoreactivity appeared normal [24]. Loss of pacemaker activity was found in both *W/W*^{v} and *Tmem16a*$^{-/-}$ mice, suggesting that ANO1 shares the same functional significance as traditional ICC marker *c-Kit* at the mRNA level. Our study showed the higher success of single-cell PCR from ICC using *Ano1*, so *Ano1* is a better marker than *c-Kit* for transcript analysis of single ICC. We expect that the use of *Ano1* as a marker for single cell identification at the mRNA level will increase the success rate of further single ICC PCR experiments in the field, allowing validation and faster up-scaling to medium and high-throughput platforms.

Acknowledgements. This study was supported by a Natural Sciences and Engineering Research Council (NSERC) research grant to Jan D. Huizinga (#386877). Raúl Loera-

Valencia was supported by CONACYT (Consejo Nacional de Ciencia y Tecnología, México, scholarship 290618). George W.J. Wright was supported by both an Ontario Graduate Scholarship and an NSERC Postgraduate Scholarship. We are grateful to Dr. Waliul Khan for the use of his thermal cycler and documentation system.

REFERENCES

1. Huizinga, J.D., Thuneberg, L., Kluppel, M., Malysz, J., Mikkelsen, H.B. and Bernstein, A. W/kit gene required for interstitial cells of Cajal and for intestinal pacemaker activity. **Nature** 373 (1995) 347–349. DOI: 10.1038/373347a0.
2. Koh, S.D., Sanders, K.M. and Ward, S.M. Spontaneous electrical rhythmicity in cultured interstitial cells of cajal from the murine small intestine. **J. Physiol.** 513 (Pt 1) (1998) 203–213.
3. Thomsen, L., Robinson, T.L., Lee, J.C., Farraway, L.A., Hughes, M.J., Andrews, D.W. and Huizinga, J.D. Interstitial cells of Cajal generate a rhythmic pacemaker current. **Nat. Med.** 4 (1998) 848–851.
4. Koh, S.D., Ward, S.M., Ordog, T., Sanders, K.M. and Horowitz, B. Conductances responsible for slow wave generation and propagation in interstitial cells of Cajal. **Curr. Opin. Pharmacol.** 3 (2003) 579–582.
5. Sanders, K.M., Koh, S.D. and Ward, S.M. Interstitial cells of cajal as pacemakers in the gastrointestinal tract. **Annu. Rev. Physiol.** 68 (2006) 307–343. DOI: 10.1146/annurev.physiol.68.040504.094718.
6. Huizinga, J.D., Berezin, I., Chorneyko, K., Thuneberg, L., Sircar, K., Hewlett, B.R. and Riddell, R.H. Interstitial cells of Cajal: pacemaker cells? **Am. J. Pathol.** 153 (1998) 2008–2011.
7. Huizinga, J.D. Gastrointestinal peristalsis: joint action of enteric nerves, smooth muscle, and interstitial cells of Cajal. **Microsc. Res. Tech.** 47 (1999) 239–247. DOI: 10.1002/(SICI)1097-0029(19991115)47:4 < 239::AID-JEMT3 > 3.0.CO;2-0.
8. Huizinga, J.D., Robinson, T.L. and Thomsen, L. The search for the origin of rhythmicity in intestinal contraction; from tissue to single cells. **Neurogastroenterol. Motil.** 12 (2000) 3–9.
9. Chen, H., Ordog, T., Chen, J., Young, D.L., Bardsley, M.R., Redelman, D., Ward, S.M. and Sanders, K.M. Differential gene expression in functional classes of interstitial cells of Cajal in murine small intestine. **Physiol. Genomics** 31 (2007) 492–509. DOI: 10.1152/physiolgenomics.00113.2007.

10. Zhu, M.H., Kim, T.W., Ro, S., Yan, W., Ward, S.M., Koh, S.D. and Sanders, K.M. A Ca(2+)-activated Cl(-) conductance in interstitial cells of Cajal linked to slow wave currents and pacemaker activity. **J. Physiol.** 587 (2009) 4905– 4918. DOI: 10.1113/jphysiol.2009.176206.
11. Sanders, K.M., Zhu, M.H., Britton, F., Koh, S.D. and Ward, S.M. Anoctamins and gastrointestinal smooth muscle excitability. **Exp. Physiol.** 97 (2012) 200– 206. DOI: 10.1113/expphysiol.2011.058248.
12. Zhu, M.H., Sung, I.K., Zheng, H., Sung, T.S., Britton, F.C., O'Driscoll, K., Koh, S.D. and Sanders, K.M. Muscarinic activation of Ca2+-activated Cl- current in interstitial cells of Cajal. **J. Physiol.** 589 (2011) 4565–4582. DOI: 10.1113/jphysiol.2011.211094.
13. Eberwine, J. Single-cell molecular biology. **Nat. Neurosci.** 4 Suppl (2001) 1155–1156. DOI: 10.1038/nn1101-1155.
14. Takeda, Y., Koh, S.D., Sanders, K.M. and Ward, S.M. Differential expression of ionic conductances in interstitial cells of Cajal in the murine gastric antrum. **J. Physiol.** 586 (2008) 859–873. DOI: 10.1113/ jphysiol.2007.140293.
15. Wouters, M.M., Gibbons, S.J., Roeder, J.L., Distad, M., Ou, Y., Strege, P.R., Szurszewski, J.H. and Farrugia, G. Exogenous serotonin regulates proliferation of interstitial cells of Cajal in mouse jejunum through 5-HT2B receptors. **Gastroenterology** 133 (2007) 897–906. DOI: 10.1053/ j.gastro.2007.06.017.
16. Li, H.H., Gyllensten, U.B., Cui, X.F., Saiki, R.K., Erlich, H.A. and Arnheim, N. Amplification and analysis of DNA sequences in single human sperm and diploid cells. **Nature** 335 (1988) 414–417. DOI: 10.1038/ 335414a0.
17. Wang, B., Kunze, W.A., Zhu, Y. and Huizinga, J.D. In situ recording from gut pacemaker cells. **Pflugers Arch.** 457 (2008) 243–251. DOI: 10.1007/ s00424008-0513-6.
18. Parsons, S.P., Kunze, W.A. and Huizinga, J.D. Maxi-channels recorded in situ from ICC and pericytes associated with the mouse myenteric plexus. **Am. J. Physiol. Cell Physiol.** 302 (2012) C1055–1069. DOI: 10.1152/ ajpcell.00334.2011.
19. Dubois, C.M., Ruscetti, F.W., Stankova, J. and Keller, J.R. Transforming growth factor-beta regulates c-kit message stability and cell-surface protein expression in hematopoietic progenitors. **Blood** 83 (1994) 3138–3145.
20. Gomez-Pinilla, P.J., Gibbons, S.J., Bardsley, M.R., Lorincz, A., Pozo, M.J., Pasricha, P.J., Van de Rijn, M., West, R.B., Sarr, M.G., Kendrick, M.L., Cima, R.R., Dozois, E.J., Larson, D.W., Ordog, T. and Farrugia, G. Ano1 is a selective marker of interstitial cells of Cajal in the human and mouse gastrointestinal tract. **Am. J. Physiol. Gastrointest. Liver Physiol.** 296 (2009) G1370–1381. DOI: 10.1152/ajpgi.00074.2009.
21. Kashyap, P., Gomez-Pinilla, P.J., Pozo, M.J., Cima, R.R., Dozois, E.J., Larson, D.W., Ordog, T., Gibbons, S.J. and Farrugia, G. Immunoreactivity for Ano1 detects depletion of Kit-positive interstitial cells of Cajal in patients with slow transit constipation. **Neurogastroenterol. Motil.** 23 (2011) 760–765. DOI: 10.1111/j.1365-2982.2011.01729.x.
22. Parsons, S.P. and Huizinga, J.D. Transient outward potassium current in ICC. **Am. J. Physiol. Gastrointest. Liver Physiol.** 298 (2010) G456–466. DOI: 10.1152/ajpgi.00340.2009.

23. Wright, G.W., Parsons, S.P. and Huizinga, J.D. Ca^{2+} sensitivity of the maxi chloride channel in interstitial cells of Cajal. **Neurogastroenterol. Motil.** 24 (2012) e221–234. DOI: 10.1111/j.1365-2982.2012.01881.x.
24. Phillips, J.K. and Lipski, J. Single-cell RT-PCR as a tool to study gene expression in central and peripheral autonomic neurones. **Auton. Neurosci.** 86 (2000) 1–12. DOI: 10.1016/S1566-0702(00)00245-9.
25. Hwang, S.J., Blair, P.J., Britton, F.C., O'Driscoll, K.E., Hennig, G., Bayguinov, Y.R., Rock, J.R., Harfe, B.D., Sanders, K.M. and Ward, S.M. Expression of anoctamin 1/TMEM16A by interstitial cells of Cajal is fundamental for slow wave activity in gastrointestinal muscles. **J. Physiol.** 587 (2009) 4887–4904. DOI: 10.1113/jphysiol.2009.176198.
26. Espinosa-Luna, R., Collins, S.M., Montano, L.M. and Barajas-Lopez, C. Slow wave and spike action potentials recorded in cell cultures from the muscularis externa of the guinea pig small intestine. **Can. J. Physiol. Pharmacol.** 77 (1999) 598–605.
27. Okada, Y., Shimizu, T., Maeno, E., Tanabe, S., Wang, X. and Takahashi, N. Volume-sensitive chloride channels involved in apoptotic volume decrease and cell death. **J. Membr. Biol.** 209 (2006) 21–29. DOI: 10.1007/s00232005-0836-6.
28. Shen, M.R., Yang, T.P. and Tang, M.J. A novel function of BCL-2 overexpression in regulatory volume decrease. Enhancing swelling-activated Ca(2+) entry and Cl(-) channel activity. **J. Biol. Chem.** 277 (2002) 15592– 15599. DOI: 10.1074/jbc.M111043200.
29. Ponce, A., Jimenez-Pena, L. and Tejeda-Guzman, C. The role of swellingactivated chloride currents (I(CL, swell)) in the regulatory volume decrease response of freshly dissociated rat articular chondrocytes. **Cell Physiol. Biochem.** 30 (2012) 1254–1270. DOI: 10.1159/000343316.
30. West, R.B., Corless, C.L., Chen, X., Rubin, B.P., Subramanian, S., Montgomery, K., Zhu, S., Ball, C.A., Nielsen, T.O., Patel, R., Goldblum, J.R., Brown, P.O., Heinrich, M.C. and van de Rijn, M. The novel marker, DOG1, is expressed ubiquitously in gastrointestinal stromal tumors irrespective of KIT or PDGFRA mutation status. **Am. J. Pathol.** 165 (2004) 107–113. DOI: 10.1016/S0002-9440(10)63279-8.
31. Robinson T.L., Sircar, K., Hewlett B.R., Chorneyko K., Riddell R.H. and Huizinga J.D. Gastrointestinal stromal tumors may originate from a subset of CD34-positive interstitial cells of Cajal. **Am. J. Pathol.** 156 (2000) 1157–1163.

2 List of Publications

Wright GWJ, Vincent A, Zhu YF, Parsons SP and Huizinga JD (2016) Chenodeoxycholic acid activates the mouse colonic inducible pacemaker via stimulation of nitrergic nerves. *J Neurogastroenterol Motil* (*Submitted*)

Huizinga JD, Wei R, Chen JH, **Wright G,** and Bardakjian B (2014) Generating bowel movements that facilitate nutrient absorption. *Can Y Sci J* **7:** 4-13.

Loera-Valencia R, Wang XY, **Wright GWJ**, Barajas-López C, and Huizinga JD (2014) Ano1 is a better marker than c-Kit for transcript analysis of single interstitial cells of cajal in culture. *Cell Mol Biol Lett* **19:** 601-610.

Wang XY, Chen JH, Li K, Zhu YF, **Wright GW,** and Huizinga JD (2014) Discrepancies between c-Kit positive and Ano1 positive ICC-SMP in the W/Wv and wild-type mouse colon; relationships with motor patterns and calcium transients. *Neurogastroenterol Motil* **26:** 1298-1310.

Wright GWJ, Parsons SP, Loera-Valencia R, Wang XY, Barajas-López C, and Huizinga JD (2013) Cholinergic signalling-regulated $K_V7.5$ currents are expressed in colonic ICC-IM but not ICC-MP. *Pflugers Arch* **466:** 1805-1818.

Wright GW, Parsons SP, and Huizinga JD (2012) Ca^{2+} sensitivity of the maxi chloride channel from interstitial cells of Cajal. *Neurogastroenterol Motil* **24:** e221-e234.

3 Permissions to Reproduce Copyright Material

JOHN WILEY AND SONS LICENSE
TERMS AND CONDITIONS
Jul 14, 2016

This Agreement between George W Wright ("You") and John Wiley and Sons ("John Wiley and Sons") consists of your license details and the terms and conditions provided by John Wiley and Sons and Copyright Clearance Center.

License Number	3907690270285
License date	Jul 14, 2016
Licensed Content Publisher	John Wiley and Sons
Licensed Content Publication	Neurogastroenterology & Motility
Licensed Content Title	Ca2+ sensitivity of the maxi chloride channel in interstitial cells of Cajal
Licensed Content Author	G. W. J. Wright,S. P. Parsons,J. D. Huizinga
Licensed Content Date	Feb 1, 2012
Licensed Content Pages	1
Type of use	Dissertation/Thesis
Requestor type	Author of this Wiley article
Format	Print and electronic
Portion	Full article
Will you be translating?	No
Title of your thesis / dissertation	Electrophysiology of Interstitial Cells of Cajal
Expected completion date	Sep 2016
Expected size (number of pages)	300
Requestor Location	George W Wright

	19 Clyde St Hamilton, ON L8L 5R5 Canada Attn: George W Wright
Publisher Tax ID	EU826007151
Billing Type	Invoice
Billing Address	George W Wright 19 Clyde St Hamilton, ON L8L 5R5 Canada Attn: George W Wright
Total	0.00 CAD

Terms and Conditions

TERMS AND CONDITIONS

This copyrighted material is owned by or exclusively licensed to John Wiley & Sons, Inc. or one of its group companies (each a"Wiley Company") or handled on behalf of a society with which a Wiley Company has exclusive publishing rights in relation to a particular work (collectively "WILEY"). By clicking "accept" in connection with completing this licensing transaction, you agree that the following terms and conditions apply to this transaction (along with the billing and payment terms and conditions established by the Copyright Clearance Center Inc., ("CCC's Billing and Payment terms and conditions"), at the time that you opened your RightsLink account (these are available at any time at http://myaccount.copyright.com).

Terms and Conditions

- The materials you have requested permission to reproduce or reuse (the "Wiley Materials") are protected by copyright.
- You are hereby granted a personal, non-exclusive, non-sub licensable (on a stand-alone basis), non-transferable, worldwide, limited license to reproduce the Wiley Materials for the purpose specified in the licensing process. This license, **and any CONTENT (PDF or image file) purchased as part of your order,** is for a one-time use only and limited to any maximum distribution number specified in the li-

cense. The first instance of republication or reuse granted by this license must be completed within two years of the date of the grant of this license (although copies prepared before the end date may be distributed thereafter). The Wiley Materials shall not be used in any other manner or for any other purpose, beyond what is granted in the license. Permission is granted subject to an appropriate acknowledgement given to the author, title of the material/book/journal and the publisher. You shall also duplicate the copyright notice that appears in the Wiley publication in your use of the Wiley Material. Permission is also granted on the understanding that nowhere in the text is a previously published source acknowledged for all or part of this Wiley Material. Any third party content is expressly excluded from this permission.

- With respect to the Wiley Materials, all rights are reserved. Except as expressly granted by the terms of the license, no part of the Wiley Materials may be copied, modified, adapted (except for minor reformatting required by the new Publication), translated, reproduced, transferred or distributed, in any form or by any means, and no derivative works may be made based on the Wiley Materials without the prior permission of the respective copyright owner.**For STM Signatory Publishers clearing permission under the terms of the STM Permissions Guidelines only, the terms of the license are extended to include subsequent editions and for editions in other languages, provided such editions are for the work as a whole in situ and does not involve the separate exploitation of the permitted figures or extracts,** You may not alter, remove or suppress in any manner any copyright, trademark or other notices displayed by the Wiley Materials. You may not license, rent, sell, loan, lease, pledge, offer as security, transfer or assign the Wiley Materials on a stand-alone basis, or any of the rights granted to you hereunder to any other person.

- The Wiley Materials and all of the intellectual property rights therein shall at all times remain the exclusive property of John Wiley & Sons Inc, the Wiley Companies, or their respective licensors, and your interest therein is only that of having possession of and the right to reproduce the Wiley Materials pursuant to Section 2 herein during the continuance of this Agreement. You agree that you own no right, title or interest in or to the Wiley Materials or any of the intellectual property rights therein. You shall have no rights hereunder other than the license as provided for above in Section 2. No right, license or interest to any trademark, trade name, service mark or other branding ("Marks") of WILEY or its licensors is granted hereunder, and you agree that you shall not assert any such right, license or interest with respect thereto

- NEITHER WILEY NOR ITS LICENSORS MAKES ANY WARRANTY OR REPRESENTATION OF ANY KIND TO YOU OR ANY THIRD PARTY, EXPRESS, IMPLIED OR STATUTORY, WITH RESPECT TO THE MATERIALS OR THE ACCURACY OF ANY INFORMATION CONTAINED IN THE MATERIALS, INCLUDING, WITHOUT LIMITATION, ANY IMPLIED WARRANTY OF MERCHANTABILITY, ACCURACY, SATISFACTORY QUALITY, FITNESS FOR A PARTICULAR PURPOSE, USABILITY, INTEGRATION OR

NON-INFRINGEMENT AND ALL SUCH WARRANTIES ARE HEREBY EXCLUDED BY WILEY AND ITS LICENSORS AND WAIVED BY YOU.

- WILEY shall have the right to terminate this Agreement immediately upon breach of this Agreement by you.

- You shall indemnify, defend and hold harmless WILEY, its Licensors and their respective directors, officers, agents and employees, from and against any actual or threatened claims, demands, causes of action or proceedings arising from any breach of this Agreement by you.

- IN NO EVENT SHALL WILEY OR ITS LICENSORS BE LIABLE TO YOU OR ANY OTHER PARTY OR ANY OTHER PERSON OR ENTITY FOR ANY SPECIAL, CONSEQUENTIAL, INCIDENTAL, INDIRECT, EXEMPLARY OR PUNITIVE DAMAGES, HOWEVER CAUSED, ARISING OUT OF OR IN CONNECTION WITH THE DOWNLOADING, PROVISIONING, VIEWING OR USE OF THE MATERIALS REGARDLESS OF THE FORM OF ACTION, WHETHER FOR BREACH OF CONTRACT, BREACH OF WARRANTY, TORT, NEGLIGENCE, INFRINGEMENT OR OTHERWISE (INCLUDING, WITHOUT LIMITATION, DAMAGES BASED ON LOSS OF PROFITS, DATA, FILES, USE, BUSINESS OPPORTUNITY OR CLAIMS OF THIRD PARTIES), AND WHETHER OR NOT THE PARTY HAS BEEN ADVISED OF THE POSSIBILITY OF SUCH DAMAGES. THIS LIMITATION SHALL APPLY NOTWITHSTANDING ANY FAILURE OF ESSENTIAL PURPOSE OF ANY LIMITED REMEDY PROVIDED HEREIN.

- Should any provision of this Agreement be held by a court of competent jurisdiction to be illegal, invalid, or unenforceable, that provision shall be deemed amended to achieve as nearly as possible the same economic effect as the original provision, and the legality, validity and enforceability of the remaining provisions of this Agreement shall not be affected or impaired thereby.

- The failure of either party to enforce any term or condition of this Agreement shall not constitute a waiver of either party's right to enforce each and every term and condition of this Agreement. No breach under this agreement shall be deemed waived or excused by either party unless such waiver or consent is in writing signed by the party granting such waiver or consent. The waiver by or consent of a party to a breach of any provision of this Agreement shall not operate or be construed as a waiver of or consent to any other or subsequent breach by such other party.

- This Agreement may not be assigned (including by operation of law or otherwise) by you without WILEY's prior written consent.

- Any fee required for this permission shall be non-refundable after thirty (30) days

from receipt by the CCC.

- These terms and conditions together with CCC's Billing and Payment terms and conditions (which are incorporated herein) form the entire agreement between you and WILEY concerning this licensing transaction and (in the absence of fraud) supersedes all prior agreements and representations of the parties, oral or written. This Agreement may not be amended except in writing signed by both parties. This Agreement shall be binding upon and inure to the benefit of the parties' successors, legal representatives, and authorized assigns.

- In the event of any conflict between your obligations established by these terms and conditions and those established by CCC's Billing and Payment terms and conditions, these terms and conditions shall prevail.

- WILEY expressly reserves all rights not specifically granted in the combination of (i) the license details provided by you and accepted in the course of this licensing transaction, (ii) these terms and conditions and (iii) CCC's Billing and Payment terms and conditions.

- This Agreement will be void if the Type of Use, Format, Circulation, or Requestor Type was misrepresented during the licensing process.

- This Agreement shall be governed by and construed in accordance with the laws of the State of New York, USA, without regards to such state's conflict of law rules. Any legal action, suit or proceeding arising out of or relating to these Terms and Conditions or the breach thereof shall be instituted in a court of competent jurisdiction in New York County in the State of New York in the United States of America and each party hereby consents and submits to the personal jurisdiction of such court, waives any objection to venue in such court and consents to service of process by registered or certified mail, return receipt requested, at the last known address of such party.

WILEY OPEN ACCESS TERMS AND CONDITIONS

Wiley Publishes Open Access Articles in fully Open Access Journals and in Subscription journals offering Online Open. Although most of the fully Open Access journals publish open access articles under the terms of the Creative Commons Attribution (CC BY) License only, the subscription journals and a few of the Open Access Journals offer a choice of Creative Commons Licenses. The license type is clearly identified on the article.

The Creative Commons Attribution License

The Creative Commons Attribution License (CC-BY) allows users to copy, distribute and transmit an article, adapt the article and make commercial use of the article. The CC-BY

license permits commercial and non-

Creative Commons Attribution Non-Commercial License

The Creative Commons Attribution Non-Commercial (CC-BY-NC)License permits use, distribution and reproduction in any medium, provided the original work is properly cited and is not used for commercial purposes.(see below)

Creative Commons Attribution-Non-Commercial-NoDerivs License

The Creative Commons Attribution Non-Commercial-NoDerivs License (CC-BY-NC-ND) permits use, distribution and reproduction in any medium, provided the original work is properly cited, is not used for commercial purposes and no modifications or adaptations are made. (see below)

Use by commercial "for-profit" organizations

Use of Wiley Open Access articles for commercial, promotional, or marketing purposes requires further explicit permission from Wiley and will be subject to a fee.

Further details can be found on Wiley Online Library
http://olabout.wiley.com/WileyCDA/Section/id-410895.html

Other Terms and Conditions:

v1.10 Last updated September 2015

Questions? customercare@copyright.com or +1-855-239-3415 (toll free in the US) or +1-978-646-2777.

SPRINGER LICENSE
TERMS AND CONDITIONS
Jul 14, 2016

This Agreement between George W Wright ("You") and Springer ("Springer") consists of your license details and the terms and conditions provided by Springer and Copyright Clearance Center.

License Number	3907701324304
License date	Jul 14, 2016
Licensed Content Publisher	Springer
Licensed Content Publication	Pflügers Archiv European Journal of Physiology
Licensed Content Title	Cholinergic signalling-regulated KV7.5 currents are expressed in colonic ICC-IM but not ICC-MP
Licensed Content Author	George W. J. Wright
Licensed Content Date	Jan 1, 2013
Licensed Content Volume Number	466
Licensed Content Issue Number	9
Type of Use	Thesis/Dissertation
Portion	Full text
Number of copies	5
Author of this Springer article	Yes and you are the sole author of the new work
Order reference number	
Title of your thesis / dissertation	Electrophysiology of Interstitial Cells of Cajal
Expected completion date	Sep 2016

Estimated size(pages)	300
Requestor Location	George W Wright 19 Clyde St Hamilton, ON L8L 5R5 Canada Attn: George W Wright
Billing Type	Invoice
Billing Address	George W Wright 19 Clyde St Hamilton, ON L8L 5R5 Canada Attn: George W Wright
Total	0.00 USD

Terms and Conditions

Introduction
The publisher for this copyrighted material is Springer. By clicking "accept" in connection with completing this licensing transaction, you agree that the following terms and conditions apply to this transaction (along with the Billing and Payment terms and conditions established by Copyright Clearance Center, Inc. ("CCC"), at the time that you opened your Rightslink account and that are available at any time at http://myaccount.copyright.com).

Limited License
With reference to your request to reuse material on which Springer controls the copyright, permission is granted for the use indicated in your enquiry under the following conditions:

- Licenses are for one-time use only with a maximum distribution equal to the number stated in your request.

- Springer material represents original material which does not carry references to other sources. If the material in question appears with a credit to another source, this permission is not valid and authorization has to be obtained from the original copyright holder.

- This permission
• is non-exclusive
• is only valid if no personal rights, trademarks, or competitive products are infringed.

• explicitly excludes the right for derivatives.

- Springer does not supply original artwork or content.

- According to the format which you have selected, the following conditions apply accordingly:
• **Print and Electronic:** This License include use in electronic form provided it is password protected, on intranet, or CD-Rom/DVD or E-book/E-journal. It may not be republished in electronic open access.
• **Print:** This License excludes use in electronic form.
• **Electronic:** This License only pertains to use in electronic form provided it is password protected, on intranet, or CD-Rom/DVD or E-book/E-journal. It may not be republished in electronic open access.
For any electronic use not mentioned, please contact Springer at permissions.springer@spi-global.com.

- Although Springer controls the copyright to the material and is entitled to negotiate on rights, this license is only valid subject to courtesy information to the author (address is given in the article/chapter).

- If you are an STM Signatory or your work will be published by an STM Signatory and you are requesting to reuse figures/tables/illustrations or single text extracts, permission is granted according to STM Permissions Guidelines: http://www.stm-assoc.org/permissions-guidelines/
For any electronic use not mentioned in the Guidelines, please contact Springer at permissions.springer@spi-global.com. If you request to reuse more content than stipulated in the STM Permissions Guidelines, you will be charged a permission fee for the excess content.

Permission is valid upon payment of the fee as indicated in the licensing process. If permission is granted free of charge on this occasion, that does not prejudice any rights we might have to charge for reproduction of our copyrighted material in the future.

-If your request is for reuse in a Thesis, permission is granted free of charge under the following conditions:

This license is valid for one-time use only for the purpose of defending your thesis and with a maximum of 100 extra copies in paper. If the thesis is going to be published, permission needs to be reobtained.
- includes use in an electronic form, provided it is an author-created version of the thesis on his/her own website and his/her university's repository, including UMI (according to the definition on the Sherpa website: http://www.sherpa.ac.uk/romeo/);
- is subject to courtesy information to the co-author or corresponding author.

Geographic Rights: Scope
Licenses may be exercised anywhere in the world.

Altering/Modifying Material: Not Permitted
Figures, tables, and illustrations may be altered minimally to serve your work. You may not alter or modify text in any manner. Abbreviations, additions, deletions and/or any other alterations shall be made only with prior written authorization of the author(s).

Reservation of Rights
Springer reserves all rights not specifically granted in the combination of (i) the license details provided by you and accepted in the course of this licensing transaction and (ii) these terms and conditions and (iii) CCC's Billing and Payment terms and conditions.

License Contingent on Payment
While you may exercise the rights licensed immediately upon issuance of the license at the end of the licensing process for the transaction, provided that you have disclosed complete and accurate details of your proposed use, no license is finally effective unless and until full payment is received from you (either by Springer or by CCC) as provided in CCC's Billing and Payment terms and conditions. If full payment is not received by the date due, then any license preliminarily granted shall be deemed automatically revoked and shall be void as if never granted. Further, in the event that you breach any of these terms and conditions or any of CCC's Billing and Payment terms and conditions, the license is automatically revoked and shall be void as if never granted. Use of materials as described in a revoked license, as well as any use of the materials beyond the scope of an unrevoked license, may constitute copyright infringement and Springer reserves the right to take any and all action to protect its copyright in the materials.

Copyright Notice: Disclaimer
You must include the following copyright and permission notice in connection with any reproduction of the licensed material:
"Springer book/journal title, chapter/article title, volume, year of publication, page, name(s) of author(s), (original copyright notice as given in the publication in which the material was originally published) "With permission of Springer"
In case of use of a graph or illustration, the caption of the graph or illustration must be included, as it is indicated in the original publication.

Warranties: None
Springer makes no representations or warranties with respect to the licensed material and adopts on its own behalf the limitations and disclaimers established by CCC on its behalf in its Billing and Payment terms and conditions for this licensing transaction.

Indemnity
You hereby indemnify and agree to hold harmless Springer and CCC, and their respective

officers, directors, employees and agents, from and against any and all claims arising out of your use of the licensed material other than as specifically authorized pursuant to this license.

No Transfer of License
This license is personal to you and may not be sublicensed, assigned, or transferred by you without Springer's written permission.

No Amendment Except in Writing
This license may not be amended except in a writing signed by both parties (or, in the case of Springer, by CCC on Springer's behalf).

Objection to Contrary Terms
Springer hereby objects to any terms contained in any purchase order, acknowledgment, check endorsement or other writing prepared by you, which terms are inconsistent with these terms and conditions or CCC's Billing and Payment terms and conditions. These terms and conditions, together with CCC's Billing and Payment terms and conditions (which are incorporated herein), comprise the entire agreement between you and Springer (and CCC) concerning this licensing transaction. In the event of any conflict between your obligations established by these terms and conditions and those established by CCC's Billing and Payment terms and conditions, these terms and conditions shall control.

Jurisdiction
All disputes that may arise in connection with this present License, or the breach thereof, shall be settled exclusively by arbitration, to be held in the Federal Republic of Germany, in accordance with German law.

Other conditions:

V 12AUG2015

Questions? customercare@copyright.com or +1-855-239-3415 (toll free in the US) or +1-978-646-2777.

Creative Commons

Attribution-NonCommercial-NoDerivs 3.0 Unported

License

1. Definitions

a. **"Adaptation"** means a work based upon the Work, or upon the Work and other pre-existing works, such as a translation, adaptation, derivative work, arrangement of music or other alterations of a literary or artistic work, or phonogram or performance and includes cinematographic adaptations or any other form in which the Work may be recast, transformed, or adapted including in any form recognizably derived from the original, except that a work that constitutes a Collection will not be considered an Adaptation for the purpose of this License. For the avoidance of doubt, where the Work is a musical work, performance or phonogram, the synchronization of the Work in timed-relation with a moving image ("synching") will be considered an Adaptation for the purpose of this License.

b. **"Collection"** means a collection of literary or artistic works, such as encyclopedias and anthologies, or performances, phonograms or broadcasts, or other works or subject matter other than works listed in Section 1(f) below, which, by reason of the selection and arrangement of their contents, constitute intellectual creations, in which the Work is included in its entirety in unmodified form along with one or more other contributions, each constituting separate and independent works in themselves, which together are assembled into a collective whole. A

work that constitutes a Collection will not be considered an Adaptation (as defined above) for the purposes of this License.

c. **"Distribute"** means to make available to the public the original and copies of the Work through sale or other transfer of ownership.
d. **"Licensor"** means the individual, individuals, entity or entities that offer(s) the Work under the terms of this License.
e. **"Original Author"** means, in the case of a literary or artistic work, the individual, individuals, entity or entities who created the Work or if no individual or entity can be identified, the publisher; and in addition (i) in the case of a performance the actors, singers, musicians, dancers, and other persons who act, sing, deliver, declaim, play in, interpret or otherwise perform literary or artistic works or expressions of folklore; (ii) in the case of a phonogram the producer being the person or legal entity who first fixes the sounds of a performance or other sounds; and, (iii) in the case of broadcasts, the organization that transmits the broadcast.
f. **"Work"** means the literary and/or artistic work offered under the terms of this License including without limitation any production in the literary, scientific and artistic domain, whatever may be the mode or form of its expression including digital form, such as a book, pamphlet and other writing; a lecture, address, sermon or other work of the same nature; a dramatic or dramatico-musical work; a choreographic work or entertainment in dumb show; a musical composition with or without words; a cinematographic work to which are assimilated works expressed by a process analogous to cinematography; a work of drawing, painting, architecture, sculpture, engraving or lithography; a photographic work to which are assimilated works expressed by a process analogous to photography; a work of applied art; an illustration, map, plan, sketch or three-dimensional work relative to geography, topography, architecture or science; a performance; a broadcast; a phonogram; a compilation of data to the extent it is protected as a copyrightable work; or a work performed by a variety or circus performer to the extent it is not otherwise considered a literary or artistic work.
g. **"You"** means an individual or entity exercising rights under this License who has not previously violated the terms of this License with respect to the Work, or who has received express permission from the Licensor to exercise rights under this License despite a previous violation.
h. **"Publicly Perform"** means to perform public recitations of the Work and to communicate to the public those public recitations, by any means or process, including by wire or wireless means or public digital performances; to make available to the public Works in such a way that members of the public may access these Works from a place and at a place individually chosen by them; to perform the Work to the public by any means or process and the communication to the public of the performances of the Work, including by public digital performance; to broadcast and rebroadcast the Work by any means including signs, sounds or images.

i. **"Reproduce"** means to make copies of the Work by any means including without limitation by sound or visual recordings and the right of fixation and reproducing fixations of the Work, including storage of a protected performance or phonogram in digital form or other electronic medium.

2. Fair Dealing Rights. Nothing in this License is intended to reduce, limit, or restrict any uses free from copyright or rights arising from limitations or exceptions that are provided for in connection with the copyright protection under copyright law or other applicable laws.

3. License Grant. Subject to the terms and conditions of this License, Licensor hereby grants You a worldwide, royalty-free, non-exclusive, perpetual (for the duration of the applicable copyright) license to exercise the rights in the Work as stated below:

a. to Reproduce the Work, to incorporate the Work into one or more Collections, and to Reproduce the Work as incorporated in the Collections; and,
b. to Distribute and Publicly Perform the Work including as incorporated in Collections.

The above rights may be exercised in all media and formats whether now known or hereafter devised. The above rights include the right to make such modifications as are technically necessary to exercise the rights in other media and formats, but otherwise you have no rights to make Adaptations. Subject to 8(f), all rights not expressly granted by Licensor are hereby reserved, including but not limited to the rights set forth in Section 4(d).

4. Restrictions. The license granted in Section 3 above is expressly made subject to and limited by the following restrictions:

a. You may Distribute or Publicly Perform the Work only under the terms of this License. You must include a copy of, or the Uniform Resource Identifier (URI) for, this License with every copy of the Work You Distribute or Publicly Perform. You may not offer or impose any terms on the Work that restrict the terms of this License or the ability of the recipient of the Work to exercise the rights granted to that recipient under the terms of the License. You may not sublicense the Work. You must keep intact all notices that refer to this License and to the disclaimer of warranties with every copy of the Work You Distribute or Publicly Perform. When You Distribute or Publicly Perform the Work, You may not impose any effective technological measures on the Work that restrict the ability of a recipient of the Work from You to exercise the rights granted to that recipient under the terms of the License. This Section 4(a) applies to the Work as incorporated in a Collection, but this does not require the Collection apart from the Work itself to be made subject to the terms of this License. If You create a Col-

lection, upon notice from any Licensor You must, to the extent practicable, remove from the Collection any credit as required by Section 4(c), as requested.

b. You may not exercise any of the rights granted to You in Section 3 above in any manner that is primarily intended for or directed toward commercial advantage or private monetary compensation. The exchange of the Work for other copyrighted works by means of digital file-sharing or otherwise shall not be considered to be intended for or directed toward commercial advantage or private monetary compensation, provided there is no payment of any monetary compensation in connection with the exchange of copyrighted works.
c. If You Distribute, or Publicly Perform the Work or Collections, You must, unless a request has been made pursuant to Section 4(a), keep intact all copyright notices for the Work and provide, reasonable to the medium or means You are utilizing: (i) the name of the Original Author (or pseudonym, if applicable) if supplied, and/or if the Original Author and/or Licensor designate another party or parties (e.g., a sponsor institute, publishing entity, journal) for attribution ("Attribution Parties") in Licensor's copyright notice, terms of service or by other reasonable means, the name of such party or parties; (ii) the title of the Work if supplied; (iii) to the extent reasonably practicable, the URI, if any, that Licensor specifies to be associated with the Work, unless such URI does not refer to the copyright notice or licensing information for the Work. The credit required by this Section 4(c) may be implemented in any reasonable manner; provided, however, that in the case of a Collection, at a minimum such credit will appear, if a credit for all contributing authors of Collection appears, then as part of these credits and in a manner at least as prominent as the credits for the other contributing authors. For the avoidance of doubt, You may only use the credit required by this Section for the purpose of attribution in the manner set out above and, by exercising Your rights under this License, You may not implicitly or explicitly assert or imply any connection with, sponsorship or endorsement by the Original Author, Licensor and/or Attribution Parties, as appropriate, of You or Your use of the Work, without the separate, express prior written permission of the Original Author, Licensor and/or Attribution Parties.
d. For the avoidance of doubt:
    i. **Non-waivable Compulsory License Schemes**. In those jurisdictions in which the right to collect royalties through any statutory or compulsory licensing scheme cannot be waived, the Licensor reserves the exclusive right to collect such royalties for any exercise by You of the rights granted under this License;
    ii. **Waivable Compulsory License Schemes**. In those jurisdictions in which the right to collect royalties through any statutory or compulsory licensing scheme can be waived, the Licensor reserves the exclusive right to collect such royalties for any exercise by You of the rights granted under this License if Your exercise of such rights is for a purpose or use which is otherwise than noncommercial as permitted under Section

4(b) and otherwise waives the right to collect royalties through any statutory or compulsory licensing scheme; and,

iii. **Voluntary License Schemes**. The Licensor reserves the right to collect royalties, whether individually or, in the event that the Licensor is a member of a collecting society that administers voluntary licensing schemes, via that society, from any exercise by You of the rights granted under this License that is for a purpose or use which is otherwise than noncommercial as permitted under Section 4(b).

e. Except as otherwise agreed in writing by the Licensor or as may be otherwise permitted by applicable law, if You Reproduce, Distribute or Publicly Perform the Work either by itself or as part of any Collections, You must not distort, mutilate, modify or take other derogatory action in relation to the Work which would be prejudicial to the Original Author's honor or reputation.

5. Representations, Warranties and Disclaimer

UNLESS OTHERWISE MUTUALLY AGREED BY THE PARTIES IN WRITING, LICENSOR OFFERS THE WORK AS-IS AND MAKES NO REPRESENTATIONS OR WARRANTIES OF ANY KIND CONCERNING THE WORK, EXPRESS, IMPLIED, STATUTORY OR OTHERWISE, INCLUDING, WITHOUT LIMITATION, WARRANTIES OF TITLE, MERCHANTIBILITY, FITNESS FOR A PARTICULAR PURPOSE, NONINFRINGEMENT, OR THE ABSENCE OF LATENT OR OTHER DEFECTS, ACCURACY, OR THE PRESENCE OF ABSENCE OF ERRORS, WHETHER OR NOT DISCOVERABLE. SOME JURISDICTIONS DO NOT ALLOW THE EXCLUSION OF IMPLIED WARRANTIES, SO SUCH EXCLUSION MAY NOT APPLY TO YOU.

6. Limitation on Liability. EXCEPT TO THE EXTENT REQUIRED BY APPLICABLE LAW, IN NO EVENT WILL LICENSOR BE LIABLE TO YOU ON ANY LEGAL THEORY FOR ANY SPECIAL, INCIDENTAL, CONSEQUENTIAL, PUNITIVE OR EXEMPLARY DAMAGES ARISING OUT OF THIS LICENSE OR THE USE OF THE WORK, EVEN IF LICENSOR HAS BEEN ADVISED OF THE POSSIBILITY OF SUCH DAMAGES.

7. Termination

a. This License and the rights granted hereunder will terminate automatically upon any breach by You of the terms of this License. Individuals or entities who have received Collections from You under this License, however, will not have their licenses terminated provided such individuals or entities remain in full compliance with those licenses. Sections 1, 2, 5, 6, 7, and 8 will survive any termination of this License.
b. Subject to the above terms and conditions, the license granted here is perpetual (for the duration of the applicable copyright in the Work). Notwithstanding the

above, Licensor reserves the right to release the Work under different license terms or to stop distributing the Work at any time; provided, however that any such election will not serve to withdraw this License (or any other license that has been, or is required to be, granted under the terms of this License), and this License will continue in full force and effect unless terminated as stated above.

8. Miscellaneous

a. Each time You Distribute or Publicly Perform the Work or a Collection, the Licensor offers to the recipient a license to the Work on the same terms and conditions as the license granted to You under this License.
b. If any provision of this License is invalid or unenforceable under applicable law, it shall not affect the validity or enforceability of the remainder of the terms of this License, and without further action by the parties to this agreement, such provision shall be reformed to the minimum extent necessary to make such provision valid and enforceable.
c. No term or provision of this License shall be deemed waived and no breach consented to unless such waiver or consent shall be in writing and signed by the party to be charged with such waiver or consent.
d. This License constitutes the entire agreement between the parties with respect to the Work licensed here. There are no understandings, agreements or representations with respect to the Work not specified here. Licensor shall not be bound by any additional provisions that may appear in any communication from You. This License may not be modified without the mutual written agreement of the Licensor and You.
e. The rights granted under, and the subject matter referenced, in this License were drafted utilizing the terminology of the Berne Convention for the Protection of Literary and Artistic Works (as amended on September 28, 1979), the Rome Convention of 1961, the WIPO Copyright Treaty of 1996, the WIPO Performances and Phonograms Treaty of 1996 and the Universal Copyright Convention (as revised on July 24, 1971). These rights and subject matter take effect in the relevant jurisdiction in which the License terms are sought to be enforced according to the corresponding provisions of the implementation of those treaty provisions in the applicable national law. If the standard suite of rights granted under applicable copyright law includes additional rights not granted under this License, such additional rights are deemed to be included in the License; this License is not intended to restrict the license of any rights under applicable law.

Creative Commons Notice

Creative Commons is not a party to this License, and makes no warranty whatsoever in connection with the Work. Creative Commons will not be liable to You or any party on any legal theory for any damages whatsoever, including without limitation any general,

References

Alberti E and Jimenez M (2005) Effect of 4-aminopyridine (4-AP) on the spontaneous activity and neuromuscular junction in the rat colon. *Pharmacol Res* **52**:447-456.

Alemi F, Poole DP, Chiu J, Schoonjans K, Cattaruzza F, Grider JR, Bunnett NW and Corvera CU (2013) The receptor TGR5 mediates the prokinetic actions of intestinal bile acids and is required for normal defecation in mice. *Gastroenterology* **144**:145-154.

Assef YA, Damiano AE, Zotta E, Ibarra C and Kotsias BA (2003) CFTR in K562 human leukemic cells. *Am J Physiol Cell Physiol* **285**:C480-C488.

Bajor A, Gillberg PG and Abrahamsson H (2010) Bile acids: short and long term effects in the intestine. *Scand J Gastroenterol* **45**:645-664.

Baker SA, Drumm BT, Saur D, Hennig GW, Ward SM and Sanders KM (2016) Spontaneous Ca(2+) transients in interstitial cells of Cajal located within the deep muscular plexus of the murine small intestine. *J Physiol* **594**:3317-3338.

Barajas-Lopez C, Berezin I, Daniel EE and Huizinga JD (1989) Pacemaker activity recorded in interstitial cells of Cajal of the gastrointestinal tract. *Am J Physiol* **257**:C830-C835.

Bayguinov O, Hennig GW and Sanders KM (2011) Movement based artifacts may contaminate extracellular electrical recordings from GI muscles. *Neurogastroenterol Motil* **23**:1029-42, e498.

Bayguinov PO, Hennig GW and Smith TK (2010) Ca2+ imaging of activity in ICC-MY during local mucosal reflexes and the colonic migrating motor complex in the murine large intestine. *J Physiol* **588**:4453-4474.

Beyder A and Farrugia G (2016) Ion channelopathies in functional GI disorders. *Am J Physiol Gastrointest Liver Physiol* **311**:G581-G586.

Block BM and Jones SW (1997) Delayed rectifier current of bullfrog sympathetic neurons: ion-ion competition, asymmetrical block and effects of ions on gating. *J Physiol* **499 (Pt 2)**:403-416.

Bogdanov KY, Vinogradova TM and Lakatta EG (2001) Sinoatrial nodal cell ryanodine receptor and Na(+)-Ca(2+) exchanger: molecular partners in pacemaker regulation. *Circ Res* **88**:1254-1258.

Brown BH, Duthie HL, Horn AR and Smallwood RH (1975) A linked oscillator model of electrical activity of human small intestine. *Am J Physiol* **229**:384-388.

Brown DA and Adams PR (1980) Muscarinic suppression of a novel voltage-sensitive K+ current in a vertebrate neurone. *Nature* **283**:673-676.

Brown DA, Hughes SA, Marsh SJ and Tinker A (2007) Regulation of M(Kv7.2/7.3) channels in neurons by PIP(2) and products of PIP(2) hydrolysis: significance for receptor-mediated inhibition. *J Physiol* **582**:917-925.

Brown DA and Passmore GM (2009) Neural KCNQ (Kv7) channels. *Br J Pharmacol* **156**:1185-1195.

Camilleri M and Gores GJ (2015) Therapeutic targeting of bile acids. *Am J Physiol Gastrointest Liver Physiol* **309**:G209-G215.

Code CF and Szurszewski JH (1970) The effect of duodenal and mid small bowel transection on the frequency gradient of the pacesetter potential in the canine small intestine. *J Physiol* **207**:281-289.

Corrias A and Buist ML (2008) Quantitative cellular description of gastric slow wave activity. *Am J Physiol Gastrointest Liver Physiol* **294**:G989-G995.

Der-Silaphet T, Malysz J, Hagel S, Larry AA and Huizinga JD (1998) Interstitial cells of cajal direct normal propulsive contractile activity in the mouse small intestine. *Gastroenterology* **114**:724-736.

Dickens EJ, Edwards FR and Hirst GD (2001) Selective knockout of intramuscular interstitial cells reveals their role in the generation of slow waves in mouse stomach. *J Physiol* **531**:827-833.

Faussone Pellegrini MS, Cortesini C and Romagnoli P (1977) [Ultrastructure of the tunica muscularis of the cardial portion of the human esophagus and stomach, with special reference to the so-called Cajal's interstitial cells]. *Arch Ital Anat Embriol* **82**:157-177.

Giorgio V, Borrelli O, Smith VV, Rampling D, Koglmeier J, Shah N, Thapar N, Curry J and Lindley KJ (2013) High-resolution colonic manometry accurately predicts colonic neuromuscular pathological phenotype in pediatric slow transit constipation. *Neurogastroenterol Motil* **25**:70-78.

Gomez-Pinilla PJ, Gibbons SJ, Bardsley MR, Lorincz A, Pozo MJ, Pasricha PJ, Van de Rijn M, West RB, Sarr MG, Kendrick ML, Cima RR, Dozois EJ, Larson DW, Ordog T and Farrugia G (2009) Ano1 is a selective marker of interstitial cells of Cajal in the human and mouse gastrointestinal tract. *Am J Physiol Gastrointest Liver Physiol* **296**:G1370-G1381.

Hamill OP, Marty A, Neher E, Sakmann B and Sigworth FJ (1981) Improved patch-clamp techniques for high-resolution current recording from cells and cell-free membrane patches. *Pflugers Arch* **391**:85-100.

Hatton WJ, Mason HS, Carl A, Doherty P, Latten MJ, Kenyon JL, Sanders KM and Horowitz B (2001) Functional and molecular expression of a voltage-dependent K(+) channel (Kv1.1) in interstitial cells of Cajal. *J Physiol* **533**:315-327.

Hernandez CC, Zaika O, Tolstykh GP and Shapiro MS (2008) Regulation of neural KCNQ channels: signalling pathways, structural motifs and functional implications. *J Physiol* **586**:1811-1821.

Hirst GD, Beckett EA, Sanders KM and Ward SM (2002) Regional variation in contribution of myenteric and intramuscular interstitial cells of Cajal to generation of slow waves in mouse gastric antrum. *J Physiol* **540**:1003-1012.

Hirst GD and Edwards FR (2004) Role of interstitial cells of Cajal in the control of gastric motility. *J Pharmacol Sci* **96**:1-10.

Huizinga JD, Berezin I, Chorneyko K, Thuneberg L, Sircar K, Hewlett BR and Riddell RH (1998) Interstitial cells of Cajal: pacemaker cells? *Am J Pathol* **153**:2008-2011.

Huizinga JD, Chen JH, Zhu YF, Pawelka A, McGinn RJ, Bardakjian BL, Parsons SP, Kunze WA, Wu RY, Bercik P, Khoshdel A, Chen S, Yin S, Zhang Q, Yu Y, Gao Q, Li K, Hu X, Zarate N, Collins P, Pistilli M, Ma J, Zhang R and Chen D (2014a) The origin of segmentation motor activity in the intestine. *Nat Commun* **5**:3326.

Huizinga JD, Martz S, Gil V, Wang XY, Jimenez M and Parsons S (2011) Two independent networks of interstitial cells of cajal work cooperatively with the enteric nervous system to create colonic motor patterns. *Front Neurosci* **5**:93.

Huizinga JD, Parsons SP, Chen JH, Pawelka A, Pistilli M, Li C, Yu Y, Ye P, Liu Q, Tong M, Zhu YF and Wei D (2015) Motor patterns of the small intestine explained by phase-amplitude coupling of two pacemaker activities: the critical importance of propagation velocity. *Am J Physiol Cell Physiol* **309**:C403-C414.

Huizinga JD, Thuneberg L, Kluppel M, Malysz J, Mikkelsen HB and Bernstein A (1995) W/kit gene required for interstitial cells of Cajal and for intestinal pacemaker activity. *Nature* **373**:347-349.

Huizinga JD, Wei R, Chen JH, Wright G and Bardakjian B (2014b) Generating bowel movements that facilitate nutrient absorption. *Canadian Young Scientist Journal* **2014**:4-13.

Huizinga JD, Zhu Y, Ye J and Molleman A (2002) High-conductance chloride channels generate pacemaker currents in interstitial cells of Cajal. *Gastroenterology* **123**:1627-1636.

Hyun JJ, Lee HS, Kim CD, Dong SH, Lee SO, Ryu JK, Lee DH, Jeong S, Kim TN, Lee J, Koh DH, Park ET, Lee IS, Yoo BM and Kim JH (2015) Efficacy of Magnesium Trihydrate of Ursodeoxycholic Acid and Chenodeoxycholic Acid for Gallstone Dissolution: A Prospective Multicenter Trial. *Gut Liver* **9**:547-555.

Kato T, Nakamura E, Imaeda K and Suzuki H (2009) Modulation of the activity of two pacemakers by transmural nerve stimulation in circular smooth muscle preparations isolated from the rat proximal colon. *J Smooth Muscle Res* **45**:249-268.

Kawamata Y, Fujii R, Hosoya M, Harada M, Yoshida H, Miwa M, Fukusumi S, Habata Y, Itoh T, Shintani Y, Hinuma S, Fujisawa Y and Fujino M (2003) A G protein-coupled receptor responsive to bile acids. *J Biol Chem* **278**:9435-9440.

Keef KD, Anderson U, O'Driscoll K, Ward SM and Sanders KM (2002) Electrical activity induced by nitric oxide in canine colonic circular muscle. *Am J Physiol Gastrointest Liver Physiol* **282**:G123-G129.

Keef KD, Murray DC, Sanders KM and Smith TK (1997) Basal release of nitric oxide induces an oscillatory motor pattern in canine colon. *J Physiol* **499 (Pt 3)**:773-786.

Kim YC, Koh SD and Sanders KM (2002) Voltage-dependent inward currents of interstitial cells of Cajal from murine colon and small intestine. *J Physiol* **541**:797-810.

Kito Y and Suzuki H (2003) Properties of pacemaker potentials recorded from myenteric interstitial cells of Cajal distributed in the mouse small intestine. *J Physiol* **553**:803-818.

Knowles CH and Farrugia G (2011) Gastrointestinal neuromuscular pathology in chronic constipation. *Best Pract Res Clin Gastroenterol* **25**:43-57.

Koh SD, Jun JY, Kim TW and Sanders KM (2002) A Ca(2+)-inhibited non-selective cation conductance contributes to pacemaker currents in mouse interstitial cell of Cajal. *J Physiol* **540**:803-814.

Komuro T (2006) Structure and organization of interstitial cells of Cajal in the gastrointestinal tract. *J Physiol* **576**:653-658.

Lakatta EG, Maltsev VA and Vinogradova TM (2010) A coupled SYSTEM of intracellular Ca2+ clocks and surface membrane voltage clocks controls the timekeeping mechanism of the heart's pacemaker. *Circ Res* **106**:659-673.

Lee HT, Hennig GW, Fleming NW, Keef KD, Spencer NJ, Ward SM, Sanders KM and Smith TK (2007) The mechanism and spread of pacemaker activity through myenteric interstitial cells of Cajal in human small intestine. *Gastroenterology* **132**:1852-1865.

Lee KJ (2015) Pharmacologic Agents for Chronic Diarrhea. *Intest Res* **13**:306-312.

Lies B, Gil V, Groneberg D, Seidler B, Saur D, Wischmeyer E, Jimenez M and Friebe A (2014) Interstitial cells of Cajal mediate nitrergic inhibitory neurotransmission in the murine gastrointestinal tract. *Am J Physiol Gastrointest Liver Physiol* **307**:G98-106.

Lowie BJ, Wang XY, White EJ and Huizinga JD (2011) On the origin of rhythmic calcium transients in the ICC-MP of the mouse small intestine. *Am J Physiol Gastrointest Liver Physiol* **301**:G835-G845.

McKay CM and Huizinga JD (2006) Muscarinic regulation of ether-a-go-go-related gene K+ currents in interstitial cells of Cajal. *J Pharmacol Exp Ther* **319**:1112-1123.

Molleman A (2003) *Patch clamping an introductory guide to patch clamp electrophysiology*. J. Wiley, New York.

Nakanishi S, Kakita S, Takahashi I, Kawahara K, Tsukuda E, Sano T, Yamada K, Yoshida M, Kase H, Matsuda Y and . (1992) Wortmannin, a microbial product inhibitor of myosin light chain kinase. *J Biol Chem* **267**:2157-2163.

Parsons SP and Huizinga JD (2010) Transient outward potassium current in ICC. *Am J Physiol Gastrointest Liver Physiol* **298**:G456-G466.

Parsons SP and Huizinga JD (2015) Effects of gap junction inhibition on contraction waves in the murine small intestine in relation to coupled oscillator theory. *Am J Physiol Gastrointest Liver Physiol* **308**:G287-G297.

Parsons SP, Kunze WA and Huizinga JD (2012) Maxi-channels recorded in situ from ICC and pericytes associated with the mouse myenteric plexus. *Am J Physiol Cell Physiol* **302**:C1055-C1069.

Parsons SP and Sanders KM (2008) An outwardly rectifying and deactivating chloride channel expressed by interstitial cells of cajal from the murine small intestine. *J Membr Biol* **221**:123-132.

Pawelka AJ and Huizinga JD (2015) Induction of rhythmic transient depolarizations associated with waxing and waning of slow wave activity in intestinal smooth muscle. *Am J Physiol Gastrointest Liver Physiol* **308**:G427-G433.

Pluja L, Alberti E, Fernandez E, Mikkelsen HB, Thuneberg L and Jimenez M (2001) Evidence supporting presence of two pacemakers in rat colon. *Am J Physiol Gastrointest Liver Physiol* **281**:G255-G266.

Poole DP, Godfrey C, Cattaruzza F, Cottrell GS, Kirkland JG, Pelayo JC, Bunnett NW and Corvera CU (2010) Expression and function of the bile acid receptor GpBAR1 (TGR5) in the murine enteric nervous system. *Neurogastroenterol Motil* **22**:814-818.

Pugsley MK (2002) Antiarrhythmic Drug Development: Historical Review and Future Perspective. *Drug Dev Res* **55**:3-16.

Quan X, Luo H, Liu Y, Xia H, Chen W and Tang Q (2015) Hydrogen sulfide regulates the colonic motility by inhibiting both L-type calcium channels and BKCa channels in smooth muscle cells of rat colon. *PLoS One* **10**:e0121331.

Rumessen JJ, Thuneberg L and Mikkelsen HB (1982) Plexus muscularis profundus and associated interstitial cells. II. Ultrastructural studies of mouse small intestine. *Anat Rec* **203**:129-146.

Sanders KM, Koh SD and Ward SM (2006) Interstitial cells of cajal as pacemakers in the gastrointestinal tract. *Annu Rev Physiol* **68**:307-343.

Sanders KM, Zhu MH, Britton F, Koh SD and Ward SM (2012) Anoctamins and gastrointestinal smooth muscle excitability. *Exp Physiol* **97**:200-206.

Schopfer LM and Salhany JM (1995) Characterization of the stilbenedisulfonate binding site on band 3. *Biochemistry* **34**:8320-8329.

Shibasaki T (1987) Conductance and kinetics of delayed rectifier potassium channels in nodal cells of the rabbit heart. *J Physiol* **387**:227-250.

Shiff SJ, Soloway RD and Snape WJ, Jr. (1982) Mechanism of deoxycholic acid stimulation of the rabbit colon. *J Clin Invest* **69**:985-992.

Smith TK, Reed JB and Sanders KM (1987) Interaction of two electrical pacemakers in muscularis of canine proximal colon. *Am J Physiol* **252**:C290-C299.

So KY, Kim SH, Sohn HM, Choi SJ, Parajuli SP, Choi S, Yeum CH, Yoon PJ and Jun JY (2009) Carbachol regulates pacemaker activities in cultured interstitial cells of Cajal from the mouse small intestine. *Mol Cells* **27**:525-531.

Strege PR, Ou Y, Sha L, Rich A, Gibbons SJ, Szurszewski JH, Sarr MG and Farrugia G (2003) Sodium current in human intestinal interstitial cells of Cajal. *Am J Physiol Gastrointest Liver Physiol* **285**:G1111-G1121.

Thomsen L, Robinson TL, Lee JC, Farraway LA, Hughes MJ, Andrews DW and Huizinga JD (1998) Interstitial cells of Cajal generate a rhythmic pacemaker current. *Nat Med* **4**:848-851.

Thuneberg L (1982) Interstitial cells of Cajal: intestinal pacemaker cells? *Adv Anat Embryol Cell Biol* **71**:1-130.

Torihashi S, Fujimoto T, Trost C and Nakayama S (2002) Calcium oscillation linked to pacemaking of interstitial cells of Cajal: requirement of calcium influx and localization of TRP4 in caveolae. *J Biol Chem* **277**:19191-19197.

Torihashi S, Ward SM, Nishikawa S, Nishi K, Kobayashi S and Sanders KM (1995) c-kit-dependent development of interstitial cells and electrical activity in the murine gastrointestinal tract. *Cell Tissue Res* **280**:97-111.

van Breemen C, Chen Q and Laher I (1995) Superficial buffer barrier function of smooth muscle sarcoplasmic reticulum. *Trends Pharmacol Sci* **16**:98-105.

van Helden DF, Laver DR, Holdsworth J and Imtiaz MS (2010) Generation and propagation of gastric slow waves. *Clin Exp Pharmacol Physiol* **37**:516-524.

Wang B, Kunze WA, Zhu Y and Huizinga JD (2008) In situ recording from gut pacemaker cells. *Pflugers Arch* **457**:243-251.

Wang XY, Paterson C and Huizinga JD (2003) Cholinergic and nitrergic innervation of ICC-DMP and ICC-IM in the human small intestine. *Neurogastroenterol Motil* **15**:531-543.

Ward SM, Beckett EA, Wang X, Baker F, Khoyi M and Sanders KM (2000) Interstitial cells of Cajal mediate cholinergic neurotransmission from enteric motor neurons. *J Neurosci* **20**:1393-1403.

Ward SM, Brennan MF, Jackson VM and Sanders KM (1999) Role of PI3-kinase in the development of interstitial cells and pacemaking in murine gastrointestinal smooth muscle. *J Physiol* **516 (Pt 3)**:835-846.

Ward SM, Burns AJ, Torihashi S and Sanders KM (1994) Mutation of the proto-oncogene c-kit blocks development of interstitial cells and electrical rhythmicity in murine intestine. *J Physiol* **480 (Pt 1)**:91-97.

Ward SM and Sanders KM (2006) Involvement of intramuscular interstitial cells of Cajal in neuroeffector transmission in the gastrointestinal tract. *J Physiol* **576**:675-682.

Yoneda S, Fukui H and Takaki M (2004) Pacemaker activity from submucosal interstitial cells of Cajal drives high-frequency and low-amplitude circular muscle contractions in the mouse proximal colon. *Neurogastroenterol Motil* **16**:621-627.

Yoneda S, Takano H, Takaki M and Suzuki H (2002) Properties of spontaneously active cells distributed in the submucosal layer of mouse proximal colon. *J Physiol* **542**:887-897.

Zhang RX, Wang XY, Chen D and Huizinga JD (2011) Role of interstitial cells of Cajal in the generation and modulation of motor activity induced by cholinergic neurotransmission in the stomach. *Neurogastroenterol Motil* **23**:e356-e371.

Zhu MH, Kim TW, Ro S, Yan W, Ward SM, Koh SD and Sanders KM (2009) A Ca(2+)-activated Cl(-) conductance in interstitial cells of Cajal linked to slow wave currents and pacemaker activity. *J Physiol* **587**:4905-4918.

Zhu MH, Sung IK, Zheng H, Sung TS, Britton FC, O'Driscoll K, Koh SD and Sanders KM (2011) Muscarinic activation of Ca2+-activated Cl- current in interstitial cells of Cajal. *J Physiol* **589**:4565-4582.

Zhu Y, Mucci A and Huizinga JD (2005) Inwardly rectifying chloride channel activity in intestinal pacemaker cells. *Am J Physiol Gastrointest Liver Physiol* **288**:G809-G821.

Zhu Y, Parsons SP and Huizinga JD (2010) Measurement of intracellular chloride ion concentration in ICC in situ and in explant culture. *Neurogastroenterol Motil* **22**:704-709.

Zhu YF, Wang XY, Lowie BJ, Parsons S, White L, Kunze W, Pawelka A and Huizinga JD (2014) Enteric sensory neurons communicate with interstitial cells of Cajal to affect pacemaker activity in the small intestine. *Pflugers Arch* **466**:1467-1475.

Zhu YF, Wang XY, Parsons SP and Huizinga JD (2016) Stimulus-induced pacemaker activity in interstitial cells of Cajal associated with the deep muscular plexus of the small intestine. *Neurogastroenterol Motil* **28**:1064-1074.